DOCTOR OF PHILOSOPHY

Investigating the structure, function and assembly of bacterial [NiFe]-hydrogenases

Bowman, Lisa

Award date:
2013

DOCTOR OF PHILOSOPHY

Investigating the structure, function and assembly of bacterial [NiFe]-hydrogenases

Lisa Bowman

2013

University of Dundee

Investigating the Structure, Function and Assembly of Bacterial [NiFe]-Hydrogenases

by

Lisa Bowman

August, 2013

Thesis submitted to the University of Dundee in partial fulfilment of the requirements for the degree of Doctor of Philosophy.

Table of Contents

Table of figures

Table of tables

Acknowledgments

The first person I must thank is my supervisor, Professor Frank Sargent. I greatly appreciate being given the opportunity to pursue my love of science in his research group. I thank him for all his encouragement, time and advice, especially in the final stages of thesis writing. I believe that I have not only acquired a variety of valuable skills under his supervision, but have also gained confidence. His enthusiasm and depth of knowledge have inspired me to continue in academia.

I must also extend thanks to Professor Tracy Palmer. Not only do I appreciate her scientific advice and guidance (that I have asked for on countless occasions), but the example she sets balancing life as a female scientist at the top of her field with being a mother.

I would like to thank all members of the TP/FS group for their helpful suggestions over the past four years. In particular, I wish to thank Dr Grant Buchanan for his advice and friendship. I don't think my laughter would have been heard half as often if I had been placed in any other office. I would also like to express my gratitude to Dr Jen McDowall for her patience and helpful discussions. Thanks are extended to all members of MMB and especially to Dr Jacqueline Heilbronn, our lab manager, for dealing with any problem, no matter how big or small.

I must also thank our collaborators Dr Alison Parkin and Professor Fraser Armstrong for electroscopic and spectroscopic data, as well as Dr Paul Fyfe and Professor William Hunter for crystallographic data. Without their helpful contributions and suggestions, some of the work in this thesis would have been impossible.

I would also like to acknowledge and express thanks to the BBSRC for funding this PhD project, and the Society of General Microbiology, FEBS-EMBO and the Biochemical Society for providing me with grants that have allowed me to present my work at national and international conferences.

I cannot finish without thanking those closest to me. First, I would like to thank Ciarán. The last four years would not have been same without you. You have given me support, love and encouragement at times when I badly needed it. Finally I owe my family a huge thank you for never growing tired of hearing about my work and providing me with support and reassurance. You have kept me motivated and I hope I have made you proud.

Declaration

I declare that I am the author of this thesis and that, unless otherwise stated, all references cited have been consulted; that the work of which this thesis is a record of has been performed by me, and that it has not been previously accepted for a higher degree: where the thesis is based upon joint research, the nature and extent of my individual contribution is defined.

Lisa Bowman

Abstract

The need to replace fossil fuel use with a viable and sustainable alternative form of energy is an issue of great importance. Biologically produced hydrogen, or 'biohydrogen' has the potential to become a key future biofuel. Furthermore, the enzymes responsible for metabolising hydrogen, termed hydrogenases, have shown promise as electrocatalysts in biological fuel cells. Understanding how these enzymes function is not only important for future biotechnology, but also has biomedical implications as a number of pathogenic bacteria rely on hydrogen as an energy source during infection. Therefore hydrogenases represent attractive drug targets.

Escherichia coli produces three [NiFe]-hydrogenases. Hyd-1 and Hyd-2 are involved in hydrogen oxidation, whereas Hyd-3 is responsible for hydrogen production. Both Hyd-1 and Hyd-2 are known twin arginine translocation (Tat) substrates and as such are synthesised as precursors bearing N-terminal signal peptides, which contain conserved SRRxFLK 'twin arginine' motifs. The signal peptides of [NiFe]-hydrogenases possess unusually extended n-regions that contain a number of conserved residues. Using the *E. coli* Hyd-1 signal peptide as a model, genetic and biochemical approaches were employed in an effort to elucidate the role of the n-region. The use of reporter fusion constructs and pulse-chase labelling experiments provided results to suggest that the n-region acts to stall protein export. Furthermore, genetic removal of the n-region from native Hyd-1 results in complete enzyme inactivity. This has led to the hypothesis that the n-region functions as a regulatory domain that controls signal peptide transport activity.

Salmonella enterica serovar Typhimurium produces homologs of the *E. coli* uptake enzymes and also encodes a third Tat-dependent hydrogenase called Hyd-5. Fascinatingly, expression of the *hyd* operon is induced aerobically; a rare property as most [NiFe]-hydrogenases are inactivated by oxygen. In this study, genetic approaches were taken to successfully upregulate expression of the *hyd* operon on the *Salmonella* chromosome. The crystal structure of Hyd-5 was solved, revealing an unusual [4Fe-3S] Fe-S cluster unique to oxygen-tolerant hydrogenases. Not only was the Fe-S cluster found to be coordinated by six cysteine residues of the small subunit, it also appeared to be ligated by a histidine of the large subunit. This residue was demonstrated to be important for the activity and oxygen-tolerance of Hyd-5. The importance of accessory proteins to Hyd-5 biosynthesis has also been established.

Publications

Parkin, A., Bowman, L., Roessler, M. M., Davies, R. A., Palmer, T., Armstrong, F. A. and Sargent, F. (2012) How *Salmonella* oxidises H_2 under aerobic conditions. FEBS Letters **586**(5): 536-544

Bowman, L., Palmer, T. and Sargent, F. (2013) A regulatory domain controls the transport activity of a twin-arginine signal peptide. FEBS Letters **587**(20): 3365-3370

Bowman, L., Fyfe, P., Flanagan, L., Parkin A., Hunter, W. N. and Sargent, F. (2013) Structure and function of an oxygen-tolerant [NiFe]-hydrogenase from *Salmonella*. In review.

Conferences and presentations

- 10th International Hydrogenase Conference, July 2012 (Szeged, Hungary). Presented a poster entitled 'Investigating the structure, function and assembly of O_2-tolerant hydrogenases from *E. coli* and *Salmonella*'.

- The Society of General Microbiology Autumn Conference, September 2011 (York, UK). Presented a poster entitled 'Assembly of uptake hydrogenases from *Escherichia coli* and *Salmonella enterica* serovar Typhimurium'.

- Joint FEBS-EMBO Advanced Lecture Course. Biomembrane Dynamics: from Molecules to Cells, June 2011 (Cargese, Corsica, France). Poster presented entitled 'Assembly of uptake hydrogenases from *Escherichia coli* and *Salmonella enterica* serovar Typhimurium'.

- 9th International Hydrogenase Conference, June 2010 (Uppsala, Sweden). Presented a poster entitled 'Investigating the assembly of uptake hydrogenases from *Escherichia coli* and *Salmonella*'.

List of common abbreviations

Å	Ångstrom (10^{-10} m; 0.1 nm)
A	Absorbance
Amp	Ampicillin
APH	Amphipathic helix
Apra	Apramycin
ATP	Adenosine triphosphate
bp	base pair
BSA	Bovine serum albumin
BV	Benzyl viologen
Cml	Chloramphenicol
C-terminus	Carboxy terminus
Da	Dalton
DMSO	Dimethyl sulphoxide
DNA	Deoxyribonucleic acid
DNase	Deoxyribonuclease
dNTP	Deoxynucleoside triphosphate
DTT	Dithiotreitol
EDTA	Ethylenediaminetetraacetate
EPR	Electron plasmon resonance
Fe-S	Iron-sulphur
FHL	Formate hydrogen lyase
x *g*	Relative centrifugal force
g	gram
GFP	Green fluorescent protein
HRP	Horse radish peroxidase
Hyd	Hydrogenase
Hyd-1	Hydrogenase-1
Hyd-2	Hydrogenase-2
Hyd-3	Hydrogenase-3
IPTG	Isopropyl β-D-1-thiogalactopyranoside
Kan	Kanamycin
kb	kilobase (1000 bp)
L	Litre
LB	Luria Bertani
µ	micro
M	Molar
m	milli
min	minute
mRNA	messenger ribonucleic acid
NAD	Nicotinamide adenine dinucleotide
NADP	Nicotinamide adenine dinucleotide phosphate
nm	nanometre
NMR	Nuclear magnetic resonance
N-terminus	Amino-terminus
OD	Optical density
PAGE	Polyacrylamide gel

PCR	Polymerase chain reaction
pmf (Δp)	Proton motive force
psi	Pounds per square inch
PFE	Protein film electrochemistry
rpm	Rotations per minute
SDS	Sodium dodecyl sulphate
Sec	Secretory
SEM	Standard error of mean
Tat	Twin arginine translocase
TEMED	N, N, N’, N’-tetramethylethylenediamine
TMAO	Trimethylamine N-oxide
Tris	Tris(hydroxymethyl)aminomethane
UV	Ultraviolet
v/v	volume per volume
w/v	weight per volume

Amino acid abbreviations

Amino-acid	Three-letter abbreviation	One-letter abbreviation
Alanine	Ala	A
Arginine	Arg	R
Asparagine	Asn	N
Aspartate	Asp	D
Cysteine	Cys	C
Glutamate	Glu	E
Glutamine	Gln	Q
Glycine	Gly	G
Histidine	His	H
Isoleucine	Ile	I
Leucine	Leu	L
Lysine	Lys	K
Methionine	Met	M
Phenylalanine	Phe	F
Proline	Pro	P
Serine	Ser	S
Threonine	Thr	T
Tryptophan	Trp	W
Tyrosine	Tyr	Y
Valine	Val	V
Any amino acid	-	X

1 Introduction

1.1 Bioenergy

The search for a clean, efficient and renewable fuel is of paramount importance for a number of reasons. The world's population is expected to reach over 9 billion by 2050. This will result in an increase in the demand for energy, the demand for food and will also impact climate change (Lal, 2010). Therefore, as well as meeting these demands, greenhouse gas emissions must also be curtailed. It has been estimated that food production and energy consumption will double within this time period (Friedrich *et al.*, 2011; Karp and Richter, 2011). Increasing awareness into the effects of burning fossil fuels and the potential future effects this may have on our planet has led to a greater attention being focussed on renewable energy. Other issues prompting bioenergy research include rising oil prices and diminishing oil reserves. In fact, a number of geologists are concerned that oil reserves may dry up before an alternative fuel has been developed (Witze, 2007). Fossil fuels (petroleum, coal and natural gas) are generated from the decomposition of organic matter over millions of years through inefficient processes, and are unsustainable. It has been estimated that the production of 3.8 L of gasoline requires about 90 metric tons of decomposed plant matter (Dukes, 2003). Alternative energy providers are thus being sought.

There are several viable options for generating electricity through the use of renewables such as wind, hydro and solar power but substitutes for liquid transport fuels are still fairly limited (Karp and Richter, 2011). There has been a great deal of interest in fuels generated from plants and organic waste (Naik *et al.*, 2010) but the conflict created between using the land for fuel production or food production is a problem (Karp and Richter, 2011).

1.1.1 First-generation biofuels

Biodiesel, bioethanol and biogas are all termed first-generation biofuels, with the former two fuels representing the most widely used of the renewable liquid transport fuels (Peralta-Yahya *et al.*, 2012). 'First-generation' refers to biofuels produced from the edible portions of crops, which are easily accessible or from organic matter sourced from land that could be used for food production. Biodiesel is composed of a mixture of fatty acid methyl and ethyl esters (FAMEs and FAEEs

respectively) and is generated from the transesterification of oils or lipids from crops including oilseed rape. Biodiesel can also be produced from processed vegetable oils (Karp and Richter, 2011; Lennen and Pfleger, 2013). Unfortunately, if the temperature falls too low, this fuel tends to form waxes (Peralta-Yahya *et al.*, 2012). Bioethanol is a product obtained following the fermentation of cornflour or canesugar but is a lot less efficient when compared with petroleum-based fuels. Ethanol only possesses about 70% of the energy that petrol has and cannot deliver enough power to fly aircraft or run heavy trucks. This fuel is also corrosive and not easily shipped (Savage, 2011). Biogas, on the other hand, is generated through the anaerobic treatment of biomass materials including manure. These 'first-generation' fuels can be blended with current petroleum-based fuels or can be used in specially designed vehicles (Naik *et al.*, 2010) but the requirement for large volumes of fuel poses problems for land use. Algae have been proposed as an alternative source of biomass as salt water instead of arable land can be used for farming but collecting and dewatering the cells have proved difficult (Peralta-Yahya *et al.*, 2012).

1.1.2 Second-generation/advanced biofuels

In order to relieve the strain created by the fuel/food conflict, 'second-generation' biofuels are being investigated. The conversion of lignocellulosic material derived from inedible and unused plant parts constitutes a viable option. Unfortunately, there are many obstacles to converting the plant cell wall sugars cellulose and hemicellulose into fuel, including high costs that exceed that of petroleum-based fuels and first-generation biofuels. The strength of cellulose's glycosidic bonds is not conducive to easy biofuel production. Harsh physiochemical treatments and multiple enzymes are required to break the strong bonds in order to release mononsaccharides that can be fermented (Jordan *et al.*, 2012). Lignin however constitutes 10-25% of lignocellulose and does not contain any sugars. Therefore lignin represents a residue of ethanol production and requires further attention if it is to be converted into a valuable product (Kumar *et al.*, 2008). Efforts have been made to improve microbial cellulase production, which could have a significant impact on biofuel production. However, this requires a better understanding of genetic and biochemical controls governing cellulase secretion (Kumar *et al.*, 2008).

Microorganisms have been exploited in a number of industrial processes for many centuries including that of alcohol production. Therefore, it is perhaps unsurprising that microorganisms, including *Saccharomyces cerevisiae* and *Escherichia coli*, are now the subjects of interest regarding microbial biofuel production. Engineering existing microbial metabolic pathways to produce fuel-like alcohols and hydrocarbons is very promising. For example, efforts have been made to refine the butanol pathway in *Clostridium* strains and interfere with the negative feedback loop that naturally prevents high levels of alcohol production (Rude and Schirmer, 2009).

Fatty acids have been regarded as natures 'petroleum' and are used by cells for energy storage. *E. coli* are naturally capable of metabolising fatty acids and through the use of synthetic biology applications; this synthesis has been directed towards fuel production (Steen *et al.*, 2010). In one study, heterologous expression of the fatty acid *O*-methyltransferase from *Mycobacterium marinum* in *E. coli* resulted in the ability of the strain to produce FAMEs (Nawabi *et al.*, 2011). Another study carried out by Steen *et al*. (2010) successfully engineered *E. coli* cells to produce fatty esters of various lengths (depending on which thioesterases were being expressed), fatty alcohols and waxes from sugars. In addition to this, the fatty ester producing cells were also engineered to express hemicellulases, allowing the bacteria to grow on hemicellulose without the addition of further enzymes. This represents a major leap forward for the production of fuel from plant biomass (Steen *et al.*, 2010). Challenges to the commercial production of FAME's and FAEE's include the need to increase yields and modify the fatty acids to possess sought after fuel properties (Lennen and Pfleger, 2013).

1.1.3 Biohydrogen as a 'future fuel'

It is generally believed that around 3.6 billion years ago, the atmosphere of early Earth was rich in hydrogen (Tian *et al.*, 2005) and provided ancient prokaryotes with an abundant source of reductant. Hydrogen is an extremely efficient fuel and still represents an energy source for many bacteria. The reaction between hydrogen and oxygen is extremely favourable and releases a large amount of energy (Vincent *et al.*, 2007) as shown in Equation 1.1.

$$2H_2\,(g) + O_2\,(g) \longrightarrow 2H_2O\,(l) \qquad \Delta H° = -286\ kJ/mol$$

Equation 1.1. The reaction of hydrogen and oxygen releases a large amount of energy.

The reaction between hydrogen and oxygen has a high specific enthalpy (Equation 1.1). The low weight to energy ratio lends itself well to being used as the fuel of choice in rocket propulsion. Although hydrogen is the most abundant element in the Universe, it is not readily accessible to us and requires intense procedures to release it (Vincent *et al.*, 2007). Among the current methods of hydrogen production is steam reforming of natural gas (Barreto *et al.*, 2003). This particular procedure requires extremely high temperatures (up to 1000 °C) and pressures (Sehested *et al.*, 2004). Water electrolysis is another approach that has been taken to generate hydrogen in a renewable manner but this technique is expensive (Barreto *et al.*, 2003).

Biohydrogen is the term used to represent biologically produced hydrogen but at the moment, is one of the less developed fuel technologies (Friedrich *et al.*, 2011). Photosynthetic microbes, including algae and cyanobacteria, are capable of converting light energy into hydrogen using enzymes called hydrogenases and nitrogenases. This is termed photobiological hydrogen production and can be performed by either oxygenic or anoxygenic microorganisms. Advantages of oxygenic photo-hydrogen production include the consumption of the greenhouse gas carbon dioxide by the Calvin cycle, the fact that readily available water constitutes the electron source and that no pollutants are formed from the reaction. The main obstacle to exploiting this system is the inhibition of hydrogen-producing enzymes by oxygen. Anoxygenic photo-hydrogen production is performed by microorganisms including purple nonsulphur bacteria. These bacteria can acquire electrons from the fermentation products present in sewage and agricultural waste, and as no oxygen is produced by these microorganisms, hydrogenase inhibition does not occur. Unfortunately, hydrogen yields are low using this process (McKinlay and Harwood, 2010).

Dark fermentation is another method of biological hydrogen production employed by a diverse range of microorganisms including *Clostridia* and *E. coli*. This involves the anaerobic breakdown of substrates rich in carbohydrates to hydrogen and a variety of other products including lactic acid, acetic acid and ethanol (Figure 1.1). The products and amounts formed are dependent on a number of factors including the

redox state of the substrate and culture pH. The conversion of formate to carbon dioxide and hydrogen is induced at acidic pH in order to relieve the cell of acid stress. The advantage of employing dark fermentation as a route to hydrogen production is that a variety of substrates can be used in this process and oxygen inhibition is not an issue of concern. Also, fermenter reactor technology exists today with no solar input required. There are however, a number of by-products that require removal and due to incomplete substrate conversion, yields are typically low (Hallenbeck and Ghosh, 2009). Advances in metabolic engineering and an increased understanding of the molecular mechanism behind hydrogen production have however resulted in dark fermentation becoming an attractive option.

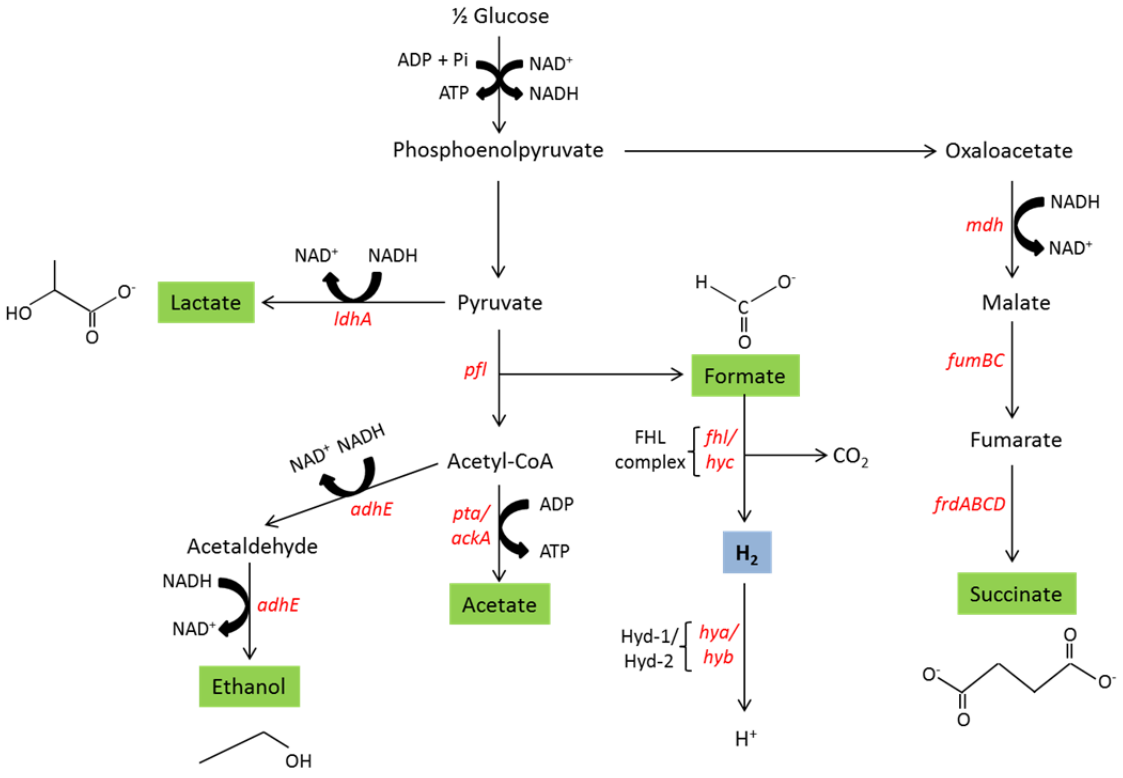

Figure 1.1. *E. coli* produces hydrogen during mixed acid fermentation.

Under anaerobic conditions, *E. coli* can break down glucose into a variety of products including lactate, acetate, ethanol, formate, succinate and hydrogen. Product proportions are balanced as to maximise ATP formation. The formate hydrogenlyase (FHL) complex serves to disproportionate formate into carbon dioxide and hydrogen. The genes encoding enzymes responsible for catalysing various reaction steps are highlighted in red: *ldhA*, lactate dehydrogenase A; *pfl*, pyruvate formatelyase; *adhE*, alcohol dehydrogenase; *pta*/*ackA*, phosphate acetyl transferase/acetate kinase; *fhl*, formate hydrogen lyase; *hyc* (representing the Hydrogenase-3 component of FHL); *hya* (representing Hydrogenase-1 oxidising activity), hyb (representing Hydrogenase -2 oxidising activity); *mdh*, malate dehydrogenase; *fumBC*, fumarate hydratase; *frdABCD*, fumarate reductase (Hallenbeck and Ghosh, 2009).

1.1.4 Fuel cell technology

Fuel cells are similar to batteries in the respect that they convert chemical energy into electrical energy. The electricity generated is continuous as long as the required chemicals are received by each electrode (Cracknell *et al.*, 2008). In the case of a hydrogen fuel cell, hydrogen represents the fuel (or reductant) and reacts at the anode, whereas oxygen is reduced at the cathode (Figure 1.2). Fuel cell electrodes are coated with electrocatalysts that catalyse the relevant reactions. The expensive metal platinum is typically used but requires a humidified gaseous environment and high temperatures reaching 100°C (Vincent *et al.*, 2007). The metal-containing enzymes responsible for microbial hydrogen metabolism (hydrogenases) make very good anode electrocatalysts, whereas fungal laccases and oxidases make good cathode electrocatalysts.

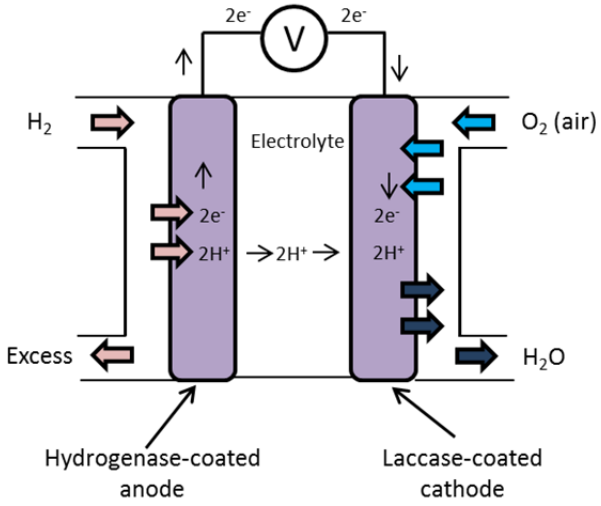

Figure 1.2. A diagrammatic representation of a biological fuel cell.

Hydrogen (the reductant/fuel) reacts at the anode of the fuel cell, which is coated with a hydrogen-oxidising hydrogenase enzyme. Hydrogen is oxidised to protons, which are conducted through the electrolyte solution, and electrons that are transferred to the cathode. Oxygen reacts at the cathode, which is coated with an enzyme capable of oxygen reduction such as a fungal laccase. Water and electricity are the only products of this reaction (Vincent *et al.*, 2007).

The use of enzymes in fuel cells allow for very specific reactions, high activity and no real need to separate the fuel and the oxidant (Cracknell *et al.*, 2008). An obstacle to using hydrogenases in biological fuel cells arises from their inactivation by oxygen. Therefore, recent research has aimed at identifying oxygen tolerant hydrogenases capable of hydrogen oxidation and understanding the molecular basis

behind this natural tolerance. The generation of electricity from biological fuel cells has in fact been demonstrated by Vincent *et al.* (2006). Hydrogenase obtained from *Ralstonia metallidurans* CH34 was used to coat the anode and the multi-copper oxidase (laccase) from the fungus *Trametes versicolor* used to coat the cathode. Only 3% hydrogen was required to generate enough electricity to power a wrist-watch for 24 hours (Vincent *et al.*, 2006). This demonstrates the potential biological fuel cells have for future electricity production.

1.2 Hydrogenase enzymes and their classification

The term 'hydrogenase' was first used to describe the enzyme responsible for activating hydrogen in bacterial species by Stephenson and Stickland in 1931. In this particular study, hydrogenase activity was assessed in *E. coli* by measuring the reversible reduction of the dye methylene blue as well as the reduction of nitrate, fumarate and molecular oxygen (Stephenson and Stickland, 1931). Subsequently, in 1933, microorganisms were isolated from anaerobic river sediments that were capable of producing methane following growth on carbon dioxide and hydrogen. The study concluded that this reaction was the result of hydrogenase activity (Stephenson and Stickland, 1933).

A wide variety of microorganisms possess the ability to metabolise hydrogen. Among these are a large number of bacterial species, including members of the Proteobacteria (e.g. *Hydrogenovibrio marinus* and *Azotobacter vinelandii*) and the Firmicutes. For example *Clostridium beijerinckii* and *Desulfovibrio desulfuricans* possess hydrogen metabolising enzymes (Vignais and Billoud, 2007). Pathogenic bacteria including *Helicobacter pylori*, *Shigella flexneri* and *Salmonella enterica* serovar Typhimurium also produce hydrogenase enzymes that may be crucial for pathogenesis (Maier, 2005). The domain of archaea also contains hydrogen metabolising microorganisms including *Methanocaldococcus jannaschii* and *Pyrococcus furiosus*. Furthermore, some lower eukaryotic organisms possess hydrogenases including species of green algae (e.g. *Chlamydomonas reinhardtii*) and fungi (e.g. *Entamoeba histolytica*) as well as a number of parasitic protozoa (Vignais and Billoud, 2007).

Certain environments or ecosystems provide an abundant source of hydrogen of which microorganisms can exploit in order to satisfy their energy needs. For example, the geothermal hot springs of Yellowstone National Park contain concentrations of hydrogen (>300 nm in some cases) that far exceed what is required for microbial energy metabolism. As determined by rRNA gene analysis, microbial communities here consist of several hundred species of bacteria, where *Aquificales* species were noted as the most abundant. The dominance of hydrogen metabolising organisms in this ecosystem suggests that hydrogen is the main energy source (Spear *et al.*, 2005). Hydrogen is also produced in abundance by microorganisms residing

within the human body. In tissues of the liver and the spleen, hydrogen concentrations have been measured at over 40 µM, which serves as an exploitable energy source for colonising *Salmonella* (Maier, 2005). Anoxic soils and sediments host a number of fermentative bacteria and methanogenic archaea that release hydrogen that can be exploited by various other microorganisms including sulphate reducers such as *Desulfovibrio* (Vignais and Billoud, 2007).

Hydrogenase enzymes typically catalyse the reversible cleavage of molecular hydrogen into protons and electrons (Equation 1.2). This reversible reaction depends on whether the enzyme is in the presence of an electron acceptor (of high potential) or electron donor (of low potential). If the enzyme interacts with hydrogen and an electron acceptor, the hydrogenase functions in hydrogen uptake. Alternatively, hydrogen is produced following the interaction between an enzyme and an electron donor and when it is necessary for the cell to dispose of excess reducing power (Vignais and Colbeau, 2004).

$$2H^+ + 2e^- \longleftrightarrow H_2\,(g)$$

Equation 1.2. Hydrogenase enzymes catalyse the reversible cleavage of hydrogen into protons and electrons.

Hydrogenases possess metal containing active sites required for hydrogen activation. Three classes of hydrogenase exist and are named depending on which metal cofactor is present. The classes are designated [NiFe]-, [FeFe]- and [Fe]-hydrogenases. These groups are thought to be products of convergent evolution as they do not do not share any sequence similarity. [NiFe]-hydrogenases are the most abundant and best studied class of hydrogenase and are involved in hydrogen uptake (oxidation). [FeFe]-hydrogenases, on the other hand, are biased towards hydrogen production. [Fe]-hydrogenases differ from the other two classes in having only one metal present in the active site (Vignais and Billoud, 2007). As this current study is focussed on understanding the structure, function and assembly of [NiFe]-hydrogenases, a limited discussion will be offered in the case of the other two classes.

1.2.1 [Fe]-hydrogenases

[Fe]-hydrogenases, formerly known as Hmd (hydrogen forming methylenetetrahydromethanopterin [methylene-H_4MPT] dehydrogenase) have only been found in methanogenic archaea and represent the least investigated of the hydrogenase enzymes (Vignais and Billoud, 2007). These enzymes are only synthesised under nickel limiting conditions and when the cells are incapable of producing the F_{420}-reducing [NiFe]-hydrogenase (Thauer *et al.*, 2010). This class of hydrogenase contains only one metal in its active site, an iron atom, and does not contain any Fe-S clusters (Zirngibl *et al.*, 1990; Zirngibl *et al.*, 1992).

$$H_2\,(g) \longrightarrow H^+ + H^-$$

Equation 1.3. [Fe]-only hydrogenases catalyse the cleavage of molecular hydrogen into a proton and a hydride.

[Fe]-hydrogenases catalyse the reaction shown in Equation 1.3 and thus differ from the [NiFe]- and [FeFe]-hydrogenases and the reactions they catalyse (Parkin and Sargent, 2012). The hydride generated from the hydrogen cleavage is then transferred to methenyltetrahydromethanopterin (methenyl-H_4MPT$^+$) resulting in its reduction to methylene-H_4MPT. This is an intermediate step in the formation of methane from carbon dioxide and hydrogen during methanogenesis (Thauer *et al.*, 2010).

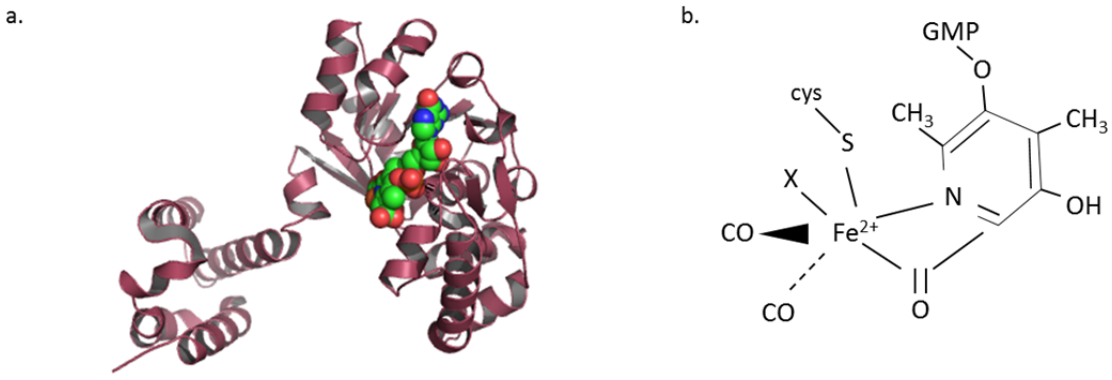

Figure 1.3. The crystal structure of an [Fe]-hydrogenase monomer and its active site.

(a) The [Fe]-hydrogenase (PDB 2B0J) exists a dimer where the two C-terminal domains are intertwined (Pilak *et al.*, 2006). The monomer is represented here. **(b)** The active site consists of one iron atom bound to a novel FeGP cofactor (Thauer *et al.*, 2010).

The crystal structure of [Fe]-hydrogenases from *Methanocaldococcus jannaschii* and *Methanopyrus kandleri* were solved in 2006 (Figure 1.3a). This study revealed that the hydrogenase exists as a homodimer composed of two globular units and one central domain. The central domain is formed as a result of the intertwining of the two C-terminal regions from the two subunits (Pilak *et al.*, 2006). The hydrogenase monomer is depicted in Figure 1.3a. Further structural analyses have led to greater insights into the active site where biologically unusual carbon monoxide molecules have been found to coordinate the iron centre (Figure 1.3b). A novel cofactor, iron-guanylylpyridinol (FeGP), is found covalently bound to the Fe atom (Shima *et al.*, 2008; Thauer *et al.*, 2010).

1.2.2 [FeFe]-hydrogenases

[FeFe]-hydrogenases have been identified from a number of anaerobic prokaryotes and are also produced by some anaerobic eukaryotes. In fact, [FeFe]-hydrogenases represent the only class of hydrogenase found in eukaryotes where they reside in either chloroplasts or in hydrogenosomes. Enzymes of this class are generally monomeric (Figure 1.4a) although the size of hydrogenases do vary considerably between microorganisms (Vignais and Billoud, 2007). These enzymes possess a novel active site containing two iron atoms, one of which is connected to a Fe-S cluster via a bridging cysteine thiolate and is termed the H-cluster (Figure 1.4a). The architecture of the active site was determined following analyses of [FeFe]-hydrogenase crystal structures obtained from *Desulfovibrio desulfuricans* and *Clostridium pasteurianum* (Peters *et al.*, 1998; Nicolet *et al.*, 1999). Similarly to the [Fe]-hydrogenase, the active sites of [FeFe]-hydrogenases are also ligated by unusual non-protein ligands. In this case, not only are carbon monoxide molecules present but also two molecules of cyanide. The two iron atoms share two bridging sulphur ligands but the exact nature of the bridging dithiolate has been a point of conjecture. It has been suggested that the bridgehead group may be a molecule of O, CH_2 or NH/NH^{2+} (Mulder *et al.*, 2011). A very recent study however has provided strong evidence to suggest that nitrogen is the bridgehead atom (Berggren *et al.*, 2013). The presence of Fe-S clusters allows the transfer of electrons to/from the active site. The number of these clusters varies extensively between microorganisms. Some [FeFe]-hydrogenases only possess the H-cluster and do not contain a single Fe-S cluster (Mulder *et al.*, 2011). A collection of

accessory genes have been discovered as necessary for the biosynthesis of [FeFe]-hydrogenase enzymes. The proteins HydE, HydF and HydG, known members of the radical S-adenosylmethionine enzyme family, are required for the assembly of an active [FeFe]-hydrogenase (Meyer, 2007).

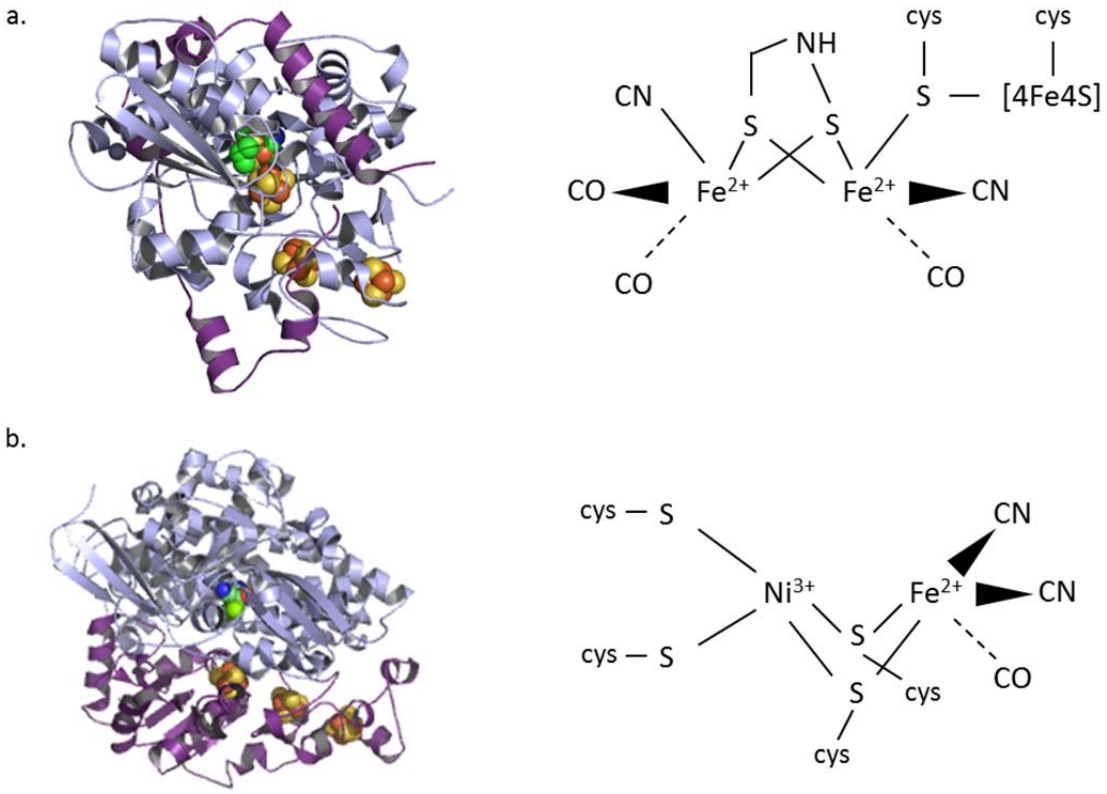

Figure 1.4. The crystal structures and active sites of [NiFe]- and [FeFe]-hydrogenases.

(a) The [FeFe]-hydrogenase of *Desulfovibrio desulfuricans* (PDB 1HFE) is a monomeric enzyme (Nicolet *et al.*, 1999). The active site, or H-cluster, consists of two Fe atoms, one of which is bound to a Fe-S cluster via a cysteine sulphur. Evidence now suggests that the bridging atom is nitrogen (Berggren *et al.*, 2013). **(b)** The [NiFe]-hydrogenase of *Desulfovibrio gigas* (PDB 1YRQ) reveals an enzyme composed of two subunits. The large subunit is coloured silver and accommodates the [NiFe]-active site. The small subunit is coloured purple and houses three Fe-S clusters. The [NiFe]-active site consists of a nickel and iron bridged by two cysteine thiolates. The nickel is bound by two additional cysteine thiolates whereas the iron atom is further bound by two cyanide molecules and one carbon monoxide molecule (Volbeda *et al.*, 2005).

Recently, efforts have been made to connect the Fe-S cluster relay of an [FeFe]-hydrogenase from *Clostridium acetobutylicum* to the Fe-S cluster of Photosystem I. Following light induction, electrons were directed to the active site and hydrogen produced (Lubner *et al.*, 2010). [FeFe]-hydrogenases are typically chosen for molecular engineering experiments as they are naturally biased towards hydrogen evolution (Mulder *et al.*, 2011).

1.2.3 [NiFe]-hydrogenases

[NiFe]-hydrogenases have been isolated from a wide range of bacteria and archaea and constitute the most numerous class of hydrogenase. The core enzyme is composed of two subunits, the large and the small subunit, which interact extensively at their interface (Figure 1.4b). The large subunit (or α-subunit) has a molecular weight of around 60 kDa and accommodates the [NiFe]-active site, which is found buried deep within the subunit. The small subunit (or β-subunit), of around 35 kDa, houses three Fe-S clusters that relay electrons to and from the active site depending on whether an electron donor or an electron acceptor is present. These Fe-S clusters are termed the 'proximal', 'medial' or 'distal' cluster depending on their distance relative to the active site. Therefore, the 'distal' cluster represents the cluster furthest from the active site (Vignais and Billoud, 2007).

Crystal structures have been determined of [NiFe]-hydrogenases, including those from *Desulfovibrio gigas* (Volbeda et al., 1995), *D. vulgaris* Miyazaki F (Higuchi *et al.*, 1997), *D. fructosovorans* (Montet *et al.*, 1997; Volbeda *et al.*, 2005), *D. desulfuricans* (Matias *et al.*, 2001) and *Allochromatium vinosum* (Ogata et al., 2010). This has provided a wealth of information regarding the coordination of each of the cofactors. The active site contains both a nickel and an iron atom that are connected *via* two cysteine thiolates. The nickel atom is further coordinated by two additional cysteine thiolates whereas the iron atom is also ligated by three non-protein and unusual ligands: two cyanide molecules and one carbon monoxide molecule. The presence of each of these molecules is thought to stabilise the iron in a low oxidation and spin state (Reissmann *et al.*, 2003). The insertion of these ligands has been of great interest due to their toxicity and rarity in biology. The use of ^{14}C labelling experiments have determined that the cyanide and carbon monoxide molecules are synthesised differently and their origins are distinct (Roseboom *et al.*, 2005). Experiments have previously suggested that the carboxyl group of acetate is incorporated into the carbon monoxide molecule (Roseboom *et al.*, 2005), while others have proposed the source to be exogenous and possibly supplied by atmospheric carbon monoxide (Forzi *et al.*, 2007; Lenz *et al.*, 2007). A more recent study using infrared spectroscopy has revealed that the carbonyl ligand may have a metabolic origin (Burstel *et al.*, 2011). The biosynthesis of carbon monoxide therefore

differs between [NiFe]- and [FeFe]-hydrogenases as tyrosine has been revealed as the substrate in the case of the latter (Shepard *et al.*, 2010). Although there is still debate concerning the source of carbon monoxide, the origin of the cyanide ligand has been better established. Paschos and co-workers (2001) found that carbamoyl phosphate was essential for maturation of the [NiFe]-active site as hydrogenase activity and large subunit processing were abolished in *E. coli* mutants incapable of synthesising carbamoyl phosphate. The maturation proteins, HypF and HypE were discovered necessary for cyanide synthesis from carbamoyl phosphate (Reissmann *et al.*, 2003).

One of the main obstacles to using [NiFe]-hydrogenases in biotechnological applications is the fact that most enzymes in this class are inactivated by oxygen (De Lacey *et al.*, 2007). There are, however, a number of unique enzymes within this class that demonstrate a tolerance or insensitivity to oxygen (Vignais and Billoud, 2007; Fritsch *et al.*, 2013).

1.2.3.1 Group 1: Uptake [NiFe]-hydrogenases

At this time, the current classification system places [NiFe]-hydrogenases into five distinct groups. The first of these, Group 1 enzymes, are found bound to the membrane and typically link hydrogen oxidation on the periplasmic side of the membrane (in Gram-negative bacteria) with cytoplasmic membrane quinone reduction in an energy-conserving manner (Dubini *et al.*, 2002). Thus, energy is recovered in the form of a proton motive force. This usually occurs under anaerobic conditions when alternative electron acceptors are present including nitrate, fumarate and sulphate, but can also be linked to oxygen reduction in some biological systems (Vignais and Colbeau, 2004). Most enzymes are anchored to the membrane *via* a C-terminal transmembrane tail on their β-subunit and are connected to the quinone pool *via* their interaction with a di-haem cytochrome *b* subunit. Other members of the group interact with low-potential c-type cytochromes (e.g. *Desulfovibrio* species) and some enzymes form larger complexes as is the case for *E. coli* Hyd-2, which is tetrameric (Vignais and Billoud, 2007). The inclusion of Hyd-2 in this group highlights the limitation of the present classification system. *E. coli* Hyd-2 does not generate a proton motive force but couples the oxidation of hydrogen to the reduction of fumarate (Dubini *et al.*, 2002). Group 1 is therefore a heterogeneous collection of enzymes, some of which have very distinct characteristics. A more recent phylogenetic

study has further divided Group 1 into subgroups of which Hyd-2 is accommodated by the HybA-hydrogenase subgroup (Pandelia *et al.*, 2012).

There is yet another interesting addition to Group 1, the selenium containing [NiFeSe]-hydrogenases (Vignais and Billoud, 2007). Here, the cysteine that is ligated to the nickel of the active site is substituted by a selenocysteine but this appears to be the only main difference. Interestingly, studies into the [NiFeSe]-hydrogenase from *Desulfomicrobium baculatum* have indicated that this enzyme is capable of producing hydrogen, even in the presence of high concentrations of gas that would normally be expected to inhibit hydrogenase activity (Parkin *et al.*, 2008). The enzyme also retained the ability to produce hydrogen under conditions of 1% oxygen (Parkin *et al.*, 2008).

A further characteristic of this group is the existence of a long N-terminal signal peptide on the small subunit of these enzymes. These peptides contain a conserved twin-arginine amino acid motif that is recognised by the twin-arginine translocation (Tat) pathway and facilitates transport of fully folded, cofactor-containing hydrogenases across the cytoplasmic membrane (Vignais and Billoud, 2007; Palmer and Berks, 2012).

1.2.3.2 Group 2: Hydrogen sensors and cyanobacterial [NiFe]-hydrogenases

Enzymes within this group do not possess signal peptides and instead of being exported, remain within the cytoplasm. Hydrogen sensors function as regulatory hydrogenases and control the biosynthesis of hydrogen oxidising enzymes when hydrogen is present. Remarkably, these enzymes are insensitive to oxygen. This property was thought to be due to the narrow, and therefore restrictive, gas channel that leads to the [NiFe]-active site (Vignais and Billoud, 2007). Mutations were engineered to widen the gas channel of the regulatory hydrogenase from *Rhodobacter capsulatus*. Substituting the two bulky residues Ile65 and Phe113 in the channel lining resulted in an acquired sensitivity to oxygen, thus confirming the theory (Duche *et al.*, 2005).

It is known that the occurrence of hydrogenases and nitrogenases in cyanobacteria are linked. Here, hydrogenases function to recycle the hydrogen that is produced during nitrogen fixation. This is apparently so efficient in fact, that very little

hydrogen production can be measured as a result of this uptake activity (Bothe *et al.*, 2010).

1.2.3.3 Group 3: Bidirectional heteromultimeric cytoplasmic [NiFe]-hydrogenases

The dimeric enzymes of Group 3 are found in association with subunits containing soluble cofactors such as NAD^+ or $NADP^+$. These hydrogenases act reversibly and, under anaerobic conditions, can re-oxidise their cofactors by utilising protons sourced from water as terminal electron acceptors (Vignais and Billoud, 2007). Although many species of archaea produce this subclass of hydrogenase including *Methanothermobacter marburgensis*, they are also synthesised by bacteria and cyanobacteria (Vignais and Colbeau, 2004). Bacterial NAD(H)-linked [NiFe]-hydrogenases are composed of two subunits termed HoxH and HoxY (the large and small subunit respectively). The dimer is associated with a diaphorase module composed of at least two subunits (HoxF and HoxU) that couple reversible hydrogen cleavage with NAD(H) oxidoreduction (Horch *et al.*, 2012). A further subunit, HoxE, is associated with cyanobacterial NAD(H)-linked bidirectional hydrogenases and is thought to interact with the membrane (Schmitz *et al.*, 2002).

1.2.3.4 Group 4: Membrane-associated, energy-conserving and hydrogen-producing hydrogenases

Enzymes of this group are composed of multiple subunits (six or more) and function to rid the cell of excess reducing equivalents. This occurs under anaerobic conditions and in the presence of a suitable carbon source such as formate or carbon monoxide. For example, Hydrogenase-3 of *E. coli* exists as part of the formate hydrogenlyase complex where formate is metabolised to produce hydrogen and carbon dioxide (Sawers *et al.*, 2004). The photosynthetic bacterium, *Rhodospirillum rubrum*, produces a hydrogenase that interacts with CO-dehydrogenase and acts to oxidise carbon monoxide to carbon dioxide. Alongside this, hydrogen is also produced. Archaea are known to be the main producers of Group 4 hydrogenases and it has been demonstrated that these enzymes couple hydrogen production with energy conservation (Vignais and Billoud, 2007). Methanogens derive almost all of their energy through methanogenesis. The Group 4 [NiFe]-hydrogenase from *Pyrococcus*

furiosus couples the reduction of ferredoxin (and electron transfer) to proton reduction and the translocation of protons (Vignais, 2008).

1.2.3.5 Group 5: 'Actinobacterial', high-affinity hydrogen-oxidising hydrogenases

Recently, a fifth group of hydrogenase has been added to the classification system. These [NiFe]-hydrogenases are found in a wide range of Actinobacteria and can oxidise hydrogen at atmospheric levels of hydrogen. A number of soil-dwelling *Streptomyces* species produce Group 5 enzymes that have been shown to exhibit a high affinity for hydrogen (Constant *et al.*, 2010). These hydrogenases consist of a large and a small subunit. The final electron acceptor is, however, unknown at this time. The genes corresponding to the synthesis of a group 5 hydrogenase of *Mycobacterium smegmatis* were found to be up-regulated under carbon limitation and oxygen limiting conditions (Berney and Cook, 2010). Homologues of the uptake genes found among the Actinobacteria have also been discovered in the genomes of some Proteobacteria. A [NiFe]-hydrogenase was discovered in the genome of *Ralstonia eutropha* with similarity to the enzymes of group 5 but does not exhibit the same high affinity to hydrogen. Fascinatingly, this particular enzyme retains hydrogen uptake activity even when oxygen is present in the reaction mixture at a concentration of 70%. Therefore, this enzyme has been described as being insensitive to oxygen (Schafer *et al.*, 2013).

1.2.4 Hydrogenases and oxygen

The presence of oxygen and carbon monoxide is a problem for many hydrogen metabolising microorganisms as these gaseous molecules compete with hydrogen for the hydrogen binding site within the metallocentre of the enzyme. The reaction with oxygen can then lead to the formation of a variety of products including sulfoxides and peroxides that inactivate the enzyme. Furthermore, Fe-S clusters are unstable when oxygen is in close vicinity. When oxygen attacks the active site of [FeFe]-hydrogenases, these enzymes become irreversibly inactivated. In contrast, oxygen-inactivated [NiFe]-hydrogenases can be reactivated under reducing conditions (Vincent *et al.*, 2007). Electron paramagnetic resonance (EPR) and fourier transform infrared spectroscopy (FTIR) experiments have been used to assess the redox states of hydrogenase active sites. The active site of [FeFe]-hydrogenases gives rise to two main redox states that

have been termed H_{ox} and H_{red} (De Lacey *et al.*, 2007). The active site of [NiFe]-hydrogenases however, acquire a number of different redox states. Two EPR signals called Ni-A and Ni-B have been detected when the active site is oxidised and constitute inactive states. However, under reducing conditions (i.e. in the presence of hydrogen) the Ni-B state can react *via* a number of transient EPR-silent states termed Ni-SI very quickly (within minutes). The Ni-A state forms an EPR-silent state called Ni-SU upon reduction but full reactivation occurs over a much longer timeframe (after several hours). Therefore the Ni-A and Ni-B states are often referred to as 'unready' and 'ready' respectively (Volbeda *et al.*, 2005; Vincent *et al.*, 2007). Structural investigations have provided insights into the bridging ligands present in the active sites of both states. Either a mono (Ogata *et al.*, 2010) or di-oxygen (Volbeda *et al.*, 2005) species is believed to be the bridging ligand of the Ni-A state, whereas a hydroxide ligand is thought to bridge the metals of the active site in the Ni-B inactive state (Volbeda *et al.*, 2005). A recent study however questions the current idea that an oxygen species is present as a ligand in the active site at all and proposes that oxygen acts as an electron acceptor instead (Abou Hamdan *et al.*, 2013). Abou Hamdan *et al*. (2013) showed that both Ni-A and Ni-B inactive states could be formed even in the absence of oxygen.

1.2.4.1 Oxygen tolerance

The inactivation of hydrogenases by oxygen presents a number of obstacles to using these enzymes in future biotechnological applications. Understanding the mechanisms behind oxygen inactivation and subsequent reactivation is crucial for the development of future technologies including biological fuel cells. Of similar importance, is dissecting the mechanism of oxygen-tolerance, a property unique to a number of [NiFe]-hydrogenases. A number of aerobic bacteria including *R. eutropha*, a knallgas bacterium, possess this subclass of [NiFe]-hydrogenase. In fact due to its aerobic lifestyle, *R. eutropha* produces three different oxygen-tolerant hydrogenases (Burgdorf *et al.*, 2005). Initial studies focussed on investigating the gas channel that connects the active site with the solvent. Hydrogen sensing hydrogenases are oxygen resistant and this is thought to be due to the presence of two bulky residues that gate the channel and act as a 'bottleneck'. Following the discovery that substituting the bulky residues for smaller amino acids resulted in oxygen sensitivity (Buhrke *et al.*,

2005; Duche *et al.*, 2005), channel residues of the oxygen-sensitive *D. fructosovorans* hydrogenase were replaced by bulkier amino acids and were found to confer oxygen-tolerance (Liebgott *et al.*, 2010). Catalytic activity however was not sustained in this mutant, suggesting that other molecular mechanisms are involved in conferring oxygen-tolerance.

Spectroscopic and electrochemical investigations into the oxygen-tolerance of hydrogenases have been performed on bacteria including *R. eutropha* (Ludwig *et al.*, 2009a; Fritsch *et al.*, 2011b), *Aquifex aeolicus* (Pandelia *et al.*, 2010) and *E. coli* (Lukey *et al.*, 2010) and have revealed characteristics specific to this subclass. For example, these enzymes only form the Ni-B ready state and are tolerant of carbon monoxide (Parkin and Sargent, 2012). This research has led to the finding that differences in the Fe-S relay of standard and oxygen-tolerant enzymes may be important for conferring the property of oxygen-tolerance. Moreover, sequence analyses have identified supernumerary cysteines at the proximal Fe-S cluster of oxygen-tolerant hydrogenases that when mutated confer oxygen-sensitivity (Goris *et al.*, 2011; Lukey *et al.*, 2011). It is clear that a modified environment surrounding this cluster is crucial to oxygen tolerance. Due to the implications for biotechnological advancement, oxygen-tolerant enzymes are currently the subject of intense research.

1.3 The hydrogenases of *E. coli* and *Salmonella*

E. coli and *Salmonella* are both Gram-negative bacteria and members of the Enterobacteriaceae. As close relatives, these microorganisms share a number of similar features but *Salmonella*, in general, express a wider array of respiratory enzymes. A search of the *E. coli* genome revealed the potential of this microorganism to produce four [NiFe]-hydrogenase enzyme (Forzi and Sawers, 2007). Hyd-1, Hyd-2 and Hyd-3 contribute to the hydrogenase activity of the cell and are expressed under different physiological conditions (Ballantine and Boxer, 1985; Sawers *et al.*, 1985). Hyd-1 and Hyd-2 perform hydrogen oxidation whereas Hyd-3 performs proton reduction as part of the FHL complex. Similarly to *E. coli*, *Salmonella* only produces hydrogenases with a [NiFe]-active site and expresses homologs of *E. coli* Hyd-1, Hyd-2 and Hyd-3. In addition to these, *Salmonella* is capable of producing a third hydrogen-oxidising hydrogenase called Hyd-5.

1.3.1 The Uptake Hydrogenases

1.3.1.1 Hyd-1 and Hyd-2 of *E. coli*

Hyd-1 and Hyd-2 are both classed as Group 1 [NiFe]-hydrogenases, although as mentioned earlier, have very distinct characteristics. However, both enzymes are synthesised as precursor proteins carrying a Tat signal peptide that ensures translocation through the Tat pathway. Hyd-1 is encoded by an operon of six genes, *hyaABCDEF* (Figure 1.5). The gene products of *hyaA* and *hyaB* represent the small and large subunits, respectively, and form the core hydrogenase enzyme (Menon *et al.*, 1991). Hyd-1 is anchored to the inner membrane via the C-terminal transmembrane tail of HyaA (Hatzixanthis *et al.*, 2003) as depicted in Figure 1.6. HyaD, HyaE and HyaF are important for the maturation of Hyd-1 with HyaD functioning as a Hyd-1 specific protease, responsible for cleaving the C-terminus of HyaB, and HyaE and HyaF functioning as potential chaperones (Menon *et al.*, 1991; Dubini and Sargent, 2003).

Initial characterisation revealed that expression of Hyd-1 was induced under fermentative conditions and enhanced by added formate (Sawers *et al.*, 1985). In addition, Hyd-1 production appears to be maximal in the stationary phase and

preferred at low pH (Brondsted and Atlung, 1994; Trchounian *et al.*, 2012). Expression of *hya* also appears to be dependent on the anaerobic regulator AppY and the global ArcB/ArcA two-component regulatory system (Richard *et al.*, 1999). ArcB phosphorylates ArcA under anaerobic conditions and acts to repress genes involved in aerobic metabolism whilst activating anaerobic gene clusters. Hyd-2 expression is also regulated by the same system (Vignais and Billoud, 2007). Expression of Hyd-1 is repressed when nitrate is present in the growth medium through the action of the NarL/NarX and NarP/NarQ regulatory systems (Richard *et al.*, 1999). Under aerobic conditions, the transcription factor IscR represses expression of the Hyd-1 operon, which is also true for Hyd-2 (Giel *et al.*, 2006).

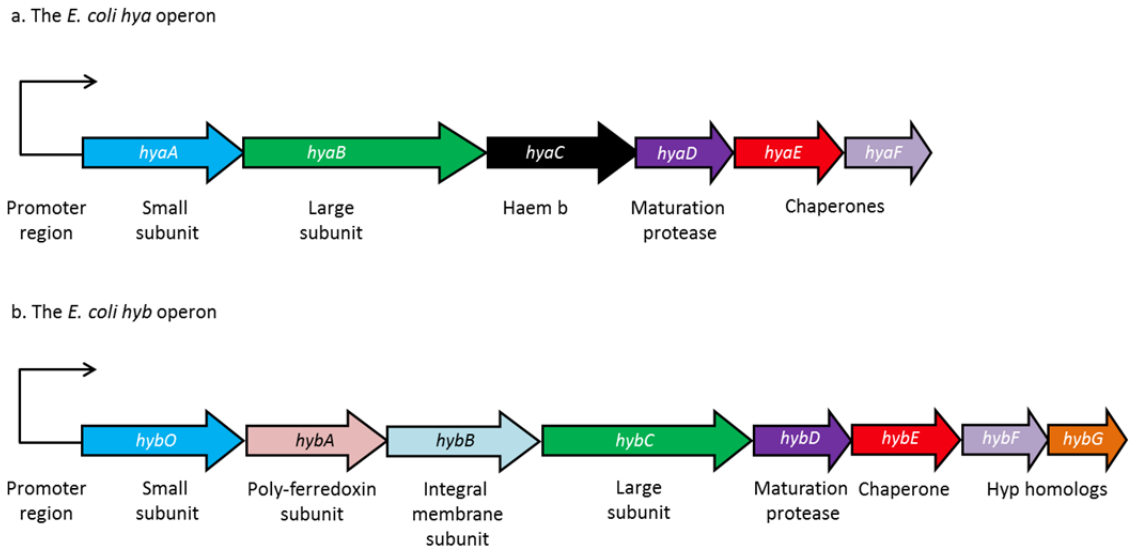

Figure 1.5. The *E. coli hya* and *hyb* operons.

(a) The *hya* operon consists of six genes and is expressed maximally under fermentative conditions (Sawers *et al.*, 1985; Menon *et al.*, 1991). **(b)** The *hyb* operon consists of eight genes and is expressed maximally under anaerobic conditions with hydrogen and fumarate or glycerol and fumarate. The promoter regions are represented with an arrow and the predicted roles/homologs of each gene product is given below each gene (Sawers *et al.*, 1985; Menon *et al.*, 1991).

Hyd-1 was isolated as a dimer of dimers by Sawers and co-workers (1986), was shown to be membrane-bound and could be released in a stable form following detergent dispersal and proteolysis. As a Group 1 membrane-bound hydrogenase, Hyd-1 couples respiratory hydrogen oxidation with the reduction of quinone. The Hyd-1 heterodimer interacts with the gene product of *hyaC*, a di-haem containing cytochrome *b* subunit, which directs electrons into the quinone pool of the respiratory

chain. This subunit also serves to anchor the enzyme to the membrane along with the HyaA transmembrane domain (Vignais, 2008).

Protein film electrochemistry (PFE) experiments have been used to establish that Hyd-1 is only capable of hydrogen oxidation (Lukey *et al.*, 2010). This is in contrast to the results of a study by Sawers and Boxer (1986) that characterised Hyd-1 as a reversible enzyme due to its ability to produce hydrogen in the presence of the artificial electron donor methyl viologen. Lukey and co-workers (2010) also determined that Hyd-1 activity can be maintained in gas mixtures containing 20% oxygen. Thus, Hyd-1 can be classed as oxygen-tolerant, a rare property in hydrogenases that makes this enzyme attractive for use in future hydrogen technologies. The physiological role of *E. coli* Hyd-1 is still however, unclear. As *hya* expression is induced by formate, Hyd-1 was initially hypothesised to have a role in recycling the hydrogen produced by the formate hydrogenlyase complex (Sawers *et al.*, 1985). Recently, it is has been suggested that due to the oxygen-tolerance of Hyd-1 and as Hyd-1 levels are highest during fermentation, this enzyme may offer 'aerobic shock protection' when under oxygen attack. This would be beneficial for microorganisms that occasionally find themselves in aerobic environments (Volbeda *et al.*, 2013). However, *E. coli* prefers to grow in the presence of oxygen and therefore does not need to be protected in any way from "oxygen attack". It is more likely that Hyd-1 is used as a respiratory enzyme during the switch between anaerobic and aerobic conditions, or under a microaerobic environment. This is backed up by genetic evidence, since there are genes for a cytochrome *bd* II oxidase at the 3' end of the *hya* operon that are co-expressed with the hydrogenase (Nesbit *et al.*, 2012).

Hyd-2 is encoded by the *hybOABCDEFG* operon (Figure 1.5) where HybO and HybC are the small and large subunits respectively. Initially, HybA was believed to be the small subunit as it possesses a twin-arginine signal peptide and Fe-S binding motifs (Menon *et al.*, 1994). This conclusion was proved incorrect following genome sequence analysis and the finding of another gene, *hybO*, upstream of *hybA* (Sargent *et al.*, 1998a). HybO was found to possess a transmembrane α helical domain that anchors Hyd-2 to the inner membrane (Hatzixanthis *et al.*, 2003) and following limited proteolysis with trypsin, Hyd-2 can be released from membranes in an active form (Ballantine and Boxer, 1986). HybA is a 'poly-ferredoxin' subunit that the HybOC dimer interacts with in the membrane (Figure 1.6). HybB is another structural component of

Hyd-2 and is an integral membrane protein with homology to HyaC of Hyd-1. Therefore it is likely that these subunits have similar roles (Sawers *et al.*, 2004). Experimental evidence suggests that Hyd-2 uses the ferredoxin HybA to reduce quinone through HybB, coupling this with hydrogen uptake (Dubini *et al.*, 2002). HybD is homologous to HyaD, the endopeptidase of Hyd-1 and HybE has been identified as a Hyd-2 specific chaperone (Menon *et al.*, 1994; Dubini and Sargent, 2003). HybF and HybG are homologues of HypA and HypC (Menon *et al.*, 1994) indicating a role in the insertion of the metal active site.

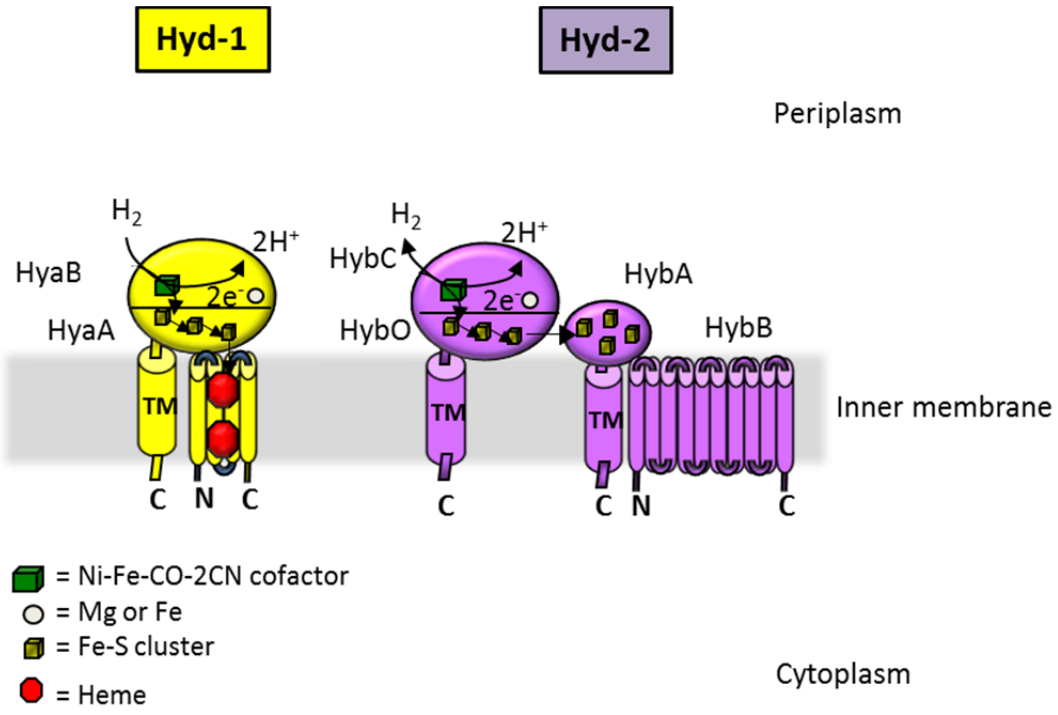

Figure 1.6. Cartoon depictions of *E. coli* Hyd-1 and Hyd-2.

Hyd-1 and Hyd-2 are both located in the inner membrane, anchored by a C-terminal transmembrane (TM) domain present on the small subunit. The HyaAB dimer interacts with a cytochrome *b* subunit in the membrane (Sawers *et al.*, 2004) whereas the HybOC dimer associates with HybA and HybB that facilitate electron transfer to the quinone pool (Dubini *et al.*, 2002). Black arrows represent the conversion of hydrogen to protons and electrons and indicate the flow of electrons through the enzyme.

Expression of the *hyb* operon is induced under anaerobic conditions by either hydrogen and fumarate or glycerol and fumarate. Instead of generating a proton electrochemical gradient, Hyd-2 donates electrons *via* menaquinol to fumarate reductase for the reduction of fumarate to succinate (Vignais and Billoud, 2007). Similarly to Hyd-1, *hyb* expression is repressed in the presence of nitrate but unlike Hyd-1 is not affected by AppY (Richard *et al.*, 1999). Mutations in the *fnr* gene results

in reduced hydrogenase activity (Sawers *et al.*, 1985), but FNR acts indirectly in this case by controlling expression of the *nik* operon, and thereby controlling availability of the essential nickel ions (Lutz *et al.*, 1991). PFE experiments have demonstrated that Hyd-2 is capable of performing both hydrogen oxidation and proton reduction, but unlike Hyd-1 does not maintain hydrogenase activity in the presence of oxygen (Lukey *et al.*, 2010).

1.3.1.2 Hyd-1 and Hyd-2 of *Salmonella*

Hyd-1 and Hyd-2 of *Salmonella* are homologs of the two uptake hydrogenases found in *E. coli* and cross-react with antibodies raised against their respective enzymes (Sawers *et al.*, 1986). Studies using transcriptional reporter fusions have provided clear insight into the expression of the *Salmonella hya* and *hyb* operons. Fusing the *hya* and *hyb* promoters to the *lacZ* gene resulted in the finding that the *hya* operon is expressed maximally under fermentative conditions (using glucose or mannose) whereas the *hyb* operon is expressed best during anaerobic respiration when using glycerol and fumarate (Zbell *et al.*, 2007). Both *hya* and *hyb* are regulated by FNR, and similarly to *E. coli* Hyd-2, *Salmonella hyb* expression is upregulated by ArcA (Zbell *et al.*, 2007). In contrast, however, *Salmonella hya* expression does not appear to be regulated by the ArcB/ArcA system (Zbell *et al.*, 2007). Another disparity in the regulation of these enzymes is the finding that *Salmonella hya* expression is not regulated by IscR (Zbell *et al.*, 2007). The expression of *hyb*, however, is repressed by IscR. Hyd-1 expression is repressed by nitrate, which appears to be mediated by the NarX/NarL two-component system (Zbell *et al.*, 2007).

An investigation by Zbell and Maier (2009) has provided evidence to suggest that *Salmonella* Hyd-1 functions to recycle hydrogen produced during fermentation. In this study, wild type *Salmonella* was not observed to produce hydrogen until Hyd-1 was deleted. Hyd-1 was also shown to be capable of using exogenous hydrogen under aerobic conditions, which would be important for bacterial survival in mammalian tissues (Zbell and Maier, 2009). These results conflict with findings of a previous study by the same group that demonstrated low *hya* expression in the presence of sodium formate (Zbell *et al.*, 2007) but agrees with the results of Sawers *et al*. (1986) who observed higher levels of Hyd-1 activity in the presence of formate.

The addition of hydrogen to a *Salmonella* culture was shown to result in an enhanced growth rate and yield (Lamichhane-Khadka *et al.*, 2010). The use of deletion mutants demonstrated that the majority of this increased growth was due to the activity of Hyd-2, which was capable of using fumarate and other electron acceptors during anaerobic respiration (Lamichhane-Khadka *et al.*, 2010). Hydrogen oxidation by Hyd-2 provided *Salmonella* with the energy required for the uptake (or transport) of amino acids essential for its growth and survival and was dependent on the PMF, and to a lesser extent, ATP (Lamichhane-Khadka *et al.*, 2010).

1.3.1.3 *Salmonella* Hyd-5

The capacity of *Salmonella* to produce three Tat-dependent, hydrogen oxidising hydrogenases was only discovered following assembly of the complete genome sequence of the bacterium (McClelland *et al.*, 2001; Maier *et al.*, 2004). Hyd-5 is encoded by the *hydABCDEFGHI* operon where HydA and HydB are the small and large subunits, respectively. HydC is a cytochrome *b* subunit responsible for directing electrons into the quinone pool whereas HydD, HydE, HydH and HydI are thought to be important for maturation of the large subunit. Of particular interest is the gene *hydH*, which has not been linked with any anaerobic gene clusters to date (Parkin *et al.*, 2012). HydH is a homolog of HoxV from *R. eutropha*, a protein that is thought to act as a scaffold for the insertion of the active site (Ludwig *et al.*, 2009b). HydF is predicted to act as a Hyd-5 specific chaperone and prevent the premature export of an immature enzyme. The role of HydG is not clear at the moment but is predicted to have a role in hydrogenase assembly (Parkin *et al.*, 2012). Hyd-5 shares high sequence homology with *E. coli* Hyd-1, with *Salmonella* HydB sharing 67% overall sequence identity with *E. coli* HyaB (Parkin *et al.*, 2012).

The use of reporter fusions to investigate the expression of the *hyd* operon yielded fascinating results. Expression from the *hyd* promoter was found to be greatest under aerobic conditions (Zbell *et al.*, 2007). This is rare for hydrogenases due to the requirement for oxygen-sensitive redox-active metals. Encountering oxygen once assembled is a major obstacle for a hydrogenase so to assemble an enzyme aerobically is a challenging task. Expression (measured as galactosidase activity) of *hyd* tripled when *arcA* was deleted from *Salmonella* so it appears that ArcA represses *hyd*

anaerobically (Zbell *et al.*, 2007). This provided another indication that Hyd is produced aerobically.

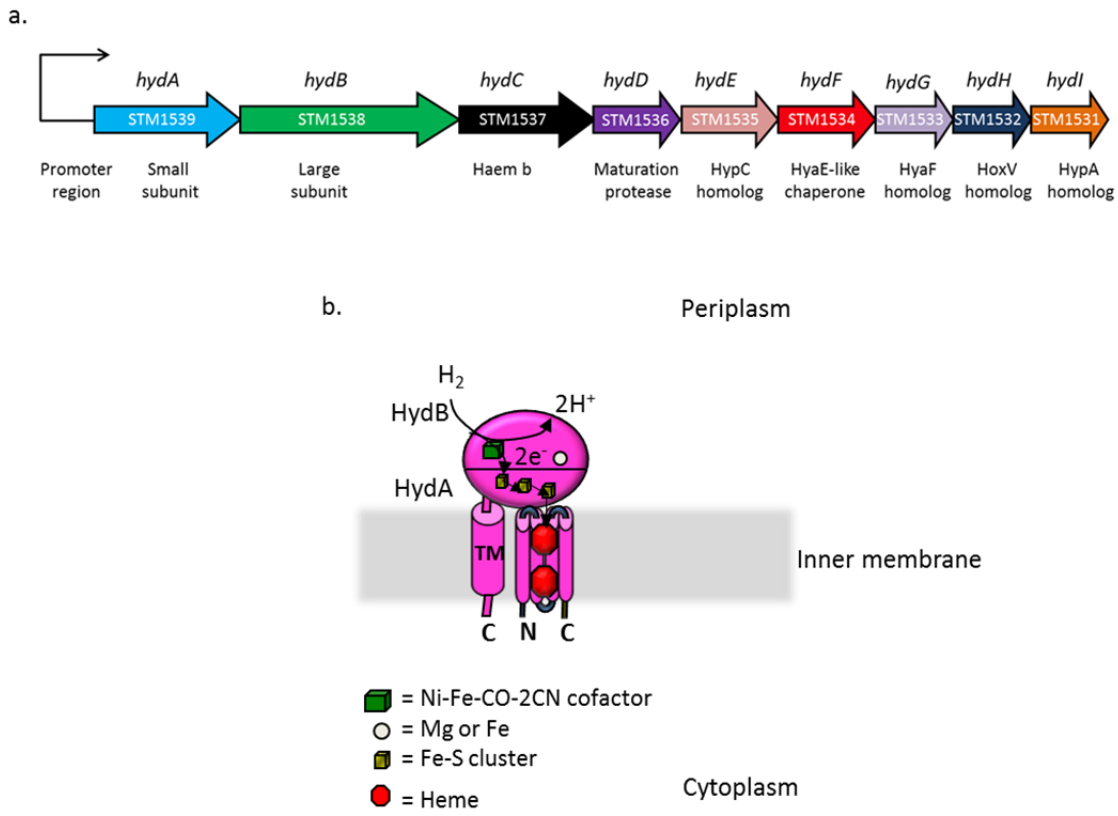

Figure 1.7. The *Salmonella hyd* operon and cartoon depiction of Hyd-5.

(a) The *hyd* operon consists of nine genes and is expressed maximally under aerobic conditions (Zbell *et al.*, 2007). The promoter region is represented here with an arrow and the predicted roles/homologs of each gene product are given below each gene. **(b)** Hyd-5 shares homology with *E. coli* and *Salmonella* Hyd-1 and is thought to be anchored to the inner membrane in a similar manner (Parkin *et al.*, 2012). Black arrows represent the conversion of hydrogen to protons and electrons and indicate the flow of electrons through the enzyme.

The role of Hyd-5 is unknown at present but has been speculated upon. As a pathogen, *Salmonella* is confronted by a number of different environmental conditions during the infection process. It is likely that the transition between aerobic and anaerobic lifestyles will occur often. Although *Salmonella* will encounter extremely anoxic conditions far down the digestive tract, this bacteria infects spleen and liver tissues, which are well oxygenated. The ability to oxidise hydrogen in both anoxic and aerobic environments will likely provide *Salmonella* with a huge survival advantage. Another environmental transition will take place when *Salmonella* is engulfed by macrophages. It might be possible that Hyd-5 activity may allow *Salmonella* to combat

the mammalian immune system by providing oxidative stress enzymes with a source of reducing power (Parkin *et al.*, 2012) or ridding of the oxygen itself through reduction.

1.3.2 The Hydrogen Producing Hydrogenases

1.3.2.1 Hyd-3 of *E. coli* and *Salmonella*

Many members of the Enterobacteriaceae are capable of producing hydrogen under anaerobic conditions, when exogenous electron acceptors are lacking. This is achieved through a process known as mixed acid fermentation (Figure 1.1). Energy metabolism through fermentation is really the 'last resort' for bacteria as the energy yield is minimal when compared to respiratory routes. The process begins with the degradation of glucose into two molecules of pyruvate, which are then cleaved to formate by pyruvate formate lyase (Sawers *et al.*, 2004). The build-up of formate in the cell leads to an increase in acidification, which if unregulated, would lead to a disruption in the proton gradient. Initially, formate is passively exported from the cell cytoplasm through the FocA channel. Interestingly, if the pH of the external medium is lowered to 6.4, formate is actively imported back into the cell by FocA and is then metabolised (Sawers, 2005).

The enzyme complex responsible for the disproportionation of formate to carbon dioxide and hydrogen is called the formate hydrogenlyase (FHL) complex. The FHL complex is composed of seven proteins, six of which are encoded by the *hyc* operon (Figure 1.8). The gene product of *fdhf* is called formate dehydrogenase-H (FDH-H) and is only produced under fermentative conditions, when formate is present (Sawers *et al.*, 1985; Sawers *et al.*, 2004). This enzyme contains selenocysteine, a Fe-S cluster, and a molybdenum atom coordinated by two molybdopterin guanine dinucleotide (MGD) cofactors at its active site and carries out formate oxidation (Boyington *et al.*, 1997). FDH-H interacts with Hyd-3 to couple this oxidation with the reduction of protons. Hyd-3 associated activity was first observed in *E. coli* by Sawers *et al*. (1985), who correlated this with synthesis of the FHL complex. Subsequently, the *hycABCDEFGHI* operon was identified and in-frame gene deletions utilised to investigate the role of each gene-product. From these studies, HycA was demonstrated to act as a regulatory protein and HycE as the large subunit of the enzyme (Bohm *et al.*, 1990; Sauter *et al.*, 1992). The genes *hycB* through to *hycG*

encode structural components of Hyd-3, where HycC and HycD are membrane embedded and HycB, HycF and HycG contain Fe-S clusters required for electron transfer. The role of HycH is currently ambiguous (Sawers *et al.*, 2004). HycI was discovered to be the endopeptidase responsible for proteolytically cleaving the C-terminus of HycE (Rossmann *et al.*, 1995).

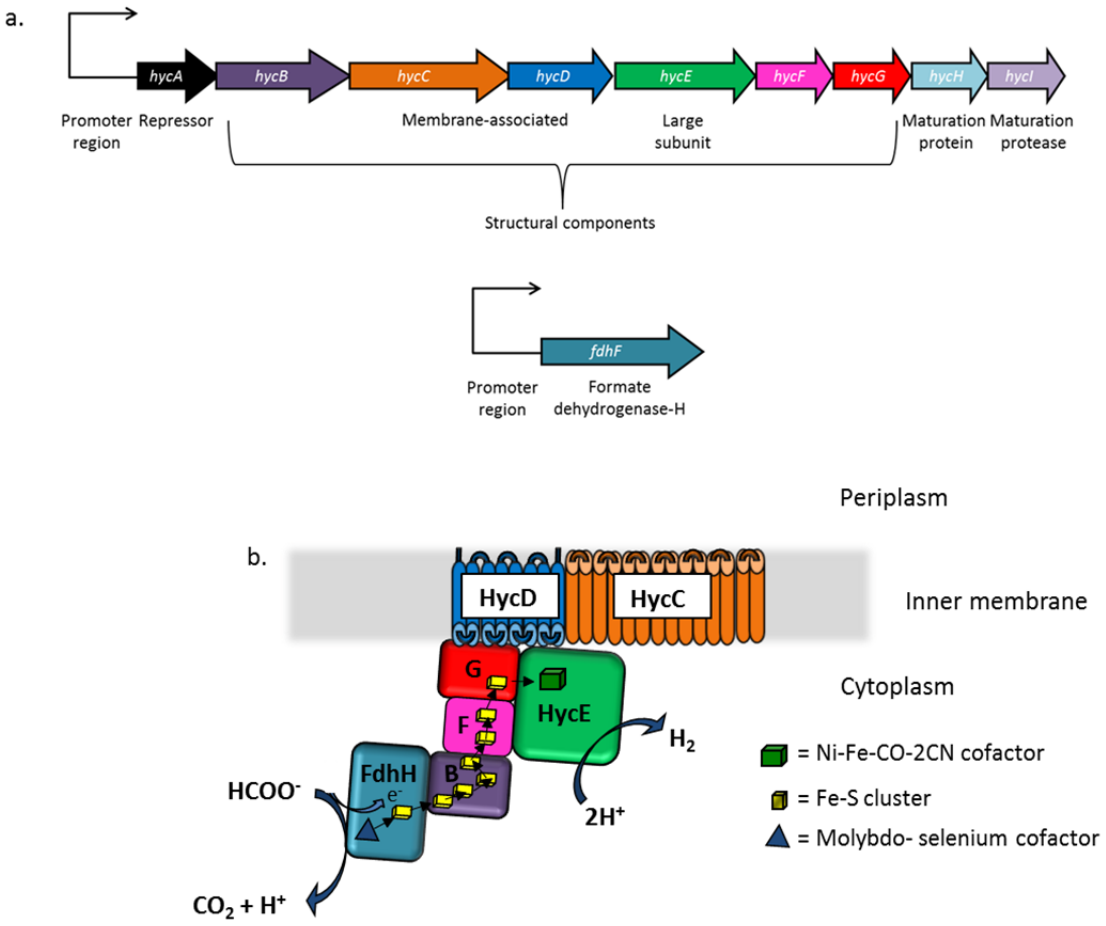

Figure 1.8. The *hyc* operon, the *fdhF* gene, and the predicted topology of the FHL complex.

(a) The *hyc* operon consists of nine genes and is expressed under anaerobic conditions and in the presence of formate. The *fdhF* gene is located elsewhere in the genome and is expressed under the same conditions as *hyc* (Bohm *et al.*, 1990; Sauter *et al.*, 1992). The promoter regions are represented with an arrow and the predicted roles/homologs of each gene product given below each gene. **(b)** Hyd-3 is composed of seven proteins, two of which are membrane associated. The active site of Hyd-3 faces into the cytoplasm (Sawers *et al.*, 2004). Black arrows indicate the flow of electrons through the enzyme complex.

Fascinatingly, HycC, HycD, HycE, HycF and HycG of Hyd-3 were discovered to share sequence similarity with components of the NADH ubiquinone oxidoreductase (or respiratory complex I) enzyme (Bohm *et al.*, 1990). Complex 1 is a large enzyme complex found in many bacteria and in the mitochondrial respiratory chain of

eukaryotes. The complex serves to couple the oxidation of a variety of electron donors and the reduction of quinone analogues in the membrane with the transport of ions against a membrane potential. This ultimately leads to the generation of a proton motive force that can be used to generate ATP within the cell, which can then be used for a number of different processes including solute uptake, flagellar rotation and protein export (Efremov and Sazanov, 2012). Recently, the crystal structure of the entire 16 subunit Complex I module from *Thermus thermophilus* was solved suggesting that one of the membrane components, Nqo8 forms part of a proton channel (Baradaran *et al.*, 2013). As this subunit shares homology with HycD, a membrane-embedded subunit of Hyd-3, it may be proposed that protons can also be translocated into the periplasm through the action of the FHL complex. HycC is the second membrane-embedded subunit of *E. coli* Hyd-3 and shares homology with NuoL/Nqo12, NuoM/Nqo13 and NuoN/Nqu14 of Complex I. HycC does however lack the NuoL amphipathic helix that spans the length of the membrane domain of Complex I and is thought to be important for proton translocation (Efremov *et al.*, 2010). Both HycC and HycD are essential for the production of hydrogen *in vivo* (Sauter *et al.*, 1992) emphasising their importance. It is still unknown whether or not protons are translocated out of the cytoplasm by the FHL complex but a study by Hakobyan *et al*. (2005) appeared to demonstrate proton translocation coupled to the oxidation of formate and the production of hydrogen. Alternatively, it has also been speculated that production of hydrogen by the FHL complex is driven by the PMF since inhibition of the F_1F_0 ATPase results in bacteria that are incapable of producing gas (Sasahara *et al.*, 1997). Recently, the use of formate as sole energy source was found to be sufficient for the growth of a number of hyperthermophiles belonging to the *Thermococcus* genus demonstrating that formate conversion can support microbial growth (Kim *et al.*, 2010).

Expression of the *fdhF* gene and the *hyp* and *hyc* operons are tightly coordinated. The gene *fhlA*, present downstream of the *hyp* operon, encodes a transcriptional activator of the FHL complex and binds to a regulatory region upstream of the *fdhF* gene and a region between the *hyc* and *hyp* operons. In addition, FhlA also binds to a site between *hycA* and *hycB*. This coordination of expression only occurs above a certain concentration of formate (Schlensog *et al.*, 1994; Sawers *et al.*, 2004). Experimental evidence suggests that FhlA binds formate directly before adopting the

conformation required for binding to the regulatory regions (Hopper and Bock, 1995). The activity of FhlA appears to be hindered by HycA, which prevents continuous FHL complex expression (Sawers *et al.*, 2004). Efforts to enhance the production of hydrogen in *E. coli* have included inactivating the repressor HycA, overexpressing or mutating FhlA and preventing the assembly of uptake hydrogenases by inactivating the Tat system (Penfold *et al.*, 2006; Maeda *et al.*, 2007; Sanchez-Torres *et al.*, 2009).

1.3.2.2 Hyd-4 of *E. coli*

E. coli is capable of producing a fourth hydrogenase, Hyd-4, encoded by the *hyfABCDEFGHIJRfocB* operon. Due to sequence similarities, the operon was believed to encode a hydrogenase with similarity to Hyd-3, where HyfB, HyfC, HyfD, HyfE and HyfF are membrane embedded and HyfA, HyfG, HyfH and HyfI are peripheral membrane proteins (Andrews *et al.*, 1997). Nine of these hydrogenase subunits share homology with 10 subunits of Complex I (Efremov and Sazanov, 2012). Hyd-4 differs from Hyd-3 in having three additional membrane subunits (HyfD, HyfE and HyfF) and a predicted formate channel, FocB. It was proposed that Hyd-4, in association with Fdh-H, could be involved in energy conserving proton translocation (Andrews *et al.*, 1997).

Further characterisation of the operon using *hyf-lacZ* fusions revealed very weak expression that was dependent on FhlA and σ^{54}. Similar to Hyd-3, expression was induced during fermentation, at low pH and when formate was present. Surprisingly, inactivation of the regulatory gene *hyfR* did not affect *hyf* expression whereas *hyfR* overexpression led to a significant induction of *hyf* expression. Although transcription was evident, protein translation was not. No Hyf proteins could be detected immunologically, no growth defects were observed for *hyf* deletion mutants and no hydrogenase activity was observed (Skibinski *et al.*, 2002). Further studies using *hyf-lacZ* fusions concluded that Hyd-4 is not produced in *E. coli* and that the *hyf* operon is in fact silent (Self *et al.*, 2004).

1.4 [NiFe]-hydrogenase biosynthesis

The assembly of hydrogenase enzymes is a complex process that requires the involvement of many biosynthetic pathways and a huge number of genes. The metallocentre must be carefully synthesised and efficiently incorporated into the large subunit of the enzyme. Fe-S clusters also must be assembled and integrated into the small subunit. These insertions, and resultant conformational changes, must occur before both subunits can unite and form the heterodimeric complex. The fully folded, cofactor containing dimer must then be recruited to the twin-arginine translocation machinery, which facilitates transfer of the enzyme across the inner membrane and into the periplasm. The signal peptide can then be cleaved and the enzyme anchored to the membrane *via* its C-terminal transmembrane domain (Forzi and Sawers, 2007).

1.4.1 Assembly of the [NiFe]-active site

Nickel acquisition is clearly essential for the formation of an active [NiFe]-metallocentre. The *nikABCDE* operon encodes for the production of a high-affinity nickel ('Nik') transporter in *E. coli* that is regulated by the FNR protein during anaerobiosis (Wu *et al.*, 1989; Navarro *et al.*, 1993). The gene products form an ATP-binding cassette (ABC)-type transport system where NikD and NikE are the ATP binding proteins. NikA functions as the periplasmic nickel binding protein whereas NikB and NikC are integral membrane subunits. Using an *E. coli nik* mutant, Rodrigue *et al*. (1996) demonstrated that intracellular nickel is absolutely required for the maturation of Hyd-2. A different method of nickel uptake is employed by *Rhizobium leguminosarum*, where HupE (encoded in the 18-gene cluster required for hydrogenase assembly) functions as a nickel permease (Brito *et al.*, 2010).

Proteins encoded by the *hyp* operon (*hypABCDEF*) are essential for assembling the [NiFe]-metallocentre and incorporating the active site into the large subunit (Figure 1.9). HypF functions as a carbamoyltransferase and thus transfers carbamoyl from carbamoyladenylate to a cysteine residue of HypE (Reissmann *et al.*, 2003; Blokesch *et al.*, 2004b). HypC and HypD form a complex that binds iron and receives the cyanide groups synthesised by HypEF. Spectroscopic analysis has revealed that the HypCD complex also carries the carbon monoxide ligand (Burstel *et al.*, 2012). The

$Fe(CN)_2CO$ moiety is then transferred to the large subunit and inserted. HypA and HypB are thought to catalyse insertion of the nickel atom into the active site to complete the process (Blokesch *et al.*, 2002). Another protein, SlyD, has also been implicated in nickel binding and [NiFe]-hydrogenase maturation in *E. coli* and *H. pylori* (Cheng *et al.*, 2012; Cheng *et al.*, 2013). It may be unsurprising that SlyD binds nickel *in vitro* however, as an inspection of the *E. coli* and *H. pylori* SlyD amino acid sequences reveal the presence of numerous histidine and cysteine residues. The importance of SlyD must be questioned however, as *Campylobacter jejuni* carrying an inactivated *slyD* gene was found to be unaffected in its ability to oxidise hydrogen (Howlett *et al.*, 2012).

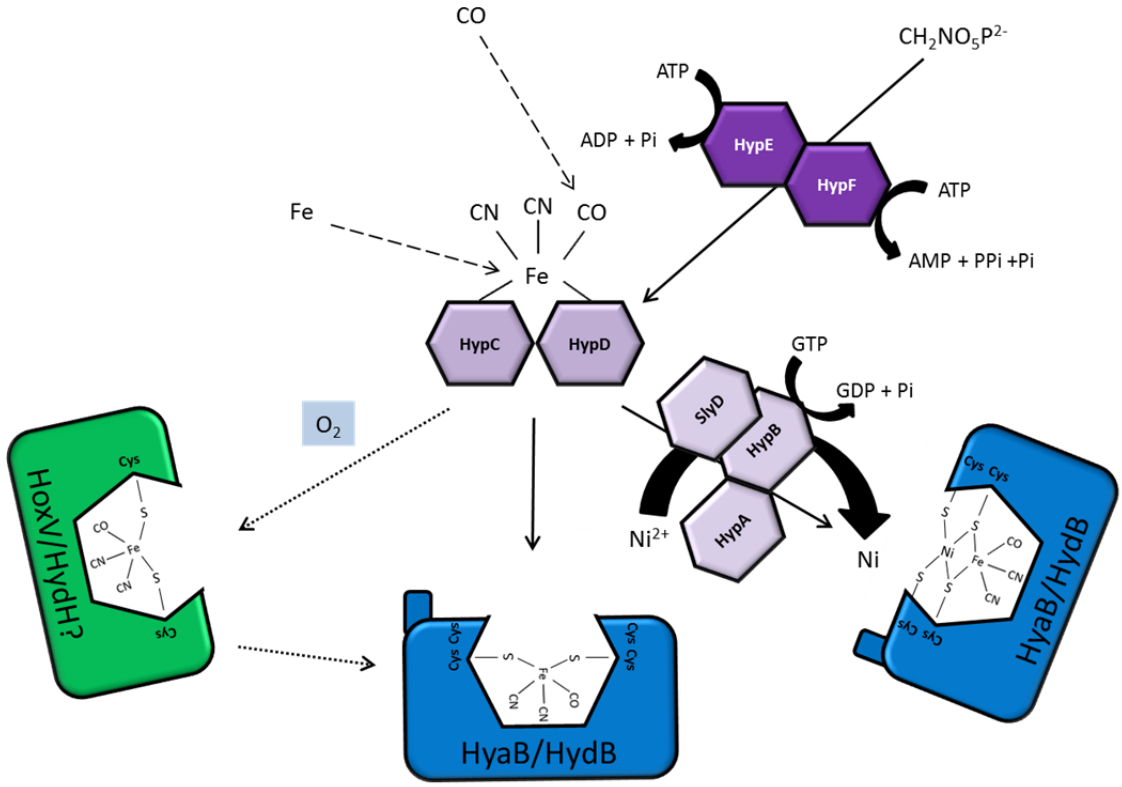

Figure 1.9. Proposed mechanism of [NiFe]-active site insertion.

The HypEF complex is thought to be responsible for generating the cyanide ligands from carbamoyl phosphate but the source of carbon monoxide and iron is still unknown (as highlighted by the use of dashed arrows). The $Fe(CN)_2CO$ moiety is assembled by the HypCD complex and is then transferred to the large subunit (Forzi and Sawers, 2007). Nickel is incorporated into the large subunit through the action of HypA, HypB and possibly SlyD in some microorganisms (Blokesch *et al.*, 2002; Cheng *et al.*, 2012; Cheng *et al.*, 2013). A subclass of [NiFe]-hydrogenase can be assembled under aerobic conditions (dotted arrow). It is thought that dedicated scaffolding chaperones are required to shield the $Fe(CN_2)CO$ moiety from oxygen attack before being transferred to the large subunit (Ludwig *et al.*, 2009b).

The aerobically expressed *hox* operon of *R. eutropha* encodes an accessory protein, HoxV, which is thought to act as a scaffolding chaperone for the insertion of the $Fe(CN)_2CO$ moiety (Ludwig *et al.*, 2009b). A homolog of this protein, *hydH*, is also encoded for in the *hyd* operon of *Salmonella*, another aerobically expressed operon and may be important for the assembly of oxygen-tolerant hydrogenases (Parkin *et al.*, 2012). Following incorporation of the fully formed [NiFe]-active site, the C-terminus of the large subunit is proteolytically cleaved by an endopeptidase rendering the insertion irreversible. Only after this cleavage has occurred is the large subunit capable of interacting with the small subunit to form the heterodimeric enzyme (Rossmann *et al.*, 1994; Vignais and Billoud, 2007).

1.4.2 Fe-S cluster biogenesis

The assembly and transfer of Fe-S clusters require yet another specialised set of proteins. The first proteins to be identified with a role in Fe-S cluster biosynthesis were found in *Azotobacter vinelandii* and were named NifS and NifU. The latter of these two proteins acts as a scaffold for the former protein to direct Fe-S cluster formation (Vignais and Billoud, 2007). Since their discovery, two other systems were discovered to be involved in Fe-S cluster biogenesis. These are named the Isc (iron sulphur cluster) and Suf (sulphur mobilisation) systems. Proteins that are involved in the transfer of Fe-S clusters are known as A-type carrier (ATC) proteins of which there are three produced in *E. coli* called IscA, SufA and ErpA (essential respiratory protein A). Both IscA and ErpA were found to be essential for the biosynthesis of active hydrogen oxidising hydrogenases in *E. coli* whereas the deletion of *sufA* did not affect hydrogenase activity (Pinske and Sawers, 2012). The precise functions of these proteins are unknown at present. It is thought that proteins of the Isc system function under normal conditions whereas proteins of the Suf system are required under conditions of stress (Vignais and Billoud, 2007). Both of these operons however appear to be induced under oxidative conditions (Zheng *et al.*, 2001; Lee *et al.*, 2004).

1.5 The Tat system

Bacterial proteins destined for a role outwith the cell cytoplasm are commonly synthesised as precursors with a signal peptide. Generally, most periplasmic proteins are transported across the bacterial inner membrane *via* the general secretory pathway (Sec), which is known to export unfolded proteins. The Sec translocon is composed of three proteins, Sec Y, E and G that interact and form a membrane embedded translocation channel (Chatzi *et al.*, 2013). In contrast to the Sec transport system, the Tat system was discovered to export fully folded, and in most cases, cofactor containing proteins (Sargent *et al.*, 1998b; Weiner *et al.*, 1998). Among these are proteins with key roles in respiratory electron transfer, membrane integrity and pathogenicity (Ochsner *et al.*, 2002; Ize *et al.*, 2003; Berks *et al.*, 2005). The Tat system has been found throughout all kingdoms of life but has been best studied in bacteria and plant chloroplasts. The number of Tat substrates varies quite considerably between microorganisms. For example, the Gram-positive *Streptomyces coelicolor* is predicted to have over 140 Tat substrates whereas *E. coli* is predicted to produce 30 Tat specific substrates (Palmer *et al.*, 2011; Palmer and Berks, 2012) that are listed in Table 1.1.

The [NiFe]-hydrogenase enzymes of Group 1 are synthesised as precursors in the cell cytoplasm and display twin-arginine signal peptides. These enzymes are found anchored to the inner membrane of Gram-negative bacteria, with their active sites facing into the periplasm. The presence of a signal peptide is essential for the correct localisation of Group 1 [NiFe]-hydrogenases as it directs translocation through the inner membrane *via* the Tat pathway. Although composed of two subunits, only the small subunit is in possession of a Tat signal peptide. Therefore, there must be a considerable degree of coordination between the two subunits to prevent translocation of one subunit without the other. Furthermore, [NiFe]-hydrogenases are complex enzymes that require careful insertion of metal cofactors before transport can occur. This must also be heavily regulated.

Tat substrate	Physiological Role	Signal Peptide Sequence
HyaA[1]	Hydrogen oxidation	MNNEETFYQAMRRQGVT**RR**SFLKYCSLAATSLGLGAGMAPKIAWA
HybO[1]	Hydrogen oxidation	MTGDNTLIHSHGIN**RR**DFMKLCAALAATMGLSSKAAA
HybA[1]	Hydrogen oxidation	MN**RR**NFIKAASCGALLTGALPSVSHA
NapG[1]	Nitrate reduction	MSRSAKPQNG**RR**RFLRDVVRTAGGLAAVGVALGLQQQTARA
NrfC[1]	Nitrite reduction	MTWS**RR**QFLTGVGVLAAVSGTAGRVVA
YagT[1]	Aldehyde oxidoreductase	MSNQGEYPEDNRVGKHEPHDLSLT**RR**DLIKVSAATAVVYPHSTLAASVPA
YdhX[1]	Part of the aldehyde ferredoxin oxidoreductase?	MSWIGWTVAATALGDNQMSFT**RR**KFVLGMGTVIFFTGSASSLLA
TorA	TMAO reduction	MNNNDLFQAS**RR**RFLAQLGGLTVAGMLGPSLLTPRRATAAQA
TorZ	TMAO reduction	MTLT**RR**EFIKHSGIAAGALVVTSAAPLPAWA
NapA[1,2]	Nitrate reduction	MKLS**RR**SFMKANAVAAAAAAAGLSVPGVA
DmsA[1,2]	DMSO/TMAO reduction	MKTKIPDAVLAAEVS**RR**GLVKTTAIGGLAMASSALTLPFSRIAHA
YnfE[1,2]	Selenate/DMSO reduction	MSKNERMVGIS**RR**TLVKSTAIGSLALAAGGFSLPFTLRNAAA
YnfF[1,2]	Selenate/DMSO reduction	MMKIHTTEALMKAEIS**RR**SLMKTSALGSLALASSAFTLPFSQMVRA
FdnG[1,2]	Formate oxidation	MDVS**RR**QFFKICAGGMAGTTVAALGFAPKQALA
FdoG[1,2]	Formate oxidation	MQVS**RR**QFFKICAGGMAGTTAAALGFAPSVALA
YedY[3]	TMAO/DMSO reduction?	MK**RR**QVLKALGISATALSLPHAAHA
CueO[4]	Copper homeostasis	MQ**RR**DFLKYSVALGVASALPLWSRAVFA
PcoA[4]	Copper resistance	MLLKTS**RR**TFLKGLTLSGVAGSLGVWSFNARSSLSLPVAA
SufI	Cell division	MSLS**RR**QFIQASGIALCAGAVPLKASA
YahJ[5]	Deaminase?	MKESNS**RR**EFLSQSGKMVTAAALFGTSVPLAHA
WcaM	Colanic acid biosynthesis	MPFKKLS**RR**TFLTASSALAFLHTPFARA
MdoD	Glucan biosynthesis	MD**RR**RFIKGSMAMAAVCGTSGIASLFSQAAFA
EfeB[6]	Iron extraction from haem	MQYKDENGVNEPS**RR**LLKVIGALALAGSCPVAHA
YaeI	Phosphodiesterase?	MIS**RR**RFLQATAATIATSSGFGYMHYC
AmiA	Cell wall amidase	MSTFKPLKTLTS**RR**QVLKAGLAALTLSGMSQAIA
AmiC	Cell wall amidase	MSGSNTAIS**RR**RLLQGAGAMWLLSVSQVSLA
FhuD	Ferrichrome binding	MSGLPLIS**RR**RLLTAMALSPLLWQMNTAHA
YcbK	Unknown	MDKFDAN**RR**KLLALGGVALGAAILPTPAFA
Pac[7]	Penicillin amidase	MKN**RN**RMIVNCVTASLMYYWSLPALA
C3736	Possible diene lactone hydrolase	MPRLTAKDFPQELLDYYDYYAHGKIS**KR**EFLNLAAKYAVGGMTALA

Table 1.1. The 30 known or predicted Tat substrates of *E. coli*.

The twin arginine residues of each Tat signal peptide are highlighted in bold and the variable n-region highlighted in red. (1) Proteins known or predicted to contain Fe-S clusters. (2) Proteins known or predicted to contain a molybdopterin guanine dinucleotide cofactor. (3) Protein containing a molybdopterin cofactor. (4) Proteins known or predicted to contain Cu ions. (5) Protein predicted to contain a Fe ion. (6) Protein contains haem. (7) Protein contains Ca^{2+}. The remaining Tat substrates either contain no cofactor or the cofactor is unknown. This table is adapted from Palmer *et al.* (2011)

1.5.1 The Tat signal peptide

Tat signal peptides share a number of characteristics typical of Sec signal peptides. This is perhaps the reason why the Tat system remained elusive for so long. Both signal peptide types have a tripartite structure and possess a positively charged 'n-region' at the N-terminus, a hydrophobic 'h-region' and a polar 'c-region' containing a typical AxA cleavage site (Figure 1.10). There are also a number of key differences including the fact that Tat signal peptides are generally much longer than Sec signal peptides. One crucial difference between the two is the occurrence of a conserved twin arginine motif (S-R-R-X-F-L-K) located between the n- and h-regions of Tat signal peptides (Palmer and Berks, 2012).

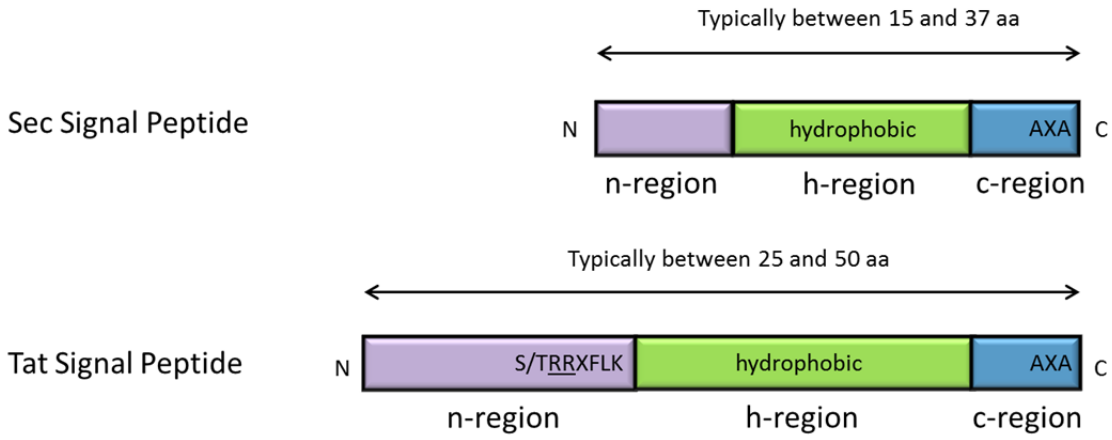

Figure 1.10. The structure of Sec and Tat signal peptides.

Both signal peptides share a common tripartite structure composed of a polar n-region, hydrophobic region and polar c-region. An 'AXA' cleavage site is present at the C-terminus of each signal peptide and is recognised by a signal peptidase. Tat signal peptides are however, typically longer due to an extended n-region and possess a twin-arginine motif, S/TRRXFLK (where X denotes any amino acid) that is specifically recognised by the components of the Tat translocon (Berks *et al.*, 2005).

The twin arginine motif was first noted in studies concerning the [NiFe]-hydrogenase of *Desulfovibrio vulgaris* Hildenborough (Niviere *et al.*, 1992). Niviere and co-workers (1992) established that substituting the first arginine of the conserved 'consensus box' resulted in the inhibition of fusion protein export. Further mutagenesis experiments using *E. coli* SufI as a model Tat substrate revealed the essentiality of both arginine residues to protein export. Substituting the twin arginines for lysines resulted in a complete block of protein processing whereas individual substitutions, although severely retarding SufI export, did not completely abolish

processing (Stanley *et al.*, 2000). These results suggested that the presence of two invariant arginine residues is not a prerequisite for Tat transport. In fact there are a number of Tat signal peptides that possess only one arginine residue including the TtrB signal peptide of *S. enterica* serovar Typhimurium tetrathionate reductase that was shown to be capable of mediating Tat-specific protein export. This signal peptide was capable of directing SufI export when fused to the N-terminus of the mature region of the protein (Hinsley *et al.*, 2001). Further analysis using GFP as a reporter protein and trimethylamine *N*-oxide reductase (TorA) signal peptide libraries demonstrated that although a basic amino acid is preferred in the position of the first arginine, the presence of a glutamine or asparagine residue in the position of the second arginine also permits protein export (DeLisa *et al.*, 2002). Of the other residues of the twin-arginine motif, substituting the phenylalanine residue has the greatest impact on protein export. Due to the observation that twin arginine residues are also present in some Sec-transported substrates, it was realised that features distinct from the twin arginine motif must also be required for ensuring Tat-specific transport (Palmer *et al.*, 2011).

The h-regions of Tat signal peptides are known to be less hydrophobic than the h-regions of Sec-targeting signal peptides. Increasing the hydrophobicity of the TorA signal peptide when fused to the leader peptidase (Lep) resulted in re-routing of protein export through the Sec pathway (Cristóbal *et al.*, 1999). It may be reasonable to assume that this stretch of hydrophobic residues might be masked in some way when the protein is in the cytoplasm. In fact, experiments have been performed that suggest that the h-region constitutes a site of chaperone binding (Hatzixanthis *et al.*, 2005; Shanmugham *et al.*, 2012).

The c-regions of Tat and Sec signal peptides both contain the same ‘AXA’ cleavage motif that is recognised by a signal peptidase. It is hypothesised that the signal peptide is cleaved following complete protein export and that this occurs close to the inner membrane in *E. coli* (Sargent et al., 2006). It is unknown whether the signal peptide is released into the cytoplasm or the periplasmic space and what the fate of the released peptide is. The c-regions of Tat signal peptides often contain one or more basic amino acids, which are thought to serve as a ‘Sec avoidance’ property (Palmer *et al.*, 2005).

Very little is known about the n-regions of Tat substrates. Tat signal peptides are generally longer than Sec signal peptides and this is mostly due to the presence of an extended n-region. When considering the list of *E. coli* Tat substrates in Table 1, it is noticeable that the length of n-region varies extensively between proteins. The reason for this variability is unknown. [NiFe]-hydrogenases in particular possess extremely long n-regions. There are also a large number of conserved residues shared between the signal peptides of hydrogenases of similar function (Berks *et al.*, 2000).

1.5.2 Tat components

In *E. coli*, four proteins have been identified to play a role in Tat transport. TatA, TatB and TatC are encoded by an operon consisting of four genes; *tatABCD*. It has been demonstrated that TatD, however, does not form part of the Tat machinery and is thought to be a water soluble metal-dependent nuclease. The *tatE* gene is monocistronic and is located elsewhere on the chromosome from the *tatABCD* operon (Bogsch *et al.*, 1998; Sargent *et al.*, 1998b; Weiner *et al.*, 1998; Wexler *et al.*, 2000). The *tatABCD* and *tatE* units are expressed constitutively under aerobic and anaerobic conditions (Jack *et al.*, 2001). Translational fusion experiments also revealed that TatA is produced at higher levels than the other Tat components and thus constitutes the major Tat protein (Jack *et al.*, 2001). TatA and TatE are homologous proteins that perform similar functions. Individual deletions of *tatA* and *tatE* do not affect protein export whereas a double mutant is unable to translocate substrates suggesting redundancy of function (Sargent *et al.*, 1998b).

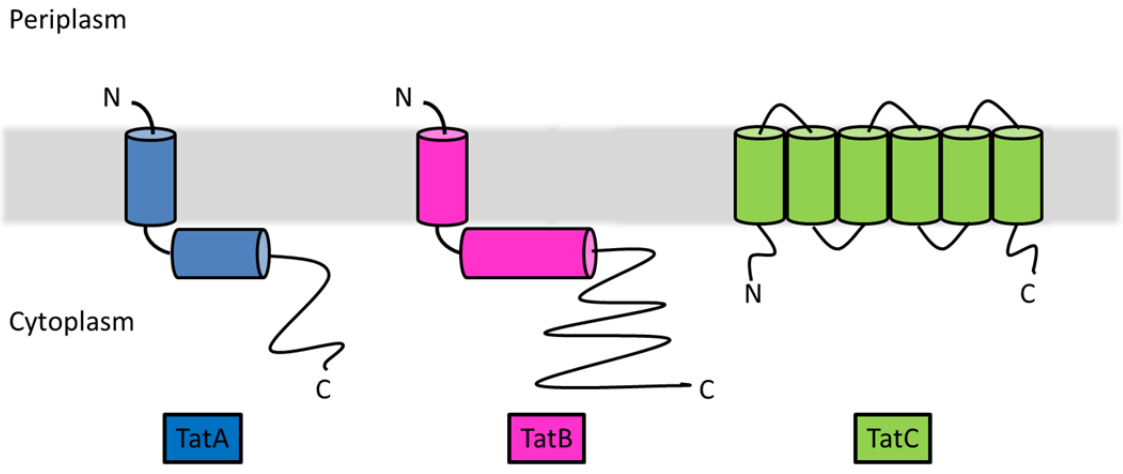

Figure 1.11. The main components of the Tat apparatus.

TatA and TatB span the cytoplasmic membrane *via* a transmembrane helix with the N-terminus predicted to face into the periplasm. The proteins also possess an adjacent amphipathic helix. TatC is composed of six transmembrane helices with the N- and C-terminus located in the cytoplasm (Palmer *et al.*, 2011).

The TatA monomer is thought to be composed of a transmembrane helix and an amphipathic helix located in the cytoplasm (Figure 1.11). It has also been established that the N-terminus faces into the periplasm whereas the C-terminus resides in the cytoplasm (Koch *et al.*, 2012). The presence of an invariant glycine residue at the junction between the transmembrane and amphipathic helices is thought to be necessary for the L-shaped arrangement of TatA (Palmer and Berks, 2012). It has also been proposed that oligomers of TatA form the channel through which Tat substrates are translocated. This proposal has been supported by negative stain electron microscopy. Here, TatA was found to form ring-like structures of various sizes that would be capable of transporting a range of substrate sizes. Another finding was the presence of a lid that is thought to act as a gate at one end of the channel (Gohlke *et al.*, 2005).

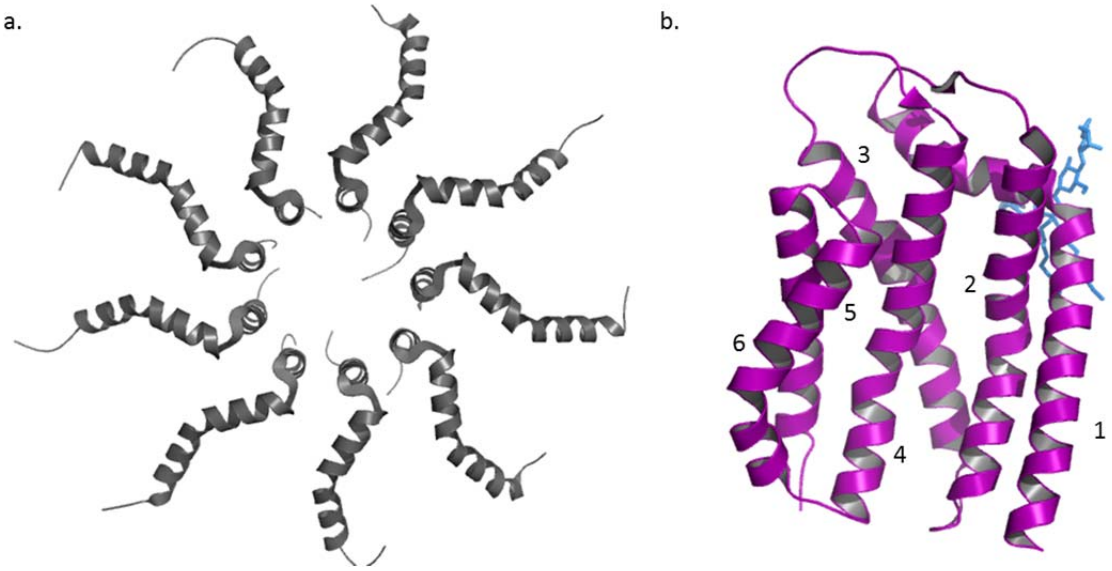

Figure 1.12. Structural representations of a TatA oligomer and TatC.

(a) TatA oligomer structures were determined by NMR following detergent solubilisation (PDB 2LZS). Nine TatA monomers appear to be assembled in a ring-like structure, with the amphipathic helices projecting outwards and the transmembrane helices bundling to form a pore (Rodriguez *et al.*, 2013). **(b)** The X-ray crystal structure of TatC from *A. aeolicus* (PDB 4B4a). TatC is composed of six transmembrane helices where TM5 and TM6 were found to be too short to completely span the membrane (Rollauer *et al.*, 2012). A molecule of the detergent lauryl maltose neopentyl glycol (LMNG) is bound and shown in blue.

Recently, the nuclear magnetic resonance (NMR) determined structure of *E. coli* TatA has been made available (Rodriguez *et al.*, 2013). TatA oligomerisation was controlled through the use of detergent and facilitated the acquisition of the TatA oligomer NMR structure shown in Figure 1.12b. Here, the definite impression of a pore is generated through the arrangement of the transmembrane helices. TatB is structurally similar to TatA but has a distinct role to play as part of the Tat machinery (Figure 1.11). TatB is also longer than TatA due to an extended C-terminus. The extreme C-terminus of both TatA and TatB do not appear to be important for Tat function (Sargent *et al.*, 2006). Interestingly, although the Tat translocase requires the function of all three proteins in Gram-negative bacteria, many Gram-positive bacteria do not produce a TatB protein. In these systems, it appears likely that TatA performs a dual function (Palmer *et al.*, 2011).

TatC is the largest component of the Tat apparatus, having six transmembrane domains, (Figure 1.11) and is highly conserved. Recently, the crystal structure of TatC was successfully solved from the thermophile *Aquifex aeolicus* (Figure 1.12b). This confirmed the presence of the six predicted transmembrane helices and also proved that both the N- and C-termini are located within the cytoplasm. Furthermore, the structure revealed that very little of TatC exists outside of the cytoplasmic membrane (Rollauer *et al.*, 2012).

1.5.3 The Tat transport cycle

A wealth of information regarding potential Tat protein interactions have been obtained from mutagenesis experiments. Unfortunately, structural information is still very weak at present, with TatC being the only component to have provided a crystal structure. A fascinating feature of the Tat system is its ability to transport a variety of substrate shapes and sizes across the cytoplasmic membrane without compromising the ionic seal. For example, transported substrates range from 20 to 70 Å in *E. coli* (Palmer and Berks, 2012). Elucidating the mechanism of Tat transport has proved difficult but a number of models have been proposed of which the most widely accepted will be presented here (Figure 1.13).

TatB and TatC are known to participate in self-self interactions and form hetero-oligomeric complexes in the membrane. These complexes are thought to recognise and bind twin-arginine signal peptides (Frobel *et al.*, 2012b). Crosslinking

experiments have identified TatC as the transport component that specifically recognises the signal peptide twin arginine motif. Furthermore, mutagenesis studies have specifically located the site of binding to the N-terminal half of TatC. Conversely, TatB was found to interact with the entire signal peptide and a region of folded, mature substrate (Alami *et al.*, 2003; Holzapfel *et al.*, 2007; Maurer *et al.*, 2010). TatC also appears to play an additional role by facilitating signal peptide membrane insertion, exposing the peptide to signal peptidase activity. The presence of TatB is thought to prevent premature exposure and signal peptide cleavage, thus regulating transport (Frobel *et al.*, 2012a). TatBC complexes have been observed by electron microscopy, in the absence and in the presence of the *E. coli* substrates SufI or CueO. The overproduction of TatBC and an affinity tag bearing SufI resulted in facile purification of the complex. Microscopy analyses suggested that substrate binding occurs at the TatBC periphery and also results in reducing the diameter of the complex. Although many copies of TatC were present in the recognition complex, a maximum number of two SufI monomers were observed to bind. On the other hand, only one molecule of CueO was found to bind the TatBC complex (Tarry *et al.*, 2009).

Initially, TatBC and TatA will be located separately in the membrane (Figure 1.13a). Tat-mediated translocation is thought to be initiated upon substrate binding to the TatBC complex (Figure 1.13b). The twin-arginine signal peptide becomes tightly bound by the recognition complex and possibly becomes inserted into the membrane (Frobel *et al.*, 2012a; Palmer and Berks, 2012). At this time, TatA will be present in the membrane as dispersed protomers. Cysteine scanning mutagenesis experiments have been performed on the helices of TatA and have shown that the transmembrane helices interact with other TatA protomers (Greene *et al.*, 2007). This is consistent with the TatA polymerisation theory, where TatA protomers interact to form the transport channel. TatA recruitment and polymerisation occurs following substrate binding to the TatBC complex and is energised by the proton motive force (Mould and Robinson, 1991; Cline *et al.*, 1992; Brock *et al.*, 1995; Yahr and Wickner, 2001). Following the assembly of TatABC (Figure 1.13c), substrate is transported across the membrane and the signal peptide cleaved by a signal peptidase (Figure 1.13d). Studies have suggested that protein translocation can only occur after TatA recruitment. Furthermore, interactions between TatA and substrate have also been identified suggesting that TatA may form a channel through which translocation occurs. The

TatBC complex does not appear to form a route for protein transport. Following protein export, the TatABC complex disassembles as is shown in Figure 1.13a (Palmer and Berks, 2012).

An alternative model of Tat-mediated transport has been proposed. This proposal suggests that due to the aggregation of transmembrane helices, the membrane becomes weakened and subsequently drags the substrate through. It is thought that this would maintain a tight membrane seal around the protein. This also suggests that the substrate is inserted into the membrane before translocation is completed (Bruser and Sanders, 2003).

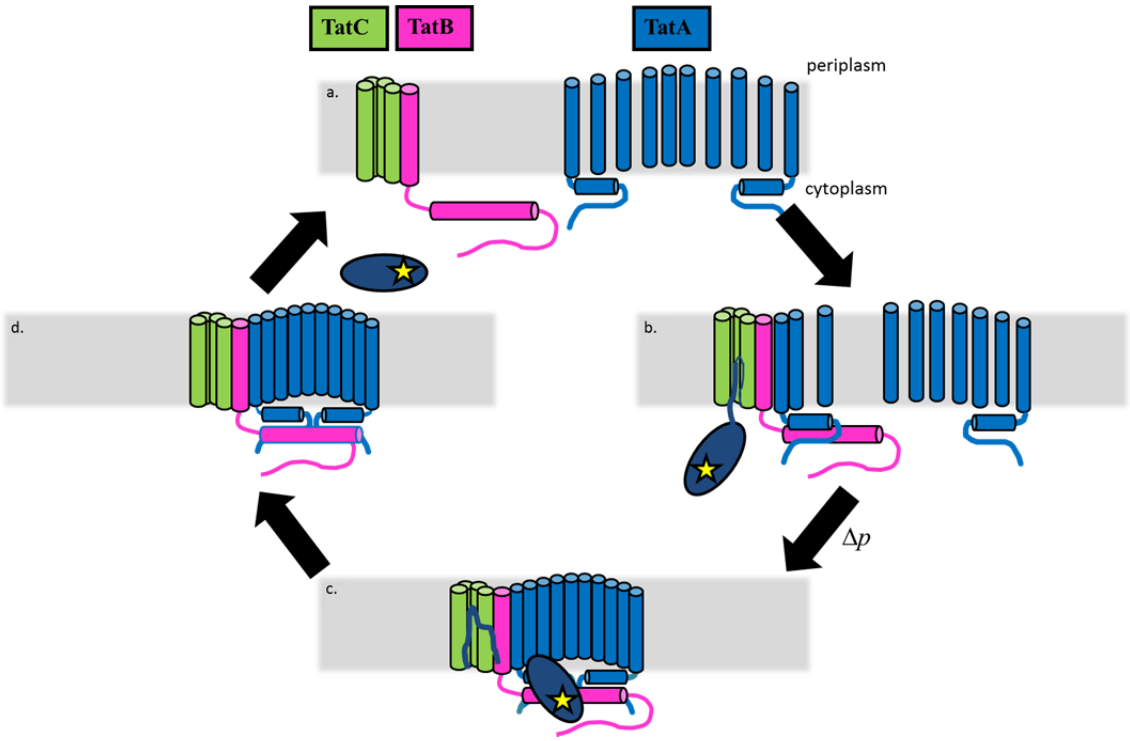

Figure 1.13. The proposed Tat transport cycle.

(a) TatB and TatC form a recognition complex in the membrane and are separated from TatA. **(b)** Substrate binds to the TatBC complex, triggering TatA recruitment and polymerisation in a PMF dependent process. **(c)** The signal peptide becomes tightly bound to the TatBC complex and is perhaps inserted into the membrane. **(d)** Protein is translocated through the TatA channel into the periplasmic space where the signal peptide is cleaved. Following protein transport, the Tat components are disassembled. Figure adapted from Palmer *et al*. (2011).

1.5.4 Proofreading and quality control

To prevent wasteful export of misfolded and incomplete Tat substrates, there must be several levels of control. It has been suggested that the translocon 'senses' proteins in their folded state as a form of 'quality control' (Figure 1.14) and prevents

transport of improperly folded forms of the protein (DeLisa *et al.*, 2003). DeLisa and co-workers (2003) demonstrated that Tat signal peptide displaying proteins requiring the formation of disulphide bonds were only transported via the Tat pathway under conditions conducive to disulphide bond formation. Earlier work however, appeared to suggest that severely malfolded proteins can still be transported by the Tat machinery (Hynds *et al.*, 1998).

Chaperones are proteins believed to bind immature substrates in the cytoplasm, prevent premature export through the Tat translocon and ensure cofactor insertion and correct assembly (Figure 1.14). Chaperone proteins have been identified for a number of cofactor containing enzymes (Sargent, 2007). For example, it was discovered that the Tat substrate nitrate reductase (NapA) is bound tightly by a chaperone called NapD (Maillard *et al.*, 2007; Grahl *et al.*, 2012). Isothermal titration calorimeter (ITC), bacterial two-hybrid assays, size exclusion chromatography (SEC) and NMR were among the methods used to specifically class NapD as a signal peptide binding chaperone. It was proposed that this partnership may act to prevent premature interactions between the signal peptide of NapA and the Tat machinery (Maillard *et al.*, 2007; Grahl *et al.*, 2012).

The interaction between dimethyl sulphoxide (DMSO) reductase and its signal peptide binding chaperone DmsD has also been extensively investigated (Oresnik *et al.*, 2001; Winstone *et al.*, 2006). Papish *et al*. (2003) have performed experiments that suggest that DmsD also interacts with the TatBC recognition complex in the membrane under anaerobic conditions. DmsD is relatively unusual in that it has been shown to interact with more than one signal peptide in the cell. In the case of DmsD, it will also bind YnfE and YnfF as well as a number of other proteins with roles in the biosynthesis of molybdenum cofactors (Palmer *et al.*, 2005; Li *et al.*, 2010).

TorD has been identified as the chaperone of TorA and was found not only to bind to the signal peptide but also to the TorA pre-protein itself (Jack *et al.*, 2004; Dow *et al.*, 2013). Binding of TorD to synthetic versions of the TorA signal peptide was investigated using ITC by Hatzixanthis *et al*. (2005). This established that TorD binds tightly and specifically to the core signal peptide, rather than the n-region when tested *in vitro* (Hatzixanthis *et al.*, 2005). Furthermore, it was found that substituting the twin arginine residues within the twin arginine motif did not have any impact on chaperone binding. TorD was also elucidated as a GTP-binding protein, which upon interacting

with the signal peptide has an increased affinity for the nucleotide and may have a regulatory role (Hatzixanthis *et al.*, 2005). Mutagenesis studies and bacterial two-hybrid assays have also been used to indicate the region of TorD binding, where the substitution of Leu31 within the h-region, was found to be sufficient to disrupt chaperone binding (Buchanan *et al.*, 2008).

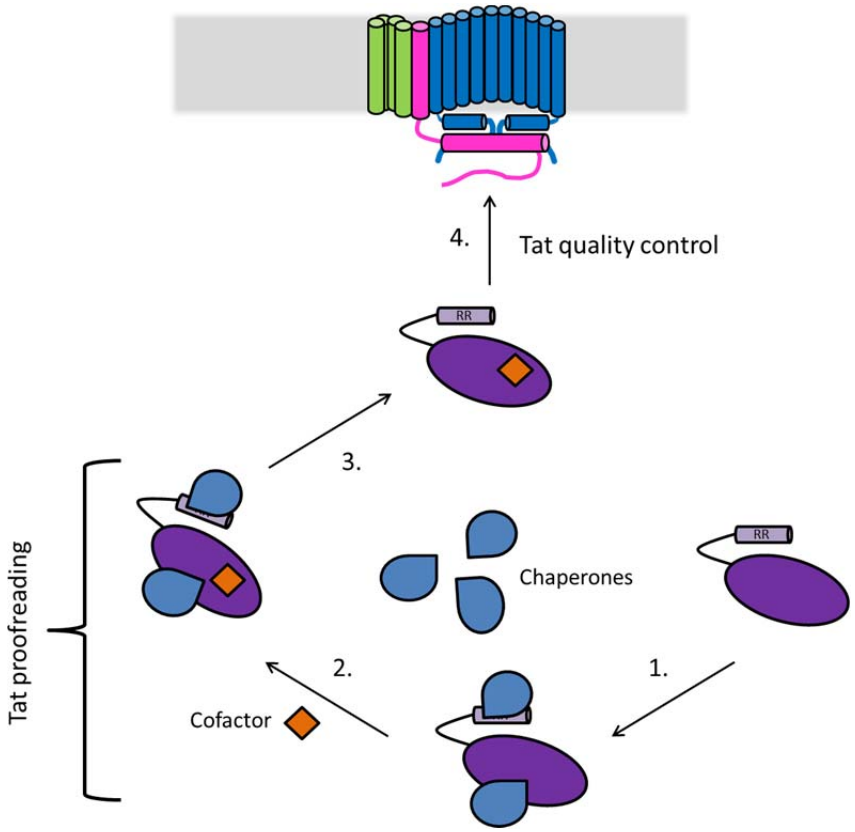

Figure 1.14. Tat proofreading and quality control.

Tat substrates are subject to a number of control measures in order to prevent wasteful transport of immature and incorrectly folded substrates. 1. It is thought that cytoplasmic chaperones bind either the signal peptide or the passenger protein (or in some cases, both) of an immature Tat substrate. 2. This prevents translocation and possibly holds the apoprotein in a conformation suitable for insertion of the relevant cofactor(s). 3. Once released, the signal peptide is recognised by TatBC. 4. The fully folded protein can now be transported across the inner membrane following Tat quality control (Palmer *et al.*, 2011).

1.5.5 Hydrogenases as Tat substrates

Membrane-bound hydrogenases are among the most complex of Tat substrates. These enzymes possess two subunits and only one Tat signal peptide. Hydrogenases also contain a number of cofactors that require efficient insertion prior to translocation. Before the identification of the Tat transport system, a 'consensus box' was observed within the signal peptide of a [NiFe]-hydrogenase produced by *D.*

vulgaris. Mutations within this consensus box were the first to establish the importance of the twin-arginine motif in protein export (Niviere *et al.*, 1992). Although the core [NiFe]-hydrogenase is composed of two subunits, only the small subunit displays a Tat signal peptide. Investigations were thus made into the translocation of the *E. coli* Hyd-2 dimer into the periplasm and revealed a fascinating interdependence. Neither the large nor the small subunit was localised in the membrane when the other subunit was missing, suggesting that complex formation occurs prior to Tat transport (Rodrigue *et al.*, 1999). Another study investigated the importance of the signal peptide to hydrogenase function. Fusing the TorA signal peptide to *E. coli* HybO resulted in a severe reduction of hydrogenase activity and prevented co-translocation of the two subunits. Overproducing the TorA chaperone, TorD, rescued hydrogenase activity, corrected hydrogenase assembly and also demonstrated the important relationship between the chaperone and its passenger protein (Jack *et al.*, 2004).

Efforts to elucidate hydrogenase chaperones have been relatively successful. To identify chaperone binding proteins specific to Hyd-1 and Hyd-2, bacterial two-hybrid assays were used. The precursor form of the small subunit (HyaA) was discovered to form a close association with the gene product of *hyaE*. This interaction was not observed if the mature form of HyaA or the large subunit of Hyd-2 (HybO) was used in the assay, indicating a very specific interaction with the HyaA signal peptide. Using the same assay, a strong association between the unprocessed small subunit of Hyd-2 (HybO) and the gene product of *hybE* was ascertained. Not only was the chaperone found to bind the small subunit but was also capable of interacting with the precursor form of the large subunit, HybC (Dubini and Sargent, 2003). A Δ*hybE E. coli* strain demonstrates very low Hyd-2 activity and although HybO was correctly localised in the cell membrane, HybC was mislocalised in the cytoplasm (Jack *et al.*, 2004). In contrast, in-frame gene deletions have demonstrated that neither HyaE nor HyaF, another predicted Hyd-1 chaperone, is absolutely necessary for [NiFe]-cofactor assembly or translocation into the periplasm (Dubini *et al.*, 2002). A *hyaE*, *hyaF* deletion strain however lacked any Hyd-1 activity (Menon *et al.*, 1991). This is perhaps indicative of the two proteins having overlapping functions.

HupH is a homolog of *E. coli* HyaF, found encoded by the *hup* operon of *Rhizobium leguminosarum bv. viciae*. Affinity chromatography experiments have revealed an interaction between HupH and the precursor form of the small subunit

(Manyani *et al.*, 2005). Furthermore, hydrogenase activity was abolished in a Δ*hupH* mutant in free living cultures regardless of the concentration of oxygen used in the tests (Manyani *et al.*, 2005). This reflects the essentiality of this protein for hydrogen uptake in this microorganism. The hydrogen oxidising activity of a Δ*hupG* (HyaE homolog) mutant was also severely reduced but in contrast, hydrogenase activity increased with decreasing oxygen concentration (Manyani *et al.*, 2005).

R. eutropha produces a membrane bound hydrogenase with similarity to Hyd-1 of *E. coli*. The *hox* operon encodes HyaE and HyaF homologues named HoxO and HoxQ, respectively. These gene products are completely required for the maturation of the hydrogenase and furthermore were shown to form a complex with the precursor form of the small subunit, HoxK (Schubert *et al.*, 2007). Removing the entire Tat signal peptide, or deleting the n-region, resulted in a loss of hydrogenase activity and reduced stability of the precursor (Schubert *et al.*, 2007). A direct interaction between both HoxO and HoxQ with the signal peptide of HoxK has also been demonstrated although the experiment makes use of a synthesised peptide with no involvement of the pre-protein (Schubert *et al.*, 2007).

1.6 Hydrogenases and virulence

In the mammalian digestive tract, hydrogen is present in abundance as a freely diffusible gas, and can also be measured in various body tissues. In mice, hydrogen levels reach an average of 168 µM in the small intestine and around 43 µM in the spleen and the stomach (Olson and Maier, 2002; Maier *et al.*, 2004). Hydrogen production is associated with the fermentation of incompletely absorbed carbohydrates by the colonic flora. As the host organism cannot utilise hydrogen, this gas is in plentiful supply (Maier, 2005). The ability of pathogens to make use of this powerful reductant is extremely advantageous for a pathogen in an environment of hydrogen abundance and high competition. A number of (mostly) enteric pathogens exist with the capability of producing active hydrogenase enzymes including *E. coli* 0157, *Shigella* (*flexeri* and *sonnei*), *Helicobacter pylori*, *Campylobacter jejuni*, *S. enterica* serovar Typhi and *S. enterica* serovar Typhimurium (Maier, 2005). Therefore, the contribution of hydrogenase enzymes to virulence and colonisation has been investigated.

C. jejuni, a causative agent of gastroenteritis, encodes a [NiFe]-hydrogenase capable of hydrogen uptake. A *hydB* mutant, however, demonstrated a very small decrease in the ability to colonise the caecum of chicks (Weerakoon *et al.*, 2009). A *hydB/fdhA* mutant on the other hand, was severely compromised in colonisation, suggesting that both formate and hydrogen are important electron donors and that the enzymes can compensate for the loss of one another (Weerakoon *et al.*, 2009). *H. pylori*, the bacterium responsible for gastric ulcers, gastritis and some gastric cancers, are capable of producing one hydrogen oxidising hydrogenase. Whereas wild type *Helicobacter* was found to be capable of colonising every inoculated mouse in a laboratory experiment, a hydrogenase mutant was only able to colonise around 20% of the infected mice (Olson and Maier, 2002). This indicates that although hydrogen uptake may be an important respiratory electron donor in the stomach, other virulence factors must exist (Olson and Maier, 2002).

Salmonella enterica serovar Typhimurium is another enteric bacterium that has the potential to cause debilitating illnesses, especially in the immunocompromised. *Salmonella* is a common cause of gastroenteritis in humans but the disease is generally

self-limiting. Unfortunately, invasive pathovariants are arising in sub-Saharan Africa that are multi-drug resistant and associated with high fatality rates (Okoro *et al.*, 2012). Another challenge facing antibiotic treatment is the existence of a bacterial persister population. Persisters were first noted in the early 1940's when it was discovered that a small number of bacterial cells survived antibiotic treatment by becoming dormant, non-dividing cells (Lewis, 2007). Persister formation appears to occur mostly in the stationary phase of growth as an altruistic behaviour trait (Lewis, 2007). It has also been demonstrated that upon removal of the antibiotic, persister cells not only resume growth but that their progeny is sensitive to antibiotic attack (Dawson *et al.*, 2011). Due to this ability to resume growth, persister populations become the source for relapse of infection. It is clear that new therapeutic strategies are required to deal with multi-drug resistance, persisters and recurrent infections. A steady stream of new antimicrobial agents should be considered a necessity.

Salmonella expresses three uptake hydrogenases under different environmental conditions *in vitro* (Zbell et al., 2007). Studies into hydrogenase expression *in vivo* found that each hydrogenase can use oxygen as a terminal electron acceptor, although Hyd-5 does appear to contribute most to aerobic hydrogen oxidation (Zbell and Maier, 2009). The whole cell half-saturation affinity of *Salmonella* for hydrogen is relatively low at 2.1 µM, so it can be safely assumed hydrogenases are saturated *in vivo* (Maier et al., 2004). Removal of the three uptake hydrogenases resulted in an avirulent strain, incapable of invading the liver or the spleen. Partial complementation (introduction of Hyd-1) restored the ability of this strain to cause death (Maier *et al.*, 2004). Maier *et al*. (2004) stress the importance of Hyd-1 to virulence as a Hyd-2/Hyd-5 deletion retained almost wild type levels of activity. Unfortunately a Hyd-1/Hyd-2 deletion mutant was not tested for its ability to cause disease. Therefore, the importance of Hyd-5 was not clarified.

Further experiments were performed to establish whether *Salmonella* hydrogenases are differentially expressed *in vivo*. Results suggested that *hya* expression was upregulated in macrophages and polymorphonuclear leukocyte-like (PMN) cells but expression was low. Hyd-1 expression was demonstrated to be important for survival in macrophages so this level of expression appears to be sufficient. Expression of *hyb* was not detected *in vivo* although qRT-PCR results suggested that *hyb* was expressed in macrophages. Expression of *hyd* was greatly

upregulated in both immune cells when compared to the medium only control. During the early stages of infection, *hyd* expression was upregulated in the liver and spleen tissues but was also measured in the ileum at a later stage (Zbell *et al.*, 2008). When *Salmonella* are phagocytosed by macrophages during infection, they are subjected to an oxidative burst and bombarded by reactive oxygen and nitrogen species (Slauch, 2011). It has been suggested that Hyd-5 may oxidise hydrogen as a way of providing reductant to enzymes responsible for combating oxidative stress (Zbell *et al.*, 2008). *Salmonella* may also use Hyd-5 to oxidise hydrogen for the purpose of conserving energy or to remove oxygen from the environment by reduction (Zbell *et al.*, 2008). As *Salmonella* will make numerous transitions from aerobic to anaerobic environments, the possession of hydrogenase enzymes that function in different conditions will extremely advantageous to this pathogen.

Although efforts are being made to fully understand hydrogenase activity for biotechnological advancement, the importance of these enzymes to the colonisation and virulence of some pathogens have implications for human health. As multi-drug resistance is increasing and our armoury of antibiotics is weakening, the design of hydrogenase inhibitors would be a welcome antimicrobial addition.

1.7 Aims

The overall aims of this work are to gain new insight into the mechanism of assembly of [NiFe]-hydrogenases from *Escherichia coli*, and to initiate a new project focussed on understanding [NiFe]-hydrogenase biosynthesis in *Salmonella*. In particular, the roles of twin-arginine signal peptides and specialised accessory proteins in the assembly of oxygen-tolerant, and aerobically expressed, [NiFe] hydrogenases will be investigated.

The specific objectives are:

1. To examine the role of the Tat signal peptide n-region in the biosynthesis of *Escherichia coli* Hyd-1, an oxygen-tolerant hydrogenase.

2. To explore the structure and function of the aerobically-expressed Hyd-5 isoenzyme from *Salmonella enterica*.

3. To investigate the involvement of specific accessory proteins in the assembly of *Salmonella* Hyd-5.

2 The role of the signal peptide in assembly of an oxygen-tolerant [NiFe]-hydrogenase from *Escherichia coli*

2.1 Introduction

Escherichia coli Hyd-1 and Hyd-2 are known Tat substrates and although Hyd-1 and Hyd-2 share a number of functional and structural similarities, a key difference between the two is that Hyd-1 is oxygen-tolerant whereas Hyd-2 is not (Lukey *et al.*, 2010). Both of these hydrogenase enzymes are synthesised as precursors in the cytoplasm with N-terminal signal peptides bearing twin-arginine motifs. [NiFe]-hydrogenase signal peptides share the structural characteristics common to all Tat signal peptides and include a polar N-terminus ('n-region'), a hydrophobic 'h-region' and a polar C-terminus ('c-region') containing an AxA cleavage site. The twin-arginine motif is, as always, found between the n-region and the h-region (Palmer and Berks, 2012). Both uptake hydrogenases are heterodimers consisting of a large and a small subunit. Interestingly, only the small subunit displays a signal peptide (Vignais and Billoud, 2007).

Signal peptides from [NiFe]-hydrogenases have played important roles in defining the function of the bacterial Tat pathway. The signal peptide from the *Desulfovibrio vulgaris* [NiFe]-hydrogenase, for example, was the first to be mutated to show the importance of the twin-arginine motif in protein transport (Niviere *et al.*, 1992). Further studies in *Ralstonia eutropha* and *Wolinella succinogenes* reinforced this observation (Bernhard *et al.*, 1996; Gross *et al.*, 1999). However, the signal peptides of [NiFe]-hydrogenases have functions beyond simply targeting of the enzyme. Studies have implicated these signal peptides in the binding of biosynthetic chaperones (Dubini and Sargent, 2003; Schubert *et al.*, 2007). Through the use of bacterial two-hybrid assays, Dubini *et al.* (2003) demonstrated binding of the accessory protein HyaE to the precursor form of HyaA, the small subunit of *E. coli* Hyd-1. In the same study, HybE was found to bind the precursor form of HybO, the small subunit of *E. coli* Hyd-2 but also exhibited binding to precursor HybC, the large subunit of Hyd-2 (Dubini and Sargent, 2003). The chaperone proteins HoxO (HyaE homolog) and HoxQ (HyaF homolog) from *R. eutropha* were shown to form a complex with the precursor form of the small subunit HoxK. Furthermore, both proteins were capable of interacting with a chemically synthesised version of the HoxK Tat signal peptide (Schubert *et al.*, 2007).

Figure 2.1. Sequence alignment of Tat signal peptides from oxygen-tolerant [NiFe]-hydrogenase.

Black shading highlights identical residues shared between 50% of the sequences; grey shading highlights conservative substitutions of these whereas residues in white indicate non-conserved amino acids. Sequences are taken from the Tat signal peptides of *E. coli* (ec) and *Salmonella* (st) uptake hydrogenases as well as from the membrane hydrogenases (Mbh) from *Ralstonia eutropha* (re), *Aquifex aeolicus* (aa) and *Hydrogenovibrio marinus* (hm).

[NiFe]-hydrogenases have unusually long signal peptides with greatly extended n-regions and exhibit remarkable sequence conservation (Berks *et al.*, 2000), which is not restricted to the twin-arginine motif (Figure 2.1). Hyd-1 from *E. coli* and Hyd-1 and Hyd-5 from *Salmonella enterica* serovar Typhimurium are similar oxygen-tolerant enzymes that share conserved residues throughout their signal peptides. An extended comparison with other signal peptides from the oxygen-tolerant class of hydrogenases again highlights the high number of conserved residues shared between enzymes of similar function (Figure 2.1). However, when the Tat signal peptides of standard [NiFe]-hydrogenases are brought in, including those of HybO from *E. coli* and *Salmonella*, clear differences begin to manifest themselves (Figure 2.2) Comparing these sequences with the Hyd-1 and Hyd-5 sequences reveals differences in the composition of the n-region in particular. This could be an indication that the region has an important role to play in hydrogenase biosynthesis and/or targeting that may be specific to enzymes performing a particular function.

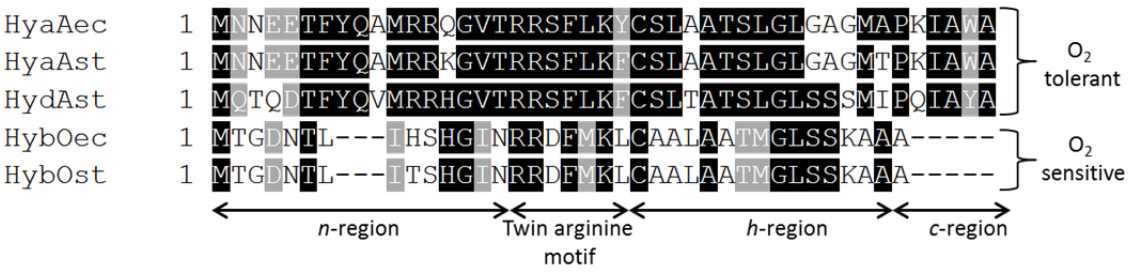

Figure 2.2. Sequence alignment of uptake hydrogenase signal peptides from *E. coli* and *Salmonella*.

Black shading highlights identical residues shared between 50% of the sequences; grey shading highlights conservative substitutions of these whereas residues in white indicate non-conserved amino acids. Sequences are taken from the Tat signal peptides of *E. coli* (ec) and *Salmonella* (st) uptake hydrogenases. Oxygen tolerance and sensitivity of the respective enzymes are indicated at the right of the figure.

2.2 Aims

The aim of this Section was to better understand the role of the signal peptide in the biosynthesis of *E. coli* Hyd-1. Understanding the assembly of Hyd-1 is of particular interest due to its ability to oxidise hydrogen under aerobic conditions. [NiFe]-hydrogenase Tat signal peptides are quite unusual and possess elongated n-regions. The role of the extended n-region is unknown and has not been extensively studied. Efforts have been made here to determine the role of the n-region and its importance in enzyme assembly.

2.3 Results

2.3.1 Investigating the role of the n-region

In an attempt to better understand the assembly and targeting of *E. coli* Hyd-1, investigations were made into the signal peptide. In particular, the role of the unusually long and conserved n-region has been studied. Hyd-1 is a sophisticated metalloenzyme and undergoes a very complex biosynthetic process requiring the involvement of many genes and biosynthetic pathways. The small subunit (HyaA) is initially synthesised in the cytoplasm as a precursor complete with signal peptide. The Fe-S clusters must be incorporated into HyaA before the large subunit (HyaB) containing the [NiFe] metallocentre can join to form the hydrogenase heterodimer. C-terminal proteolytic processing of the large subunit renders this interaction irreversible. The enzyme is then targeted to the Tat machinery and translocated *via* the Tat pathway before being integrated into the membrane (Vignais and Billoud, 2007).

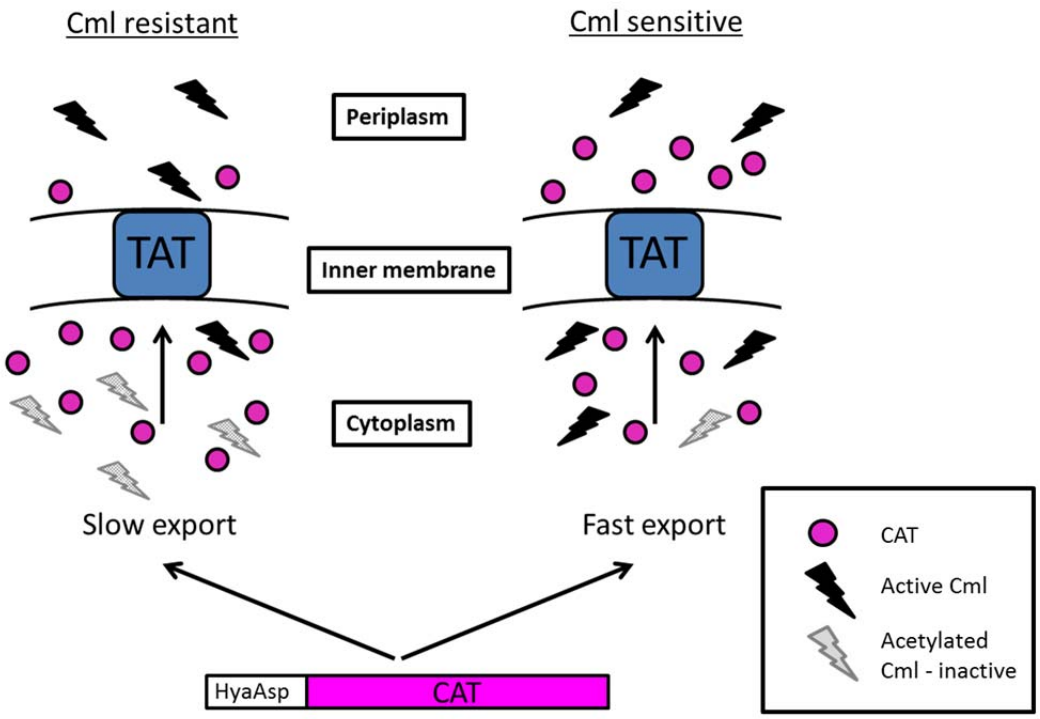

Figure 2.3. Diagram of signal peptide targeted CAT transport.

Inefficient Tat transport results in accumulation of CAT in the cytoplasm and inactivation of chloramphenicol by acetylation. Efficient export of the signal peptide fused reporter results in antibiotic sensitivity as the cell is incapable of inactivating Cm.

Due to the complexity of this process, it was decided that the Hyd-1 signal peptide would be analysed in isolation from the enzyme and fused to a reporter protein, chloramphenicol acetyl transferase (CAT). Previous studies using fusions between this reporter and various twin-arginine signal peptides have shown that CAT is exported solely by the Tat system and cannot default to the Sec pathway. CAT deactivates chloramphenicol (Cml) using acetyl coenzyme-A (Co-A) that acetylates the antibiotic. Acetyl Co-A only exists within the cell cytoplasm so this reaction cannot occur in the periplasm (Stanley *et al.*, 2002; Hicks *et al.*, 2005). Therefore, cells that export CAT fusions efficiently out of the cytoplasm are sensitive to the antibiotic, whereas retarded export results in antibiotic inactivation and cell survival (Figure 2.3).

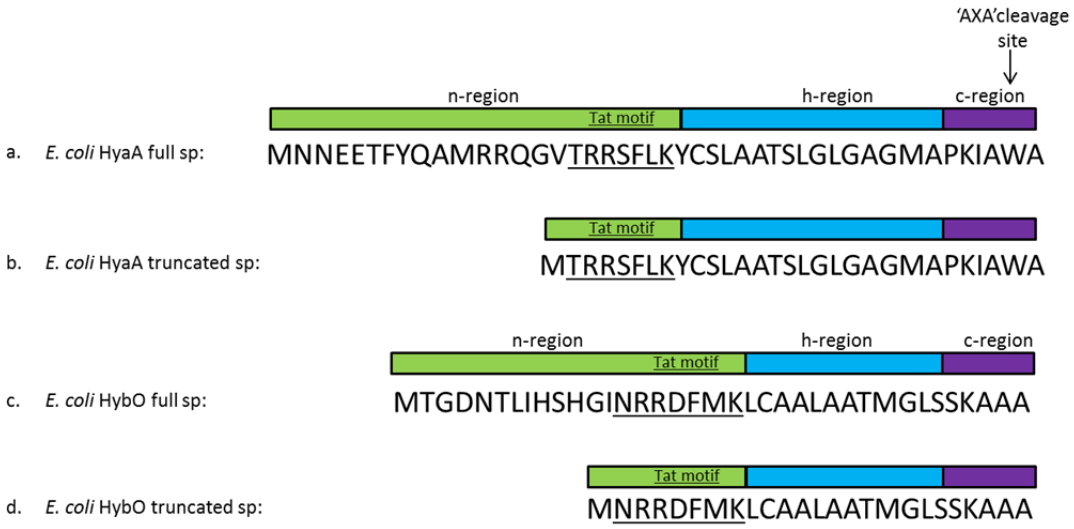

Figure 2.4. The structure and sequence of the full-length and truncated hydrogenase signal peptides.

(a) The full signal peptide of *E. coli* Hydrogenase-1 (encoded by pUniCAT-HyaA). The signal peptide shares the tripartite structure characteristic of all Tat signal peptides, comprising of a polar n-region at the N-terminus, a hydrophobic h-region and a c-region containing the signal peptide cleavage site. The Tat motif is situated at the boundary between the n- and h-regions. **(b)** The signal peptide of *E. coli* Hydrogenase-1 lacking its n-region (encoded by pUniCAT-HyaAsstrunc). **(c)** The full signal peptide of *E. coli* Hydrogenase-2 (encoded by pUniCAT-HybO). **(d)** The signal peptide of *E. coli* Hydrogenase-2 lacking its n-region (encoded by pUniCAT-HybOsstrunc).

In order to better understand the function of the [NiFe]-hydrogenase signal peptide, fusions to the reporter protein CAT were investigated. Previously constructed HyaA- and HybO-CAT signal peptide fusion vectors were used initially to determine whether or not varying the structure of the signal peptides would have any effect on overall transport efficiency. The CAT assay acts as a negative transport test. Cells with

active CAT present in the cytoplasm are resistant to the antibiotic chloramphenicol. If CAT is transported out of the cell cytoplasm and into the periplasm the cell will become sensitive to chloramphenicol. The pUniCAT-HyaA and pUniCAT-HybO plasmids encode the full HyaA/HybO signal sequences fused to CAT (Figure 2.4), whereas pUniREP-HyaAlong and pUniCATHybOlong encode the full HyaA/HybO signal sequence plus part of the mature protein sequence fused to CAT. The pUniCAT-HyaAsstrunc and pUniCat-HybOsstrunc plasmids are the final two fusion vectors and encode truncated signal peptides where the n-region has been removed (Figure 2.4).

2.3.2 A truncated HyaA signal peptide is more efficient at reporter protein transport

Plate tests were used initially to determine the efficiency of reporter transport. MG1655 cells (*E. coli* wild-type with an active Tat translocase, *tat*$^{+}$) were transformed separately with the set of vectors encoding signal peptide fusions to the CAT protein. Strains expressing these fusions were streaked out onto solid media plates, supplemented with increasing concentrations of chloramphenicol. MG1655 expressing CAT without a Tat signal peptide fusion (pUniREP) was used as positive control. Without a signal peptide, CAT persists in the cytoplasm and confers antibiotic resistance to the cell. MG1655 was used as a negative control. Results of the plate tests are presented in Figure 2.5.

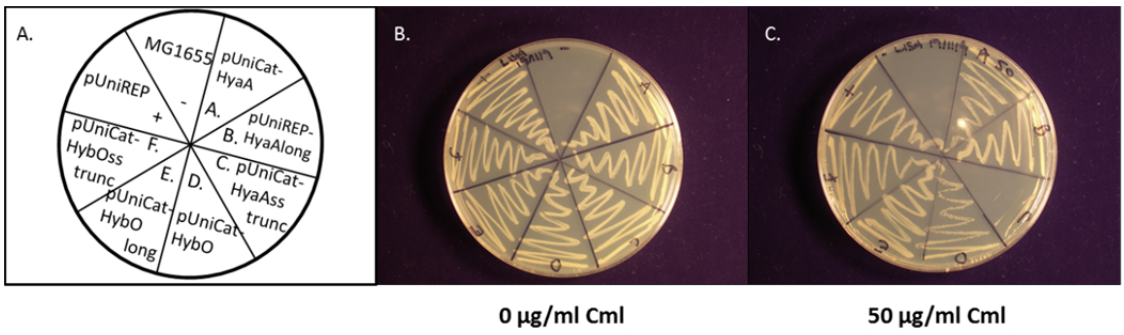

Figure 2.5. Plate tests suggest that varying signal peptide structure can affect transport efficiency.

(a) The plates were split into eight segments and each transformed strain, positive and negative control streaked into a segment as depicted. MG1655 cells were transformed individually with one of the fusion vectors and streaked out onto LB-agar supplemented with **(b)** ampicillin only and onto LB-agar supplemented with **(c)** ampicillin and 50 µg/ml chloramphenicol.

When chloramphenicol was omitted from the agar, all cells grew well (no selective pressure) except for MG1655, which is sensitive to the ampicillin used to select for pUniREP transformed cells. When chloramphenicol was supplemented at a concentration of 50 µg/ml, one of the transformed cell types was clearly sensitive to the antibiotic. The signal peptide that appeared to be most efficient at exporting CAT to the periplasm, and thus rendering the cell sensitive to chloramphenicol, belonged to Hyd-1 and was lacking the n-region. As mentioned before, n-regions of hydrogenase signal peptides are unusually long and contain conserved amino acids, but the biological role of this region is currently unknown. A comparison between the truncated signal peptides and the full length signal peptides is depicted in Figure 2.4. Varying the Hyd-2 signal peptide structure did not result in any growth defect on the chloramphenicol supplemented agar plates so was not investigated further.

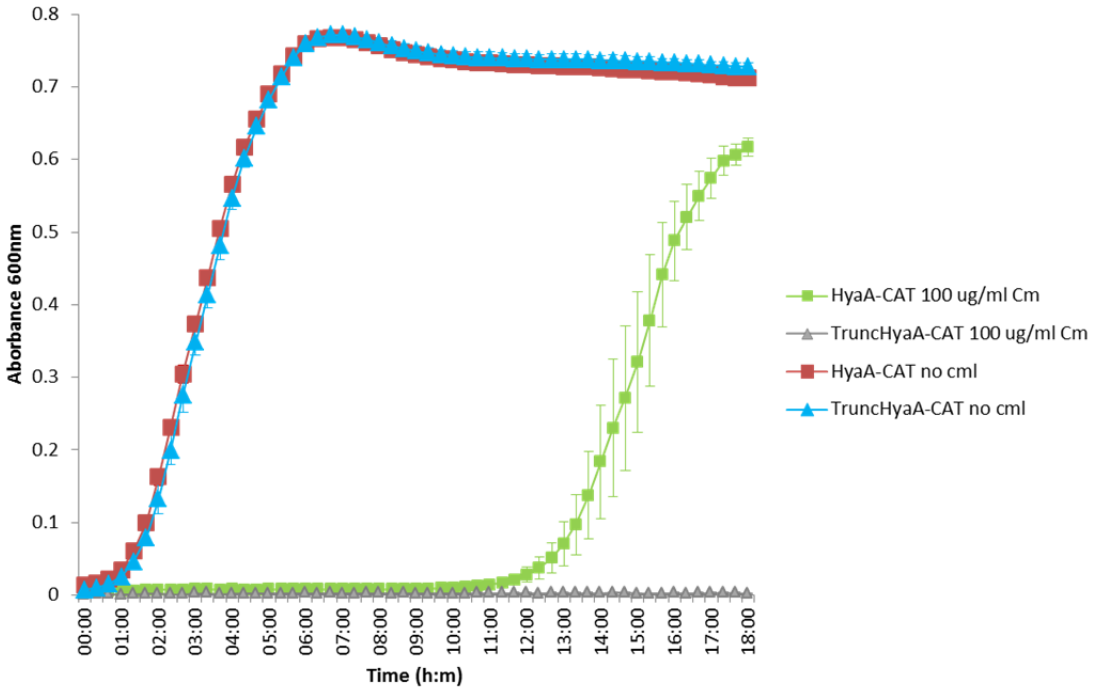

Figure 2.6. Liquid growth tests verify that varying signal peptide structure can affect transport efficiency.
MG1655 cells were transformed separately with HyaA-CAT and TruncHyaA-CAT. Cells were grown in rich media supplemented with ampicillin only or with ampicillin and 100 ug/ml chloramphenicol. Absorbance was measured at 600nm, every 20 minutes, over a period of 18 hours in three independent experiments. Error bars indicate standard error of the mean.

In order to validate these initial findings, a liquid media growth test was performed. MG1655 (*tat*$^+$) cells expressing either the full length signal peptide CAT fusion (HyaA-CAT) or the 'truncated' signal peptide CAT fusion (TruncHyaA-CAT) were

grown in LB medium with or without the addition of chloramphenicol. In media without added chloramphenicol, the two cell types grew well and similarly to one another (Figure 2.6). In media supplemented with 100 μg/ml chloramphenicol, cells expressing HyaA-CAT grew eventually but only after a very long lag phase (Figure 2.6). Cells expressing the TruncHyaA-CAT fusion vector did not grow in the presence of the antibiotic (Figure 2.6). The results of this experiment imply that the truncated signal peptide is more efficient at transporting the reporter out of the cytoplasm and verify the results obtained from previous plate tests.

To establish the subcellular localisation of CAT within the cell, fractionations were performed on cells expressing the fusion vectors and on MG1655 as a control. Whole cell, periplasm and sphaeroplast fractions were separated by SDS-PAGE, immunoblotted and CAT detected using an antibody specific to CAT (Figure 2.7). The molecular weight difference between the precursor (30.6 kDa for HyaA-CAT and 28.8 kDa for TruncHyaA-CAT) and the mature form (25.6 kDa) is sufficient to allow detection of both forms of the protein when analysed following SDS-PAGE. Qualitative analysis of the Western blot suggests that the CAT protein is present at similar levels in cells expressing HyaA-CAT or TruncHyaA-CAT. Less CAT remained in the sphaeroplast fraction of the strain expressing TruncHyaA-CAT than in the sphaeroplasts of cells expressing the full length signal peptide (Figure 2.7). The increased levels of precursor (and perhaps signal-degraded fusion protein) that was visible when analysing cells expressing full-length HyaA-CAT would account for the increased resistance of these cells to chloramphenicol.

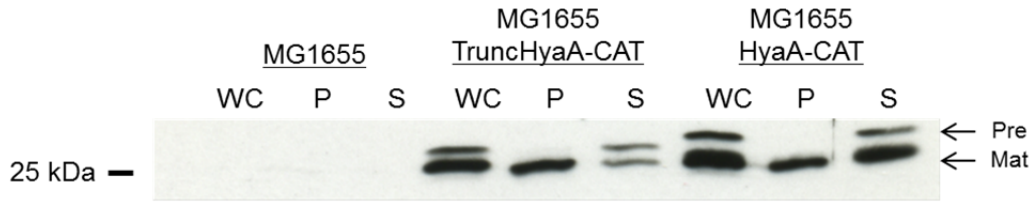

Figure 2.7. Cellular localisation of CAT.

MG1655 cells were transformed with TruncHyaA-CAT and HyaA-CAT. Cells were grown aerobically in LB media supplemented with 0.5% glycerol for 3.5 hours. Whole cell, periplasm and sphaeroplast fractions were separated by SDS-PAGE, immunoblotted and CAT detected using a CAT specific antibody. Fractionation of MG1655 cells was performed as a control. WC = whole cell, P = periplasm, S = sphaeroplast, Pre = precursor, Mat = mature.

2.3.3 The signal peptide n-region regulates the rate or efficiency of protein transport

The next aim of the project was to obtain more quantitative results. To analyse the rate of protein export, pulse-chase experiments were performed. Put briefly, K38[pGP1-2] cells are transformed with a fusion vector, where expression of the gene of interest is under control of the T7 promoter. A temperature increase induces expression of the T7 polymerase (encoded on pGP1-2) and rifampicin is added to block transcription from *E. coli* promoters. Cells are pulsed with radiolabelled [^{35}S]-methionine, which becomes incorporated into the translated protein. Labelled methionine is then 'chased' with unlabelled methionine, allowing protein processing to be followed. Samples from specified time points are then analysed by SDS-PAGE followed by autoradiography.

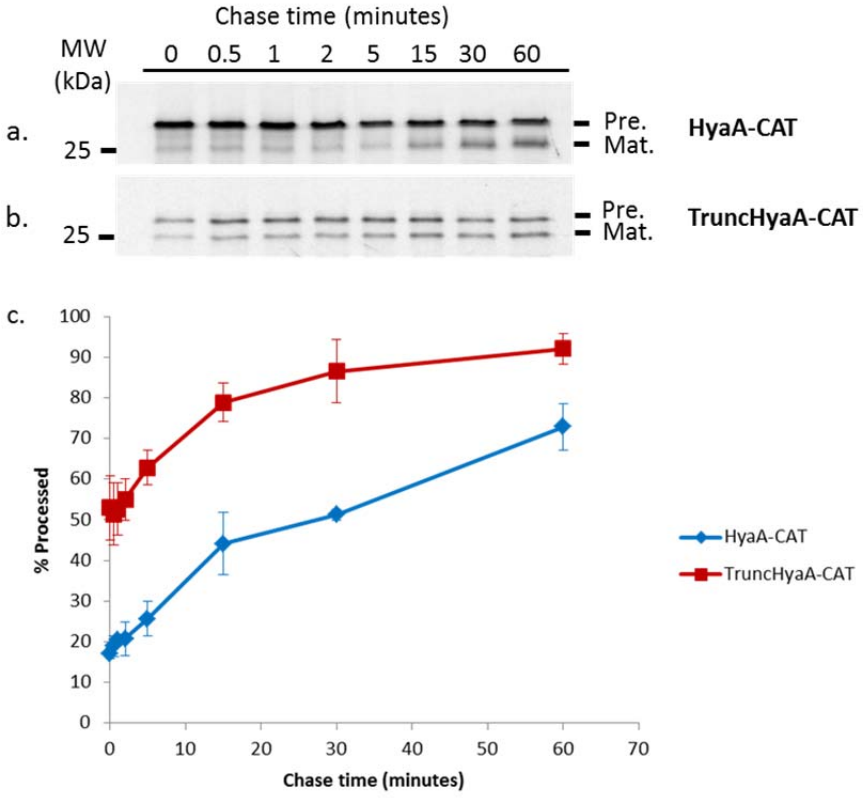

Figure 2.8. Pulse-chase analysis of chloramphenicol acetyl transferase (CAT) export.

K38[pGp1-2] cells expressing CAT fusion signal peptides were radioactively pulse labelled with ^{35}[S] methionine for two minutes and then chased with unlabelled methionine for a total of 60 minutes. Samples were removed at specified time points, and protein processing analysed using SDS-PAGE followed by autoradiography. Autoradiographs of **(a)** HyaA-CAT and **(b)** TruncHyA-CAT processing are shown. **(c)** Autoradiographs were quantified using QuantityOne software and are based on three independent experiments. The standard error of the mean is shown for each time point.

Over the course of the experiment, the labelled protein with a mass corresponding to that of the precursor protein is processed to its smaller mature form. CAT was however, never processed to completion. Chase time was extended from 60 to 90 minutes but processing remained incomplete (not shown). Using this method, it was established that the truncated signal peptide, when fused to CAT, does appear to be more efficient at transporting the reporter protein into the periplasm than the full length signal peptide (Figure 2.8a and b). In fact, within half a minute, it appears that almost 50% of the labelled protein is processed. Autoradiographs were quantified using Quantity One software (Figure 2.8c). Quantification verifies that there is a clear and immediate difference in processing rate that is dependent on the presence of the n-region. From these results, it is clear that processing and export is purposely slowed when the full length signal peptide is present.

2.3.4 Amino acid substitutions in the n-region affect the rate of CAT export

With the aim of elucidating important amino acid residues within the n-region of the HyaA signal peptide, individual amino acid substitutions were introduced using site directed mutagenesis. Each amino acid residue of the n-region, from Asn2 to Val16, was substituted with a bulky tryptophan residue with the intention of disrupting any putative protein-protein interactions that may be occurring. Schubert *et al.* (2007) identified the n-region as a potential site for chaperone binding as its deletion disrupted complex formation between precursor HoxK and the two chaperones HoxO and HoxQ. If disruption to the structure and function of the n-region is indeed caused, it might be possible to replicate the increased export rate observed when the signal peptide n-region is completely removed. Alternatively, major disruptions may abolish protein export. The resulting signal peptides are designated so that the native amino acid precedes the position and the substituting amino acid. For example HyaAN2W-CAT is a fusion vector where the asparagine residue at position 2 of the signal peptide is substituted with a tryptophan residue. All substitution fusion vectors were checked for expression of CAT by Western immunoblotting (data not shown).

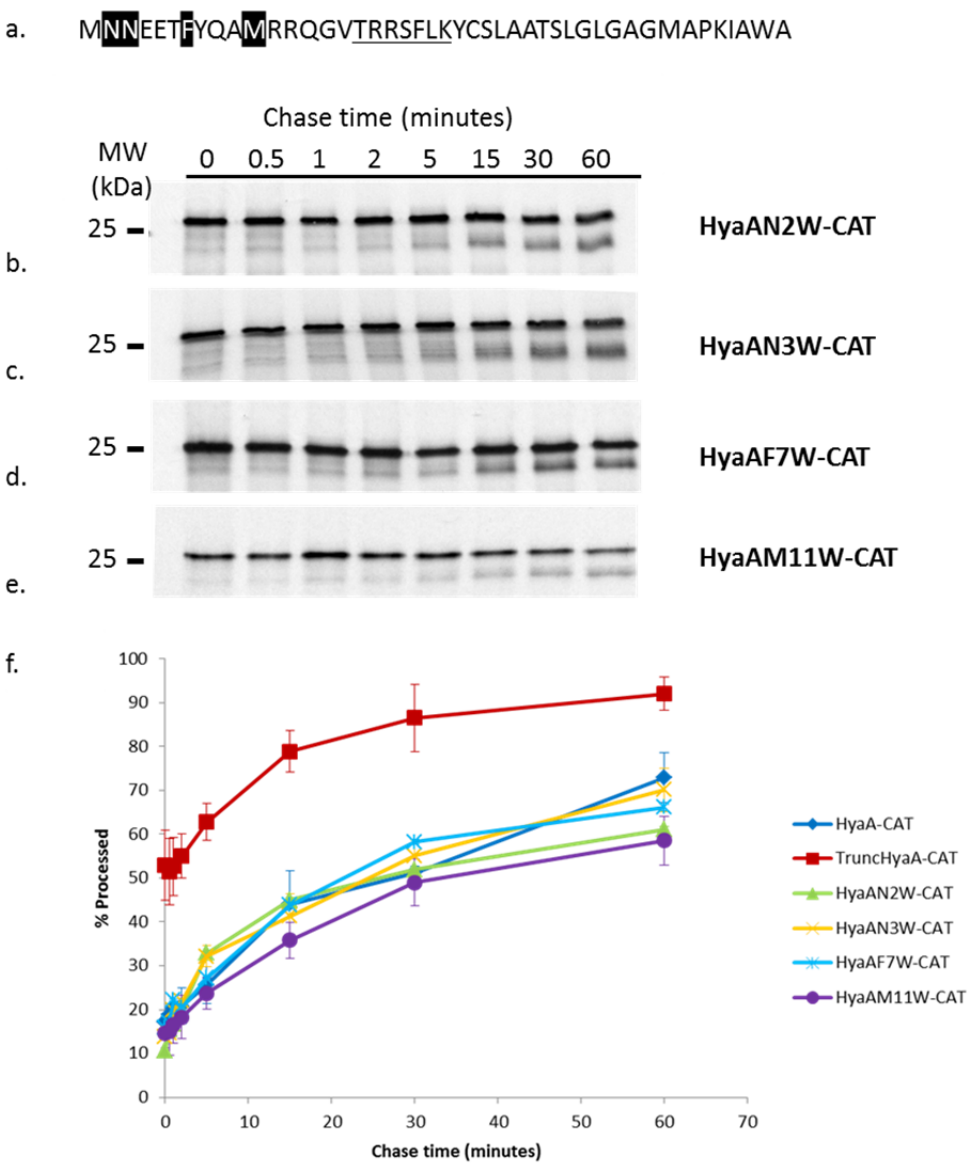

Figure 2.9. CAT export was unaffected by some signal peptide amino acid substitutions.

K38[pGp1-2] cells expressing CAT fusion signal peptides were radioactively pulse labelled with ^{35}[S] methionine for two minutes and then chased with unlabelled methionine for a total of 60 minutes. Samples were removed at specified time points, and protein processing analysed using SDS-PAGE followed by autoradiography. **(a)** The Hyd-1 Tat signal sequence is shown with amino acid substitutions highlighted in black. Autoradiographs of **(b)** HyaAN2W, **(c)** HyaAN3W-CAT, **(d)** HyaAF7W and **(e)** HyaAM11W-CAT processing are shown. **(f)** Autoradiographs were quantified using QuantityOne software and are based on three independent experiments. The standard error of the mean is shown for each time point. CAT export from HyaA-CAT and TruncHyaA-CAT are compared with CAT export from the signal peptides carrying substitutions.

K38[pGP1-2] cells were transformed separately with the fusion vectors and the effects of the substitutions assessed by performing further pulse-chase experiments. A number of amino acid substitutions did not result in any significant difference in CAT export when compared with the full length signal peptide (Figure 2.9). Amino acids Asn2, Asn3, Phe7 and Met11 did not appear to impact the rate of CAT processing.

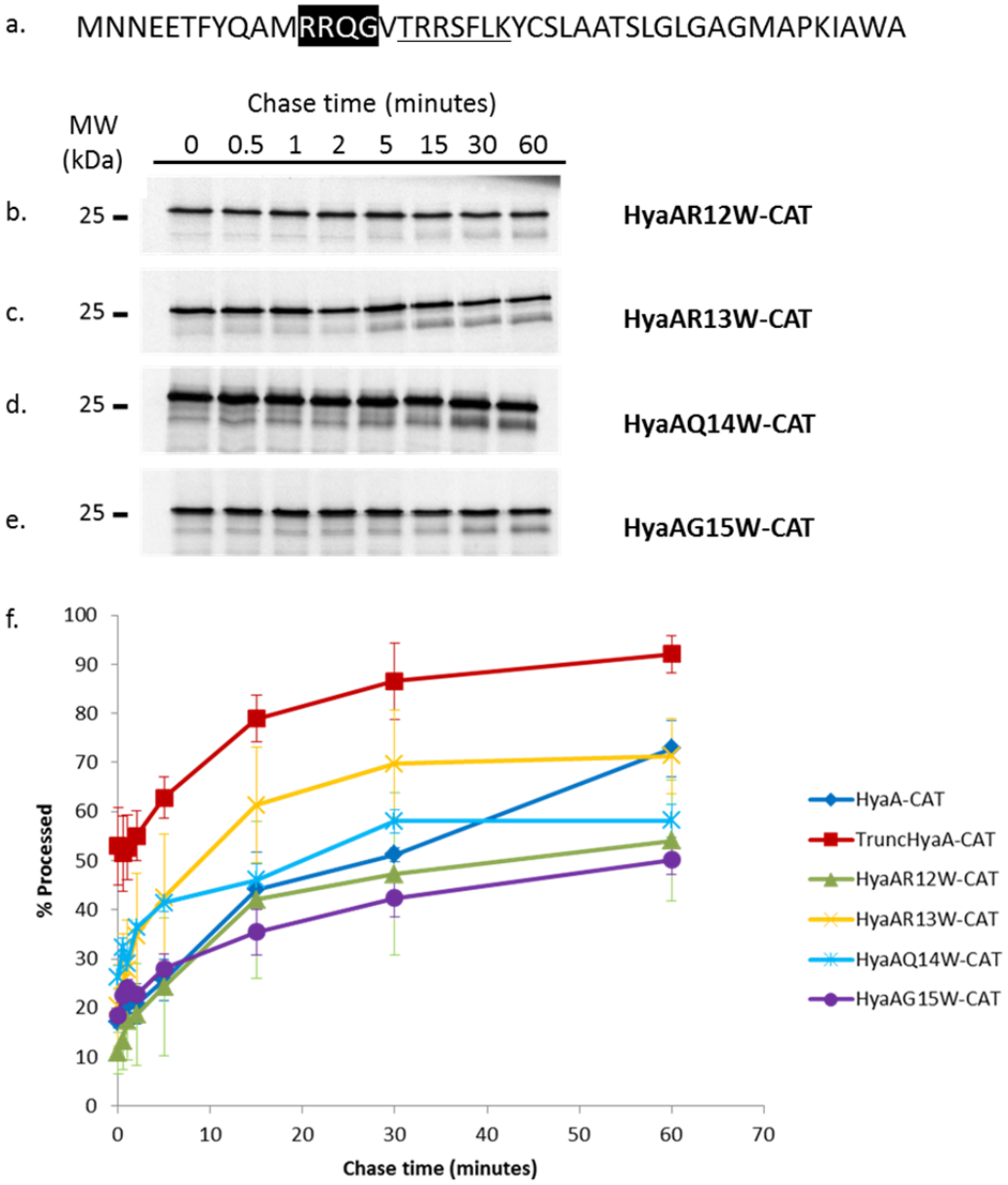

Figure 2.10. Substituting Arg13 for tryptophan leads to an increase in the initial rate of processing whereas Arg12, Gln14 and Gly15 substitution do not greatly impact the rate of CAT processing.

K38[pGp1-2] cells expressing CAT fusion signal peptides were radioactively pulse labelled with ^{35}[S] methionine for two minutes and then chased with unlabelled methionine for a total of 60 minutes. Samples were removed at specified time points, and protein processing analysed using SDS-PAGE followed by autoradiography. **(a)** The Hyd-1 Tat signal sequence is shown with amino acid substitutions highlighted in black. Autoradiographs of **(b)** HyaAR12W, **(c)** HyaAR13W-CAT, **(d)** HyaAQ14W and **(e)** HyaAG15W-CAT processing are shown. **(f)** Autoradiograph bands were quantified using QuantityOne software and are based on three independent experiments. The standard error of the mean is shown for each time point. CAT export from HyaA-CAT and TruncHyaA-CAT are compared with CAT export from the signal peptides carrying substitutions.

The amino acids, Arg12, Arg13, Gln14 and Gly15 when substituted with tryptophan, demonstrated export rates similar to that of HyaA-CAT (Figure 2.10). One of the substitutions however did appear to affect the early processing of the reporter

protein. This was the substitution of Arg13, which resulted in a slightly faster initial rate of processing until it reached a plateau of processing similar to that of HyaA-CAT (Figure 2.10). Arg13 is highly conserved between the signal peptides of oxygen-tolerant [NiFe]-hydrogenases (Figure 2.1) and may be an important residue for the function of the n-region.

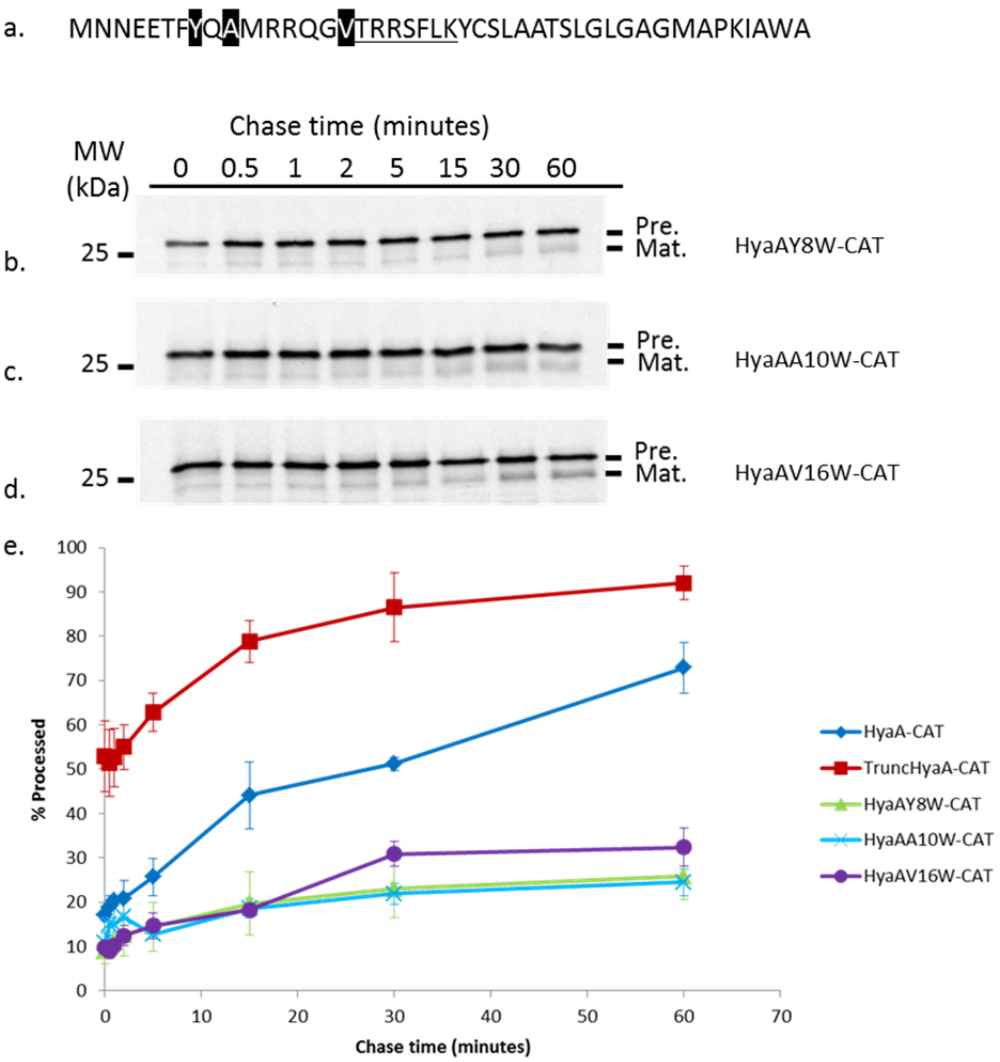

Figure 2.11. Tyr8, Ala10 and Val16 substitutions severely retarded CAT export.

K38[pGp1-2] cells expressing CAT fusion signal peptides were radioactively pulse labelled with ^{35}[S] methionine for two minutes and then chased with unlabelled methionine for a total of 60 minutes. Samples were removed at specified time points, and protein processing analysed using SDS-PAGE followed by autoradiography. **(a)** The Hyd-1 Tat signal sequence is shown with amino acid substitutions highlighted in black. Autoradiographs of **(b)** HyaAY8W, **(c)** HyaAA10W-CAT and **(d)** HyaAV16W processing are shown. **(e)** Autoradiograph bands were quantified using QuantityOne software and are based on three independent experiments. The standard error of the mean is shown for each time point. CAT export from HyaA-CAT and TruncHyaA-CAT are compared with CAT export from the signal peptides carrying substitutions.

There were a number of substitutions however that appeared to severely impede export of CAT. Substituting Tyr8, Ala10 and Val16 with tryptophan almost completely abolished processing of the reporter protein (Figure 2.11). Processing barely began so that the percentage of processed protein at each time point resembles that of time zero. The signal sequence alignment between homologous enzymes (Figure 2.1) highlights Tyr8 as a highly conserved amino acid. The only hydrogenase with an alternative residue to tryrosine at position 8 is that from *Aquifex aeolicus*, a thermophile. Here, the residue has already been substituted for a tryptophan (Figure 2.1). There are, however, further differences within the h-region between the *Aquifex* hydrogenase Tat signal peptide and those of other oxygen-tolerant hydrogenases (Figure 2.1).

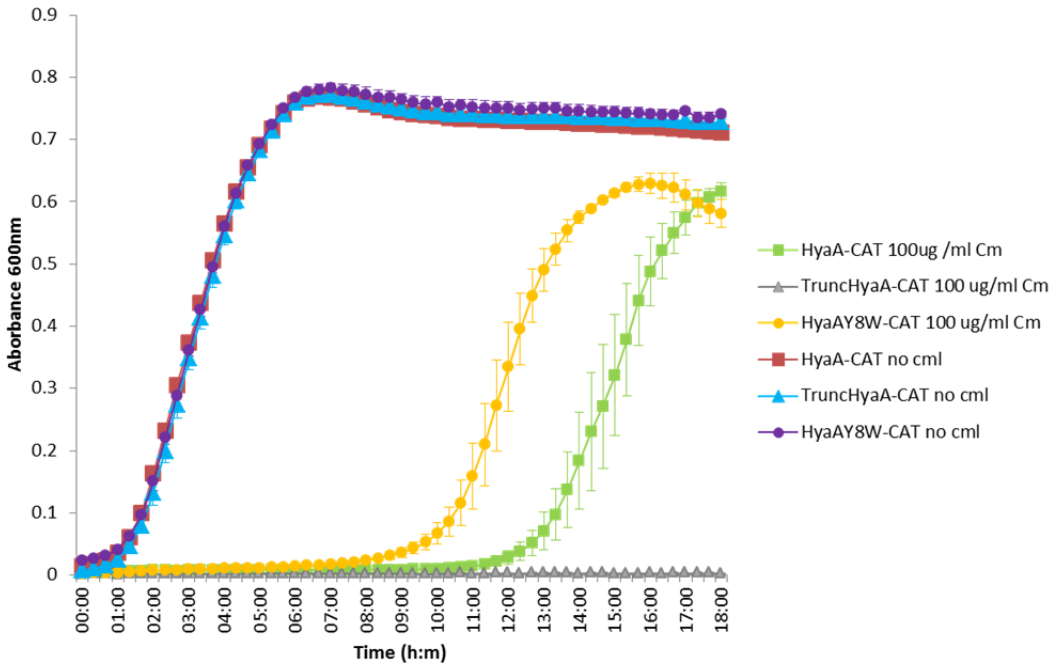

Figure 2.12. Substituting Tyr8 with tryptophan results in reduced CAT transport.

MG1655 cells were transformed separately with HyaA-CAT, TruncHyaA-CAT and HyaAY8W-CAT. Cells were grown in rich media supplemented with ampicillin or with ampicillin and 100 ug/ml chloramphenicol. Absorbance was measured at 600nm, every 20 minutes, over a period of 18 hours in three independent experiments. Error bars indicate standard error of the mean.

MG1655 cells expressing the HyaAY8W-CAT fusion vector were subjected to a liquid media assay to determine if this signal peptide truly was less efficient at exporting CAT. With no added chloramphenicol, cells expressing HyaAY8W-CAT grew well and similarly to cells expressing HyaA-CAT and TruncHyaA-CAT. When the media

was supplemented with 100 ug/ml chloramphenicol, MG1655 expressing HyaAY8W exhibited a similar lag phase to cells expressing the full length signal peptide fusion but entered exponential phase at an earlier time point. This implies that the HyaAY8W signal peptide is less efficient at exporting CAT. CAT is retained within the cytoplasm and thus confers resistance to chloramphenicol (Figure 2.12).

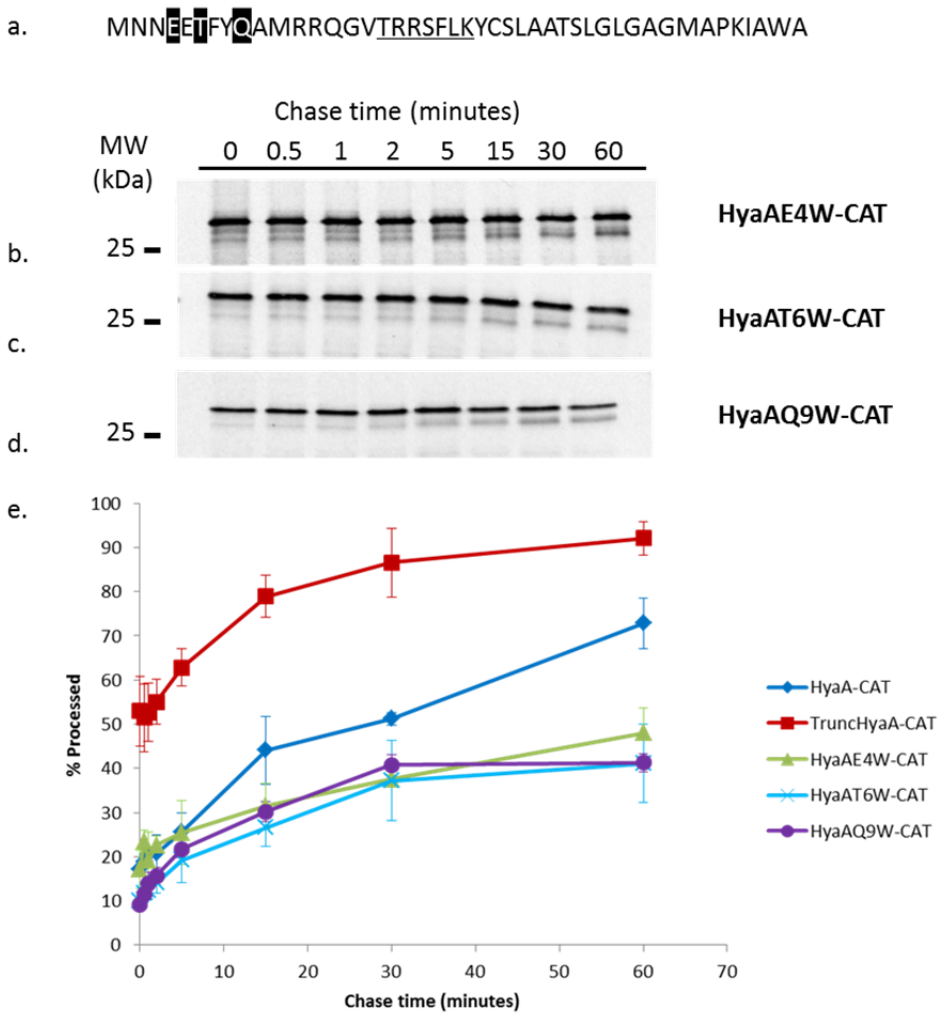

Figure 2.13. Substituting Glu4, Thr6 and Gln9 with tryptophan reduced the rate of CAT export.
K38[pGp1-2] cells expressing CAT fusion signal peptides were radioactively pulse labelled with ^{35}[S] methionine for two minutes and then chased with unlabelled methionine for a total of 60 minutes. Samples were removed at specified time points, and protein processing analysed using SDS-PAGE followed by autoradiography. **(a)** The Hyd-1 Tat signal sequence with amino acid substitutions highlighted in black. Autoradiographs of **(b)** HyaAE4W, **(c)** HyaAT6W-CAT and **(d)** HyaAQ9W processing are shown. **(e)** Autoradiograph bands were quantified using QuantityOne software and are based on three independent experiments. The standard error of the mean is shown for each time point. CAT export from HyaA-CAT and TruncHyaA-CAT are compared with CAT export from the signal peptides carrying substitutions.

A number of other amino acid substitutions resulted in slow CAT export (Figure 2.13). Substituting Glu4, Thr6 and Gln9 with tryptophan affected the rate of protein

processing. Thr6 is completely conserved among the five homologous enzyme signal peptides chosen in the introduction (Figure 2.1). Glu4 is only conserved between Hyd-1 of *E. coli* and *Salmonella*. Gln9 is also conserved between Hyd-1 of *E. coli* and *Salmonella* but is also found in the signal peptide of *Salmonella* Hyd-5.

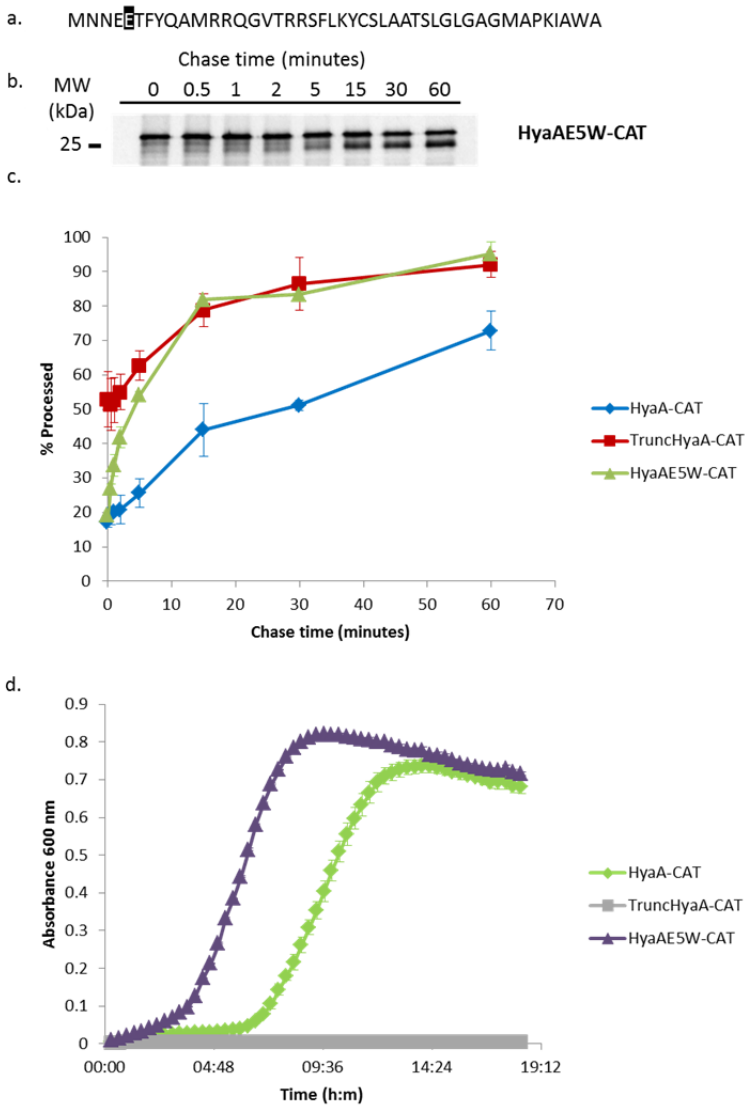

Figure 2.14. Substituting Glu5 with tryptophan leads to a degradation of the signal peptide in the cytoplasm.
K38[pGp1-2] cells expressing CAT fusion signal peptides were radioactively pulse labelled with ^{35}[S] methionine for two minutes and then chased with unlabelled methionine for a total of 60 minutes. Samples were removed at specified time points, and protein processing analysed using SDS-PAGE followed by autoradiography. **(a)** The Hyd-1 Tat signal sequence with amino acid substitution highlighted in black. **(b)** An autoradiograph of HyaAE5W is shown. **(c)** Autoradiograph bands were quantified using QuantityOne software and are based on three independent experiments. The standard error of the mean is shown for each time point. CAT export from HyaA-CAT and TruncHyaA-CAT are compared with CAT export from the signal peptides carrying substitutions. **(d)** MG1655 cells were transformed separately with HyaA-CAT, TruncHyaA-CAT and HyaAY8W-CAT. Cells were grown in rich media supplemented with ampicillin and 75 µg/ml chloramphenicol. Absorbance was measured at 600nm, every 20 minutes, over a period of 18 hours. Error bars indicate standard error of the mean.

One of the variant signal peptides, HyaAE5W, appeared to act similarly to the truncated signal peptide and apparently demonstrated the same rate of processing (Figure 2.14a, b and c). Unfortunately, further experiments using this fusion revealed that the signal peptide was probably degraded in the cytoplasm (Figure 2.14d). In particular, cells expressing HyaAE5W-CAT grew well in the presence of chloramphenicol, better, in fact, than the full length signal peptide. This indicates that CAT has remained within the cell cytoplasm, thus conferring antibiotic resistance. If HyaAE5W truly behaved similarly to TruncHyaA-CAT, cells expressing the fusion vector would be unable to survive in the presence of chloramphenicol.

2.3.5 The signal peptide n-region is essential for stability of the Hyd-1 complex

So far, the experiments performed here have made use of an artificial system where the signal peptide is fused to a reporter protein. Investigations into the physiological role of the signal peptide, i.e. when attached to the native hydrogenase enzyme rather than the CAT reporter, were made next. DNA encoding the HyaA signal peptide lacking its n-region was synthesised along with 500 base pairs upstream and downstream of the region and suitable restriction sites incorporated to assist cloning. The synthetic region of DNA was cloned into the vector pMAK705, which facilitates the introduction of DNA sequences or deletions onto the chromosome *via* homologous recombination (Hamilton *et al.*, 1989). This method was used to introduce an allele encoding the n-region-deleted signal peptide onto the chromosome of strain IC009 (MC4100 Δ*hybC*, Δ*hycE*), which does not produce a functional Hyd-2 or Hyd-3 enzyme. The aim was to discover whether or not Hyd-1 is assembled when the signal peptide n-region is absent.

A new antibody specific to Hyd-1 was prepared for the purposes of this study. Membranes were isolated from the different strains and analysed by rocket immunoelectrophoresis. In this technique samples were loaded to small wells of an agarose gel containing Hyd-1 antisera and were then electrophoresed into the gel. As the protein migrates through the gel, the antibody binds and begins to form precipitin, which eventually stalls electrophoresis of the protein complex. The precipitin arcs can then be stained for hydrogenase activity following immersion of the gel in hydrogen saturated buffer containing BV and triphenyl tetrazolium chloride (Tetrazolium red or TTc), an activity indicator. While active Hyd-1 was detected in the membranes of

IC009, no detectable Hyd-1 activity was detected in the membranes of IC009 ΔNR (Δn-region [Figure 2.15]). No trace of activity was observed in the cytoplasm (not shown).

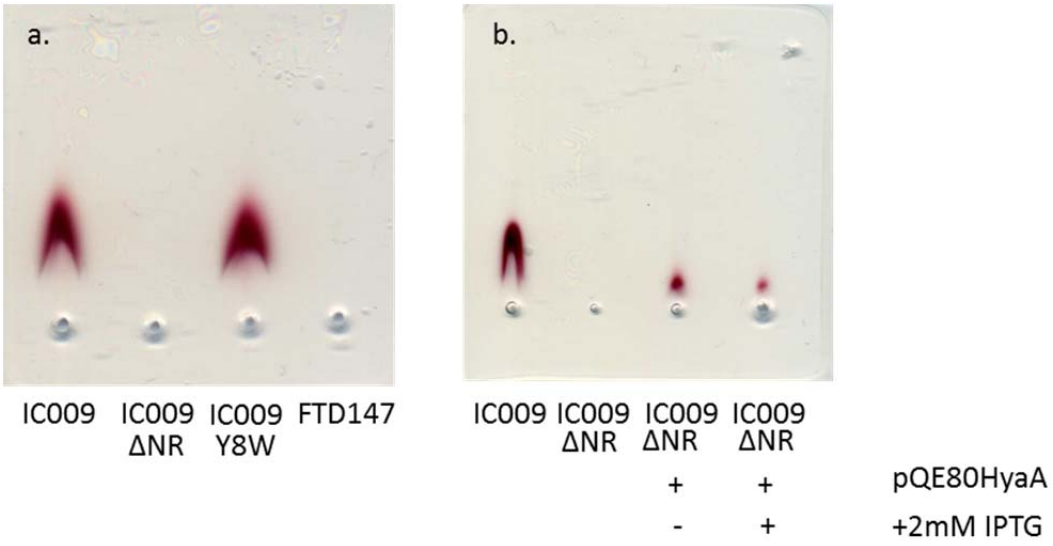

Figure 2.15. Hyd-1 activity is not present in the membranes of IC009 carrying the n-region deletion.
Strains were grown in rich media supplemented with 0.5% glycerol and 0.4% fumarate. Cells were harvested, lysed under pressure and membranes obtained. Membranes were solubilised using 4% Triton X-100 and electrophoresed through an agarose gel containing Hyd-1 antibody. Activity was stained using BV and TTc under hydrogen saturated conditions. **(a)** IC009, IC009 ΔNR, IC009 Y8W and FTD147 membranes were stained for activity. **(b)** Membranes from IC009 ΔNR expressing *hyaA* from pQE80 (grown with or without 2mM IPTG) were also stained for activity.

Next, Western immunoblotting was turned to in an attempt to localise Hyd-1 in the Δn-region strain. Unfortunately, the Hyd-1 antibody detects a number of non-specific protein bands and requires various methods of clean-up before use. For detection of the large subunit, it was sufficient to incubate the antibody with the crude extract of FTD147 (MC4100 Δ*hyaB* Δ*hybC*, Δ*hycE*) a strain deleted for the genes encoding the large subunits of all active hydrogenases, centrifuge to remove precipitates, and then use for immunoblotting. For detection of the small subunit, purified Hyd-1 was separated by SDS-PAGE, blotted, stained with ponceau and the section of nitrocellulose membrane containing the small subunit incubated with Hyd-1 antibody. An acidic glycine wash was then used to strip the antibody from the membrane, the pH increased to prevent denaturation and then used for immunoblotting.

The large subunit of Hyd-1 (HyaB) was detected in both the cytoplasm and membranes of IC009. In contrast, HyaB was only weakly detected in the cytoplasm of

IC009 when the n-region of the signal peptide was absent, and was completely missing from the membranes. Interestingly, as HyaB was detected in the cytoplasm as a faint band, this suggests that the subunit was being degraded or that there was an expression problem (Figure 2.16). The small subunit (HyaA) could not be detected in the cytoplasm of either strain but was present in the membranes of IC009. HyaA was not detected in the membranes of the n-region deletion strain (Figure 2.16). These results suggest that the n-region has an extremely important role in regulating the assembly of Hyd-1.

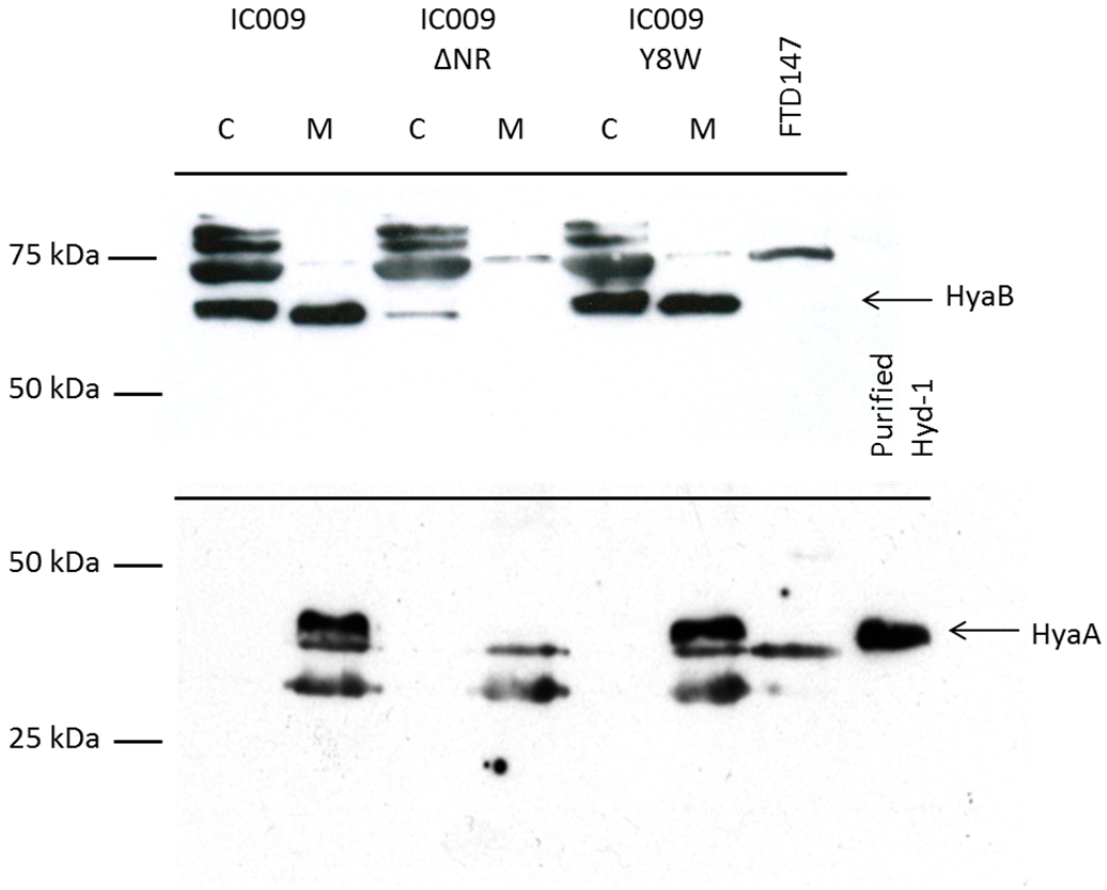

Figure 2.16. The n-region is important in regulating the export of Hyd-1.

Strains IC009, IC009 ΔNR and IC009 Y8W were grown anaerobically in rich media supplemented with 0.5% glycerol and 0.4% sodium fumarate before whole cells were harvested. Cells were lysed under pressure and cytoplasm (C) and membrane (M) fractions separated by SDS-PAGE. For identification of HydB, protein was separated on a 10% polyacrylamide gel. For detection of HydA, protein was separated on a 14% polyacrylamide gel. Western immunoblotting was performed using an antibody specific to Hyd-1. The large subunit (HyaB) was identified and unspecific bands ruled out by comparison with FTD147 (Δ*hyaB*, Δ*hybC*, Δ*hycE*) whole cells. The small subunit (HyaA) was identified, compared with FTD147 whole cells and run alongside HyaA purified from FTH004 (MC4100 *hya*A^{his}).

Efforts to complement the n-region deletion proved largely unsuccessful. DNA encoding the entire HyaA sequence (including the signal peptide), plus part of *hyaB*, was cloned into the IPTG inducible over-expression vector, pQE80. Membranes were obtained from IC009 ΔNR expressing *hyaA* from pQE80 either grown with or without the addition of 2 mM IPTG. Hyd-1 activity was then tested by rocket immunoelectrophoresis. A hint of Hyd-1 activity was detected from the strain regardless of the addition of IPTG but was not comparable to that of IC009 (Figure 2.15b). No hydrogenase activity was observed in the cytoplasm (not shown). Expressing *hyaA* from vectors pbluescript SK+ and pUniprom gave similar results.

In order to rule out the possibility of expression problems explaining the failed detection of HyaA and the faint detection of HyaB from the n-region deletion strain, reverse transcriptase-PCR (RT-PCR) was utilised. RNA was extracted from both IC009 and IC009 ΔNR, and cDNA synthesised. PCR analysis of the cDNA was performed using primers to amplify 500bp of *hyaA* and *hyaB* and 400bp of *hyaE*. Amplification of genomic DNA was used as a positive control and cDNA untreated with reverse transcriptase used as a negative control. No amplification product was visualised for any of the genes using this negative control. A product corresponding to the expected molecular weight of all gene regions was obtained using genomic DNA and RT-generated cDNA. Gene expression levels appear to be similar between IC009 and IC009 ΔNR. Furthermore, deletion of the n-region has not caused any polar effects downstream (Figure 2.17).

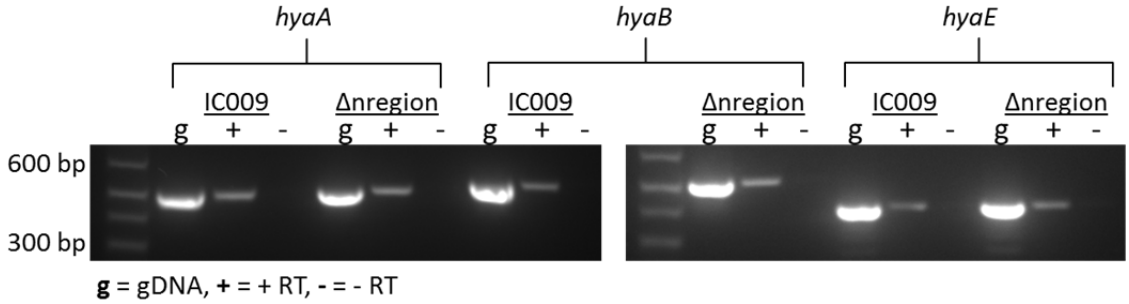

Figure 2.17. RT-PCR detection of *hya* genes indicate expression levels are similar for strains IC009 and IC009 ΔNR. cDNA was generated from *hyaA*, *hyaB* and *hyaE* regions and PCRs were performed. Lanes containing genomic DNA positive controls, +RT PCR on cDNA and –RT negative controls are specified.

2.3.6 Assessing the role of a Y8W substitution in the physiological context

Substituting the tyrosine residue at position eight of the Hyd-1 signal peptide for a bulkier amino acid residue appeared to abolish CAT export (Figure 2.11). The codon for Tyr8 was thus substituted for that encoding tryptophan on the chromosome of IC009 using the pMAK705 recombination method. The substitution did not affect targeting of either HyaA or HyaB to the membranes (Figure 2.16). Furthermore, Hyd-1 activity was observed in the membranes of IC009 expressing the Tyr8 substitution within the signal peptide, and at similar levels to that of IC009 (Figure 2.15).

2.4 Discussion

Hydrogenase enzymes are included among the most complex and sophisticated of the substrates transported by Tat. Not only do these enzymes contain redox active cofactors that require careful insertion before export, the two subunits also have to form a heterodimer within the cytoplasm. Moreover, hydrogenases possess a C-terminal 'tail' that anchors it to the inner membrane. The enzyme complex is targeted to the membrane *via* a Tat signal peptide present on the small subunit. The large subunit does not possess any signal peptide and must 'hitch-hike' across the membrane with its partner protein (Rodrigue *et al.*, 1999). A number of reviews have addressed the overall structure of the signal peptide from a variety of Tat substrates and have attempted to assign roles to some of the regions of the signal peptide. A glaring omission however is the role of the n-region. The purpose of this study was to reveal the function of the n-region using the oxygen-tolerant Hyd-1 from *E. coli* as a model.

The n-regions of [NiFe]-hydrogenases are particularly fascinating as they are unusually long and share a number of conserved residues between homologous enzymes. This suggests that the region must have an important function although this has remained elusive as yet. The results of this Section have provided a number of insights into the significance of this region. To test the function of the Hyd-1 signal peptide, reporter fusions were constructed. The signal peptide was investigated in isolation from its native protein due to the complex nature of hydrogenase assembly. Using reporter fusion constructs and pulse-chase experiments, it was revealed that the rate of reporter export was faster when the signal peptide n-region was removed. Unfortunately, processing of the reporter protein was never observed to completion even when the length of chase time was extended. This is in contrast to what has been shown for the signal peptides of some other Tat dependent substrates including *Salmonella* tetrathionate reductase and *E. coli* SufI, which promote full processing of reporter fusion proteins (Stanley *et al.*, 2000; Hinsley *et al.*, 2001; Hatzixanthis *et al.*, 2003). The reason for this is unknown. It would be useful to repeat the pulse-chase experiments using cells cultured under anaerobic conditions. It is conceivable that a protein required for more efficient processing is only produced under anoxic

conditions. An increase in the efficiency of a [NiFe]-hydrogenase signal peptide has previously been demonstrated under anaerobic conditions for the export of β-lactamase (Niviere *et al.*, 1992).

Protein export appears to be purposely stalled when the n-region is present suggesting that it may have a role in regulating the rate or the efficiency of protein transport. This delay might exist to ensure that the necessary cofactors have been successfully incorporated into the hydrogenase enzyme before export *via* the Tat pathway. It is also possible that this region may serve as a binding site for a protein that has an important role in regulating protein export. The signal peptide therefore may not only be essential in permitting protein export into the periplasm, but for signalling enzyme maturity.

2.4.1 What is the role of the n-region?

It is plausible that residues of the n-region are involved in specific protein-protein interactions with accessory proteins, the Tat translocon, with other residues of the signal peptide, or possibly unfolded regions of the mature protein sequence (Figure 2.18). In an attempt to identify amino acid residues that may be important in protein-protein interactions, site-specific substitutions were introduced to the Hyd-1 signal peptide fused to the reporter. In this study, Tyr8, Ala10 and Val16 substitutions resulted in an almost complete block of reporter export. The implication is that these residues are important in maintaining efficient protein processing and suggests they may form an important interaction with other amino acids. In fact, substituting any of the amino acids from positions 4 to 10, with the exception of Phe7, appeared to affect the rate of processing and export so this may indeed be an important region involved in various interactions. Substituting Tyr8 did not affect enzyme targeting or Hyd-1 specific hydrogen oxidising activity. This residue was chosen for further investigation due to the effect of its substitution on reporter export. In the physiological setting, this substitution is not sufficient to cause transport defects. Ala10 and Val16 should also be substituted on the *E. coli* chromosome to analyse the impact these residues have on Hyd-1 export and activity. CAT and Hyd-1 are structurally very different. The presence of the native hydrogenase may have induced conformational changes within the signal peptide or may directly interact with the signal peptide. Therefore it is

possible that the results obtained from experiments using the native enzyme will differ from reporter protein experiments.

To gain physiologically relevant results, DNA encoding the n-region of the Hyd-1 signal peptide was deleted from the *E. coli* chromosome and the presence of the n-region was clearly shown to be critical for Hyd-1 assembly. Here, it was demonstrated that without the n-region, neither the large nor the small subunit of Hyd-1 was correctly localised in the membranes of cells. The large subunit was however detected in the cytoplasm of cells, but at a much lower level compared to the parent strain (Figure 2.16). A similar result was reported in the case of the membrane bound hydrogenase from *R. eutropha*, where the n-region of the small subunit (HoxK) signal peptide was deleted up to residue Gln12: two amino acids away from the twin-arginine motif. The *R. eutropha* strain expressing the n-region deleted signal peptide was incapable of demonstrating hydrogen oxidation activity and the content of precursor HoxK was greatly reduced when compared with wild type levels (Schubert *et al.*, 2007). Schubert *et al.* (2007) did not attempt to detect the large subunit from *R. eutropha* cells carrying the n-region deletion.

Efforts were then made to assay hydrogenase activity and determine conclusively whether or not active enzyme was present in the membranes of IC009 carrying the n-region deletion. The established method exploits the hydrogenase-dependent reduction of an artificial electron acceptor, benzyl viologen (BV) and is measured in a cuvette. This method was used initially in the attempt to determine Hyd-1 activity from whole cells. In this experiment, whole cells are added to hydrogen saturated buffer and BV reduction measured as a change in absorbance at a wavelength of 600nm. Unfortunately, Hyd-1 did not react well with BV in this assay and no difference was measured between the Hyd-1 only expressing strain and the strain devoid of hydrogenase activity. This has been noted before for this particular enzyme in whole cell assays (Pinske *et al.*, 2011) and may be due to its conformation when attached to the membrane. Rocket immunoelectrophoresis was performed instead, which involves prolonged hydrogen activation. This method was successful and demonstrated that the loss of the signal peptide n-region results in loss of Hyd-1 specific activity, similar to what was observed in *R. eutropha* (Schubert *et al.*, 2007).

It is highly apparent that the n-region is essential for correct assembly of Hyd-1. Whether this is due to a direct interaction with the Tat apparatus in a ‘quality control’

manner or an interaction with a chaperone that permits cofactor insertion is unknown (Figure 2.18a and e). It may also be possible that the n-region binds to its passenger protein holding it in a certain conformation for specific assembly events to occur (Figure 2.18c). If this does not occur, the enzyme may be destined for degradation. A specific protein interaction with the n-region may be required in order to protect Hyd-1 from undergoing this degradation.

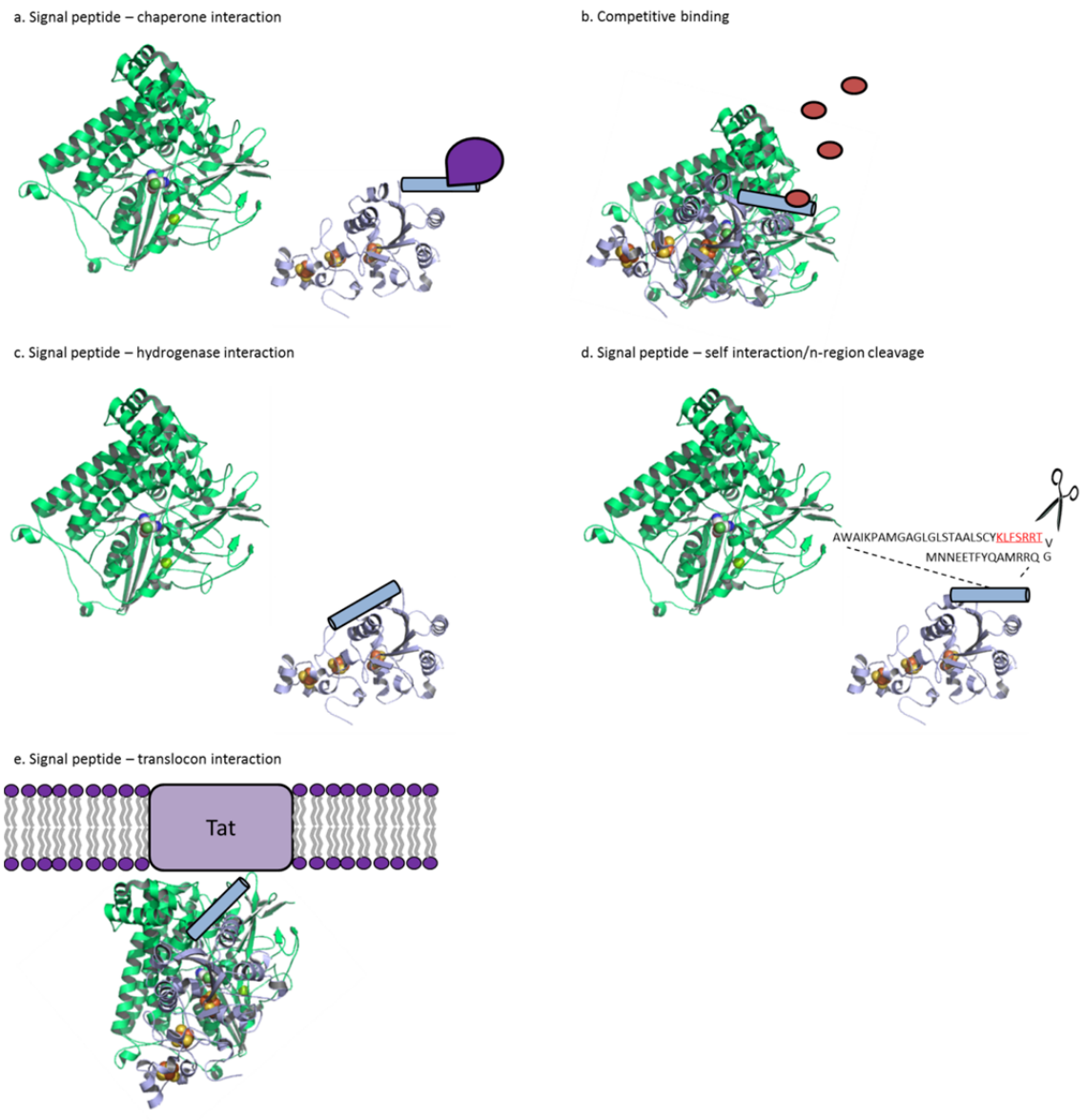

Figure 2.18. Possible roles for the n-region of the *E. coli* Hyd-1 signal peptide.

The n-region may **(a)** act as a binding site for a chaperone protein, **(b)** bind other molecules in a competitive manner, **(c)** interact with the native hydrogenase, **(d)** fold back on itself, become cleaved or **(e)** interact with the translocon machinery.

2.4.1.1 Does the signal peptide n-region interact with chaperone proteins?

Hydrogenase assembly is complicated. How does the Tat machinery recognise that the enzyme has been assembled correctly, and is ready for export? There must be a variety of measures in place to curtail transport of malformed proteins and prevent wasteful export. Assembly is further complicated by the involvement of 'specialist factors' that are necessary in assembling oxygen-tolerant hydrogenases. Bacterial two hybrid assays identified HyaE as a chaperone that binds to the small subunit of *E. coli* Hyd-1, although there was no evidence of direct binding to the signal peptide. Although Hyd-1 and Hyd-2 are structurally and functionally similar enzymes, they bind different chaperones. HyaE was shown to interact very weakly with Hyd-2. HybE was identified as the precursor-binding chaperone of *E. coli* Hyd-2 small subunit, and this protein was also found to bind the precursor form of the large subunit (Dubini and Sargent, 2003). Signal-swapping experiments where the signal peptide of Hyd-2 was replaced with that of TorA resulted in reduced hydrogenase activity and prevented the co-translocation of the two subunits. This was rescued only after co-expression with the TorA chaperone TorD (Jack *et al.*, 2004). This highlights the importance of the signal peptide-chaperone interaction in facilitating complex assembly before translocation.

The only data predicting HyaE as a possible signal peptide binding chaperone has been derived from bacterial two-hybrid experiments (Dubini and Sargent, 2003). Next, the small subunit, HyaA, should be affinity-tagged and co-purification experiments performed. This should be attempted in a *tat* deletion mutant and also a *hyaB* deletion mutant in order to obtain a precursor complex. If co-purifying proteins are obtained, these should be identified by mass spectrometry and Western analysis using antibodies specific to the proteins if possible. It might also be possible to affinity-tag various lengths of the signal peptide (e.g. the n-region only or the full length signal peptide). Immobilisation of these peptides to a column and the subsequent loading of soluble extract from wild type or *tat* mutant cells might result in the pull down of interacting proteins that bind specifically to this peptide. Another option is to immobilise various lengths of synthesised peptides onto a nitrocellulose membrane. Incubating the membrane with purified chaperone proteins, or indeed the precursor form of the small subunit, may result in the identification of an interaction upon immunological analysis using an affinity tag specific antibody. Isothermal

titration calorimetry (ITC) is an *in vitro* method of assessing protein-protein interactions. The Hyd-1 signal peptide n-region fused to a reporter protein should be titrated against each of the predicted chaperone proteins in an attempt to establish whether or not the n-region interacts with a chaperone.

R. eutropha produces a membrane bound hydrogenase with similarity to Hyd-1 of *E. coli*. The *hox* operon encodes HyaE and HyaF homologs named HoxO and HoxQ respectively. These gene products are completely required for the maturation of the hydrogenase and furthermore were shown to form a complex with the precursor form of the small subunit (HoxK). Removing the entire Tat signal peptide and deleting the n-region from the signal peptide resulted in a loss of hydrogenase activity and reduced stability of pre-HoxK. A direct interaction between the chaperones and the signal peptide of HoxK was also demonstrated *in vitro* using a synthetic peptide (Schubert *et al.*, 2007). It is interesting that the group did not synthesise a peptide covering the n-region sequence only and test for chaperone interactions as the study implies an important interaction between this region and the chaperone. Other studies of signal binding chaperones have localised chaperone binding to the h-region. This is not surprising as some Tat substrates do not possess long n-regions and it would be reasonable to assume that this hydrophobic stretch of amino acids would be masked in some way in the cytoplasm (Hatzixanthis *et al.*, 2005; Shanmugham *et al.*, 2012).

2.4.1.2 Is the n-region capable of binding RNA molecules?

The Human Immunodeficiency Virus Type I (HIV-1) encodes a transcriptional transactivator, coincidentally called TAT, important for viral gene expression. This protein displays a peptide rich in arginine residues where the first eight amino acids are proposed to act as a nuclear localisation signal (Truant and Cullen, 1999; Cardarelli *et al.*, 2007). Further to this, an interaction between the final three amino acids (Arg-Arg-Arg) of the peptide and intracellular moieties has also been demonstrated, indicating a dual functionality of this peptide. As arginine-rich regions are found in many proteins capable of binding RNA, such an interaction was investigated for the HIV TAT peptide. Substituting the three C-terminal arginine residues from the TAT peptide resulted in a decrease in affinity between the peptide and RNA molecules. Subsequent treatment with ribonuclease led to a complete abolishment of peptide-

RNA binding (Cardarelli *et al.*, 2008). Competition therefore exists between the two functions of the peptide and it is tempting to speculate that a similar scenario exists for the signal peptides of [NiFe]-hydrogenases. It is possible that the signal peptide not only acts as an export signal but also binds intracellular moieties in a competitive manner (Figure 2.18b) and this might result in the stalling of enzyme export. This is supported by the demonstration that an Arg13 substitution results in an increase in the initial rate of reporter processing (Figure 2.10). If this residue was responsible for stalling export through RNA binding, it would be expected that its substitution would increase the rate of reporter export. Alternatively, RNA binding may induce a conformational change. It is known that the binding of small RNAs by proteins often results in the stabilisation of a protein in a particular conformation required for complex formation (Pichon and Felden, 2007). Therefore, the binding of RNA molecules by the n-region of [NiFe]-hydrogenases may induce a conformational change within the small subunit that is required for docking of the large subunit. In this study, it was shown that removal of the n-region increases the rate or efficiency of reporter export. If the n-region was indeed an area of binding which acted to hinder protein export, it is reasonable to expect that when the n-region is removed the efficiency of protein export would increase. This period of stalling may be necessary to allow insertion of relevant cofactors.

When attached to the native enzyme, removal of the n-region from the signal peptide results in abolished transport and enzyme degradation. If the n-region does indeed stall enzyme export to allow cofactor insertion, without it the hydrogenase may be rejected by the Tat machinery and degraded due to its incomplete assembly. [NiFe]-hydrogenase signal peptides also contain an arginine rich area similar to HIV-1 TAT. The *E. coli* Hyd-1 n-region contains two conserved arginine residues with a further two found within the twin-arginine motif. It is tempting to speculate that these positively charged amino acids may also bind RNA. An *in vitro* binding assay may be useful here to determine whether or not the signal peptide binds RNA. Fluorescently labelled signal peptides would be added to a solution containing fluorescently labelled random oligo-RNAs and any binding monitored by fluorescence resonance energy transfer (FRET) signal analysis. Individual amino acids could then be substituted in order to identify interacting residues. The two arginine residues within the n-region would be prime candidates for this.

2.4.1.3 Is the signal peptide folded and does the n-region interact with the native hydrogenase?

Secondary structure predictions of signal peptides propose that Tat signal peptides assume an alpha-helical conformation but in reality, these peptides can be quite dynamic (Sargent *et al.*, 2006). The Hyd-1 signal peptide is also predicted to be alpha-helical when the sequence is entered into a structure prediction program (Figure 2.19). Methods including NMR and circular dichroism have been used to investigate Tat signal peptide structure. The signal peptide of the High Potential Iron-Sulphur Protein precursor of *Allochromatium vinosum* was found to be unstructured and the SufI signal peptide did not reveal any secondary structure until the hydrophobicity of the environment was increased (Kipping *et al.*, 2003; San Miguel *et al.*, 2003). The PhoD signal peptide from *Bacillus subtilis* was analysed using NMR and detergent micelles. A helical stretch of amino acid residues was discovered and found parallel to the membrane (Klein *et al.*, 2012). The crystal structure of the Tat signal peptide from the Rieske iron-sulphur protein of the cytochrome b_6f complex from *Mastigocladus laminosus* is anchored to the inner membrane *via* an uncleaved signal peptide. The structure of the protein complete with signal peptide was solved and revealed an amazingly dynamic signal peptide. The h-region is α-helical and the Tat motif forms an interesting structure where the side groups have collapsed away from the polar environment (Kurisu *et al.*, 2003). Involvement of the signal peptide in the control of protein synthesis has been demonstrated to occur at the translational level in a study by Punginelli *et al.* (2004). The Tat dependent formate dehydrogenase N (FDH-N) enzyme of *E. coli* displays a signal peptide on its Fdn-G subunit. This signal peptide possesses a very small n-region: only three amino acids precede the twin arginine motif. The mRNA specific to the first 17 amino acids of the signal peptide is predicted to form a stem-loop structure that modulates FDH-N translation. The hairpin structure is disrupted by an Arg5 substitution, which results in a 60-fold increase in the level of synthesised protein (Punginelli *et al.*, 2004). It is tempting to speculate that this modulation of translation is necessary for the complete maturation of FDH-N and that similar mechanisms of stalled assembly exist for other complex enzymes.

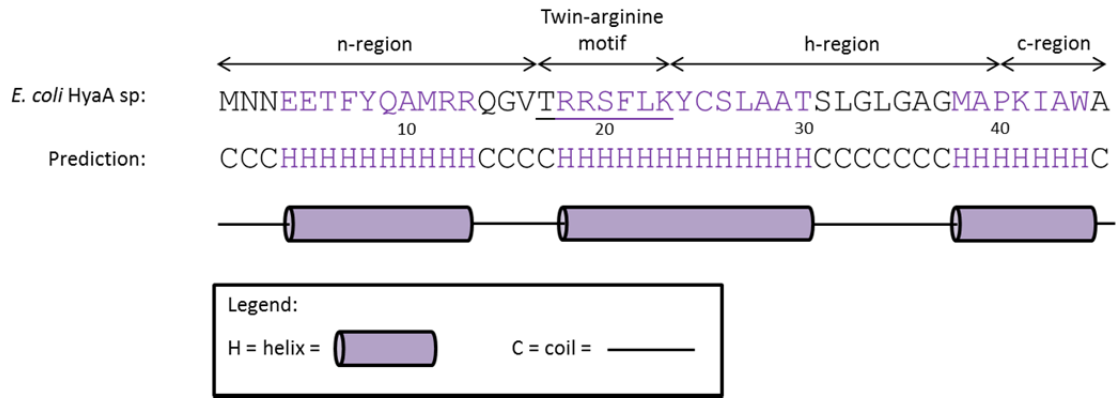

Figure 2.19. Secondary structure prediction of the *E. coli* Hyd-1 signal peptide.

Secondary structure was predicted using the PSIPRED Protein Sequence Analysis Workbench and edited as above. The structure is predicted to be predominately alpha-helical as depicted by the purple cylinders.

At the moment, it is unknown what conformation the *E. coli* Hyd-1 signal peptide assumes in physiologically relevant terms. The structure it adopts might depend largely on the structure of the passenger protein and may change as the unfolded protein folds around cofactors and interactions between subunits occur. The signal peptide may be hidden within the unfolded protein and is then revealed when the protein is in a state where it can be exported. Structural analyses of [NiFe]-hydrogenases has revealed that the processed N-terminus of the small subunit is located at the interface of the two subunits, which might suggest that the signal peptide lies along this interface before heterodimer formation (Volbeda *et al.*, 1995; Berks *et al.*, 2000). Only one of the hydrogenase subunits bears a signal peptide. This suggests that there must be mechanisms in place to prevent translocation of one subunit without the other. Is it possible that the signal peptide does indeed lie across the HyaA/HyaB interface before HyaB docks, and does so in a conformation that is not recognised by the Tat translocon (Figure 2.18c)? The recruitment of HyaB would then displace and free the signal peptide, which would then be recognised by the Tat machinery. It would be of interest to substitute some of the amino acids that lie along this interface and possibly interfere with this interaction. This might prove difficult however as the large subunit must also dock here. A bacterial two hybrid experiment may be useful in this case to identify intramolecular protein-protein interactions. The full signal peptide DNA sequences should be cloned into a vector expressing one of the adenylate cyclase fragments and the mature sequence of HyaA should be cloned into the other. This would test whether the two have any affinity for one another. If an

interaction was identified, interaction sites could be mapped using site directed mutagenesis or region deletions.

Cysteine cross-linking experiments would also provide an insight into whether or not the [NiFe]-signal peptide folds onto itself. It can be hypothesised that due to its extended length the n-region is capable of folding over and masking the twin-arginine motif (Figure 2.18d). The signal peptide should be fused to a reporter protein such as maltose binding protein (MBP), a protein that does not contain a single cysteine residue. Taking advantage of the conserved cysteine that immediately follows the twin-arginine motif of the signal peptide, amino acids of the n-region should be individually substituted with cysteines. A membrane permeable cross-linking agent should be used for these experiments. If the signal peptide does fold and cysteine residues do cross-link, it is possible that the protein's movement would be retarded during gel electrophoresis.

Obtaining a crystal structure of the precursor small subunit would be highly desirable. This would provide information on the conformation and binding of the signal peptide. It would also be useful to obtain a structure of the precursor heterodimer complex displaying the signal peptide. If this was not possible, nuclear magnetic resonance (NMR) spectroscopy should be used in an attempt to establish any signal peptide interactions with itself or the passenger protein. ITC experiments using the signal peptide n-region fused to a reporter protein titrated with the precursor HyaA/HyaAB complex should also be employed.

2.4.1.4 Does the signal peptide n-region interact with the Tat translocon?

Tat signal peptides are known to bind the TatBC complex where the twin arginine motif is recognised by a site in TatC, possibly forming a specific binding site. The signal peptide h-region and the mature protein are believed to lie close to TatB (Palmer and Berks, 2012). Available data therefore suggest that the Tat components bind the twin-arginine motif and the signal peptide immediately following the motif. Is the n-region recognised by the Tat translocon (Figure 2.18e)? As a number of Tat substrates do not possess a lengthy n-region, this interaction has not been investigated to any great extent. Cysteine cross linking experiments should be employed to assess whether or not the elongated n-region of [NiFe]-hydrogenases associates with any of the Tat components. The N-terminus of the signal peptide is thought to be located at

the cytoplasmic side of the membrane during protein transport. This is also based on observations made of the orientation of Rieske iron sulphur protein signal peptides that remain un-cleaved and become membrane anchoring domains (Sargent *et al.*, 2006). In this study, Hyd-1 was degraded in the cytoplasm of cells expressing an n-region deleted signal peptide (Figure 2.16). It is not known whether or not the n-region deleted signal peptide has interacted with the Tat translocon, been deemed unsuitable for export and then marked for degradation. Attempts should be made to detect the large and small subunits carrying the n-deleted signal peptide in a *tat* mutant. If the subunits are found degraded in the cytoplasm, this would imply that events earlier to Tat translocon recognition lead to its degradation.

Numerous studies have suggested that TatA polymerises to form a pore through which the Tat substrate is translocated. This is the most widely held assumption and is supported by imaging studies (Palmer and Berks, 2012). Others have hypothesised that TatA oligomer assembly weakens the membrane and that the Tat substrate is pulled through after TatC undergoes a conformational change (Bruser and Sanders, 2003). Further to this, it was demonstrated that the size of oligomer assembled depended on the presence of a signal peptide (Dabney-Smith *et al.*, 2006). It has also been demonstrated that increasing length of precursor correlates with stalled transport implying that there are various factors involved in influencing efficiency of transport. The authors suggested a 'molecular' drag that might result from interactions between the protein and a channel wall or lipid bilayer (Cline and McCaffery, 2007). It might be possible that the n-region itself imposes a 'molecular drag' slowing export down so that final checks on the maturity of the enzyme can be made. This however, would not entirely explain the degree of conservation maintained within the n-region. Not all Tat substrates possess elongated n-regions so it might be unlikely that this region is involved in general Tat machinery recognition.

2.4.2 Is the n-region cleaved from the signal peptide?

How can we reconcile the fact that removal of the n-region results in fast and efficient export of a reporter protein but that the n-region is absolutely required for export of the native enzyme? One hypothesis might be that the n-region is necessary at the beginning of enzyme assembly and its presence required until a number of maturation processes including cofactor insertion has been achieved. The n-region

may then be cleaved from the signal peptide (Figure 2.18d), signalling maturity of the enzyme and its readiness for export. The same problem would not be faced when the signal peptide missing its n-region was fused to the reporter protein as it does not require insertion of any cofactors. Recognition of the signal peptide by the Tat machinery is all that is required in this case.

The AxA motif present in the c-region of many Tat substrates forms the recognition site that is cleaved by Type 1 signal peptidases (Yahr and Wickner, 2001). Protease activity is proposed to occur very close to the lipid bilayer on the periplasmic side. Therefore, it is assumed that peptide cleavage only occurs after the complete translocation of the passenger protein (Sargent *et al.*, 2006). Unfortunately it is unknown whether the cleaved signal peptide is released into the cytoplasm or into the periplasm. It is likely, however, that the signal peptide remains at the cytoplasmic side of the inner membrane. Experiments where a domain was fused to the N-terminus of a signal peptide demonstrated that this domain was not transported. This fusion did not interfere with signal peptide recognition or Tat-mediated transport (Fincher *et al.*, 1998). Therefore it will be difficult to determine whether the n-region is cleaved in the cytoplasm as there is a possibility that the whole signal peptide is released into the same compartment. It would be of interest to chemically synthesise the entire Hyd-1 signal peptide with an affinity tag present at each end. Incubation of the peptide with cytoplasm of anaerobically cultured *E. coli* cells and subsequent Western analysis would allow the facile detection of peptide fragments. Samples treated with protease inhibitors should be performed alongside as a control. A collection of peptide fusions containing individual amino acid substitutions should then be used to localise the point of cleavage.

2.4.3 The n-region may constitute a regulatory domain

Although the role of the signal peptide n-region remains elusive, the results of this study do offer several insights into what the function may be. We propose that the n-region should be termed a 'regulatory region' as it is clearly involved in regulating the rate and efficiency of protein export (Figure 2.20). The n-region is evidently essential for the stability, assembly and, consequently, the localisation of Hyd-1. Without this important region, the hydrogenase does not appear to be regarded competent for Tat transport and is degraded within the cytoplasm. This

results in a loss of Hyd-1 specific activity from the membranes of *E. coli* cells. A fascinating find of this study was that fusing an n-region deleted signal peptide to a reporter protein led to an increased rate of protein export. This suggests that that the n-region acts in a regulatory manner to hinder protein export, which may be required for the complete assembly of the hydrogenase enzyme. It is tempting to hypothesise that the n-region is capable of taking part in a variety of protein-protein interactions, whether this is with chaperone proteins or the precursor enzyme. It might also be possible that this region interacts with RNA molecules either in specific or unspecific associations. Another intriguing speculation is that the n-region folds back to mask the twin-arginine motif. It may then be a requirement for the n-region to be cleaved signalling readiness for Tat transport. The n-region clearly constitutes a regulatory domain regardless of which interaction transpires as genuine. The binding of proteins to other proteins often results in conformational changes, so it is conceivable that the signal peptide performs a number of different functions depending on the stage of enzyme assembly.

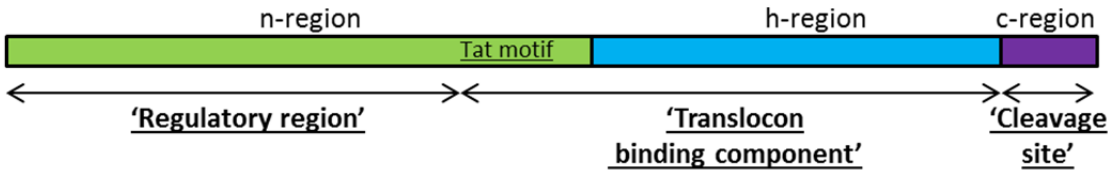

Figure 2.20. Suggested roles for regions of the signal peptide.

The n-region is proposed to function as a 'regulatory region'; the h-region is suggested to bind to the translocon machinery, whereas the c-region contains the cleavage site recognised by a signal peptidase in the periplasm.

3 Investigating the structure and function of the oxygen-tolerant Hyd-5 from *Salmonella enterica* serovar Typhimurium

3.1 Introduction

Hydrogen is an important energy source for a number of pathogenic bacteria including *Helicobacter pylori* and *Salmonella* (Maier, 2005). *Salmonella* expresses three uptake-type hydrogenases encoded by the *hya, hyb and hyd* operons. These are Tat-dependent enzymes and are found bound to the periplasmic face of the inner membrane. Two of these (*hya* and *hyb*) are homologs of the Hyd-1 and Hyd-2 hydrogenase enzymes found in *Escherichia coli* (Zbell *et al.*, 2007). The existence of the third isoenzyme (encoded by the *hyd* operon) was a surprise revealed after the assembly of the complete genome sequence (McClelland *et al.*, 2001; Maier *et al.*, 2004). These uptake hydrogenases were found to be expressed under different conditions and were also demonstrated to be utilized at different stages of infection (Zbell *et al.*, 2008). Whereas the *hya* and *hyb* operons are best expressed during fermentation and anaerobic respiration respectively, the *hyd* operon is expressed at its greatest under aerobic conditions (Zbell *et al.*, 2007).

It has been proposed that the energy generated by the oxidation of hydrogen is crucial for pathogenesis within the host (Maier, 2005). In fact, removal of the three uptake hydrogenases from *Salmonella* results in an avirulent strain incapable of invading spleen or liver tissue (Maier *et al.*, 2004). Therefore, investigations into the structure and the assembly of these enzymes are relevant for biomedical as well as biotechnological reasons. Indeed, the design of hydrogenase inhibitors would be a great contribution to the dwindling collection of antibacterial therapeutics used currently.

Although the *Salmonella* genome encodes only four hydrogenases, the aerobically-expressed uptake hydrogenase has been termed Hyd-5 here so as not to confuse this enzyme as having any similarity to Hyd-4 of *E. coli*. Hyd-5 is of great interest as it may represent a new class of oxygen-tolerant enzyme in enteric bacteria. Hyd-5 is encoded by the *hydABCDEFGHI* operon where the gene *hydA* encodes the small subunit and *hydB* encodes the large subunit. This operon is particularly interesting due to the presence of a number of 'accessory genes' that are absent from the operons encoding hydrogenases expressed under anoxic conditions. One of the main challenges to using hydrogenases in future biotechnological applications is the

fact that many of these enzymes are irreversibly inactivated by oxygen. The oxygen tolerance exhibited by enzymes like Hyd-5 is an extremely attractive feature that has become the focus of intense research. Understanding the molecular basis behind this tolerance, how a microorganism is capable of expressing such a hydrogenase, and what processes are involved in enzyme biosynthesis are vital to engineering oxygen-tolerance into synthetic hydrogenases.

3.2 Aims

The aim of this Chapter was to isolate and further characterise the aerobically expressed Hyd-5 from *S. enterica* serovar Typhimurium. At the outset of this work, no structural information was available for any oxygen-tolerant hydrogenases. One objective of this Chapter, therefore, was to collaborate with a structural biology group in order to obtain a high resolution crystal structure of *Salmonella* Hyd-5, and thus gain further insights into the molecular basis of oxygen-tolerance.

3.3 Results

3.3.1 Isolation of the Hyd-5 enzyme

Very high overproduction of plasmid-encoded hydrogenases and especially heterologous overexpression is difficult. This is most likely due to the complex biosynthetic pathways involved in enzyme maturation and the inability of the host cell to keep up with the insertion of cofactors, protein export, etc. *E. coli* is often used as the choice host microorganism for heterologous gene expression. This is especially relevant when studying hydrogen production as *E. coli* does not produce any [FeFe]-hydrogenases, which are biased towards hydrogen production. Any analytical measurements are therefore simplified (Kuchenreuther *et al.*, 2010). Enzyme purified from these recombinant systems are often of similar yields when compared from enzyme produced from the native microorganism but activities are considerably lower. This is thought to be due to incomplete hydrogenase maturation (Akhtar and Jones, 2008; Laffly *et al.*, 2010). A study by Voordouw *et al*. (1987) attempted the recombinant expression of two genes encoding the structural subunits of the periplasmic *Desulfovibrio vulgaris* hydrogenase in *E. coli*. Although both subunits were expressed successfully, the recombinant enzyme did not display any detectable hydrogenase activity. EPR analysis led to the conclusion that one of the Fe-S clusters was missing from the synthesised enzyme. Further to this, expression of the *D. vulgaris* hydrogenase genes led to enzyme mislocalisation in *E. coli* (van Dongen *et al.*, 1988). The majority of enzyme was detected within the cytoplasm of *E. coli* cells instead of within the periplasm, its native location. In fact, it was estimated that no more than 20% of enzyme was successfully translocated across the inner membrane. Both Voordouw *et al*. (1987) and van Dongen *et al*. (1988) hypothesised that additional factors must be required for the complete assembly of the *D. vulgaris* enzyme, which are not present in *E. coli*.

In an attempt to overcome some of the obstacles faced when using plasmid overexpression systems, the decision was taken to genetically modify the chromosome of the native organism, *S. enterica* serovar Typhimurium LT2a. Using the pMAK705 homologous recombination method (Hamilton *et al.*, 1989), DNA encoding a hexa-histidine affinity tag was added to the 3' end of the gene encoding the small subunit

(*hydA*), yielding the strain SFTH01. Western analysis of SFTH01 whole cells revealed low levels of $HydA^{HIS}$ when the strain was cultured aerobically, and no protein at all when grown under anaerobic conditions (Figure 3.1a and b).

Attempts were made to purify Hyd-5 from strain SFTH01 but were hindered by the natural low level of expression from the native *hyd* promoter. SFTH01 was thus further modified in order to up-regulate *hyd* expression. Two strains were constructed: one where the constitutive *tat* promoter (p_{tat}) from *E. coli* (Jack *et al.*, 2001) was incorporated upstream of the *hyd* operon (SFTH05), and another where the LacI-repressible T5 promoter (p_{T5}) from the pQE70 overexpression plasmid (Qiagen Inc.) was incorporated (SFTH06). These strains were relatively easy to generate. As the T5 promoter was cloned as an *Eco*RI-*Bam*HI fragment, colonies could be screened for the insertion of T5 by digesting the amplified region with *Bam*HI and analysing the bands following agarose gel electrophoresis. Increased levels of $HydA^{HIS}$ were detected from both strains following Western analysis of whole cells (Figure 3.1a). Supplementing the media with IPTG did not appear to result in increased expression from the T5 promoter (Figure 3.1a), suggesting that the strong promoter is not repressed in this strain. Indeed, *Salmonella* LT2a does not appear to encode any LacI homologues on its chromosome that would be responsible for transcriptional repression. Evidently, high levels of $HydA^{HIS}$ are produced by SFTH06 but it is the precursor form of the protein that apparently dominates under aerobic conditions (Figure 3.1a). It may be that the Tat machinery is saturated by the engineered overexpression and cannot keep up with production of enzyme. Another possibility is that, under aerobic expression, cofactor levels are not sufficient to allow maturation of the protein. In fact, in *E. coli*, [NiFe] cofactor levels are at their greatest under anaerobic conditions (Lutz *et al.*, 1991) and this is probably also the case in *Salmonella*. Therefore, to allow efficient cofactor mobilisation, strains were cultured under anoxic conditions into late stationary phase (Figure 3.1b). Subcellular fractionation was performed on SFTH06 to obtain cytoplasm and membrane fractions. The mature form of the enzyme was found firmly associated with membranes whereas the precursor appeared to be unstable and was rapidly degraded in the cytoplasm (Figure 3.1b). SFTH06 was therefore chosen as the strain most appropriate for isolating Hyd-5 (Figure 3.1c).

SFTH06 was cultured anaerobically and cells harvested and then lysed using a chemical cocktail. Immobilised metal affinity chromatography (IMAC) was used to purify Hyd-5 under aerobic conditions. Peak fractions were separated by SDS-PAGE (Figure 3.1d) and the presence of HydA and HydB confirmed by tryptic peptide mass fingerprinting. A smaller form of HydB was also present in the sample that appears to be proteolytically truncated towards its C-terminus (Figure 3.1d). Protein yield from this strain was good. For example, from 9 g (wet weight) of cells, 1.4 mg protein was obtained.

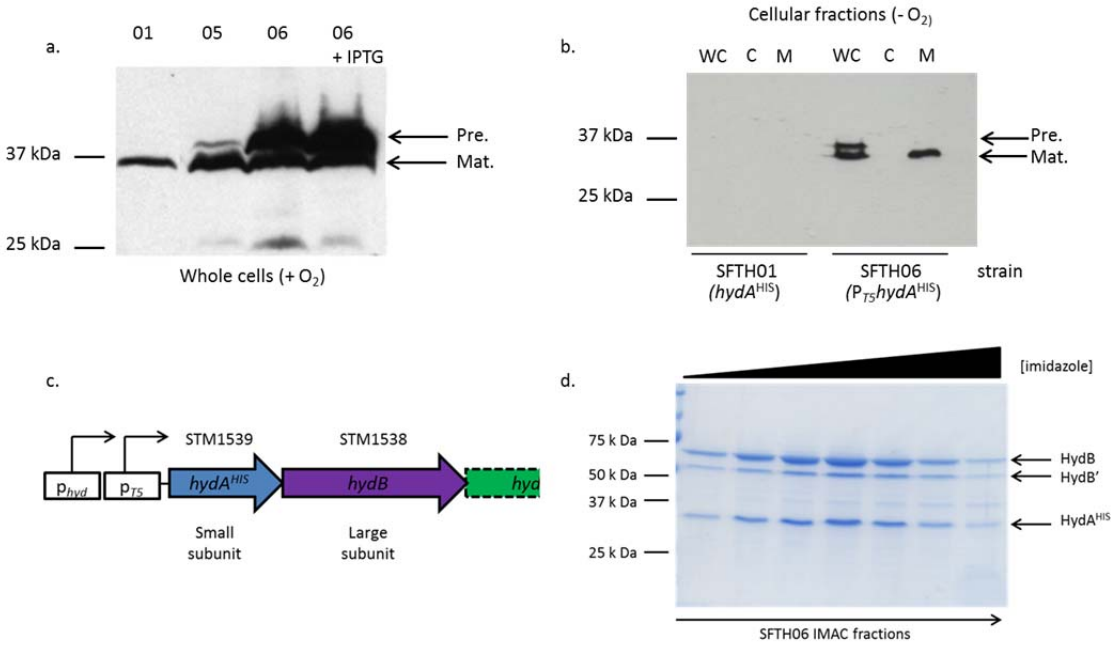

Figure 3.1. The *Salmonella* chromosome was genetically modified to allow isolation of Hyd-5.

(a) Strains SFTH01 (*hydA*^{HIS}), SFTH05 (P_{tat}*hydA*^{HIS}) and SFTH06 (P_{T5}*hydA*^{HIS}) were grown aerobically in LB medium, and whole cells subjected to Western immunoblotting. SFTH06 cells were cultured with and without the addition of 2 mM IPTG. Whole cells were separated by SDS-PAGE, blotted and protein detected using antibody specific to the affinity tag. **(b)** Strains SFTH01 and SFTH06 were grown anaerobically in LB and whole cells harvested. Cells were lysed under pressure and subcellular fractions obtained. Whole cells (WC), cytoplasm (C) and membrane (M) fractions were separated by SDS-PAGE, blotted and protein detected using antibody specific to the affinity tag. **(c)** A diagram highlighting the promoter region of SFTH06 (P_{T5}*hydA*^{HIS}), chosen as the most suitable strain for isolating Hyd-5. **(d)** Hyd-5 was purified by IMAC and elution fractions separated by SDS-PAGE. HydA and HydB are indicated. A degraded fragment of HydB is also indicated (HydB').

In collaboration with Dr Paul K. Fyfe and Prof William N. Hunter from the Division of Biological Chemistry & Drug Discovery, Dundee, Hyd-5 obtained from SFTH06 was further purified by size-exclusion chromatography and entered into crystallisation trials. Unfortunately, these initial trials proved unsuccessful. One

possible reason for this may have been the choice of detergent used during the purification process, which was Triton X-100. The critical micelle concentration (CMC) of this detergent is very low (0.23 mM). Therefore, this detergent was substituted with *N, N*-Dimethyldodecylamine *N*-oxide (LDAO) and used throughout the entire purification. LDAO is a detergent with a larger CMC (1 mM) so will tend to form smaller micelles around hydrophobic regions. Again, crystallisation trials failed.

3.3.2 Cleavage of the C-terminal transmembrane domain by limited trypsinolysis

It is possible that the presence of the C-terminal transmembrane domain of HydA was creating problems for crystal formation. Consequently, attempts were made to remove this hydrophobic region (and concomitantly the hexa-Histidine tag) using limited trypsinolysis, thus generating a soluble form of the enzyme. This idea stemmed from the work of Ballantine and Boxer (1986) who demonstrated that adding trypsin to *E. coli* membrane vesicles resulted in the release of an active fragment of Hydrogenase-2. Similar experiments demonstrated that *E. coli* Hyd-1 was also susceptible to trypsinolysis (Sawers and Boxer, 1986). This limited proteolytic treatment is obviously applied after enzyme assembly, when the enzyme is anchored to the periplasmic face of the inner membrane. Ballantine & Boxer (1986) also showed that similar trypsinolysis of the Hyd-1 and Hyd-2 small subunits could be performed after dispersal of the lipid bilayer with detergents.

Trypsin cleaves peptides at the C-terminal side of exposed arginine and lysine residues and the C-terminal tail of HydB contains six residues that provide a potential site for trypsinolysis (Figure 3.3a). Experiments involved incubating 1.4 mgs of purified enzyme with 0.2% (w/v) trypsin over a time period of 60 minutes. Samples were taken every 10 minutes and separated by SDS-PAGE. During this time-course, $HydA^{HIS}$ was hydrolysed, yielding a smaller stable fragment of around 30 kDa. A degradation fragment of HydB was also visible but was almost completely undetectable by the end of the treatment (Figure 3.2a). As the cleavage of $HydA^{HIS}$ was possibly achieved too rapidly, the concentration of trypsin was lowered to 0.02% (w/v). This yielded a similar tryptic fragment of HydA to that observed previously. Purified Hyd-5 was therefore incubated with 0.02% (w/v) trypsin for 1 hour at 37°C. To remove trypsin from the purified enzyme, anion exchange chromatography was performed. Following this additional purification, the only proteins observed were HydB and the truncated HydA

subunit (Figure 3.2b). Unfortunately, the yield of protein was extremely low and inadequate for entry into crystallisation trials. From 1.4 mgs of protein, only 0.4 mgs was recovered following anion exchange chromatography.

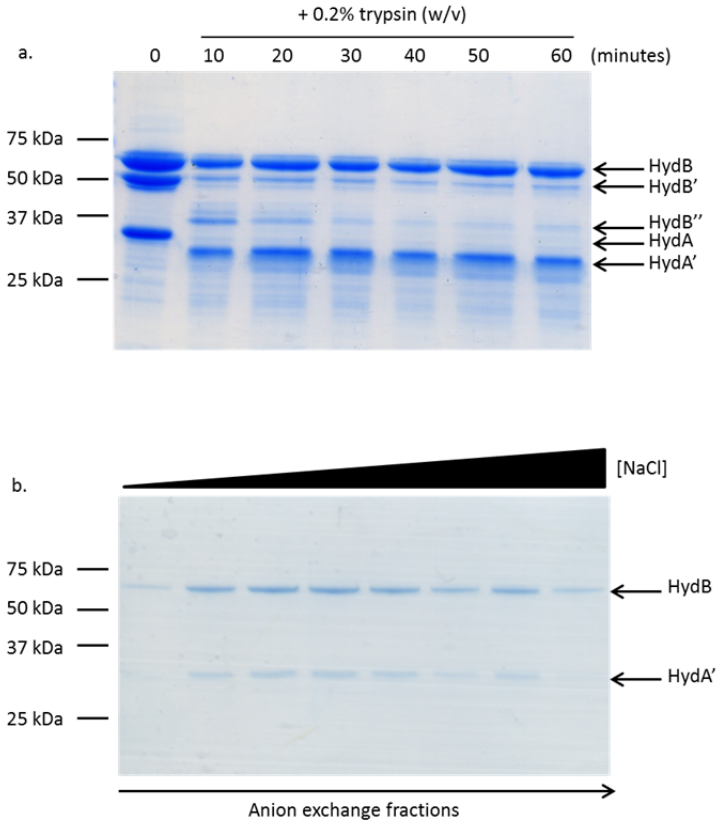

Figure 3.2. Limited trypsinolysis of purified Hyd-5.

(a) Hyd-5 was purified by IMAC and incubated with 0.2% (w/v) trypsin, at 37°C, over a time period of 60 minutes. Samples were removed every 10 minutes, added to Laemmli buffer, boiled and analysed by SDS-PAGE. A 5µl sample untreated with trypsin was included for comparison and is shown at time 0. HydB and degraded fragments (HydB' and HydB'') are indicated as well as HydA and the tryptic fragment HydA'. **(b)** Following purification by IMAC and incubation with 0.02% (w/v) trypsin, Hyd-5 was further purified by anion exchange chromatography and fractions analysed by SDS-PAGE.

3.3.3 Genetic deletion of the Hyd-5 transmembrane domain

Due to the very low yield of enzyme obtained after trypsinolysis, this method was abandoned. Next, a genetic approach was taken to solve the problem. Hyd-5 small subunit residues Gly314 (using nomenclature previous to processing) up to and including Lys367 were genetically deleted from SFTH06 using the pMAK705 recombination method, leaving the affinity tag intact (Figure 3.3a). The transmembrane deleted strain generated was designated LB03. Of the *E. coli* hydrogenases, *Salmonella* Hyd-5 most closely resembles Hyd-1. As *E. coli* Hyd-1 has

been shown to possess a C-terminal transmembrane helix, or C-tail (Hatzixanthis *et al.*, 2003), and *E. coli* Hyd-2 was found to be soluble in the periplasm after genetic removal of its C-tail (Hatzixanthis et al., 2003), *Salmonella* Hyd-5 was presumed now water-soluble and detergents were no longer necessary to disrupt the membranes during the purification protocol. The LB03 strain was cultured under anoxic conditions, cells disrupted under pressure, and IMAC employed as before to purify the enzyme from the crude extract. Eluted fractions were assessed following SDS-PAGE resulting in the identification of the large subunit and a truncated small subunit with a molecular weight of around 30 kDa (Figure 3.3b). Isolated Hyd-5 was further purified by size-exclusion chromatography (SEC) and entered into crystallisation trials in collaboration with Dr Paul K. Fyfe and Prof William N. Hunter from the Division of Biological Chemistry & Drug Discovery, Dundee. Using the hanging drop method of crystallisation, dark brown crystals formed (Figure 3.3c) under the following reservoir conditions: 19% (w/v) PEG4000, 0.1 M MES pH 6, 0.24 M lithium sulphate.

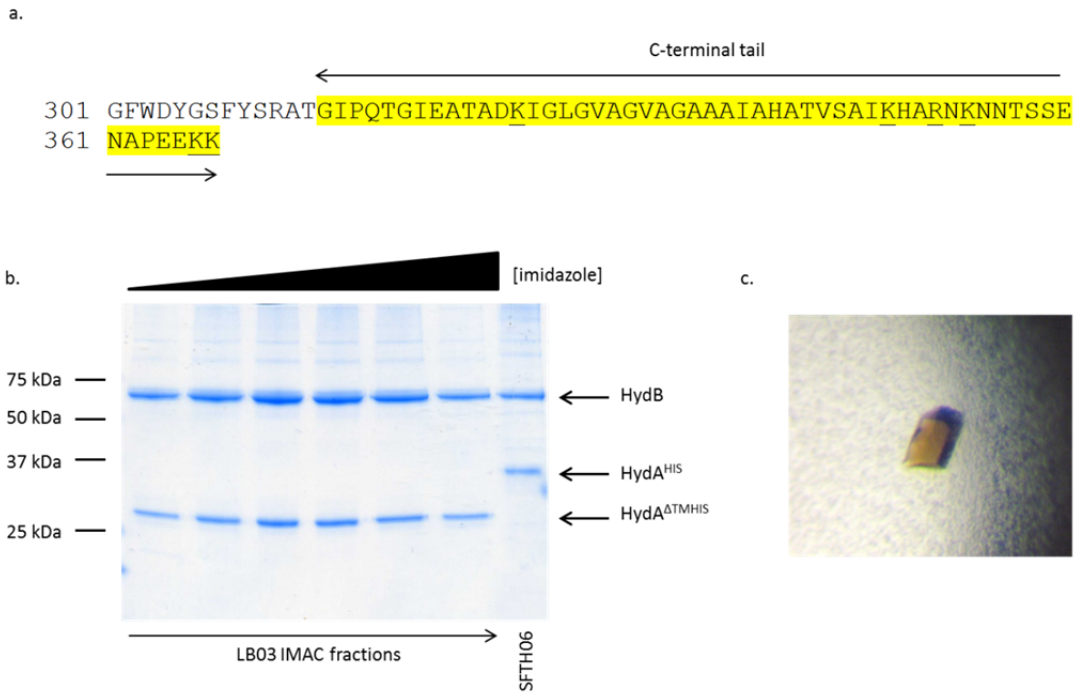

Figure 3.3. Hyd-5 crystals formed from protein isolated from LB03.

(a) The C-terminal sequence of HydA from *Salmonella* Hyd-5 is highlighted in yellow and tryptic residues underlined. **(b)** LB03 was cultured anaerobically, cells harvested and then lysed under pressure. Hyd-5 was purified by IMAC and fractions analysed by SDS-PAGE. HydB and truncated HydA ($HydA^{\Delta TMHIS}$) were identified. A sample containing Hyd-5 purified from SFTH06 was run alongside for comparison. **(c)** An example of the dark brown crystals formed from Hyd-5 is shown. Crystal dimensions are roughly 70 µM x 50 µM. Reservoir conditions consisted of 19% PEG4000, 0.1 M MES pH6 and 0.24 M lithium sulphate.

3.3.4 The crystal structure of *Salmonella* Hyd-5

The water-soluble Hyd-5 isolated from strain LB03 crystallised with three core hydrogenase dimers in the asymmetric unit (Figure 3.4). The structure was solved by molecular replacement using the structure of the membrane bound [NiFe]-hydrogenase of *Ralstonia eutropha* (Protein Data Bank Accession 3RGW) to 3.2 Å resolution (Figure 3.4). Two of the hydrogenase dimers appeared to be associated with each other (Figure 3.5a), suggesting that Hyd-5 may exist as a dimer of heterodimers – the classic $\alpha_2\beta_2$ arrangement observed for other [NiFe]-hydrogenases (Ballantine and Boxer, 1986; Sawers and Boxer, 1986; Ogata *et al.*, 2010). In this arrangement, the two distal [4Fe-4S] clusters from the two small subunits lie in close proximity to each another. This may have physiological relevance that will be discussed later.

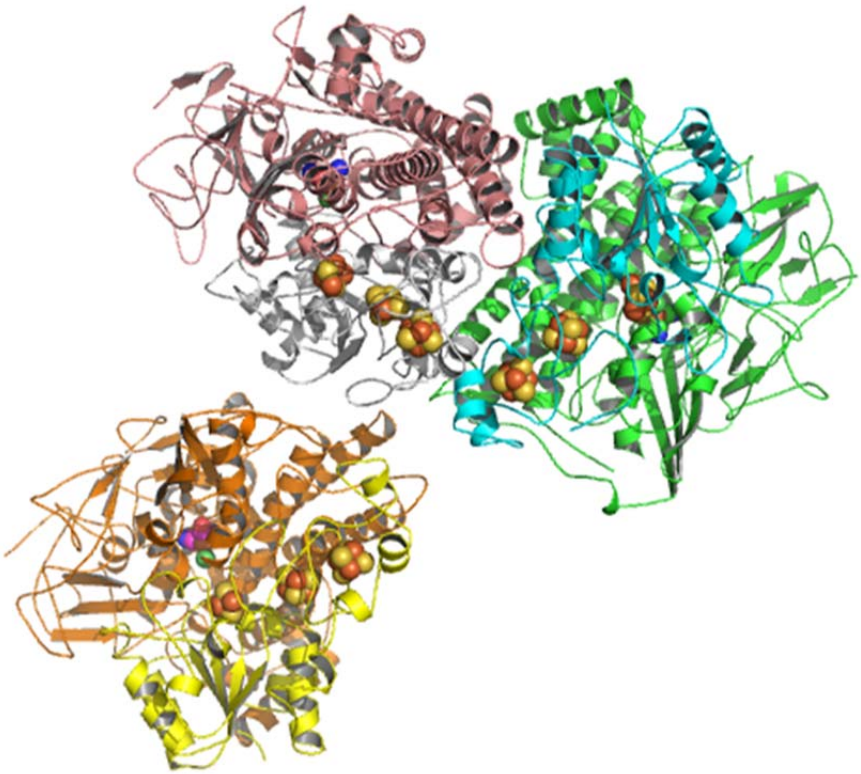

Figure 3.4. Hyd-5 crystallised with three hydrogenase dimers in the asymmetric unit.
Large subunits are coloured pink, green and orange with the small subunits depicted in grey, blue and yellow. Spheres are coloured as follows: orange = iron, yellow = sulphur, dark green = nickel, blue = nitrogen, light green = carbon.

The structure of Hyd-5 represents that of an oxygen-tolerant hydrogenase. The two subunits of the heterodimer share the structure typical of standard [NiFe]-

hydrogenases that have already been crystallised (Volbeda *et al.*, 1995; Volbeda *et al.*, 2005; Ogata *et al.*, 2010). The large subunit contains the [Ni-Fe] active site whereas the small subunit accommodates three Fe-S clusters (Figure 3.5b). The distances between the four redox active centres are between 8 and 11 Å in each case. The C-terminus of the large subunit is well buried within the structure, which is to be expected as hydrogenase large subunits are known to be C-terminally processed and locked in position prior to docking onto their small subunit partners (Vignais and Billoud, 2007). Available [NiFe]-hydrogenase structures have revealed a magnesium ion that interacts with the terminal histidine residue of HydB (e.g. Ogata *et al.*, 2010). The Hyd-5 structure does appear to have a region of density where the magnesium should be positioned so it might be possible that this ion is also present in Hyd-5.

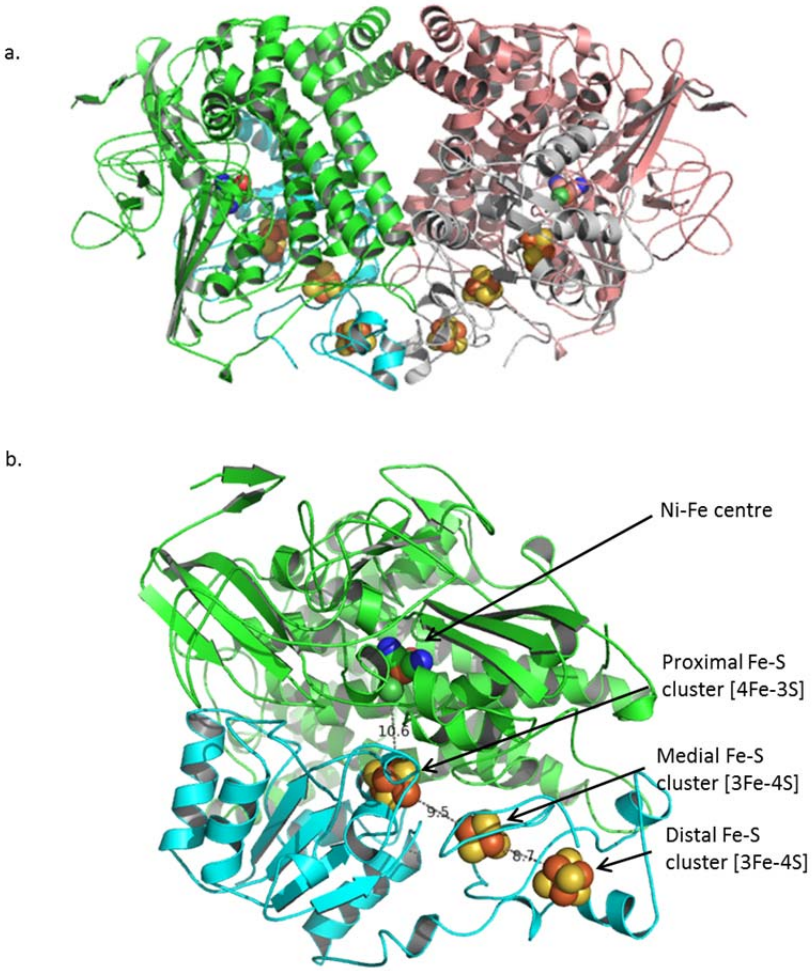

Figure 3.5. Crystal structure of [NiFe]-hydrogenase-5 from *Salmonella*.

Large subunits are coloured pink and green with the small subunits depicted in grey and blue. Spheres are coloured as follows: orange = iron, yellow = sulphur, dark green = nickel, blue = nitrogen, light green = carbon. **(a)** Hyd-5 appears to form a dimer of heterodimers. **(b)** The structure of the Hyd-5 heterodimer is depicted with the distance measured between redox active centres highlighted in Å.

3.3.4.1 The structure of Hyd-5 reveals a unique [4Fe-3S] proximal Fe-S cluster

The Hyd-5 structure revealed at least four metal cofactors in each large subunit/small subunit core hydrogenase heterodimer. Unfortunately, the [Ni-Fe] centre within the large subunit proved difficult to solve, which may be a consequence of the purification conditions, i.e. the active site was exposed to oxygen attack (Figure 3.6a). The small subunit houses three Fe-S clusters that relay electrons both to and from the active site depending on whether an electron donor or acceptor is present. The medial Fe-S cluster is arranged as a [3Fe-4S] cluster, coordinated by three cysteine residues (Figure 3.6c) whereas the distal cluster is a cubane [4Fe-4S] Fe-S cluster coordinated by three cysteines and one histidine (Figure 3.6d).

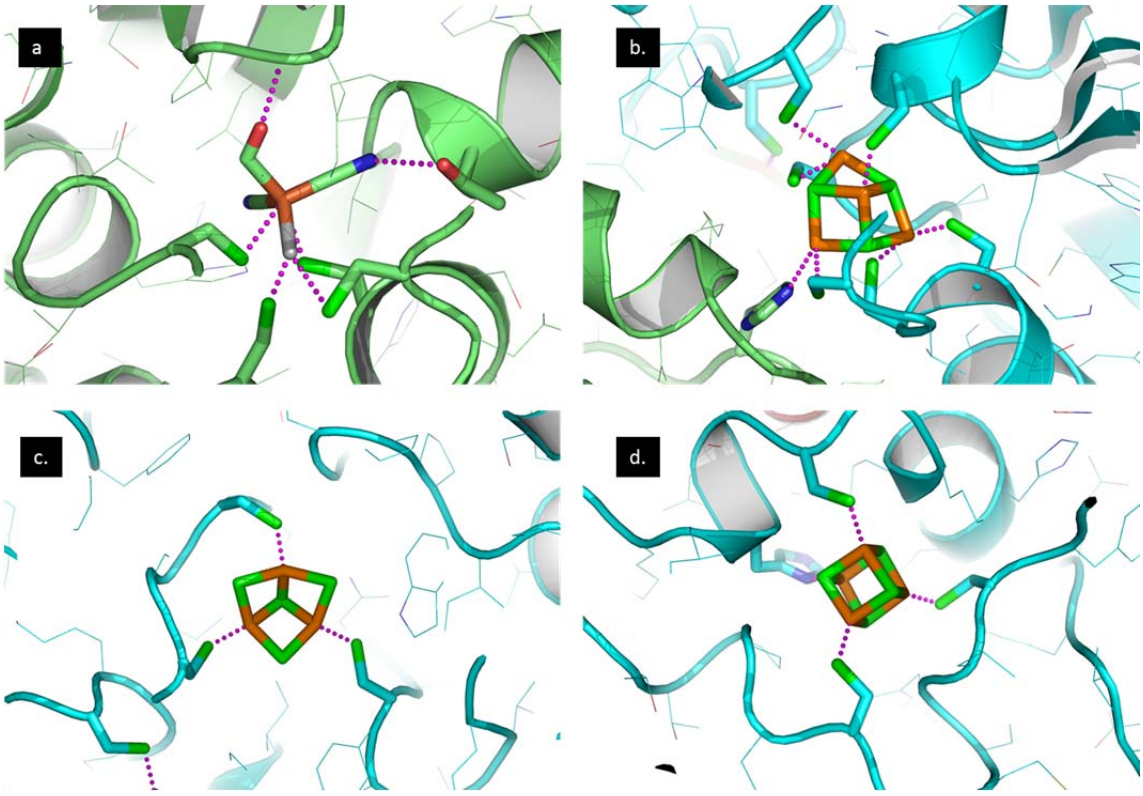

Figure 3.6. Co-ordinating residues of the Hyd-5 active site and the three Fe-S clusters.

(a) The Ni-Fe active site. **(b)** The [4Fe-3S] proximal Fe-S cluster is co-ordinated by six cysteine residues of the small subunit and a histidine residue of the large subunit. **(c)** The [3Fe-4S] medial Fe-S cluster is coordinated by three cysteine residues of the small subunit. **(d)** The distal Fe-S cluster is a cuboidal [4Fe-4S] cluster coordinated by three cysteines and one histidine of the small subunit.

The proximal Fe-S cluster proved to be extremely interesting as it differs from those found in standard oxygen-sensitive hydrogenases, and is so far unique in nature. The proximal Fe-S cluster of the oxygen-tolerant Hyd-5 is a [4Fe-3S] type coordinated by six cysteines (Figure 3.6b). This contrasts with the standard [4Fe-4S] cluster, which

is coordinated by four cysteine residues. The importance of the two additional ligating cysteines (termed CysS19 and CysS120 using nomenclature after signal peptide processing and where 'S' denotes the small subunit) to the oxygen-tolerance mechanism has been well studied during the course of this research (Lukey *et al.*, 2011; Pandelia *et al.*, 2011). A comparison of small subunit sequences from oxygen-sensitive and oxygen-tolerant hydrogenases is shown in Figure 3.7 to highlight these supernumerary cysteines.

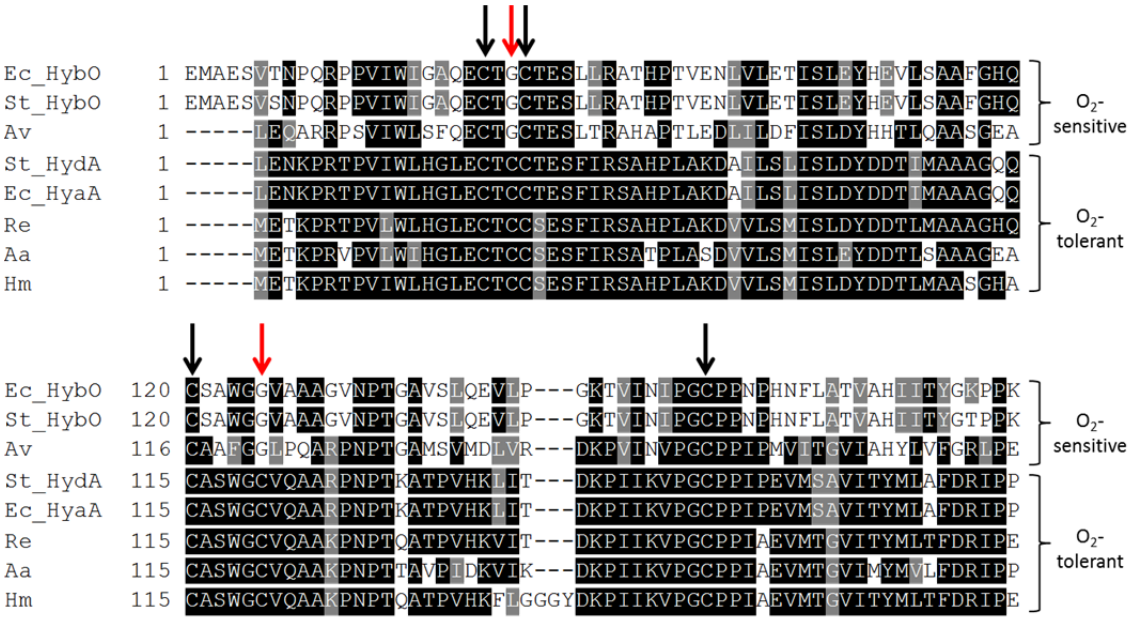

Figure 3.7. Amino acid sequence alignment comparing the small subunits of standard and oxygen-tolerant hydrogenases.

Cysteine residues responsible for ligating the proximal Fe-S cluster are marked with an arrow. Red arrows indicate the positions occupied by supernumerary cysteines found only in oxygen-tolerant hydrogenases. Black shading highlights identical residues shared between 50% of the sequences; grey shading highlights conservative substitutions of these whereas residues in white indicate non-conserved amino acids. Sequences are taken from *E. coli* (Ec), *Salmonella* (St), *Allochromatium vinosum* (Av), *Ralstonia eutropha* (Re), *Aquifex aeolicus* (Aa) and *Hydrogenovibrio marinus* (Hm).

Oxygen-sensitive hydrogenases possess glycines at the equivalent positions of the additional cysteines. Substituting the conserved cysteines present in oxygen-tolerant enzymes with glycine residues results in an enzyme sensitive to low levels of oxygen (Lukey *et al.*, 2011; Pandelia *et al.*, 2011). In *E. coli* Hyd-1, tolerance was found to be largely due to the occurrence of CysS19 (Lukey *et al.*, 2011). A unique environment immediately surrounding the proximal Fe-S cluster is obviously crucial in conferring oxygen-tolerance to hydrogenase enzymes. The effect these

supernumerary cysteines (CysS19 and CysS120) have on the proximal Fe-S cluster of *Salmonella* Hyd-5 is to distort and enlarge the cluster (Figure 3.6b). This contrasts starkly with the cubane architecture of the proximal [4Fe-4S] cluster of oxygen-sensitive hydrogenases. Interestingly, the proximal Fe-S cluster also appears to be coordinated by a histidine residue, HisL229, where 'L' denotes the large subunit.

3.3.5 HisL229 may be important in ligating the proximal Fe-S cluster with GluL73 stabilising the interaction

HisL229 of the large subunit may be an important coordinating residue of the proximal Fe-S cluster (Figure 3.8a). This amino acid is conserved between both oxygen-tolerant and oxygen-sensitive hydrogenases (Figure 3.8b). The equivalent of *Salmonella* HisL229 has been implicated in the ligation of the proximal Fe-S cluster from the oxygen-sensitive [NiFe]-hydrogenase from *D. gigas* (Volbeda *et al.*, 1995). However the equivalent residue was not regarded as a possible ligand of the proximal Fe-S clusters from the other oxygen-tolerant structures solved recently (Fritsch *et al.*, 2011c; Shomura *et al.*, 2011; Volbeda *et al.*, 2012; Volbeda *et al.*, 2013). Observing a close interaction between HisL229 equivalents and the proximal cluster may depend on the general conditions of crystallisation or which state (oxidised or reduced) the enzyme is crystallised in. It is likely that HisL229 may be able to reposition itself due to the flexible region it occupies, which is rich in proline and glycine residues.

Another residue of interest is the buried glutamic acid at position 73 of the large subunit that could possibly interact with HisL229 (Figure 3.8a). The presence of these two residues may be important in coordinating and stabilising the unique proximal Fe-S cluster in its unusual conformation. GluL73 is conserved between the oxygen-tolerant hydrogenases of *E. coli* and *Salmonella* and is replaced by a glutamine in standard oxygen-sensitive hydrogenases (Figure 3.8c). This suggests that GluL73 has an important role within the structure of oxygen-tolerant hydrogenases in particular.

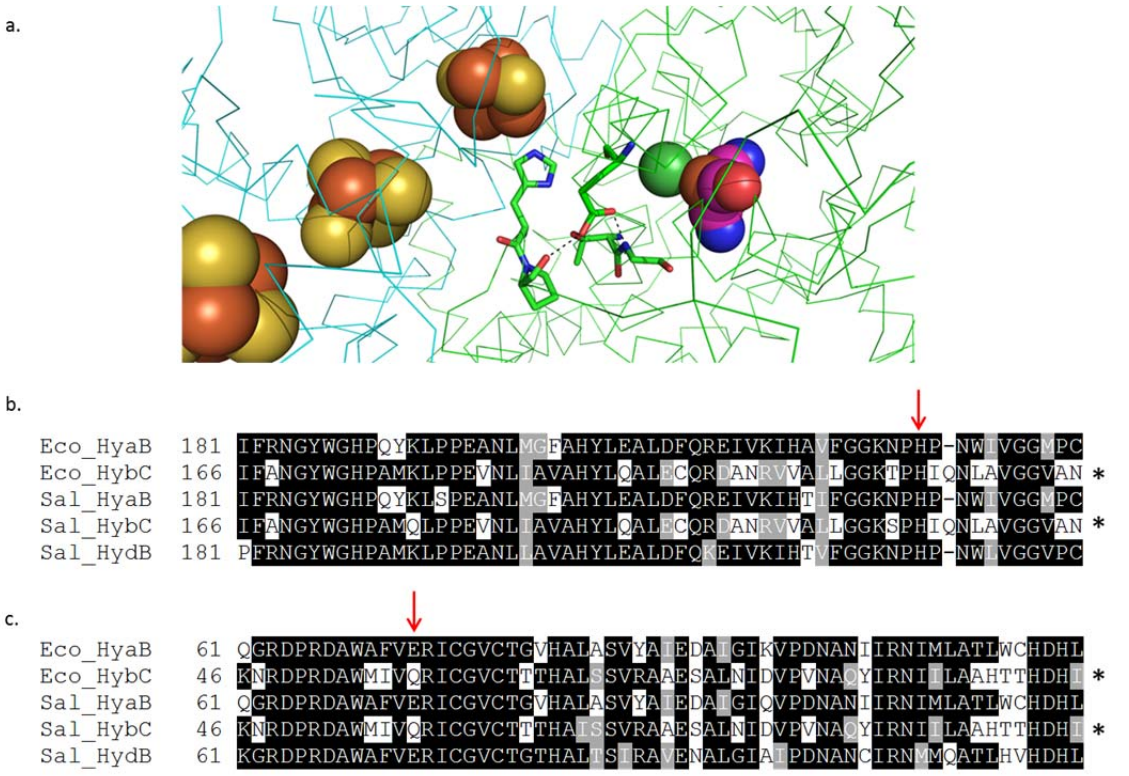

Figure 3.8. HisL229 and GluL73 may have an important involvement in coordinating the proximal Fe-S cluster.
(a) The locations of HisL229 and GluL73 relative to each other, the NiFe active site and the three Fe-S clusters. Spheres are coloured as follows: yellow = sulphur, brown = iron, green = nickel, red = oxygen, purple = carbon and blue = nitrogen. The backbone of the small subunit is traced in blue, while the backbone of the large subunit is traced in green. Dashed lines indicate hydrogen bonding between protonated GluL73 and the carbonyl of ProL230 and the amide of GlyL81. **(b)** HisL229 is conserved between the large subunits of *E. coli* (Eco) and *Salmonella* (Sal) uptake hydrogenases. His229 is indicated with a red arrow. **(c)** GluL73 is conserved between the oxygen-tolerant Hyd-1 from *E. coli* and Hyd-5 from *Salmonella* but is missing from oxygen-sensitive sequences. GluL73 is indicated with a red arrow. Sequences marked with an asterisk are from oxygen-sensitive hydrogenases.

To assess whether HisL229 and GluL73 are genuinely important for the oxygen-tolerance of Hyd-5, the codons for these residues were substituted on the chromosome using site-directed mutagenesis and the pMAK705 recombination method (Hamilton *et al.*, 1989). Substitutions were made independently, with each residue replaced with an alanine residue to yield strains LB03 H229A and LB03 E73A. To check the stability of the enzymes produced by these strains, protein was purified by IMAC and fractions analysed by SDS-PAGE (Figure 3.9). Hyd-5 obtained from strain LB03 H229A appeared stable and both the large and the truncated small subunits were visualised. No contaminating or co-purified proteins were observed (Figure 3.9a). Enzyme produced by strain LB03 E73A also appeared to be stable with the truncated HydA and HydB subunits visible. Also observed was a protein with a molecular weight

higher than that of the large subunit (Figure 3.9b). This corresponds to the size of the heterodimeric complex (around 90 kDa), although this protein has not been identified using mass spectrometry. Why the presence of an SDS-stable Hyd-5 complex would be more apparent when purified from LB03 E73A is unclear. There does not appear to be any degradation of enzyme when purified from either of the substitution strains. The substitution carrying enzymes also appear to resemble enzyme purified from LB03 when assessed after SDS-PAGE. It is possible however that there may be more subtle changes generated within the enzyme that have affected its ability to function under aerobic conditions.

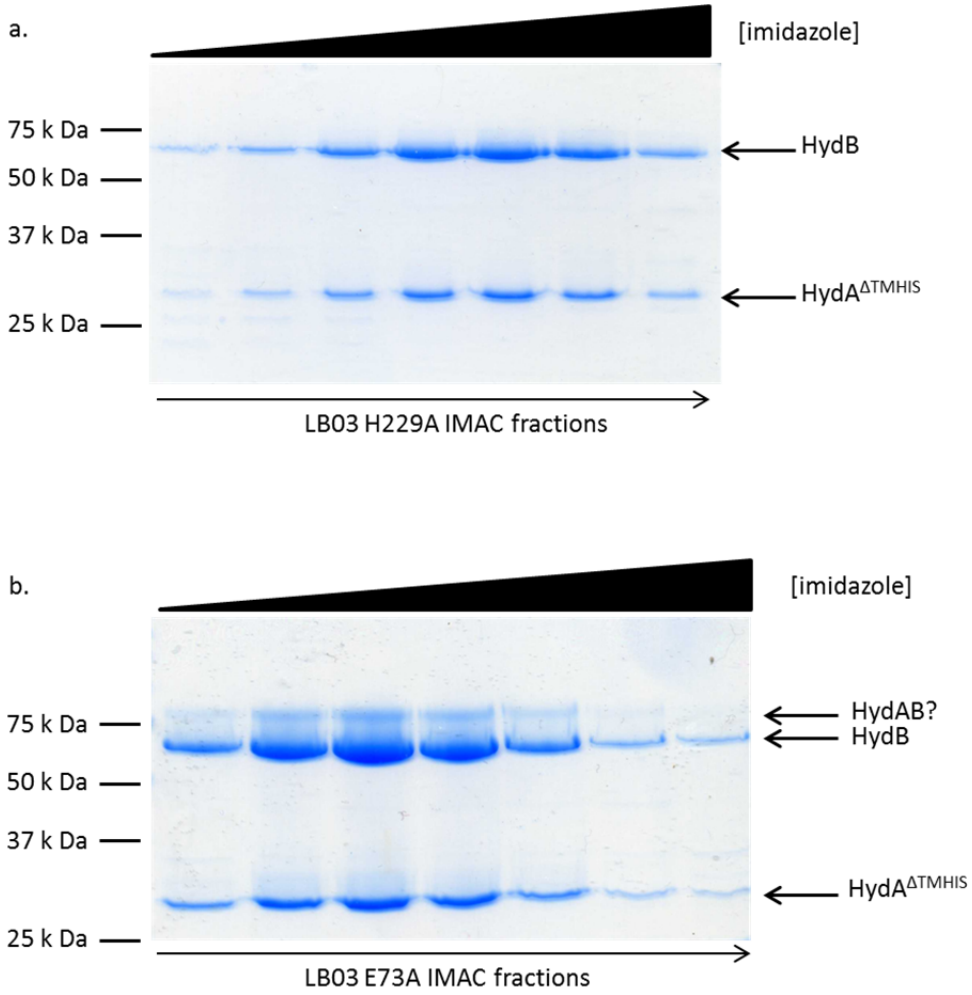

Figure 3.9. Hyd-5 purified from LB03 H229A and LB03 E73A is stable.

Both strains were cultured anaerobically, cells harvested and then disrupted under pressure. Enzyme was purified from **(a)** LB03 H229A and **(b)** LB03 E73A by IMAC and fractions analysed by SDS-PAGE.

To ascertain whether or not the variant enzymes were capable of hydrogen oxidation activity, various assays were performed (Figure 3.10). First, strains LB03,

LT2a, LB03 H229A and LB03 E73A were cultured anaerobically and the hydrogen oxidising activity of whole cell samples assessed using the artificial electron acceptor BV. Total hydrogenase activity was slightly reduced in cells expressing Hyd-5 carrying either of the large subunit substitutions (Figure 3.10a). Next, periplasmic fractions were prepared from the same strains and samples analysed by rocket immunoelectrophoresis. This technique reports on the relative levels of enzyme in different samples and also gives an indication if the enzyme is active. Rocket immunoelectrophoresis cannot give an indication on the specific activities in any sample, however. Activity was stained for using BV and tetrazolium red under hydrogen-saturated conditions at 37 °C (Figure 3.10a). No Hyd-5 activity arcs were observed in the periplasm of LT2a (Figure 3.10a) since Hyd-5 is anchored to the membrane in this strain. The rocket immunoelectrophoresis results suggest that the enzymes carrying the substitutions retain enzymatic activity but are slightly less abundant in the periplasm (Figure 3.10a).

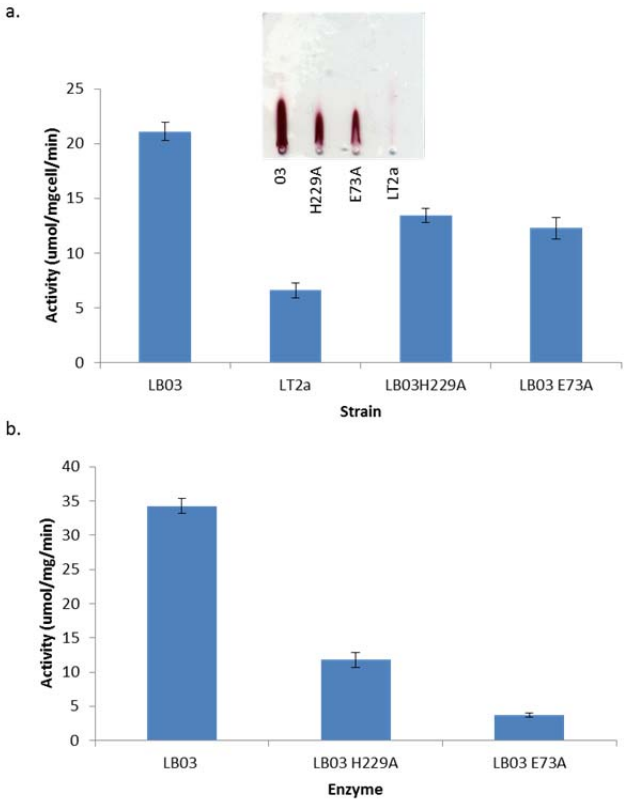

Figure 3.10. His229 and Glu73 substitutions affect the ability of Hyd-5 to oxidise hydrogen under aerobic conditions.

(a) Strains LB03, LT2a, LB03H229A and LB03E73A were cultured anaerobically and whole cells subjected to BV activity assays. Error bars indicate the SEM from three independent experiments. Rocket immunoelectrophoresis was performed on the periplasm fractions of these strains and is shown inset. **(b)** Hyd-5 was purified from strains

LB03, LB03H229A and LB03E73A by IMAC and subjected to BV activity assays. Error bars indicate that assays were performed in triplicate for each enzyme.

Finally, the specific hydrogen oxidising activity of purified Hyd-5 from LB03, LB03 H229A and LB03 E73A was then assessed using BV (Figure 3.10b). In this case, a more dramatic decrease in activity was observed for both variant enzymes. Substituting GluL73 with alanine resulted in the greatest reduction in hydrogen uptake activity. In fact, activity was almost abolished (Figure 3.10b). Therefore residue GluL73 seems to be critical for the activity of Hyd-5.

3.4 Discussion

Salmonella is closely related to *E. coli*, but in general expresses a wider array of respiratory enzymes. *Salmonella* expresses homologs of the Hyd-1 and Hyd-2 uptake hydrogenase enzymes of *E. coli* and also expresses a hydrogen evolving hydrogenase similar to that of *E. coli* (Sawers *et al*., 1986). One important difference between the two however, is the presence of a fascinating third Tat-dependent [NiFe] uptake hydrogenase in *Salmonella* called Hyd-5. Hyd-5 is especially unusual as it is best expressed under aerobic conditions (Zbell *et al.*, 2007). The main objective of this Chapter was to isolate and characterise this aerobically expressed hydrogenase, and add to the knowledge required for biotechnological and biomedical advancement.

3.4.1 Characterising and isolating *Salmonella* Hyd-5

Although Hyd-5 is composed of only two subunits, assembly of the enzyme requires the involvement of nine gene products encoded by the *hyd* operon. Further to this, operons independent from the *hyd* operon are also involved in Hyd-5 biosynthesis. For example, the *isc* operon is required for Fe-S complex formation (Shepard *et al.*, 2011). Due to the complexity of hydrogenase biosynthesis and the desire to avoid potential assembly bottlenecks, expression of the *hyd* operon was upregulated at the native level, on the *Salmonella* chromosome. The addition of a C-terminal his-tag to the small subunit permitted successful purification of the Hyd-5 complex and also facilitated detection of the protein by Western analysis. Biochemical analyses demonstrated that the small subunit was produced under oxygenic conditions but repressed under anoxic conditions. This agrees with recent investigations into gene expression profiles (Zbell *et al.*, 2007). It may be that under anaerobic conditions, Hyd-1 and Hyd-2 are being produced at such an elevated level that the activity of Hyd-5 is redundant.

The fact that the Hyd-5 operon is maximally expressed under aerobic conditions suggests that the enzyme may be capable of performing hydrogen oxidation when oxygen is present. As part of this project a number of complementary electrochemistry experiments were performed on Hyd-5 by the Armstrong Group in Oxford. First, protein film electrochemistry (PFE) was employed to analyse the effect

of varying hydrogen partial pressure on the activity of Hyd-5 (Parkin *et al.*, 2012). This is a well-established technique used to study hydrogenase activity. Enzymes are adsorbed onto electrode materials and electron transfer between the electrode and protein are measured (Vincent *et al.*, 2007). The enzyme's catalytic activity is measured as a function of the applied potential and the electrical current produced relates to the frequency of enzyme turnover in the presence of substrate. Experiments take place in an anaerobic glove-box where both the temperature and pH are controlled and gas mixtures are supplied at a constant flow rate. Once the enzyme has been adsorbed, the electrode is rotated at a constant rate to ensure the efficient provision of substrate and removal of product. Using PFE, a positive electrical current was generated by the hydrogen oxidising activity of Hyd-5 (complete with transmembrane domain). As there was no negative current measured at low potentials, it was concluded that Hyd-5 was capable of hydrogen oxidation but not proton reduction. It was demonstrated that hydrogen oxidation was initiated at potentials more positive than -0.28V, which was described as an "overpotential requirement". This requirement was not altered as the percentage of hydrogen supplied was varied (Parkin *et al.*, 2012).

The ability of Hyd-5 to exhibit hydrogen oxidising activity in the presence of physiologically relevant levels of oxygen was also tested. Positive currents were measured under both oxygenic and anaerobic conditions although this was substantially reduced when 3% oxygen was included in the gas mixture (Figure 3.11). Oxygen does inhibit all hydrogenases to an extent and Hyd-5 is no different. It is therefore not surprising to see a decreased rate of hydrogen oxidation. At potentials lower than 0 V, a negative current was measured that does offset the positive current to an extent. At potentials greater than 0 V, hydrogen oxidation is abolished (Figure 3.11). This suggests the occurrence of an oxygen species bound to the active site, generating an inactive enzyme. This state is reversible however, as when the potential is decreased, electrical current increases (Figure 3.11). This suggests that the enzyme forms the "ready" inactive state when oxygen is present.

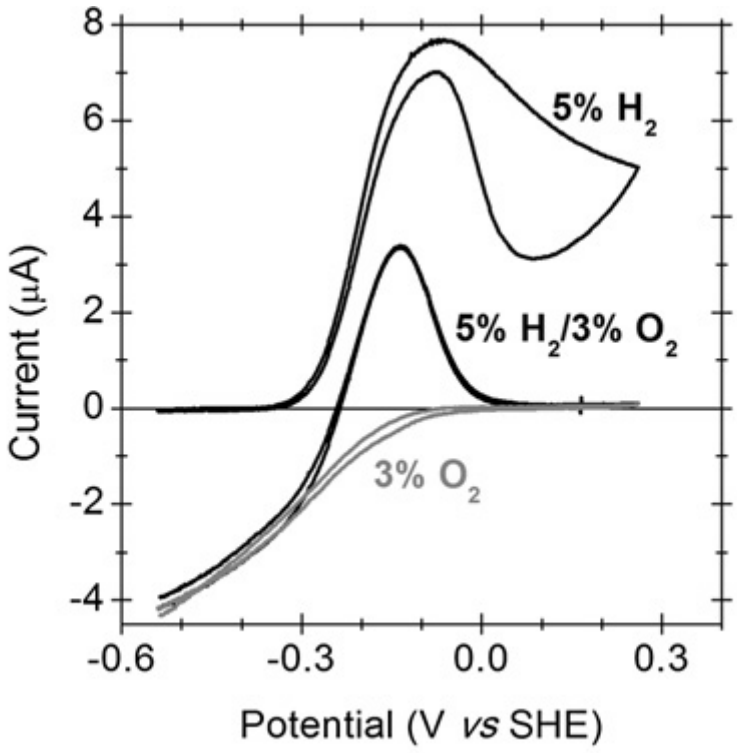

Figure 3.11. Cyclic voltammogram reveals the ability of Hyd-5 to oxidise hydrogen in the presence of oxygen. Cyclic voltammograms were measured at 2 mV s^{1} and buffer maintained at 37°C and at pH 7.4. Three separate gas mixtures of 5% hydrogen; 5% hydrogen and 3% oxygen; and 3% oxygen were used. PFE was performed by the Armstrong Group, Oxford University (Parkin *et al.*, 2012).

Electron paramagnetic resonance (EPR) experiments were also performed to characterise the redox-active centres of Hyd-5 including the [NiFe] active site and the three Fe-S clusters. EPR signals revealed that the active site was present in two states: the "ready" and the "unready" states. This is similar to what has been observed for the oxygen-tolerant Hyd-1 of *E. coli* (Lukey *et al.*, 2010). A "high potential" centre was observed in the Fe-S region of the spectrum that had previously been believed to represent the proximal [4Fe-4S] Fe-S cluster (Pandelia *et al.*, 2011). Of course, now it is known that the proximal Fe-S cluster has an unusual architecture and is actually a [4Fe-3S] cluster.

Hyd-5 can thus be classified as an oxygen-tolerant enzyme and its production induced under aerobic conditions. This enzyme has great potential for future biotechnological applications.

3.4.2 What is the mechanism of oxygen-tolerance?

At the beginning of this project, molecular insights into the basis of oxygen-tolerance were emerging but crucial structural information was still unavailable. As the [NiFe] active site is the target of molecular oxygen, initial experiments focussed on this region. In fact, amino acid substitutions located within the gas channels of the oxygen-sensitive hydrogenase from *Desulfovibrio fructosovorans* were found to dramatically increase its oxygen-tolerance (Liebgott *et al.*, 2010). The catalytic activity of this enzyme however did not match that of 'true' oxygen-tolerant enzymes. Therefore, it was suggested that the mechanism of oxygen-tolerance must involve a number of different factors (Friedrich *et al.*, 2011). The presence of two extra conserved cysteine residues close to the proximal Fe-S cluster of oxygen-tolerant hydrogenases pointed towards an unusual modification in this region. Mutagenesis experiments were performed to alter these cysteines and monitor changes in oxygen-tolerance. Substituting the cysteines of oxygen-tolerant enzymes from *E. coli* and *R. eutropha* H16 for glycines resulted in an acquired sensitivity to oxygen reflecting the importance of these residues (Goris *et al.*, 2011; Lukey *et al.*, 2011). Spectroscopic analyses also indicated a modified environment surrounding a unique proximal Fe-S cluster in oxygen-tolerant hydrogenases (Lukey *et al.*, 2010; Fritsch *et al.*, 2011b; Lukey *et al.*, 2011; Pandelia *et al.*, 2011).

In 2011, structural information emerged that validated results obtained from both spectroscopic and biochemical studies. Crystal structures of the membrane bound hydrogenases (MBH) from *R. eutropha* and *Hydrogenovibrio marinus* were solved, offering great insight into the basis of oxygen-tolerance (Fritsch *et al.*, 2011c; Shomura *et al.*, 2011). Whereas Fritsch *et al*. (2011c) reported the structure of a heterodimeric hydrogenase from *R. eutropha*, Shomura *et al*. (2011) reported that the *H. marinus* enzyme formed a dimer of heterodimers, similar to that of *Salmonella* Hyd-5. Shomura and co-workers (2011) believe this dimer to be biologically correct for a number of reasons. First, the area of contact between the two heterodimers is high at almost 11% of the total surface area. Secondly, the distal clusters and the C-termini of both small subunits are arranged facing each other (Shomura *et al.*, 2011). The standard [NiFe]-hydrogenase from *A. vinosum* also crystallised as a heterotetramer (Ogata *et al.*, 2010) so this association does not appear to be restricted to oxygen-tolerant hydrogenases. Neither of the oxygen-tolerant structures revealed any

significant differences between the active sites of oxygen-tolerant and oxygen-sensitive hydrogenases, which suggest that oxygen-tolerance is dependent on modifications elsewhere. Both structures however reveal the modified architecture of the proximal Fe-S cluster. Like *Salmonella* Hyd-5, these enzymes also contain a [4Fe-3S] proximal Fe-S cluster indicative of a conformation unique to oxygen-tolerant hydrogenases. The sulphide of CysS19 in *R. eutropha* (or CysS25 in *H. marinus*) appears to replace the missing sulphide that is present in standard hydrogenases. Fritsch *et al*. (2011c) also note that CysS120 and CysS149 serve to enlarge the Fe-S cluster by withdrawing an iron atom from its usual cubane shape. Additional information gained from the study by Fritsch *et al*. (2011c) was the presence of water filled cavities situated between the active site and the solvent. The authors suggest the controlled translocation of water through gated salt-bridges following the complete reduction of oxygen.

Shortly after these structures were published, the crystal structure of *E. coli* Hyd-1 was solved (Volbeda *et al.*, 2012). Again, similar to *Salmonella* Hyd-5, *E. coli* Hyd-1 appears to exist as a dimer of heterodimers. In the mid-1980's, characterisation of both *E. coli* Hyd-1 and Hyd-2 from detergent dispersed membranes led to the finding that both enzymes were likely to be heterotetramers (Ballantine and Boxer, 1986; Sawers and Boxer, 1986). Volbeda *et al*. (2012) also believe that this is relevant in biological terms as the arrangement agrees with previous observations where one hydrogenase was able to "jump-start" another by donating electrons (Wait *et al.*, 2010). Volbeda *et al*. (2012) also found water molecules within their structure but these appear to be confined to the hydrophobic gas channel. The *E. coli* study also implicated GluL76 in coordinating the proximal Fe-S cluster. It is thought that GluL76 could deprotonate CysS20, triggering a movement in the Fe-S cluster, which makes this cluster highly dynamic (Volbeda *et al.*, 2012; Mouesca *et al.*, 2013). The structure of *E. coli* Hyd-1 has since been solved in partial complex with cytochrome *b*, its integral membrane partner, in a 2:1 ratio (Volbeda *et al.*, 2013). A representation of this is depicted in Figure 3.12.

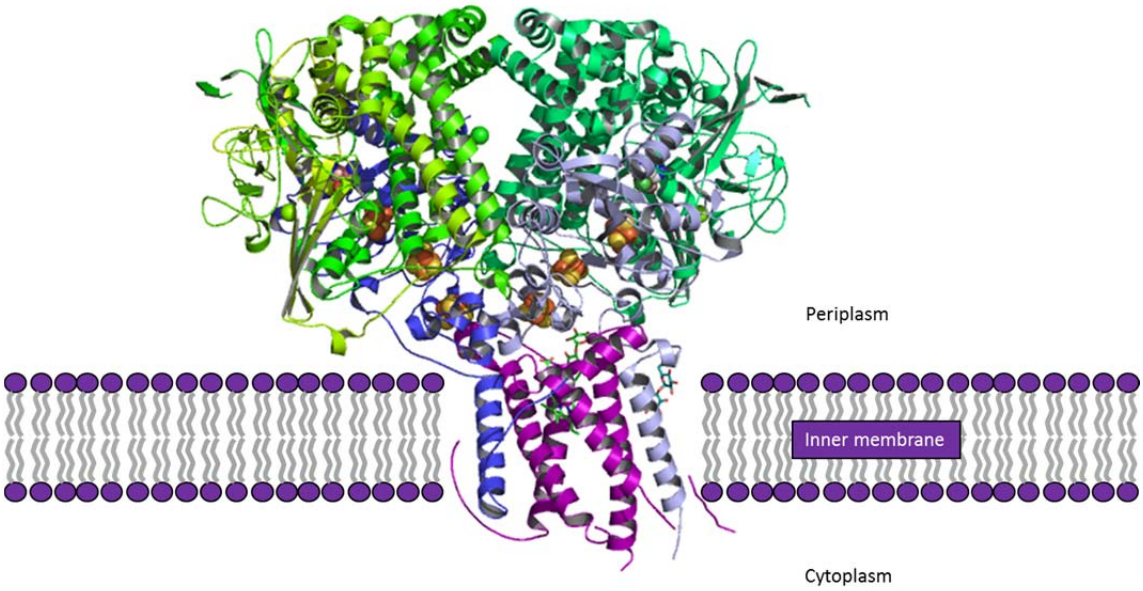

Figure 3.12. The crystal structure of *E. coli* Hyd-1 associated with cytochrome b.

Hyd-1 crystallised as a dimer of dimers. Both hydrogenase transmembrane domains were solved as was one haem-containing cytochrome *b*. Cytochrome *b* was found to contain a single haem cofactor. Subunits are coloured as follows: the large subunit in dark and light green, the small subunits in dark and light blue and cytochrome *b* in purple. Atoms are coloured as follows: iron atoms in orange, sulphur atoms in yellow, nickel atoms in dark green, nitrogen in blue, carbon in pink and magnesium in green.

Volbeda *et al*. (2013) highlight a number of points that support an *in vivo* interaction between cytochrome *b* and one of the hydrogenase small subunits of *E. coli* Hyd-1. Firstly, the interfaces of both proteins contain a number of conserved residues. Secondly, the shape and charge of the interface is complementary. Thirdly, a similar interaction between the small subunit of *E. coli* formate dehydrogenase-N (FDH-N) and its cognate cytochrome has been observed. Lastly, the cytochrome can be partially reduced with hydrogen suggesting that electrons can be transferred from the distal Fe-S cluster to the cytochrome haem. There are however, key omissions from the crystal structure solved by Volbeda *et al*. (2013). Only one cytochrome *b* subunit was revealed per hydrogenase dimer of dimers where two would be expected. Furthermore, analysis of the *E. coli* HyaC amino acid sequence leads to the prediction that this subunit contains two haem groups (Figure 3.13). Unfortunately, only one haem was visible per cytochrome *b*. The region of the cytochrome furthest from the hydrogenase is disordered and not folded as tightly as regions closer to the hydrogenase (Volbeda *et al.*, 2013). This may have resulted in loss of the 'distal' haem, a particularly important feature as this would constitute the site of ubiquinone binding to the enzyme.

E. coli HyaC and *Salmonella* HydC share a number of conserved amino acid residues (Figure 3.13). Many of the conserved residues of cytochrome *b* have also been implicated in forming interactions with the two *E. coli* Hyd-1 small subunits of the heterotetramer. Therefore it is likely that *Salmonella* HydC forms similar interactions with Hyd-5 as *E. coli* HyaC does with Hyd-1. It is likely that the extended N-terminus that *Salmonella* HydC is predicted to possess does not actually exist. A closer look at the nucleotide sequence reveals the presence of a ribosome binding site upstream of Met24. Therefore, it is possible that Met24 constitutes the true start site.

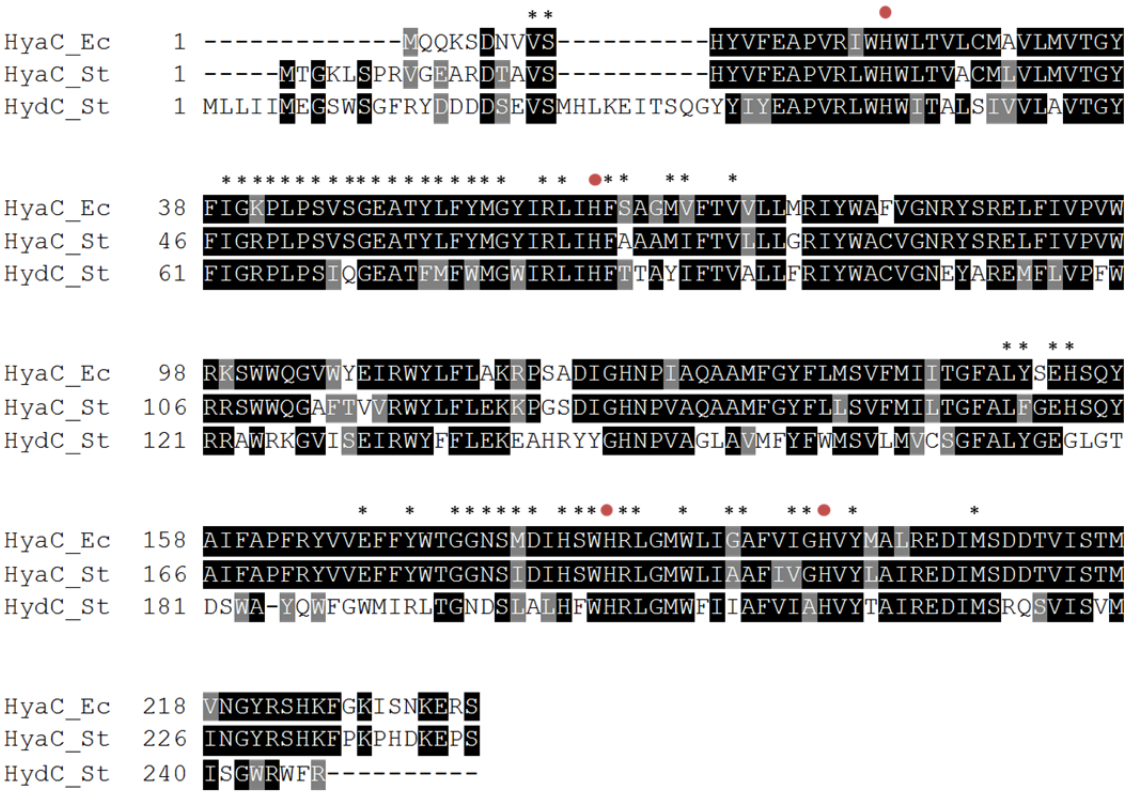

Figure 3.13. Amino acid sequence alignment of cytochrome *b* subunits from *E. coli* (Ec) and *Salmonella* (St). Residues thought to interact with the small subunits of *E. coli* Hyd-1 are marked with an asterisk, based on the observations of Volbeda *et al*. (2013). Histidine residues marked with a red circle represent amino acids involved in ligating the haem groups. Black shading highlights identical residues shared between 50% of the sequences; grey shading highlights conservative substitutions of these whereas residues in white indicate non-conserved amino acids.

The proximal Fe-S cluster was an unprecedented find. There is one other known Fe-S cluster with remarkable similarity to that of the proximal Fe-S clusters of oxygen-tolerant hydrogenases: the nitrogenase P-cluster. As with the proximal Fe-S cluster of hydrogenases, the coordination and the structure of the P-cluster was a

subject of controversy. It was unknown whether the P-cluster contained 8 Fe atoms and 8 S atoms or 8 Fe atoms and 7 S atoms. The structure of the P-cluster was solved by Peters *et al*. (1997) who demonstrated that the cluster was a 8Fe-7S cluster containing two 4Fe-3S clusters, one of which was found in a distorted state similar to the proximal Fe-S cluster of oxygen-tolerant hydrogenases.

The presence of two additional cysteine residues in oxygen-tolerant hydrogenases imparts unusual electronic properties upon the proximal Fe-S cluster. Remarkably, this cluster is stable in three different oxidation states by virtue of its unique structure and plasticity. Clearly, when oxygen attacks the active site, its removal has to be highly efficient. The complete reduction of oxygen to water requires four electrons and protons to prevent the formation of reactive oxygen species that would render the enzyme inactive (Friedrich *et al.*, 2011). When oxygen attacks the [NiFe] active site of oxygen-sensitive hydrogenases, two spectroscopically distinctive inactive states of Ni (III) can be formed. The first is termed Ni-A, or the "unready state", which forms under electron-poor conditions and is slow to reactivate (De Lacey *et al.*, 2007). The oxygen species bridging the Ni and Fe atoms of the Ni-A state is unknown but is hypothesised to be either a mono (Ogata *et al.*, 2010) or di-oxygen species (Volbeda *et al.*, 2005). This is in contrast to Ni-B or the "ready state", which is favoured under electron-rich conditions and can be reactivated rapidly (De Lacey *et al.*, 2007). In this case, a hydroxide ligand is believed to bridge the atoms of the metallocentre (Volbeda *et al.*, 2005). This is highlighted in Figure 3.14. One of the characteristics shared by oxygen-tolerant hydrogenases is that only the Ni-B inactive state is generated upon oxygen attack (Parkin and Sargent, 2012).

Each of the oxygen-tolerant structural studies highlight the unique redox transitions of which the proximal Fe-S is capable of undergoing (Fritsch *et al.*, 2011c; Shomura *et al.*, 2011; Volbeda *et al.*, 2012). The suggestion is that this cluster can rapidly deliver two electrons to the active site for the reduction of oxygen instead of the single donation that the proximal clusters of oxygen-sensitive hydrogenases are restricted to. The final two electrons can be sourced from redox transitions of the medial cluster and the [Ni-Fe] active site itself. As the distal Fe-S cluster is not required to contribute an electron, the thermodynamic hurdle is lowered, resulting in faster electron delivery. Therefore, only the Ni-B state is generated, resulting in rapid reactivation of the enzyme (Parkin and Sargent, 2012). Avoidance of the Ni-A state,

and consequently slow reactivation, is important for oxygen-tolerance and the rapid reduction of oxygen to water (Figure 3.14).

Interestingly, six cysteine coordinated [4Fe-3S] clusters are not confined to aero-tolerant microorganisms but have also been found in strict anaerobes including Chlorobi and Heliobacteria. Evolutionary analyses now support the suggestion that [4Fe-3S] clusters existed before the emergence of oxygen and were possibly required for the successful reduction of the photo-oxidised reaction centre pigment, which has a relatively high potential (Pandelia *et al.*, 2012).

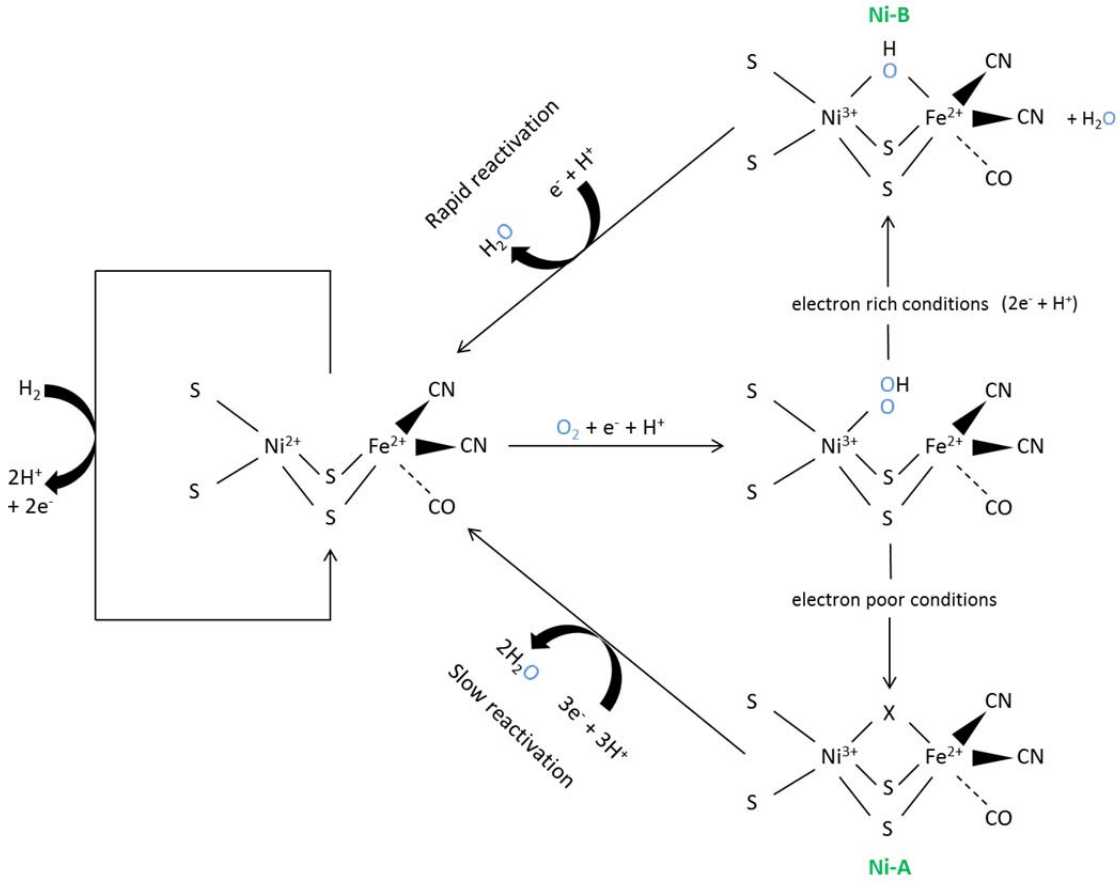

Figure 3.14. A model of oxygen reduction by [NiFe]-hydrogenases.

The Ni-B state is formed after the reduction of oxygen by four electrons whereas the Ni-A state results from the two electron reduction of oxygen. The bridging ligand between Ni and Fe of the Ni-A state is unknown so is depicted as X.

The unique proximal Fe-S cluster, although critical for oxygen-tolerance, does not appear to be the only feature responsible for conferring oxygen-tolerance. The experiments referred to previously where cysteine replacements were made did result in engineered oxygen-sensitivity, but only after several minutes of exposure (Goris *et*

al., 2011; Lukey *et al.*, 2011). True oxygen-sensitive hydrogenases are inactivated within seconds under the same conditions, indicating that oxygen-tolerant enzymes possess additional characteristics that influence their ability to function aerobically. A common determinant of oxygen-tolerance is the resistance of the enzyme to carbon monoxide inactivation (Fritsch *et al.*, 2013). Engineering oxygen-sensitivity into oxygen-tolerant enzymes through cysteine substitutions at the proximal Fe-S cluster does not result in an acquired sensitivity to carbon monoxide (Goris *et al.*, 2011; Lukey *et al.*, 2011). The fact that carbon monoxide exposure does not lead to inactivation of the enzyme whereas oxygen does, suggests that properties unique to the active site are involved here. The medial [3Fe-4S] cluster is also thought to contribute to oxygen-tolerance even though this conformation is shared between oxygen-tolerant and standard hydrogenases. Altering this cluster has been demonstrated to affect the stability of hydrogenases under aerobic conditions (Fritsch *et al.*, 2013).

The oxygen-tolerant hydrogenase enzymes investigated to date appear to be dedicated to hydrogen oxidation only. The mechanism of oxygen-tolerance clearly demonstrates that electron flow can be reversed so as to reduce oxygen at the active site. Is it possible that these enzymes are also capable of reducing protons and therefore aerobic hydrogen production? If not, there are perhaps uncharacterised enzymes with this ability, which would be a great leap forward for hydrogen based technologies.

3.4.3 Are HisL229 and GluL73 important for coordinating the proximal Fe-S cluster?

In contrast to the other available oxygen-tolerant hydrogenase structures, the *Salmonella* Hyd-5 structure appears to indicate a further coordination of the proximal Fe-S cluster by a histidine residue (HisL229) present in the large subunit (Figure 3.8a). The main difference between the isolated *Salmonella* Hyd-5 enzyme and the others is the fact that this enzyme has never been "turned over" *in vivo* and has not delivered electrons to the quinone pool due to its transmembrane deletion. Further to this, Hyd-5 was purified aerobically and crystallised under naturally oxidising conditions. The other crystals were obtained either under reducing conditions, chemically oxidised conditions or under anaerobic conditions with or without the addition of hydrogen (Fritsch *et al.*, 2011c; Shomura *et al.*, 2011; Volbeda *et al.*, 2012; Volbeda *et al.*, 2013). Therefore it is possible, that the structure of *Salmonella* Hyd-5 has revealed something

the others could not. The fact that substituting this histidine for an alanine resulted in a reduction of hydrogen oxidising activity (Figure 3.10) suggests that this residue does have a role in coordinating and possibly stabilising the proximal Fe-S cluster.

The crystal structure of the [NiFe]-hydrogenase from *Desulfovibrio gigas* provided valuable information regarding the coordination of its proximal Fe-S cluster (Volbeda *et al.*, 1995). In addition to four coordinating cysteine residues within the small subunit, the proximal Fe-S cluster also appeared to be ligated by a histidine residue present in the large subunit (Volbeda *et al.*, 1995). This histidine residue (HisL219) is equivalent to HisL229 in *Salmonella* (Figure 3.15) and supports the suggestion that HisL229 is a true ligand of the proximal Fe-S cluster in *Salmonella* Hyd-5. Further validation is provided following analysis of complex I mutagenesis studies (Kashani-Poor *et al.*, 2001; Grgic *et al.*, 2004). Respiratory complex I is a multi-subunit membrane bound oxidoreductase, conserved in all kingdoms of life. These enzymes oxidise a variety of electron donors, coupling this with the reduction of quinone and translocation of protons across the inner mitochondrial or bacterial membrane (Efremov and Sazanov, 2012). The complete crystal structure of complex I from *Thermus thermophilus* has recently been solved: a huge achievement as this particular complex consists of sixteen subunits, seven of which are membrane embedded (Baradaran *et al.*, 2013). Interestingly, complex I shares homology with [NiFe]-hydrogenases. Subunits Nqo6 (NuoB) and Nqo4 (NuoD) of complex I are homologous in sequence and structure to [NiFe]-hydrogenase small and large subunits respectively (Efremov and Sazanov, 2012). Complex I also accommodates an equivalent to the proximal Fe-S cluster of [NiFe]-hydrogenases called N2, present in Nqo6. This cluster is coordinated by four cysteine residues, two of which are unusual tandem cysteines (Cys45 and Cys46 in *T. thermophilus*) that strain the geometry of the cluster and increase the flexibility of the region (Berrisford and Sazanov, 2009). The possibility that both adjacent cysteine residues could ligate cluster N2 was originally considered unlikely due to steric reasons. An earlier study using the yeast *Yarrowia lipolytica* as a model, concentrated on identifying the fourth N2 cluster ligand (Grgic *et al.*, 2004). As the N2 cluster is situated at the interface of the PSST subunit (homologous to Nqo6/NuoB/HydA) and the 49 kDa subunit (homologous to Nqo4/NuoD/HydB), Grgic *et al*. (2004) substituted a number of conserved histidine and arginine residues within the 49 kDa subunit, as ligand options within the PSST subunit had already been ruled

out (Kashani-Poor *et al.*, 2001). One of the histidine residues investigated, His226, is equivalent to *Salmonella* HisL229 and to *D. gigas* HisL219 (Figure 3.15), both of which have been implicated in the ligating of a proximal Fe-S cluster. Substituting His226 for alanine impacted the ubiquinone reductase activity of the enzyme significantly, reducing it by 80%. Complex I assembly however appeared normal as evaluated by blue native-PAGE. Moreover, the substitution had a drastic effect on N2 as no EPR signal could be detected for this cluster from purified protein or mitochondrial membranes (Grgic *et al.*, 2004). Clearly this residue is significant in influencing the properties of the N2 cluster. Due to the conserved nature of this residue, it is likely that this histidine performs a similar function in hydrogenase enzymes.

Figure 3.15. Partial amino acid sequence alignment of [NiFe]-hydrogenase large subunits and the 49 kDa subunit of complex I.

Sequences are taken from the large subunits of *Salmonella* (St), *D. gigas* (Dg) and *D. fructosovorans* (Df) and also the 49 kDa subunit of complex I from *Y. lipolytica* (Yl). The conserved histidine residue (HisL229 in *Salmonella*) is indicated with an arrow. Black shading highlights identical residues shared between 50% of the sequences; grey shading highlights conservative substitutions of these whereas residues in white indicate non-conserved amino acids.

Substituting HisL229 for the small hydrophobic alanine resulted in a reduction of hydrogen oxidising activity of *Salmonella* Hyd-5 (Figure 3.10). Rocket immunoelectrophoresis was performed to further assess the activity of Hyd-5 from this variant strain. As the transmembrane domain of the enzyme has been genetically deleted from this strain, Hyd-5 activity is no longer associated with cell membranes but is located in the periplasm instead. Thus, periplasmic samples were assessed for Hyd-5 specific activity. A reduction in the levels of active Hyd-5 was observed from the variant strains using this method. This was also true for GluL73.

Based on observations of the *Salmonella* Hyd-5 structure, GluL73 was hypothesised as interacting with residue HisL229 (Figure 3.8a). Substituting GluL73 for alanine resulted in a more drastic reduction in hydrogen uptake activity, especially when the enzyme was isolated from the cell (Figure 3.10). This charged residue has

been noted before by Shomura *et al*. (2011) as one of the only two acidic amino acids around the proximal Fe-S cluster of *H. marinus* that is not conserved in standard hydrogenase enzymes. The importance of GluL73 was dismissed however as the residue is not completely conserved between membrane bound hydrogenases. This was viewed as evidence that the residue was unimportant for conferring any electronic properties to the proximal Fe-S cluster. However, GluL73 is largely conserved between oxygen-tolerant hydrogenases (Figure 3.8c). From the comparisons made by Shomura *et al*. (2011), the only hydrogenase found to have an alternative residue in place of Glu73 was from *A. vinosum*. This hydrogenase is not oxygen-tolerant as the small subunit of this enzyme does not possess the extra cysteine residues required for ligation of the proximal Fe-S cluster unique to oxygen-tolerant hydrogenases (Figure 3.7). It is possible that GluL73 is important for stabilising the Fe-S cluster in a particular conformation required for oxygen-tolerance.

Next, both *Salmonella* mutant strains described here should be cultured anaerobically and anaerobic activity assays performed on intact cells and on anaerobically purified protein. This would indicate whether or not the residues impact on the hydrogen oxidising activity of the enzyme when oxygen is omitted. Hyd-5 isolated from both LB03 H229A and LB03 E73A should also be entered into crystallisation trials. This would provide an insight into the effect these substitutions are having locally and more specifically on the proximal Fe-S cluster. Understanding which residues are important in coordinating and stabilising vital cofactors like Fe-S clusters, especially those involved in oxygen-tolerance, is crucial for the engineering of oxygen-tolerant hydrogenase enzymes.

3.4.3.1 Electrochemical characterisation of Hyd-5 obtained from LB03 H229A and E73A

To assess the importance of His229 and Glu73 to the catalytic activity of native Hyd-5 and Hyd-5 variants H229A and E73A, PFE experiments were performed in collaboration with Lindsey Flanagan and Dr Alison Parkin from the Department of Chemistry, University of York. First, the effect of varying the concentration of hydrogen was tested. At each percentage of hydrogen in the gas mixture, the E73A variant behaved similarly to native Hyd-5. In contrast, the H229A variant exhibited a different wave shape to native Hyd-5 and the E73A variant. The overpotential

requirement of native Hyd-5 and the E73A variant was not present in the H229A variant, indicating that this histidine affects the potential of the proximal Fe-S cluster. In addition, as the electrode potential is increased, the H229A variant becomes anaerobically inactivated. The enzyme is however, almost fully reactivated on the reverse scan (Figure 3.16a).

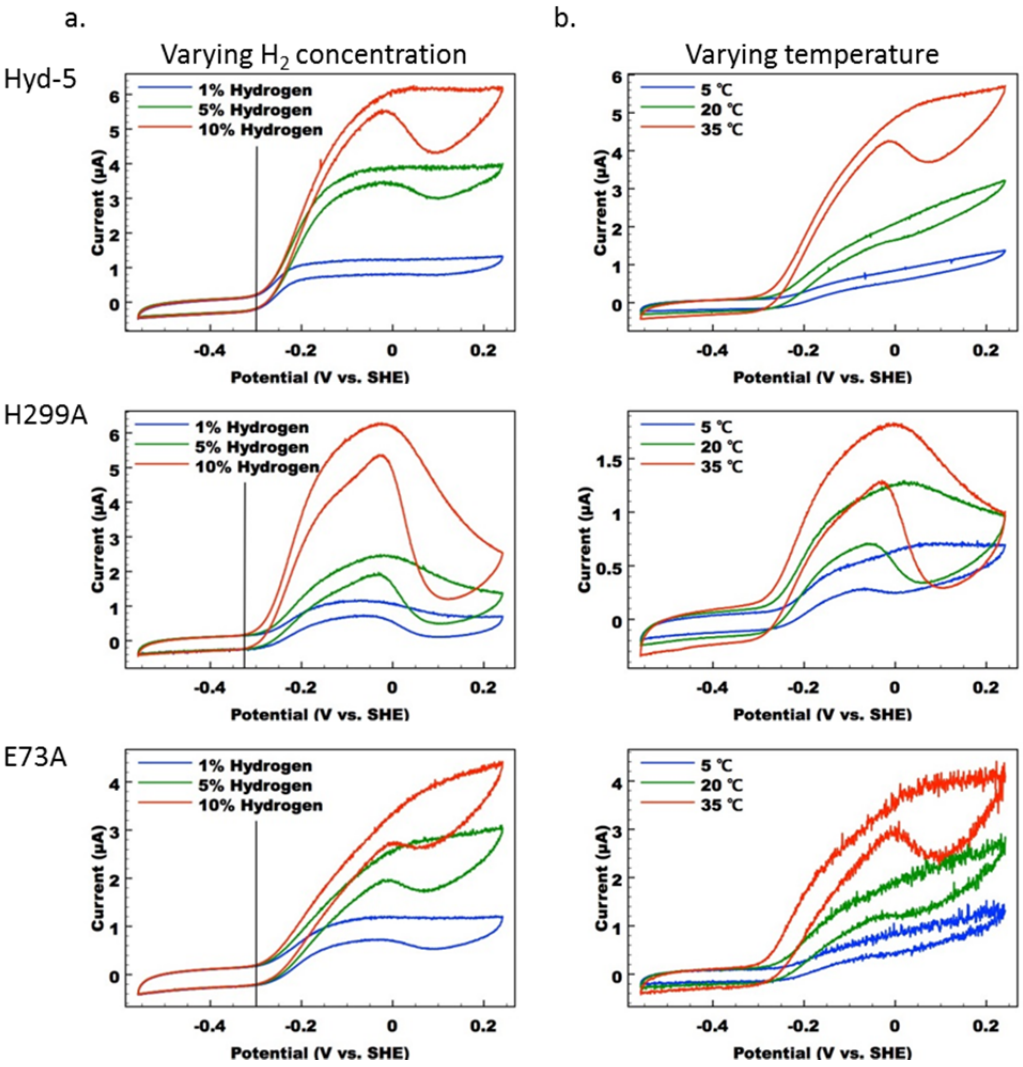

Figure 3.16. The effect of varying hydrogen concentration and temperature on the catalytic response of native Hyd-5 and Hyd-5 variants.

Cyclic voltammograms were measured at 5 mV s^{-1}, the buffer maintained at pH 6. 0 and the electrode rotated at 4000 rpm for Hyd-5 isolated from LB03, LB03 H229A and LB03 E73A. **(a)** The catalytic response to hydrogen was measured under three separate gas mixtures of 1%, 5% and 10% hydrogen at a constant temperature of 37°C. A vertical line indicates the hydrogen oxygen potential for each variant enzyme. **(b)** The catalytic response to temperature was measured at 5°C, 20°C and 35°C at a concentration of 10% hydrogen. Experiments were performed by Dr Alison Parkin and Lindsey Flanagan from the Department of Chemistry, University of York.

As the H229A variant is inactivated at a much lower potential, it is likely that the Ni(III) state (probably Ni-B) is formed more easily than for native Hyd-5. If Ni(II) became Ni(III) by delivering one electron to the proximal Fe-S cluster, this would indicate the cluster has a lower reduction potential. This would also suggest that above -0.05 V, H229A contains a $[4Fe3S]^{4+}$ proximal cluster capable of accepting electrons and facilitating the oxidation (and inactivation) of the active site. This is in contrast to native Hyd-5 and the E73A variant that possess a $[4Fe3S]^{3+}$ proximal cluster incapable of accepting electrons to potentials up to and above 0.1 V. Therefore, it appears that the presence of His229 in the native enzyme impedes the transfer of electrons to the proximal Fe-S cluster and serves to create an overpotential requirement.

Secondly, the effect of varying temperature was assessed. As before, the cyclic voltammograms looked similar for native Hyd-5 and E73A at each temperature (Figure 3.16b). At 5°C, anaerobic inactivation was hardly observed for either of these two enzymes. The H229A variant, on the other hand, displayed some inactivation at high potentials and at each temperature tested. This indicates that the activation energy required for Ni-B formation by H229A is different from that of native Hyd-5 and E73A.

Finally, the catalytic response of native Hyd-5 and the two variants to oxygen was investigated. This was performed in a step-wise manner. Initially, the gas mixture contained 3% hydrogen only, which was then altered to 3% hydrogen and 3% oxygen. The enzyme was then given a recovery period when the oxygen was turned off and the environment contained 3% hydrogen once more. Finally, the gas mixture contained 3% oxygen. Native enzyme did not appear to be strongly affected by the presence of oxygen as Hyd-5 retained 80% of its hydrogen oxidising activity at -0.059 V under these conditions Figure 3.17). Inactivated enzyme was presumed to be in the Ni-B state as active enzyme was observed once the oxygen flow was turned off. The H229A and E73A variants were more affected by oxygen as they demonstrated less activity in this environment. It is presumed that most of the inactivated enzyme was present in the Ni-A state as the activity levels achieved before the addition of oxygen were not reached once removed (Figure 3.17). In contrast to native Hyd-5, no hydrogen oxidising activity was observed at higher potentials for either of these mutant enzymes, although it must be stated that H229A was more affected by oxygen than E73A. From these results, it has been hypothesised that His229 acts to stabilise the

proximal Fe-S cluster in an 'open' $[4Fe3S]^{5+}$ state that may only be possible if Glu73 deprotonates the histidine. The formation of this open state would be less favourable upon loss of either of these residues and the formation of Ni-A more likely.

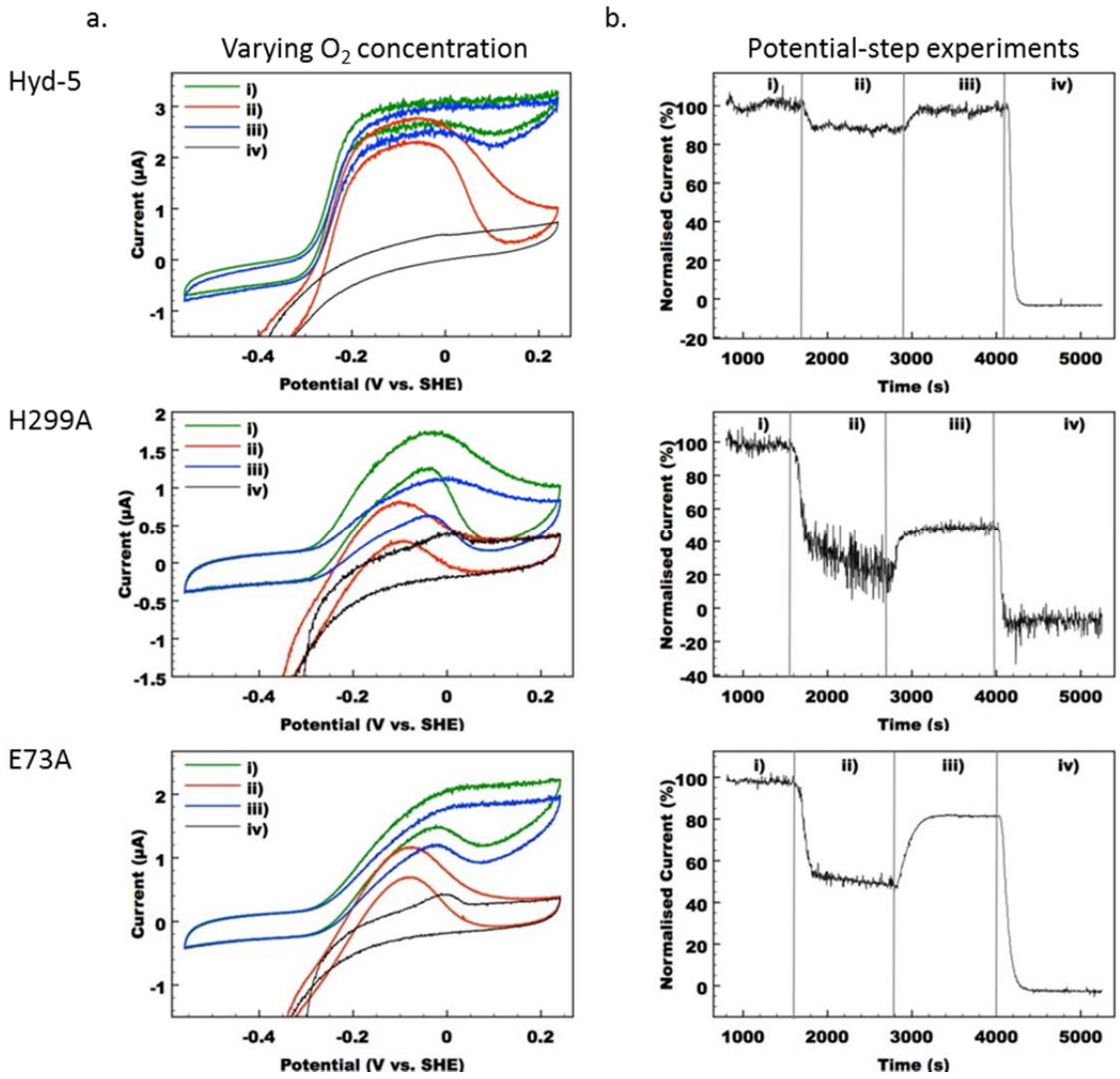

Figure 3.17. The response of native Hyd-5 and Hyd-5 variants to varying oxygen concentrations.

(a) Cyclic voltammograms and chronoamperometry were measured at gas mixtures of (i) 3% hydrogen only (ii) 3% hydrogen and 3% oxygen (iii) 3% hydrogen (recovery) and (iv) 3% oxygen only for native Hyd-5 and variants H229A and E73A. Measurements were taken at 5 mV s^{-1} and the buffer maintained at pH 6. 0 and at 37°C. **(b)** Chronoamperometry experiments were performed at a constant potential of -0.3V. Experiments were performed by Dr Alison Parkin and Lindsey Flanagan from the Department of Chemistry, University of York.

As it was only possible to assume the redox states of the variant enzyme proximal Fe-S clusters, it would be useful to perform more definitive experiments. EPR spectroscopy should be performed on each of the variant enzymes to gain an insight into what state the proximal Fe-S cluster may be and what inactivation state (Ni-A or Ni-B) the enzyme forms.

3.4.4 Oxygen-tolerance in the physiological context

Salmonella produces three similar uptake hydrogenase enzymes but does so under different environmental conditions (Zbell *et al.*, 2007). The periplasmic environment of cells varies significantly during infection. Many [NiFe]-uptake hydrogenase active sites, including that of *Salmonella* Hyd-5, face into the periplasm so it may not be surprising that a variety of hydrogenases are required. For example, *E. coli* Hyd-1 is active under oxidising conditions whereas Hyd-2 is inactive when oxygen is present (Lukey *et al.*, 2010). Hydrogen oxidation is an important method of obtaining energy for a pathogen such as *Salmonella*. As the human host does not use the hydrogen generated by microorganisms residing within the gut, hydrogen is an abundant energy source (Maier, 2005). In fact, it has been demonstrated that hydrogen uptake is essential for the pathogenicity of *Salmonella* (Maier *et al.*, 2004). Evading the host immune response is critical for the survival of a pathogen so the fact that *Salmonella* has the capability of producing a hydrogenase under aerobic conditions may assist this process. *Salmonella* is an intracellular pathogen. It was revealed that *hyd* expression was up-regulated within murine macrophages and human polymorphonuclear leukocyte (PMN) - like cells when compared with controls containing media only (Zbell *et al.*, 2008). Reactive oxygen species such as superoxide anions (O_2^-) and hydrogen peroxide (H_2O_2) are generated within macrophages during an immune response known as a 'oxidative burst' (Slauch, 2011). It might be possible that such elevated oxygen levels would lead to the up-regulation of *hyd* genes and that the reductant generated by hydrogen oxidation would then be available for enzymes involved in combatting oxidative stress (Zbell *et al.*, 2008). It might also be possible that Hyd-5 enables *Salmonella* to conserve energy in the form of ATP by using hydrogen as the reductant and oxygen as the terminal electron acceptor (Maier *et al.*, 2004; Zbell *et al.*, 2007; Zbell *et al.*, 2008; Zbell and Maier, 2009).

Salmonella Hyd-5 and *E. coli* Hyd-1 share high sequence homology. There is 67% identity and 80% similarity between the large subunits of *Salmonella* Hyd-5 and *E. coli* Hyd-1 (Parkin *et al.*, 2012). Although both of these enzymes can tolerate oxygen, *Salmonella* Hyd-5 is expressed best under aerobic conditions whereas *E. coli* Hyd-1 expression levels are greatest during anaerobic fermentation (Sawers *et al.*, 1985; Zbell *et al.*, 2007). *Salmonella* actually has the ability to produce a second oxygen-tolerant

hydrogenase that shares more similarity with *E. coli* Hyd-1 than *Salmonella* Hyd-5 does. The small subunits of *E. coli* Hyd-1 and *Salmonella* Hyd-1 share 92% sequence identity and 98% similarity (Parkin *et al.*, 2012). *Salmonella* Hyd-1 is maximally expressed under anaerobic conditions. Therefore *Salmonella* produces two types of oxygen-tolerant hydrogenase: one that is aerobically expressed and assembles in the presence of oxygen, and the second that is expressed during anaerobic fermentation but retains hydrogen oxidising activity under aerobic conditions.

Solving the crystal structure of *Salmonella* Hyd-5 is not only useful for better understanding the molecular basis of oxygen-tolerance but is also important for the development of hydrogenase inhibitors. Rational drug design can now be attempted due to the knowledge gained of the biological target.

4 Investigating the involvement of accessory proteins in the biosynthesis of *Salmonella* Hyd-5

4.1 Introduction

The ability of a [NiFe]-hydrogenase to maintain hydrogen oxidising activity in the presence of oxygen is no small feat since standard hydrogenase enzymes are almost instantly inactivated when in contact with this gaseous molecule (De Lacey *et al.*, 2007). Oxygen tolerance confers upon microorganisms a selective advantage in environments that may occasionally be subjected to oxygen invasion. Importantly, the molecular basis behind oxygen tolerance is now becoming clear. The combination of gas, water, proton and electron pathway adaptations have contributed to the oxygen tolerance of some [NiFe]-hydrogenases (Fritsch *et al.*, 2013). Notably, however, not all oxygen-tolerant [NiFe]-hydrogenases are actually assembled under aerobic conditions. *Escherichia coli* Hyd-1, for example, is expressed maximally under anaerobic conditions (Sawers *et al.*, 1985) but demonstrates hydrogen uptake capabilities under oxidising conditions (Lukey *et al.*, 2010). One reason for this might be to allow *E. coli* to continue using hydrogen as an electron donor during the transition from anaerobic to aerobic conditions. The *Salmonella hyd* operon, on the other hand, is optimally expressed under oxic conditions and repressed anaerobically (Zbell *et al.*, 2007). During infection, *Salmonella* will be confronted with a wide range of environmental conditions. In the early stages of infection, *Salmonella* may require the activity of Hyd-5 to oxidise hydrogen in a low oxygen environment. Conditions will become increasingly anaerobic as cells pass through the digestive system. Anaerobiosis will then favour the expression of alternative hydrogenase enzymes that can further exploit the abundance of hydrogen and generate energy. It is also possible that *hyd* expression permits cell survival within macrophages (Zbell *et al.*, 2008). On the other hand, *Salmonella* may require Hyd-5 activity further on in the infection process, once it has infected the well-oxygenated liver and spleen tissues. Not only is Hyd-5 expressed under aerobic conditions, the enzyme is also assembled under aerobic conditions. This presents the bacterial cell with additional challenges.

4.1.1 General assembly factors required for [NiFe]-hydrogenase biosynthesis

The biosynthesis of [NiFe]-hydrogenase enzymes requires the involvement of multiple assembly factors and a collection of biosynthetic pathways. One of the major

requirements for the assembly of [NiFe]-hydrogenases is the acquisition of nickel under anaerobic conditions (Ballantine and Boxer, 1985). It is thought that nickel enters the periplasm of *E. coli via* a porin in the outer membrane. Once in the periplasm, nickel is then imported into the cell cytoplasm via a 'Nik' transporter, encoded by the *nikABCDE* operon (Navarro *et al.*, 1993). A loss of [NiFe]-hydrogenase activity has been demonstrated when mutations in the *nik* operon are generated (Wu and Mandrand-Berthelot, 1986). The Nik transporter is composed of a periplasmic binding protein (NikA), two transmembrane proteins (NikB and NikC), and two cytoplasmic nucleotide-binding proteins (NikD and NikE) that are associated with the inner membrane (Navarro *et al.*, 1993; de Pina *et al.*, 1995). Expression of the *E. coli nik* operon is regulated by FNR during anaerobiosis (Wu *et al.*, 1989).

The *E. coli hyp* operon (*hypABCDEF*) encodes proteins that are involved in assembling the [NiFe]-active site and incorporating the metallocentre into the large subunit (Vignais and Billoud, 2007). Another protein, SlyD, has also been implicated in binding nickel and participating in hydrogenase biosynthesis (Cheng *et al.*, 2012). In *E. coli*, HypB, HypD and HypE were demonstrated to be essential for the maturation of each of the three hydrogenase enzymes. While addition of nickel to the medium rescued activity in a *hypB* mutant, the other mutants could not be chemically complemented (Jacobi *et al.*, 1992). HypE and HypF proteins are responsible for synthesising cyanide from carbamoyl phosphate (Blokesch *et al.*, 2004b), which are then transferred to a complex composed of HypC and HypD (Blokesch *et al.*, 2004a). HypA, HypB and SlyD are thought to be responsible for inserting nickel into the metallocentre (Chan Chung and Zamble, 2011; Cheng *et al.*, 2013). Similar to the *nik* operon, the *hyp* operon is also regulated by FNR under anaerobiosis (Lutz *et al.*, 1991).

4.1.2 System specific accessory genes required for [NiFe]-hydrogenase assembly

How is *Salmonella* capable of assembling Hyd-5 under aerobic conditions? This is an especially pertinent question considering that in its *E. coli* cousin, the *nik* and *hyp* operons are both up-regulated in response to anaerobiosis. It is clear that the biosynthetic machinery used to synthesise aerobically expressed hydrogenases must differ from that used to assemble anaerobically expressed enzymes. A comparison between the operon of aerobically expressed *Salmonella* Hyd-5 and the operons of the anaerobically expressed *Salmonella* Hyd-1 and *E. coli* Hyd-1 enzymes reveal the

existence of three additional 'accessory' genes (Figure 4.1). *E. coli* Hyd-1 is encoded by the *hyaABCDEF* operon whereas *Salmonella* Hyd-5 is encoded by the *hydABCDEFGHI* operon. The *hyd* operon encodes homologs of the *E. coli* Hyd-1 structural proteins HyaA, HyaB and HyaC, (HydA, HydB and HydC) and the predicted chaperone proteins HyaE (HydF) and HyaF (HydG). HydE, HydH and HydI are the three remaining 'accessory proteins' encoded by the *hyd* operon. HydI and HydE are homologues of HypA and HypC respectively, which indicate a specific role in [NiFe]-cofactor insertion (Chan Chung and Zamble, 2011; Burstel *et al.*, 2012). HydH is the third additional gene product encoded by the *hyd* operon and is particularly fascinating. HydH has no equivalent in *E. coli* but is a homolog of HoxV, a protein found in *Ralstonia eutropha*. This protein is thought to act as a scaffolding chaperone for the insertion of the [NiFe]-cofactor, offering protection from the detrimental effects of oxygen (Ludwig *et al.*, 2009b).

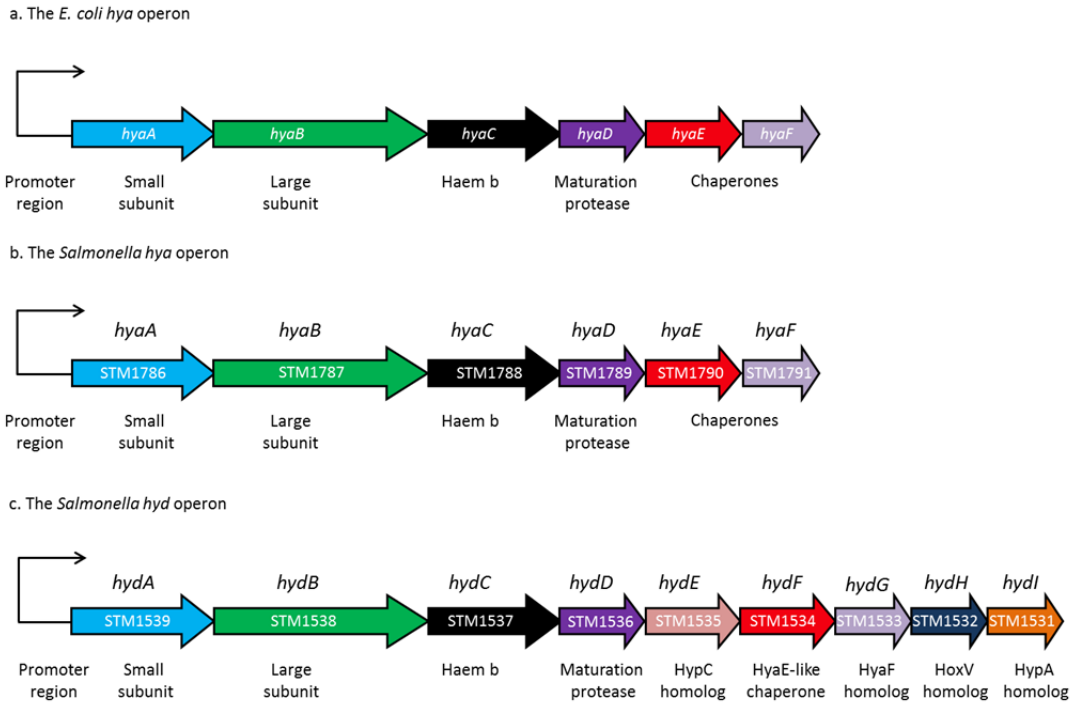

Figure 4.1. A comparison of anaerobically and aerobically expressed [NiFe]-hydrogenase operons.

(a) The *E. coli* Hyd-1 operon (*hyaABCDEF*) is optimally expressed under anoxic conditions (Sawers *et al.*, 1985). **(b)** The *Salmonella* Hyd-1 operon (*hyaABCDEF*) is expressed best under anoxic conditions (Zbell *et al.*, 2007). **(c)** The *Salmonella* Hyd-5 operon (*hydABCDEFGHI*) is maximally expressed under aerobic conditions and contains three additional genes (Zbell *et al.*, 2007). The promoter regions are represented with an arrow and the predicted roles/homologs of each gene product given below each gene.

A number of studies have provided insights into the involvement of ‘accessory proteins’ in the biosynthesis of oxygen-tolerant hydrogenases (Dubini and Sargent, 2003; Schubert *et al.*, 2007; Ludwig *et al.*, 2009b; Fritsch *et al.*, 2011a). Due to the complexity of the biosynthetic process, the roles of these proteins are still uncertain and may differ between oxygen-tolerant hydrogenases of different microorganisms.

4.2 Aims

The aim of this Chapter was to explore the roles of accessory proteins in the biosynthesis of the oxygen-tolerant Hyd-5 from *Salmonella*. This was to be achieved using a combination of genetic and biochemical techniques. The role of HydH is of particular interest as the gene encoding this protein has never been found linked to known anaerobic gene clusters. Understanding the assembly factors required for the biosynthesis of hydrogenases under oxygenic conditions is crucial for the successful engineering of synthetic microorganisms capable of producing bio-hydrogen, or in the synthesis of air-stable enzymes to be used in biological fuel cells.

4.3 Results

A large collection of genes and a variety of biosynthetic pathways are required for the successful incorporation of redox-active cofactors into hydrogenase subunits. The genetically modified *Salmonella* LB03 strain was used in this study to generate a *tat* mutant and accessory gene deletion mutants. LB03 encodes a modified HydA protein that bears a hexa-histidine tag at its C-terminus and does not possess a transmembrane domain. The *hyd* operon was also engineered to contain a strong promoter, T5, in order to up-regulate expression. This approach proved successful in the isolation of Hyd-5 and facilitated crystal formation (Chapter 3). The *Salmonella* Hyd-5 operon encodes six accessory proteins arranged in the gene cluster as *hydDEFGHI*. Three of these proteins are believed to be important for the maturation of Hyd-5 and were chosen to be investigated in this specific study. In-frame deletions of the accessory genes *hydF*, *hydG* and *hydH* were generated using the pMAK homologous recombination method (Hamilton *et al.*, 1989) to yield strains LB05, LB04 and LB06 respectively from the background strain LB03 (Table 4.1).

Strain Name	Gene Deletion
LB03	-
LB04	*hydG* (STM1533)
LB05	*hydF* (STM1534)
LB06	*hydH* (STM1532)

Table 4.1. Accessory gene deletion strains.

All strains overproduce Hyd5 due to the presence of a T5 promoter upstream of the *hyd* operon and encode enzymes bearing hexa-histidine affinity tags at the C-terminus of HyaA in place of the usual transmembrane domain.

4.3.1 Characterisation of strains carrying in-frame chromosomal deletions of Hyd-5-specific accessory genes

The hydrogen oxidising activity of Hyd-5 from each of the deletion strains LB05 (Δ*hydF*), LB04 (Δ*hydG*) and LB06 (Δ*hydH*) was investigated in intact cells. Each strain was cultured anaerobically, cells harvested, washed and then resuspended in 50 mM Tris.HCl buffer. Hydrogen oxidising activity was measured in cuvettes containing hydrogen-saturated buffer and the artificial electron acceptor BV. The reaction was initiated by the addition of intact cells (Figure 4.2). Cells carrying an in-frame deletion

in *hydF* (strain LB05) were not dramatically affected in terms of hydrogen oxidising activity (Figure 4.2a). In contrast, in-frame deletions of both *hydG* and *hydH* greatly impacted hydrogen uptake activity (Figure 4.2). In fact, activity levels from these strains resemble the low basal levels measured in non-modified *Salmonella* LT2a (Figure 4.2a). The low activity measured should not be attributed to Hyd-1 as previous experiments using *E. coli* devoid of all hydrogenases except membrane anchored Hyd-1 only demonstrated background levels of activity (Pinske *et al.*, 2011). Therefore, the activity should be assigned to Hyd-2, as this enzyme's activity can be measured in *E. coli* whole cells (Jack *et al.*, 2004). The situation should be presumed similar for closely related *Salmonella*.

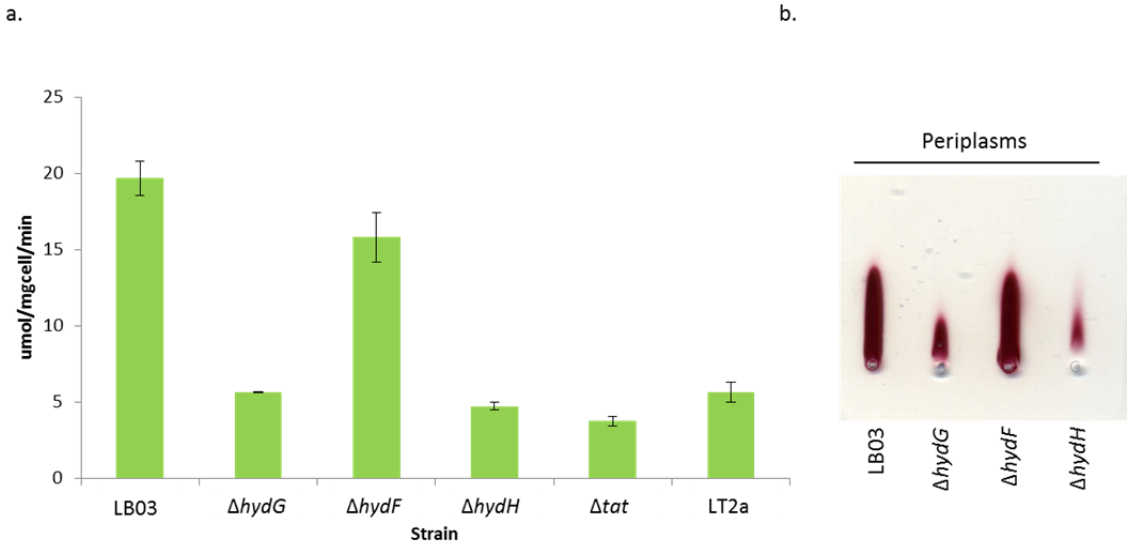

Figure 4.2. Hydrogen oxidising activities of whole cells and periplasms from the deletion strains.

(a) LB03, LB04 (Δ*hydG*), LB05 (Δ*hydF*), LB06 (Δ*hydH*) and LB03T (Δ*tat*) were cultured anaerobically in low salt LB media. The LB03T (Δ*tat*) culture was supplemented with 50 µg/ml apramycin. Cells were harvested, washed and 100 mg of cells resupended in 200 µl of 50 mM Tris.HCl. Hydrogen dependent benzyl viologen reduction was measured at an absorbance of 600nm. **(b)** LB03, LB04 (Δ*hydG*), LB05 (Δ*hydF*), LB06 (Δ*hydH*) were cultured anaerobically in low salt LB media, cells harvested, periplasms obtained and then subjected to rocket electrophoresis. Periplasm samples were electrophoresed into agar containing Hyd-5 specific antibody and incubated under hydrogen saturated conditions with BV and Tetrazolium Red at 37°C.

Next, periplasmic fractions were prepared from anaerobically-cultured strains LB03, LB04 (Δ*hydG*), LB05 (Δ*hydF*) and LB06 (Δ*hydH*) and then subjected to rocket immunoelectrophoresis. Periplasmic samples were electrophoresed into agarose containing Hyd-5-specific antibody and incubated under hydrogen saturated conditions with the redox dyes BV and tetrazolium red. The levels of periplasmic Hyd-

5 in LB05 (Δ*hydF*) were found to be similar to those observed in the LB03 periplasms (Figure 4.2b) . However, reduced levels of active Hyd-5 were noted in the periplasms of both LB04 (Δ*hydG)* and LB06 (Δ*hydH* [Figure 4.2b]). It is possible that in the absence of HydG or HydH there is a decrease in the amount of enzyme competent for export out of the cytoplasm.

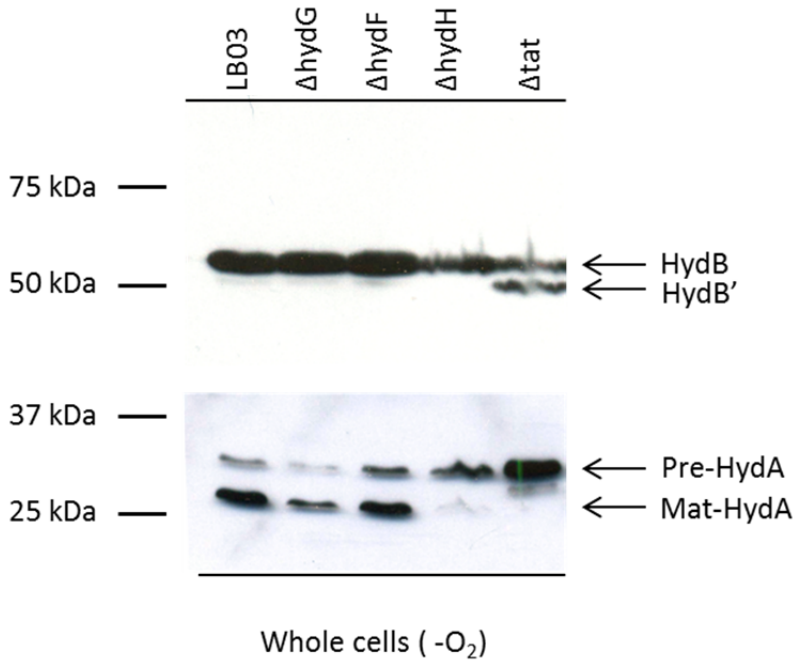

Figure 4.3. Western analysis of the large and small subunits of deletion strains.

LB03, LB04 (Δ*hydG*), LB05 (Δ*hydF)*, LB06 (Δ*hydH*) and LB03 Δ*tat* were cultured anaerobically in low salt LB media. The LB03 Δ*tat* culture was supplemented with 50 µg/ml apramycin. Whole cells were separated on a 10% SDS-polyacrylamide gel, blotted and challenged with an antibody specific to Hyd-5 for HydB identification. Whole cells were separated on a 14% SDS-polyacrylamide gel blotted and challenged with an antibody specific to the his-tag for HydA identification.

To further examine whether deletions of the accessory genes had an effect on the maturation of Hyd-5, whole cells were subjected to Western immunoblotting analysis. Strains were grown anaerobically, cells harvested, boiled in Laemmli sample buffer and separated by SDS-PAGE. The Hyd-5 antibody generated for the purposes of this study unfortunately detects many nonspecific proteins when used in a Western blot. The antibody was thus 'purified' by incubating the serum with the crude extract of an anaerobically-cultured Hyd-1-deletion strain (LB03H1). Following this pre-treatment, immunoreactive bands corresponding to the molecular weight of HydB were detected at similar levels in all extracts (Figure 4.3). A degraded form of HydB

(HydB') was observed in the *tat* deletion mutant. The Hyd-5 small subunit was also detected in each of the strains (Figure 4.3). Both the precursor and the processed form of HydA were present in LB03, LB04 (Δ*hydG*) and LB05 (Δ*hydF*) whole cells. Only the precursor form of HydA was observed from the *tat* mutant, which is unsurprising as the Tat pathway is not functional in this strain and the enzyme would be retained in the cytoplasm. Western immunoanalysis proved very revealing in the case of LB06 (Δ*hydH*) in particular (Figure 4.3). Pre-HydA is clearly the predominant form of the small subunit in the cells of the *hydH* deletion mutant. This suggests that the enzyme has not been recognised as competent for Tat dependent export and therefore remains N-terminally unprocessed.

4.1.2.1 Isolation of Hyd-5 from strains lacking specific accessory genes

To determine the importance of HydF, HydG and HydH in the biosynthesis and stability of Hyd-5, enzyme was purified from each deletion strain using IMAC and subsequently analysed by SDS-PAGE. Hyd-5 isolated from LB04 (Δ*hydG*) appeared to behave in a similar manner to Hyd-5 purified from the background strain LB03 (Figure 4.4). HydB and the processed form of $HydA^{\Delta TMHIS}$ were both identified with no co-purifying proteins observed. However, to obtain a concentration of purified Hyd-5 from the Δ*hydG* strain comparable to that from LB03, double the volume of culture had to be utilised. Clearly, the LB04 strain is struggling to produce Hyd-5 when *hydG* is not expressed. Hyd-5 purified from LB05 (Δ*hydF*) appeared to behave in a similar manner to enzyme isolated from LB03, but in this case no yield issues were encountered (Figure 4.4).

Enzyme purified from LB06 (Δ*hydH*) generated the most interesting result. Firstly, to obtain enzyme yields comparable to that from LB03, at least triple the volume of LB06 culture had to be utilised. Only 0.4 mg of enzyme was isolated from 9 g of cells. HydH therefore appears to have an important role in the biosynthesis of Hyd-5. Secondly, when analysed by SDS-PAGE, Hyd-5 isolated from LB06 (Δ*hydH*) displayed fragmented large and small subunits (Figure 4.4). A very faint band corresponding to the molecular weight of pre-$HydA^{\Delta TMHIS}$ is visible as well as a possible degradation product (Figure 4.4). This is indicative of serious protein processing problems not encountered in the other strains. A protein band corresponding to the molecular weight of mature $HydA^{\Delta TMHIS}$ is also evident (Figure 4.4). The only other

enzyme exhibiting various forms of the small subunit was purified from the Δ*tat* strain where enzyme was prevented from leaving the cell cytoplasm (Figure 4.4)

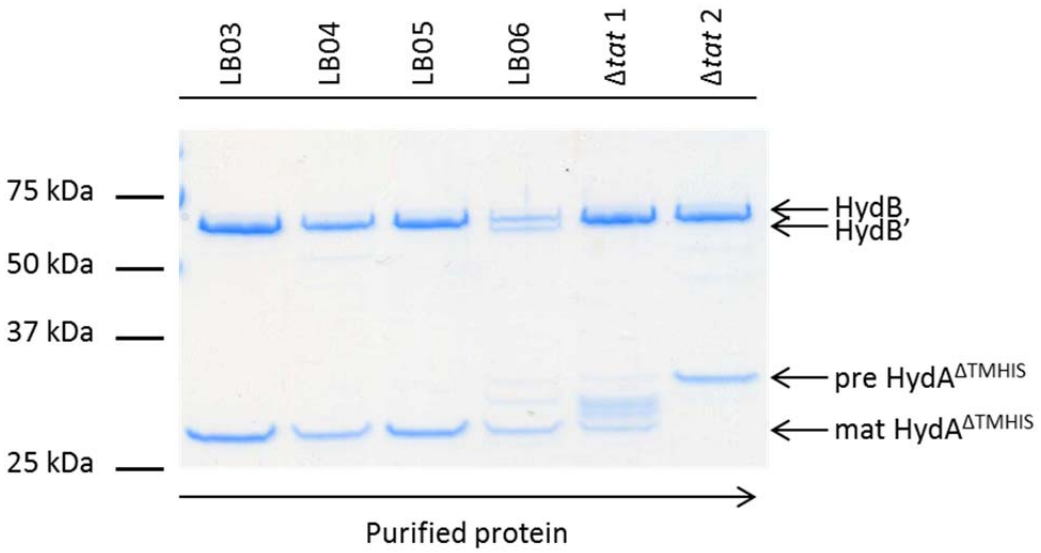

Figure 4.4. Hyd-5 was isolated from each deletion strain.

LB03, LB04 (Δ*hydG*), LB05 (Δ*hydF*), LB06 (Δ*hydH*) and LB03T (Δ*tat*) were cultured anaerobically in low salt LB. The LB03T (Δ*tat*) culture was also supplemented with 50 μg/ml apramycin. Cells were disrupted under pressure and soluble extracts subjected to IMAC. Main peak fractions containing Hyd-5 were concentrated and 10 μg of each protein analysed by SDS-PAGE. Hyd-5 purified in two peaks from LB03T (Δ*tat*). The lanes containing protein pooled and concentrated from these peaks are headed Δ*tat* 1 and Δ*tat* 2.

To ascertain whether or not enzyme isolated from the deletion strains was capable of oxidising hydrogen, BV uptake activity assays were performed on purified protein. Hyd-5 isolated from LB05 (Δ*hydF*) demonstrated hydrogen oxidising activity comparable to that of Hyd-5 purified from LB03 (Figure 4.5). In contrast, hydrogen uptake activity was clearly reduced in enzyme isolated from LB04 (Δ*hydG* [Figure 4.5]). The most striking reduction in Hyd-5 specific hydrogen oxidising activity was observed from enzyme isolated from LB06 (Δ*hydH* [Figure 4.5]). This further supports the idea that HydH is critical for Hyd-5 maturation and consequently enzyme activity. Similar to the results obtained from BV assays using intact cells (Figure 4.2a), HydG and HydH appear to be critical for normal levels of activity.

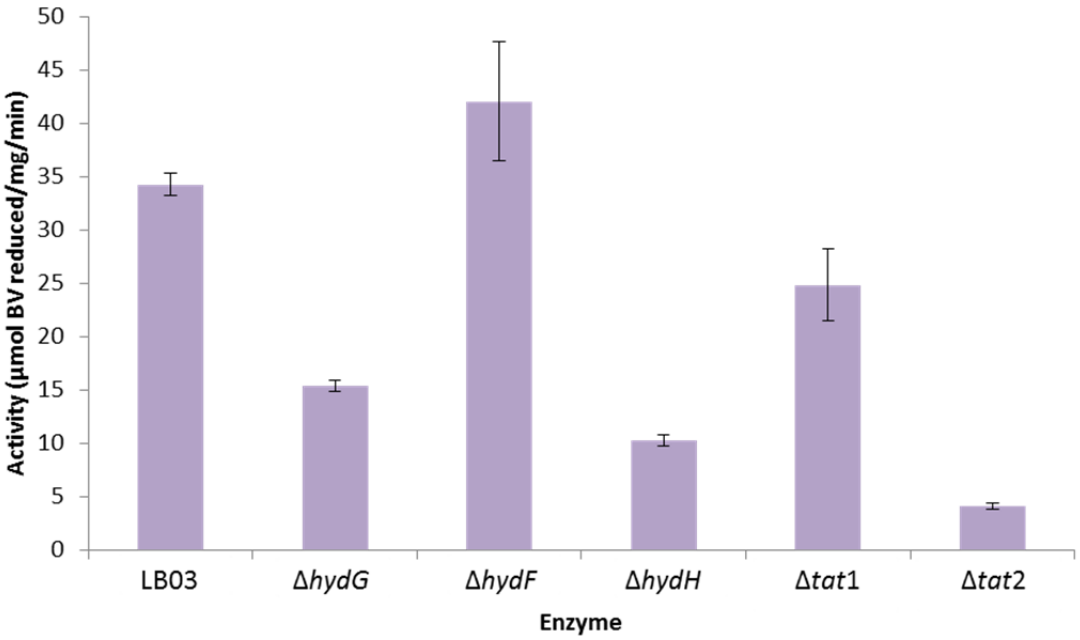

Figure 4.5. Hydrogen oxidising activities of purified Hyd-5 obtained from specific deletion strains.
LB03, LB04 (Δ*hydG*), LB05 (Δ*hydF*), LB06 (Δ*hydH*) and LB03T (Δ*tat*) were cultured anaerobically in low salt LB. The LB03T (Δ*tat*) culture was supplemented with 50 µg/ml apramycin. Cells were harvested, lysed under pressure and soluble extracts subjected to IMAC. Peak fractions were pooled and concentrated following purification. Hydrogen dependent benzyl viologen reduction was measured at an absorbance of 600nm. The SEM from three independent measurements is indicated for each purified enzyme.

4.3.2 Purification of Hyd-5 from a *Salmonella tat* mutant

In an attempt to purify Hyd-5 in complex with accessory proteins, a *Salmonella tat* strain (LB03T) was generated. The lambda redirect method was used to replace the *tatABC* genes with an apramycin resistance cassette on the *Salmonella* chromosome. This replacement occurs *via* a homologous recombination event using a PCR product specific to the target region. Replacement of the *tat* genes was confirmed by PCR of apramycin resistant colonies. Further confirmation of a non-functional Tat pathway was achieved by streaking the apramycin resistant strain onto agar supplemented with 2% (w/v) SDS. This test is useful because the cell wall amidases AmiA and AmiC are Tat substrates with a critical role in maintaining outer membrane integrity. Defects in the Tat pathway result in amidase mislocalisation and a strain that is sensitive to SDS (Ize *et al.*, 2003). The apramycin resistant strain was unable to grow on agar containing 2% (w/v) SDS, confirming the correct phenotype of a pleiotropic *tat* mutant (Figure 4.6a).

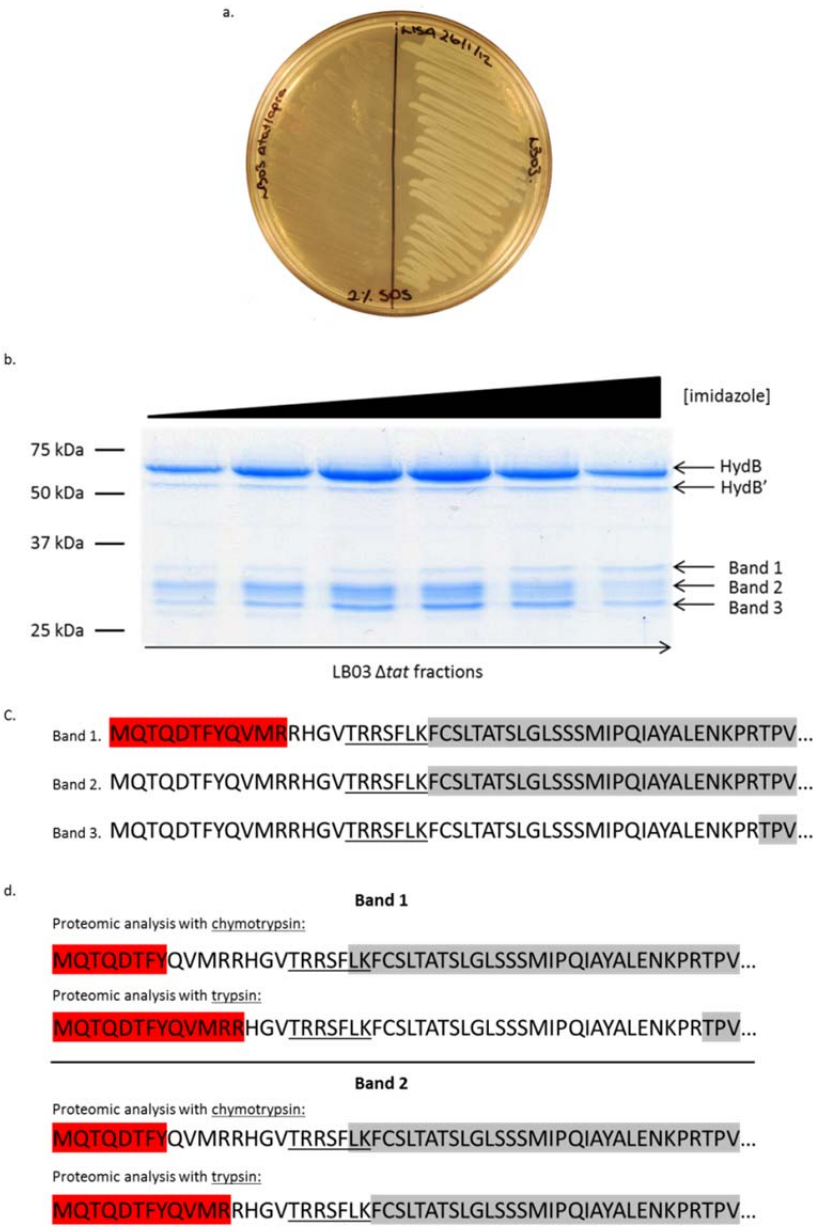

Figure 4.6. Hyd-5 was isolated from a *Salmonella tat* mutant.

(a) A single colony of the *tat* deletion strain (LB03T) and LB03 were streaked onto agar supplemented with 2% SDS. **(b)** LB03T (Δ*tat*) was cultured anaerobically in low salt LB supplemented with 50 µg/ml apramycin. Cells were harvested and then disrupted under pressure. Soluble extract was subjected to IMAC and fractions separated by SDS-PAGE. **(c)** Bands 1, 2 and 3 were analysed by tryptic peptide mass fingerprinting by the Dundee Fingerprints Service and revealed three different forms of $HydA^{\Delta TMHIS}$. Amino acids highlighted in red and grey were peptides discovered following standard tryptic digest. **(d)** Protein bands 1 and 2 were excised from a 14% SDS polyacrylamide gel and 'in-gel' digestion performed separately with chymotrypsin and trypsin to yield peptide fragments. Peptide fragments were sent to the MRC Protein Phosphorylation and Ubiquitylation proteomics facility for mass fingerprinting and LC-MS analysis.

When crude extract obtained from the *Salmonella tat* mutant was subjected to IMAC, Hyd-5 eluted in two separate peaks. Enzyme obtained from the first peak demonstrated good hydrogen uptake activity, although this was still reduced in

comparison with Hyd-5 isolated from LB03 (Figure 4.5). SDS-PAGE analysis revealed that a proportion of HydA$^{\Delta TMHIS}$ in this peak was present in the mature form (Figure 4.4). Hydrogen uptake activity is still fairly high to be attributed to the mature form alone and may also be contributed to by the unprocessed form of the enzyme present. Protein obtained from the second peak was almost completely inactive (Figure 4.5). This may represent a labile form of the enzyme.

Fractions of the first, and main, peak were separated by SDS-PAGE and revealed an interesting result where three distinct electrophoretic forms of HydA$^{\Delta TMHIS}$ were observed (Figure 4.6b). Each of these protein bands was sent for standard mass spectrometry analysis and identification. The resulting peptide matches proved intriguing (Figure 4.6c). The protein with the highest molecular weight of the three (Band 1) was identified as pre-HydA$^{\Delta TMHIS}$, complete with signal peptide (Figure 4.6c). The protein with the smallest molecular weight of the three (Band 3) was identified as the mature form of HydA$^{\Delta TMHIS}$, lacking the entire signal peptide (Figure 4.6c). While this may seem unusual for a *tat* mutant, following cell lysis the signal peptidase LepB, which is usually exposed to the periplasm, becomes accessible to cytoplasmic contents. Therefore, a proportion of mat-HydA$^{\Delta TMHIS}$ is probably formed following cleavage of the signal peptide at this stage. This seems likely as no mat-HydA$^{\Delta TMHIS}$ was identified following Western immunoanalysis of LB03T whole cells (Figure 4.3). Curiously, the middle protein band (Band 2) consisted of the precursor small subunit missing its n-region (Figure 4.6c). There are two plausible explanations as to why the n-region was not identified: it may be that the n-region has been cleaved from HydA$^{\Delta TMHIS}$ or that the n-region has been post-translationally modified and therefore could not be detected in the mass spectrometer.

4.1.2.2 Is the n-region of the Hyd-5 signal peptide phosphorylated?

MALDI-TOF and direct N-terminal Edman sequencing were both performed in an attempt to determine whether the n-region was present on 'band 2', the second form of HydA$^{\Delta TMHIS}$ but proved mostly unsuccessful. The results of N-terminal Edman sequencing confirmed 'band 1' and 'band 3' as precursor and mature HydA respectively. The first five amino acids of 'band 2' however were identified as 'LTATS', which are present in the signal peptide sequence but do not immediately follow the twin arginine motif. The residues between the twin arginine motif and the amino acids

'LTATS' were however identified by initial mass spectrometry (Figure 4.6c). Therefore, it could not be conclusively determined as to whether the n-region was present or not from these results.

Due to the unusual electrophoretic movement of band 2 (Figure 4.6b), it was hypothesised that the n-region may be phosphorylated. This proposal was supported by the observation of a possible phosphorylation site, [D/E]XXpY, present in the n-region of the *Salmonella* Hyd-5 signal peptide and the n-region of the *E. coli* Hyd-1 signal peptide (Figure 4.7). Protein phosphorylation has been extensively studied in eukaryotes and was initially thought to be confined to this Domain of life. Serine, threonine, tyrosine, and arginine kinases and phosphatases have since been discovered in bacteria (Bechet *et al.*, 2009; Pereira *et al.*, 2011; Elsholz *et al.*, 2012). Hyd-5 signal peptide residues Tyr8, Thr17 and Ser20 are conserved amino acids and were considered potential phosphorylated amino acid residues (Figure 4.7).

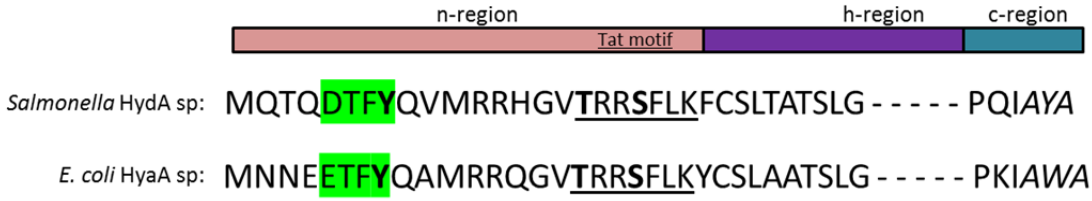

Figure 4.7. The signal peptides of *Salmonella* HydA and *E. coli* HydA possess a predicted 'phospho-motif'.
The predicted phosphorylation sites are highlighted in green, where the tyrosine residue is the expected phosphorylated residue. Tyr8, Thr17 and Ser20 were also considered possible phosphorylated residues and are highlighted in bold.

To address this directly, in-gel proteolytic digestion was performed on the slowest running form of HydA$^{\Delta TMHIS}$ (Band 1) and the unusual middle band (Band 2). Two proteases were used in the investigation: trypsin, which cleaves at the C-terminal side of arginine and lysine residues, and chymotrypsin, which cleaves at the C-terminal side of tyrosine, tryptophan, phenylalanine and leucine residues. A phospho-peptide search was then conducted by Dr David Campbell of the MRC-PPU proteomics facility run by Dr Matthias Trost in the MRC Protein Phosphorylation and Ubiquitylation Unit, Dundee. Unfortunately, no phosphorylated peptides were discovered, but surprisingly the n-region of HydA$^{\Delta TMHIS}$ from Band 2 was detected after proteomic analysis using both chymotrypsin and trypsin (Figure 4.6d). This appears to suggest that band 2 does represent full-length HydA$^{\Delta TMHIS}$. Frustratingly, a peptide covering the twin-arginine

motif, TRRSFLK, was never identified by mass spectrometry, probably due to the fact that this peptide is too small or too highly positively charged (Figure 4.6d).

4.3.3 Isolation of Hyd-5 expressed under aerobic conditions

When SFTH06 (a strain that is up-regulated for the full-length $HydA^{HIS}$ protein) was cultured aerobically, the precursor form of the enzyme appeared to dominate (Chapter 3, Figure 3.1a). It is possible that, under these conditions, a number of bottlenecks exist that prevent the complete assembly of Hyd-5 and so hinder the isolation process. Anaerobic conditions were therefore initially used to culture the strains for enzyme purification. It was now considered a possibility, however, that Hyd-5 could be isolated in complex with key accessory proteins if LB03 was cultured aerobically.

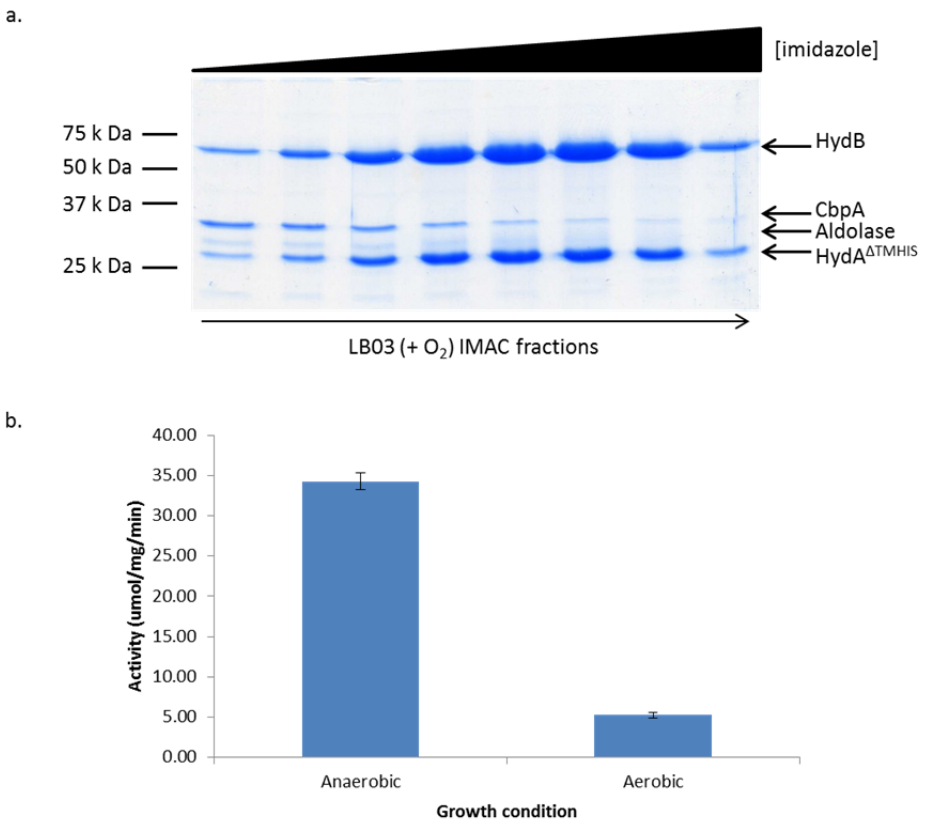

Figure 4.8. Hyd-5 is inactive when LB03 is cultured aerobically.

(a) Cells were harvested from aerobically grown LB03 cultures supplemented with 0.5% glycerol, lysed and subjected to IMAC. Eluted fractions were analysed after separation by SDS-PAGE and co-purifying protein bands were sent for MS analysis. **(b)** LB03 was cultured both anaerobically and aerobically, Hyd-5 isolated and BV uptake activity assays performed on the purified enzyme.

To test this, cells were grown under strict aerobic conditions (small volumes in large baffled flasks with vigorous shaking), harvested, and Hyd-5 purified by IMAC. SDS-PAGE analysis revealed the presence of HydB and the transmembrane deleted form of HydA as well as two co-purifying bands (Figure 4.8). Mass spectrometry (MS) results determined that the larger of the bands (~35 kDa) was Curved DNA-binding protein (CbpA) whereas the smaller (~31 kDa) of the bands was aldolase, suggesting both were non-specific interactions. Unfortunately, no known hydrogenase-specific chaperone proteins were identified.

Due to the original observation that the Hyd-5 precursor form predominates when cells were grown aerobically, it was surprising that the enzyme appeared to be fully intact and assembled in the current experiment (Figure 4.8). To ascertain whether or not Hyd-5 isolated from aerobically grown LB03 was enzymatically active, uptake activity assays were performed using BV. Interestingly, Hyd-5 displayed almost no activity when purified from cells grown under aerobic conditions (Figure 4.8b).

Hyd-5 clearly behaves differently when isolated from cells grown in the presence of oxygen. The reasons for this are not immediately obvious as the protein does appear to be stable following purification and SDS-PAGE analysis. As Hyd-5 isolated from anaerobically grown LB03 was successfully crystallised and the structure solved, it was thought that under similar conditions, Hyd-5 purified from aerobically cultured LB03 could also be crystallised. The two structures could then be compared and any subtle differences determined. Following IMAC, Hyd-5 was further purified by size exclusion chromatography (SEC [Figure 4.9a]). Samples were taken from main peak fractions and analysed following SDS-PAGE. Both the large and truncated small subunits were identified (Figure 4.9b). Enzyme was then entered into crystallisation trials. Trays were set up with reservoirs containing a range of PEG 4000 concentrations, from 16% to 23%, 0.1 M MES ranging from pH 5.5 to 6 and 0.24 M lithium sulphate. Unfortunately, crystals did not form under the selected conditions.

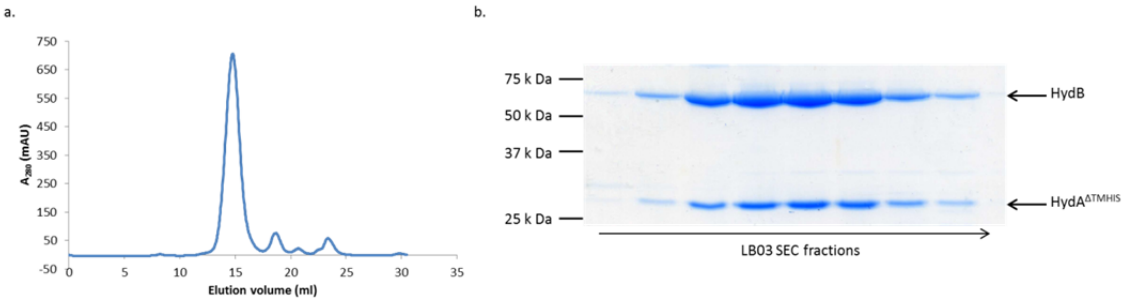

Figure 4.9. Purified Hyd-5 isolated from aerobically grown LB03.

LB03 was cultured aerobically and Hyd-5 purified by IMAC. **(a)** The enzyme was further purified by SEC and **(b)** main peak fractions analysed following separation by SDS-PAGE.

To determine whether the aerobically-expressed Hyd-5 was initially active in the cells, but was then rapidly inactivated during purification, hydrogenase activity assays were also performed on intact cells from each of the deletion strains cultured aerobically. In this case the hydrogen oxidising activity of each deletion strain was very low, resembling background levels. Furthermore, to assess whether low levels of nickel were a limiting factor to enzyme biosynthesis (as the *nik* operon is anaerobically regulated by FNR), aerobic cultures were supplemented with 10 µM $NiSO_4$. Unfortunately, activity levels were not affected by this addition. Finally, periplasmic fractions obtained from aerobically grown strains were also subjected to rocket immunoelectrophoresis. Surprisingly, the results matched those of the anaerobically cultured strains (Figure 4.2b) in so far as clear enzyme arcs of precipitin were detected and these arcs were capable of demonstrating hydrogen dependent BV reduction.

Although inactive, a very high yield of Hyd-5 was purified from aerobically cultured LB03. From 2 litres of culture, approximately 2 mg of enzyme was purified. As Hyd-5 was difficult to isolate from anaerobically grown LB06 (Δ*hydH*), this strain was cultured under aerobic conditions to investigate what effect this would have on the assembly of the enzyme and whether or not it would co-purify in complex with accessory proteins. Hyd-5 could not be isolated from LB06 using these altered growth conditions, again suggesting that HydH is critical for the assembly of Hyd-5.

4.4 Discussion

Oxygenic conditions not only pose problems for the sustained activity of [NiFe]-hydrogenases but also for the assembly of these sophisticated cofactor containing enzymes. The biosynthetic process appears to be more complex for aerobically assembled hydrogenases and requires the involvement of an increased number of accessory proteins (Figure 4.1). The aim of this Chapter was to investigate the importance of these extra proteins in the biosynthesis of the aerobically expressed and oxygen-tolerant *Salmonella* Hyd-5. Three forms of HydA were identified from Hyd-5 isolated from a *tat* mutant. Although the screen for phosphorylated peptides proved unsuccessful, it is tempting to speculate that the signal peptide is post-translationally modified in some way within the regulatory domain at the N-terminus.

The construction of individual *hydF*, *hydG* and *hydH* in-frame deletion strains revealed that both HydG and HydH have an impact on hydrogenase uptake activity.

4.4.1 What is the role of *Salmonella* HydF?

Salmonella HydF is a homolog of *E. coli* HyaE and of *R. eutropha* HoxO. Previous studies have suggested that HyaE and HoxO function as signal peptide binding chaperones (Dubini and Sargent, 2003; Schubert *et al.*, 2007). The HyaE family of proteins have not been linked with the assembly of standard oxygen-sensitive hydrogenases but only with oxygen-tolerant hydrogenases (Parkin and Sargent, 2012). Although HyaE was found to be expendable for the biosynthesis of *E. coli* Hyd-1, HoxO was demonstrated to be essential for the assembly of *R. eutropha* MBH (Dubini *et al.*, 2002; Schubert *et al.*, 2007). HupG of *R. leguminosarum*, another homolog of *Salmonella* HydF, was found to be essential for the maturation of the hydrogenase small subunit in this organism. A *hupG* deletion mutant displayed a 50 % reduction in hydrogenase activity in free living cells, but displayed a higher activity when in symbiosis with plant roots. This was taken to indicate that oxygen was an important factor affecting uptake activity in this deletion mutant (Manyani *et al.*, 2005). Further to this, investigations into the biochemistry of HoxO and HupG suggest that these proteins interact directly with the small subunit (Manyani *et al.*, 2005; Schubert *et al.*, 2007).

An NMR structure of *E. coli* HyaE is available (Parish *et al.*, 2008) and is depicted in Figure 4.10a. The structure reveals a thioredoxin-like fold, possibly indicative of a role for the protein in sulphur redox chemistry. This protein, however, does not contain any cysteine side chains but instead possesses highly conserved acidic residues (Glu50, Asp44 and Asp53) that are surface exposed and are structurally positioned where the cysteines are usually located in thioredoxins (Figure 4.10a). Parish *et al*. (2008) proposed that this negatively charged region may interact with the positively charged Tat motif of the signal peptide. It has also been suggested, however, that the negatively charged region of HyaE may be involved in protecting the unique proximal [4Fe-3S] cluster before the heterodimeric hydrogenase complex is finally formed (Parkin and Sargent, 2012).

Similar to *E. coli* HyaE, *Salmonella* HydF was demonstrated to be dispensable for Hyd-5 maturation in this study. It would be of interest to affinity-tag HydF on the upregulated *Salmonella* chromosome and attempt co-purification experiments to identify interacting proteins. As well as being performed in the *tat*$^{+}$ strain, this should also be performed in a *tat*$^{-}$ or a Δ*hydB* strain to obtain precursor complex.

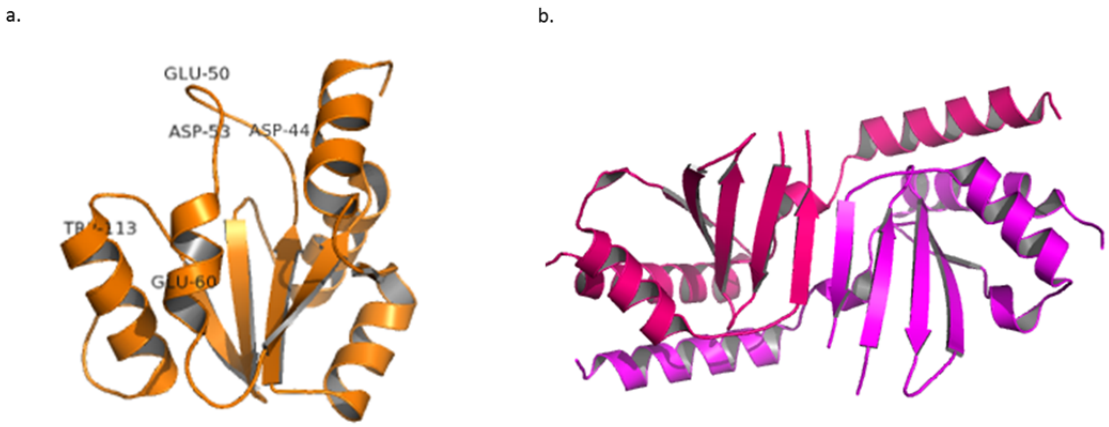

Figure 4.10. Structural representations of HyaE and HyaF-family proteins.

(a) NMR structure of HyaE (PDB 2HFD) from *E. coli* reveals a thioredoxin-like fold (Parish *et al.*, 2008). The protein sequence contains conserved acid residues (GLU-50, ASP-44 and ASP-53) that are located in a flexible loop between helices II and III and are highlighted on the structure. Another conserved acid residue lies in helix III (GLU-60) in close proximity to a conserved residue (TRP-113) in helix V. **(b)** The crystal structure of HupH, a HyaF homolog (PDB 3SB1) from *Thiobacillus denitrificans*. HupH appears to form a C-terminal domain-swapped homodimer. Adapted from Parkin and Sargent (2012).

Enzyme isolated from a Δ*hydF* mutant strain should be further characterised. Protein film electrochemistry (PFE) experiments should be performed to confirm that

the hydrogen-oxidising activity of enzyme isolated from LB05 is unaffected by a deletion in *hydF*. Electron paramagnetic resonance (EPR) spectroscopy experiments would also provide information regarding the state of the redox-active cofactors. The results of this might provide an insight into the functional role of HydF. If this protein is indeed necessary for the insertion of particular cofactors, EPR could be very informative.

4.4.2 What is the role of *Salmonella* HydG?

Salmonella HydG is homologous to *E. coli* HyaF and the C-terminus of the protein also shares homology with HoxR of *R. eutropha* (Figure 4.11). HoxR is predicted to be an iron-binding rubredoxin protein and homologues are commonly found in bacteria that produce [NiFe]-hydrogenases under aerobic conditions (Manyani *et al.*, 2005). Rubredoxins are small (~5-6 kDa) iron containing proteins that are thought to have roles in electron transfer reactions and in the oxidative stress response (Wildschut *et al.*, 2006; Hagelueken *et al.*, 2007). These enzymes are identifiable by two classical CXXCG motifs that are involved in direct ligation of Fe ions. In the HoxR-type rubredoxins, these motifs are modified to CXXCW and CXXCD/E (Fritsch *et al.*, 2011a).

Salmonella HydG contains two rubredoxin motifs that are conserved in *R. eutropha* HoxR but lacking in *E. coli* HyaF (Figure 4.11). *Salmonella* HydG therefore appears to represent a fusion between a HyaF-like protein and a HoxR rubredoxin-like protein. It has been suggested that *R. eutropha* HoxR functions to synthesise and/or repair Fe-S clusters at elevated oxygen concentrations (Fritsch *et al.*, 2011a). Fe-S clusters are susceptible to oxidative attack and the available oxygen-tolerant hydrogenase structures predict that both the proximal and medial Fe-S clusters are exposed at the enzyme surface. It is not yet known how the proximal Fe-S cluster is assembled but may require the assistance of a dedicated accessory protein (Fritsch *et al.*, 2013). An unusual Fe-S cluster profile was identified when *R. eutropha* MBH was isolated from a *hoxR* deletion mutant (Fritsch *et al.*, 2011a). Whether or not HoxR is responsible for the assembly of the proximal Fe-S cluster under aerobic conditions is now a point of conjecture. HoxR related proteins only appear to be linked with aerobically expressed [NiFe]-hydrogenases possessing a [4Fe-3S] proximal Fe-S cluster. This includes hydrogenases produced by *R. eutropha* (Fritsch *et al.*, 2011a), *Salmonella*,

Rhizobium leguminosarum (Manyani *et al.*, 2005) and *Bradyrhizobium japonicum* (Fu and Maier, 1994). *E. coli* Hyd-1, which also possesses a [4Fe-3S] cluster, does not produce a HoxR-like protein but this is perhaps not surprising as Hyd-1 is always assembled under anaerobic conditions. This lends further credence to the idea that the protein has a specific role in the aerobic assembly of a Fe-S cluster. Co-purification experiments have also indicated that HoxR is a critical constituent of the maturation complex (Fritsch *et al.*, 2011a). Moreover, HupI, the HoxR homolog present in *R. leguminosarum*, has been demonstrated to be essential for hydrogenase maturation in that organism (Manyani *et al.*, 2005).

The N-terminus of *Salmonella* HydG shares homology with *E. coli* HyaF (Figure 4.11). The HyaF family of proteins have not been found associated with operons encoding oxygen-sensitive hydrogenases (Parkin and Sargent, 2012). It would be reasonable to expect subtle differences to exist between accessory proteins even if they share a high number of the same residues. There are however, notable differences between the protein sequences of *E. coli* HyaF and *Salmonella* HydG (Figure 4.11). In fact, *E. coli* HyaF and *Salmonella* HydG only share 32% sequence identity. Whereas *E. coli* HyaF is not essential for the assembly of Hyd-1, the HoxQ homolog from *R. eutropha* has been demonstrated as critical for MBH activity (Menon *et al.*, 1991; Schubert *et al.*, 2007). HupH from *R. leguminosarum*, a homolog of the HydG/HyaF/HoxQ, is also essential for hydrogenase biosynthesis in that organism where a *hupH* deletion strain was demonstrated to be devoid of hydrogen oxidising activity in free living cells, regardless of the oxygen concentrations tested (Manyani *et al.*, 2005).

Salmonella HydG is clearly important for the assembly of fully active Hyd-5 and may have evolved to function in the insertion/assembly and/or repair of the unusual proximal Fe-S cluster. It might be of interest to mutate the conserved rubredoxin motifs of HydG to investigate the importance of these residues in maintaining the biosynthesis of active enzyme. It would also be of interest to affinity-tag HydG on the *Salmonella* chromosome, isolate the protein and enter it into crystallisation trials. This structure should differ from the crystal structure of the HyaF homologue HupH from *Thiobacillus denitrificans* (Figure 4.10) given the two domain structure. It might also be possible to isolate HydG in complex with pre-Hyd-5 or another accessory protein using the affinity-tagged version of the protein.

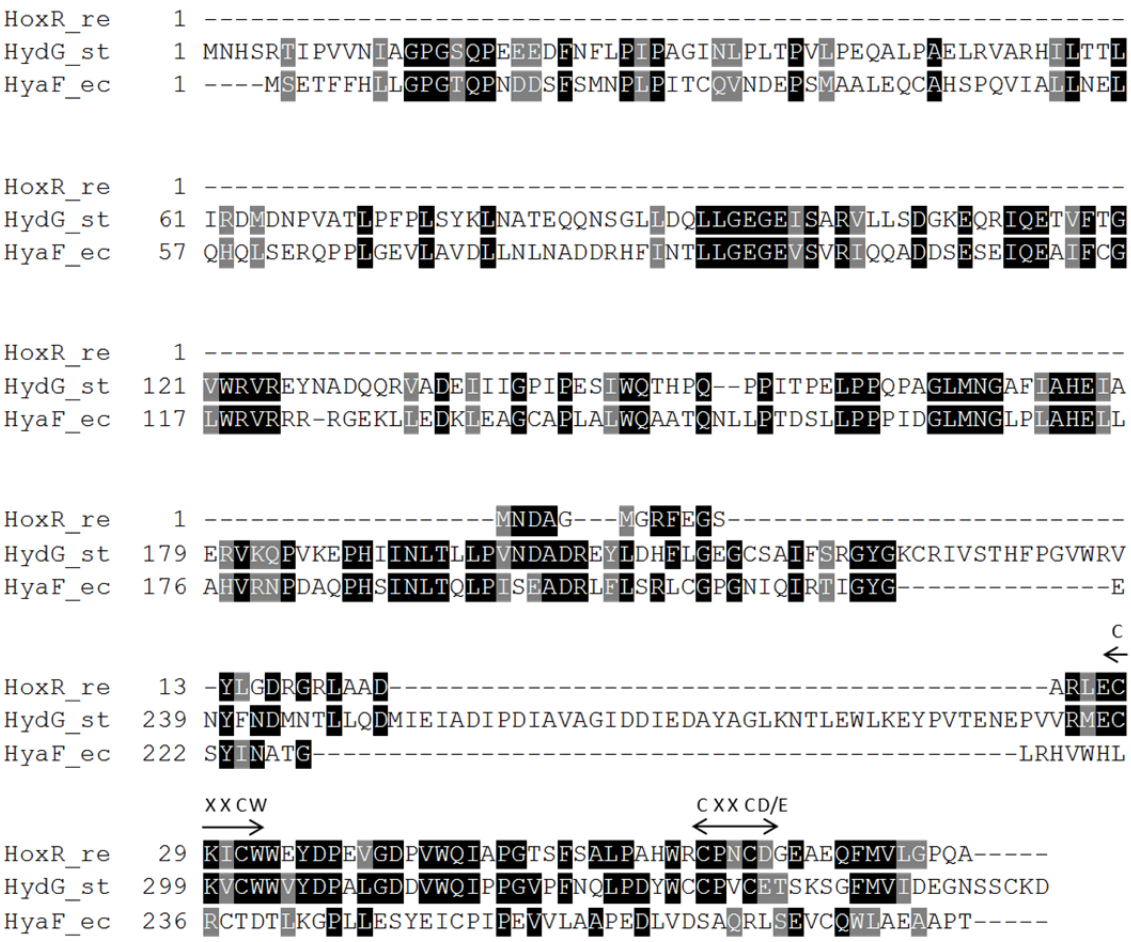

Figure 4.11. Sequence alignment between rubredoxin-like proteins and *E. coli* HyaF.

The N-terminus of *Salmonella* (st) HydG shares homology with HyaF from *E. coli* (ec). The C-terminus of HydG however shares homology with HoxR from *R. eutropha* and contains two rubredoxin-like motifs (CXXCW and CXXCD/E) that are highlighted in the figure.

In this study, *Salmonella* HydG was demonstrated to impact the hydrogen oxidising activity of Hyd-5 and it is tempting to speculate that this protein has a protective role to play in the insertion of the proximal Fe-S cluster. PFE should be used to demonstrate, unequivocally, whether or not purified Hyd-5 obtained from LB04 (Δ*hydG*) is enzymatically inactive. This should also be tested in the presence of various levels of oxygen. EPR spectroscopy should also be employed in an effort to characterise the redox-active cofactors in this mutant enzyme. The EPR spectrum can then be analysed and unusual signals revealed, with particular attention given to the signals from the [NiFe]-active site and the proximal [4Fe-3S] cluster.

4.4.3 What is the role of *Salmonella* HydH?

HydH is an extremely fascinating protein as it appears to be dedicated to the assembly of aerobically expressed [NiFe]-hydrogenases. In this Chapter, it was demonstrated that HydH is critical to the hydrogen oxidising activity of Hyd-5. Without HydH, the small subunit remains unprocessed (Figure 4.3) suggesting that this protein is essential for the complete maturation of the enzyme. Furthermore, SDS-PAGE analysis of protein purified from LB06 (Δ*hydH*) revealed a number of small subunit forms similar to what is observed from protein purified from a Δ*tat* strain (Figure 4.4). This suggests that Hyd-5 is retained within the cytoplasm when HydH is missing from *Salmonella*. This may be due to the incomplete assembly of the enzyme and subsequent rejection by the Tat apparatus. This suggests that HydH is a key player in the maturation of Hyd-5.

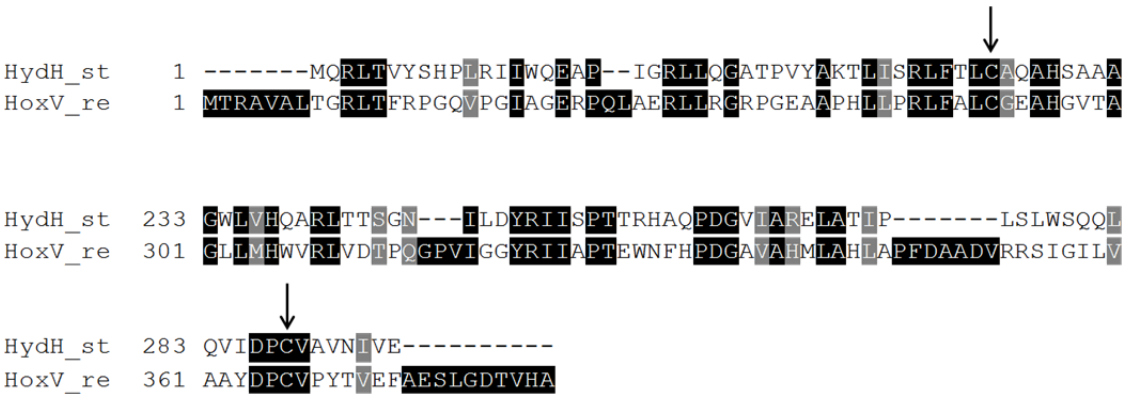

Figure 4.12. Sequence alignment of *Salmonella* HydH and HoxV from *R. eutropha*.

Only the N-terminus and the C-terminus of *Salmonella* (st) HydH and *R. eutropha* (re) HoxV are shown in this alignment. The conserved cysteine residues responsible for metal ligation are indicated by arrows.

The gene product of *hydH* is predicted to be a homolog of HoxV found in *R. eutropha*. It has been demonstrated that HoxV is essential for the hydrogen oxidising activity of *R. eutropha* MBH as a *hoxV* deletion mutant displayed only 3% of the activity exhibited by the wild type control strain (Ludwig *et al.*, 2009b). Co-purification studies also demonstrated that HoxV interacts with the MBH large subunit HoxG, the accessory protein HypC, and with HoxL, a HypC homologue (Ludwig *et al.*, 2009b). Ludwig *et al*. (2009b) used infrared spectroscopy and metal analysis to identify the coordination of $Fe(CN^-)_2CO$ to HoxV and suggested that the protein acts as a scaffolding chaperone required for insertion of the active site. This was also concluded

for the HoxV homolog, HupK, from *R. leguminosarum* (Albareda *et al.*, 2012). *R. eutropha* HoxV contains two conserved cysteine residues that have been shown to be important for hydrogenase activity and ligation of the metal cofactor (Ludwig *et al.*, 2009b). These structural motifs are shared between these two proteins and the hydrogenase large subunit. Another study revealed the presence of these motifs in the HoxV homolog HupK from *R. leguminosarum* (Imperial *et al.*, 1993). These two cysteines are also conserved in *Salmonella* HydH (Figure 4.12) so it is likely that this protein performs a similar role to *R. eutroph*a HoxV.

A clear band of precursor HydA was detected from the extracts of a *Salmonella* mutant lacking HydH with barely any processed small subunit being observed (Figure 4.3). Investigations into the function of the HydH homologs HoxV from *R. eutropha* and HupK from *R. leguminosarum* have uncovered their importance for hydrogen oxidising activity but only processing of the large subunit has been shown to be affected by gene deletions (Bernhard *et al.*, 1996; Albareda *et al.*, 2012). Therefore this study presents the first evidence to suggest that the presence of a HoxV-like protein is critical to the processing of the small subunit. It can be speculated that due to the inefficiency of [NiFe]-metallocentre assembly, the hydrogenase subunits fail to pass quality control and are not exported across the inner membrane. Wasteful translocation is thus avoided. Only one form of HydB was detected in the extracts of the deletion strains following Western analysis (Figure 4.3). It is therefore difficult to conclude anything about the processing of the large subunit.

Although when assayed *in vitro* (over a few minutes timescale) Hyd-5 isolated from the *hydH* background appeared inactive, a small amount of active Hyd-5 is evidently produced by the *hydH* deletion strain as observed by rocket immunoelectrophoresis (Figure 4.2). This activity only became evident following the prolonged incubation of gel-bound enzyme with substrate over many hours. This suggests that the [NiFe]-metallocentre has been incorporated into a small proportion of the large subunits resulting in a complex capable of hydrogen oxidation. It has been shown that BV hydrogen oxidation also depends on the presence of a small subunit (Pinske *et al.*, 2011) indicating that Hyd-5 is probably present here as a heterodimer at least.

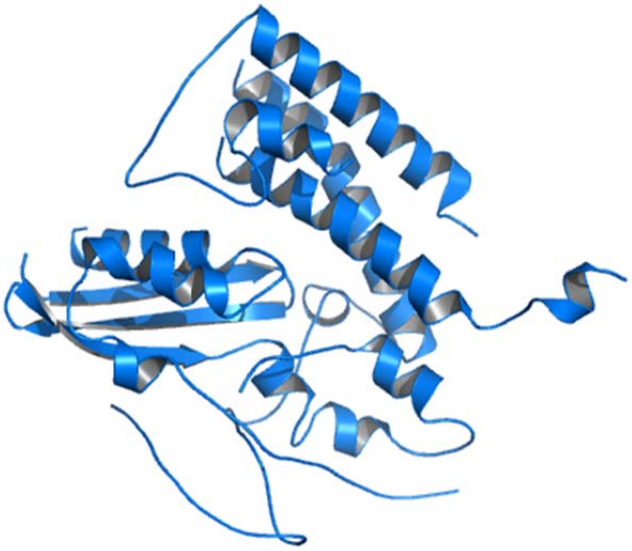

Figure 4.13. Phyre[2] model of HydH.

HydH is predicted to be mostly alpha-helical and shares homology with the large subunit of [NiFe]-hydrogenases (Kelley and Sternberg, 2009).

At the present time, no structure exists for a HydH homolog. However, a Phyre[2] model has been generated and is shown in Figure 4.13. Phyre[2] is a computational tool used to predict the structure of a protein by comparing a query amino acid sequence with a library of sequences of known protein structures. A predicted structure can then be generated (Kelley and Sternberg, 2009). HydH is predicted to be primarily alpha-helical but also to contain beta strands. The highest scoring template, sharing 22% identity with HydH, was the standard [NiFe]-hydrogenase large subunit. If HydH truly functions as a scaffolding protein for the biosynthesis of the active site, a degree of similarity between HydH and HydB would be expected.

Due to the important role these proteins are expected to play in the biosynthesis of aerobically assembled hydrogenases, it would be of interest to gain an X-ray crystal structure of HydH. This may lead to a better understanding of HydH function. An affinity-tagged version of HydH should be isolated from the upregulated *hyd* operon containing the T5 promoter. This might also lead to the identification of interacting proteins. Antibodies specific to HydH should also be generated to localise the protein within the cell under various physiological conditions. It would also be useful to perform PFE and EPR spectroscopy on Hyd-5 isolated from LB06 (Δ*hydH*). This will determine whether or not Hyd-5 is enzymatically active and will also indicate any unusual signals pertaining to the redox-active cofactors.

It is clear that the accessory gene products HydG and HydH impact the hydrogen oxidising ability of *Salmonella* Hyd-5. It would be interesting to discover whether or not this is oxygen dependent. Future experiments should begin with isolating Hyd-5 from the *hydG* and *hydH* deletion strains under strict anaerobic conditions following anaerobic culture. The hydrogen dependent reduction of BV should then be assessed using the purified enzyme. Will this enzyme demonstrate wild type levels of activity? Hydrogen oxidation should then be tested under increasing concentrations of oxygen. The detection of HydA and HydB from cell extracts should also be performed from cells cultured under different oxygenic conditions. The presence and formation of each of the subunits should then be assessed through Western immunoanalysis.

4.4.4 What are the roles of the remaining accessory proteins encoded by the *hyd* operon?

HydD shares homology with *E. coli* HyaD and HoxM of *R. eutropha*. This protein is a specific protease required for the carboxy-terminal cleavage of the large subunit and is necessary for irreversible complex formation between the small and large subunits following [NiFe]-cofactor assembly (Bernhard *et al.*, 1996; Vignais and Billoud, 2007). HydE and HydI are another two proteins that are not linked with the anaerobic assembly of [NiFe]-hydrogenases but are encoded for by the operon of *Salmonella* Hyd-5. HydE and HydI are homologs of HypC and HypA respectively. As the *hyp* operon is maximally expressed under anaerobic conditions, it might be expected that [NiFe]-cofactor assembly would be severely compromised in the presence of oxygen (Lutz *et al.*, 1991). It may be that the *hyd* operon encodes two Hyp homologues as a way of countering this problem. HypA and HypC are both involved in the assembly of the [NiFe]-active site. HypA is thought to act as a scaffold for the assembly of nickel insertion proteins whereas HypC is believed to form a complex with HypD and supports the maturation of the $Fe(CN)_2(CO)$ moiety (Chan Chung and Zamble, 2011; Burstel *et al.*, 2012). The complete assembly of the metallocentre however requires the involvement of at least six Hyp gene products that are synthesised under anoxic conditions. This poses a significant challenge to the assembly of an aerobically expressed hydrogenase regardless of the presence of the two Hyp homologues

4.4.5 Is the Hyd-5 signal peptide post-translationally modified?

A *Salmonella tat* mutant was generated with the objective being to co-purify accessory proteins in complex with the enzyme precursor. Surprisingly, no co-purifying proteins were identified following purification of Hyd-5 from this strain. Instead, three forms of $HydA^{\Delta TMHIS}$ were revealed. The precursor and mature forms of the small subunit were present along with a version of $HydA^{\Delta TMHIS}$ that possessed an n-region that could not be detected by standard mass spectrometry. It was hypothesised that the n-region of the Hyd-5 Tat signal peptide was phosphorylated, accounting for its unusual electrophoretic mobility. This was substantiated by the finding of a phospho-motif (D/EXXpY) that is almost completely conserved between the signal peptides of oxygen-tolerant [NiFe]-hydrogenases (See Chapter 2, Figure 2.1). Unfortunately, the screen for phosphorylated proteins proved unsuccessful. The n-region was however detected in this screen indicating that this region is probably modified in some way and difficult to detect using standard mass spectrometry.

Recent studies into protein phosphorylation have revealed the importance of arginine phosphorylation in a number of vital cellular processes including protein degradation and stress responses (Elsholz *et al.*, 2012). The Hyd-5 signal peptide contains two essential arginine residues that are critical for enzyme translocation by the Tat pathway. Disappointingly, this particular region of the signal peptide was never identified by proteomic analysis, even following digestion with chymotrypsin (Figure 4.6d). The twin arginine residues are essential to protein export so mutating these residues should generally be avoided. However, substituting the arginine residues from an enzyme that will never be exported from the cell cytoplasm is an option. Future experiments should involve mutating the signal peptide twin arginine residues and isolating the enzyme from the *tat* mutant. Will the same electrophoretic mobility of the small subunit be observed following SDS-PAGE analysis? This can also be performed for various other residues within the signal peptide n-region in an attempt to identify amino acids that are modified within the cell. The Hyd-5 signal peptide also contains two further well conserved arginine residues outwith the twin arginine motif but still within the n-region. These amino acids must also be investigated. It might be possible that the n-region is post-translationally modified and then cleaved. This would also support the results obtained in Chapter 2 where a Hyd-1 signal peptide n-region deletion resulted in faster export of a reporter protein.

It should be considered that the Tat signal peptide not only functions in targeting enzyme to the periplasm, but also acts to bind intracellular moieties. Is it possible that the arginine-rich/positively charged signal peptide constitutes an RNA-binding motif? Arginine-rich motifs have been shown to bind RNA in viruses and bacterial cells. Although these types of interactions are mostly unspecific, many others are extremely specific (Bayer *et al.*, 2005). The Tat peptide of HIV-1 has not only been demonstrated as having a role in nuclear localisation but the arginine-rich motif it contains has been shown to bind intracellular moieties including RNA's (Cardarelli *et al.*, 2008). It is tempting to speculate that the Hyd-5 signal peptide is responsible for performing various functions. Competition may exist between the binding of the signal peptide to the Tat machinery and to RNA's present in the cytoplasm. This would hinder the transport process and allow sufficient time for the incorporation of essential cofactors. Hyd-5 should be isolated from the cytoplasmic fraction of a *Salmonella tat* mutant and analysed for any protein-RNA interactions by performing an Electrophoretic Mobility Shift Assay (EMSA). Using a non-denaturing poly-acrylamide gel, the electrophoretic mobility of purified Hyd-5 can be compared with that of Hyd-5 treated with RNase. Post-translational modification of the signal peptide has never been considered before. The extended length and the high degree of conservation between residues of [NiFe]-hydrogenase signal peptide n-regions suggest an important role for this region. This was discussed at length in chapter 2 where we proposed that the n-region constituted a 'regulatory' region. The n-region is fascinating and was shown to be important for the stability of *E. coli* Hyd-1 (Chapter 2). Again, the role of the n-region is being questioned but this time for *Salmonella* Hyd-5.

4.4.6 Why do aerobically cultured strains produce, apparently assembled, but inactive enzyme?

The results from this study indicate that although Hyd-5 is expressed at its greatest level under aerobic conditions, enzyme isolated under these conditions is almost completely inactive. In contrast to this, enzyme isolated from anaerobically cultured *Salmonella* is capable of hydrogen oxidation. This may be due to the extremely high levels of Hyd-5 produced by the genetically manipulated strain under oxic conditions. The cofactor biosynthetic machinery may be unable to keep up with enzyme assembly. It is however extremely surprising that Hyd-5 has formed an

assembled heterodimer, that can be isolated form aerobically grown, overexpressing *Salmonella* (Figure 4.9). It is has been demonstrated that the incorporation of nickel into the hydrogenase large subunit is a prerequisite for enzyme maturation as deletion of the *hyp* genes resulted in an unprocessed enzyme devoid of nickel (Rossmann *et al.*, 1994). The *hyp* operon also requires activation by FNR under anoxic conditions, as does the *nik* operon (Wu *et al.*, 1989; Lutz *et al.*, 1991). Moreover, it has been established that the small subunit forms a complex with the large subunit following nickel incorporation and C-terminal endoproteolytic cleavage (Magalon and Bock, 2000). Here however, both subunits appear to have been isolated together from aerobically cultured *Salmonella*, conditions where it would be expected that the *hyp* and *nik* operons are not being expressed. The aerobically isolated protein was brown in colour so it can be assumed to contain Fe-S clusters. It is possible that HydB does not contain nickel but interestingly, has still been assembled. EPR and metal analysis should be performed to ascertain if the enzyme contains the relevant cofactors and to what level. The band corresponding to the large subunit of the aerobically isolated hydrogenase (Figure 4.9) must be identified by mass spectrometry to determine unequivocally whether or not the C-terminus is present. The subcellular localisation of Hyd-5 produced from aerobically grown *Salmonella* should also be established. Subcellular fractionation and Western analysis will provide an insight into whether or not Hyd-5 is properly processed.

Hyd-5 biosynthesis may require the involvement of genes expressed from operons that are repressed under oxygenic conditions resulting in the incomplete assembly of the enzyme. Whereas expression from the *isc* and *suf* operons (responsible for Fe-S cluster biosynthesis) is induced under oxidative conditions, expression from the *hyp* operon is induced under anaerobic conditions (Lutz *et al.*, 1991; Zheng *et al.*, 2001; Lee *et al.*, 2004). The expression of the anaerobically induced *hyp* operon and the aerobically induced *hyd* operon must require careful coordination and multiple levels of regulation that are not understood as yet. To add another level of complexity, the FNR protein has also been proposed to function under aerobic conditions, possibly reflecting the necessity of this protein under a variety of physiological conditions (Sawers *et al.*, 1988). It has been demonstrated that in *R. leguminosarum*, the *hyp* operon can be induced under 'microaerobic' conditions (Rey

et al., 1993). Thus expression of the *hyp* operon may depend on a number of different factors under various physiological conditions.

The addition of $NiSO_4$ did not affect the hydrogen oxidising activity of any of the aerobically grown strains. This indicates that nickel uptake is not a key limiting factor under aerobic conditions. Future experiments should involve up-regulating the *hyp* operon on the *Salmonella* chromosome by incorporating the T5 promoter upstream and deleting the native *hyp* promoter. The *hyp* operon will thus be constitutively expressed as *Salmonella* does not produce a lacI homologue. If the production of Hyp proteins is affecting the ability of these strains to oxidise hydrogen, upregulated expression of this operon may result in rescued activity. It might also be necessary to upregulate expression of the *tat* operon. Further attempts should be made to obtain crystals of Hyd-5 isolated from aerobically cultured *Salmonella*. This would be important for determining whether the Hyd-5 structure is altered in some way that is not obvious from SDS-PAGE analysis.

Also of interest would be the aerobic expression and purification of Hyd-5 from each of the accessory mutants. It might be possible to disrupt complex formation through the deletion of one of the accessory genes. This would provide an insight into which of the proteins are essential for the biosynthesis of Hyd-5. This was already performed for LB06 (*ΔhydH*) and resulted in the complete loss of Hyd-5 assembly. Therefore it can be concluded (albeit tentatively) that HydH may be essential for the biosynthesis of Hyd-5 under oxic conditions. If HydH does function as a scaffolding chaperone responsible for inserting the [NiFe]-active site during aerobic expression, the failure of complex formation may be expected. It would be difficult to reconcile this with the successful formation of Hyd-5 from aerobically grown LB03 if the active site is missing from this particular enzyme.

5 Future perspectives

5.1 Hydrogen-based technologies

The search for alternative fuels and energy sources has been necessitated by diminishing oil reserves, increasing oil prices and the need to decrease carbon dioxide emissions. Although it is extremely likely that a variety of renewable energy sources will ultimately be required, hydrogen has been termed by some as the 'fuel of the future'. Current methods of hydrogen production are very expensive and require intense extraction conditions. As hydrogen is produced naturally by a number of microorganisms, this offers a viable and sustainable alternative. Recent research has focussed on exploiting hydrogenase enzymes as biotechnological tools, either in hydrogen production or in biological fuel cells (Friedrich *et al.*, 2011). Efforts to elucidate the mechanism of oxygen-tolerance have been successful and have established that the unique co-ordination of the proximal Fe-S cluster of [NiFe]-hydrogenases is crucial for conferring this property. The mechanisms behind a number of other features specific to oxygen-tolerant hydrogenases, including carbon monoxide tolerance, are still unknown and require further analysis. Although [NiFe]-hydrogenases are suitable for use as electrocatalysts in biological fuel cells, this class of enzyme are catalytically biased to hydrogen uptake so are not generally used in hydrogen production studies. The finding that oxygen-tolerant hydrogenases are capable of reverse electron transfer prompts the question as to whether or not this enzyme subclass can reduce protons. The advances in genetic engineering and synthetic biology are now proving very helpful in incorporating desired properties into specific enzymes.

5.1.1 Fermentative hydrogen production

Dark fermentation is advantageous as a method of hydrogen production as there is no possibility that hydrogenase activity will be inhibited by oxygen. Also, a number of carbon rich sources, including waste crops, can be utilised by a variety of different fermenting bacteria (Hallenbeck and Ghosh, 2009). A major drawback however is that the yield of hydrogen is low per substrate consumed, which appears to be a general consequence of bacterial metabolism. Therefore efforts should be made to remove metabolic bottlenecks (Rittmann and Herwig, 2012). Modifying the existing

pathways that exist in fermentation is an option that has attracted a lot of interest. Inactivating pathways that divert electrons away from the pyruvate pool, the source of electrons for proton reduction should increase the yield of hydrogen. For example, inactivation of the *ldhA* gene results in increased hydrogen production, albeit modest (Hallenbeck and Ghosh, 2009). Deletion of the uptake hydrogenases in *E. coli* was also found to increase the amount of hydrogen produced by 37% (Redwood *et al.*, 2008). Furthermore, the inactivation of *hycA*, which encodes a repressor of the *hyc* operon, and the overexpression of *fhlA*, which encodes for an activator of the FHL complex have also resulted in higher hydrogen yields (Penfold *et al.*, 2006; Maeda *et al.*, 2007; Sanchez-Torres *et al.*, 2009). Clearly, obtaining commercially useful volumes of hydrogen produced from metabolically engineered bacteria during fermentation will require multiple pathway disruptions or enhancements. Furthermore, heterologous overexpression of an extremely efficient hydrogen producing hydrogenase may also be necessary. There are advantages to be gained from taking a cellular approach to hydrogen production as enzymes do seem to be superior when functioning *in vivo* when compared with those that have been isolated or synthesised (e.g. in the ability to self-repair).

5.1.2 Photobiological hydrogen production

Although fermentative hydrogen production is proving difficult to augment, advances in photobiological hydrogen production are emerging. One of the main obstacles in using algae and cyanobacteria to produce hydrogen photobiologically is the problem of hydrogenase inactivation upon oxygen attack. As oxygen is produced during photosynthesis, this is clearly a major problem. The recent availability of oxygen-tolerant hydrogenase structures (Fritsch *et al.*, 2011c; Shomura *et al.*, 2011; Volbeda *et al.*, 2012; Volbeda *et al.*, 2013), including the structure solved in this work, have led to the elucidation of mechanisms critical for oxygen-tolerance and represent a huge leap forward for the improvement of this process.

During oxygenic photosynthesis, protons and electrons are extracted from water by photosystem II (PS II) and oxygen produced. Electrons are transferred to PS I and then relayed to $NADP^+$, *via* a ferredoxin, yielding NADPH. Under normal conditions, NADPH is used to by the Calvin cycle to fix carbon dioxide into organic carbon. Alternatively, under conditions of redox imbalance, hydrogen is produced by

bidirectional [NiFe]-hydrogenases in an attempt to rid the cells of excess NAD(P)H. Experiments have been performed with the aim of coupling PSI to hydrogen producing hydrogenases *in vitro*, providing a system that ensures the direct conversion of light to hydrogen production. One such study employed the method of artificially fusing the oxygen-tolerant, membrane bound [NiFe]-hydrogenase from *R. eutropha* with the PsaE subunit of PSI from *Synechocystis* sp. PCC 6803. The fusion was designed in such a way that ensured the close arrangement of the peripheral Fe-S cluster of PSI with the distal Fe-S cluster of HoxK from *R. eutropha*. The fusion protein was found to successfully and spontaneously associate with a PsaE deleted form of PSI in solution. Unfortunately, a very low yield of hydrogen was obtained upon illumination (Ihara *et al.*, 2006). This method was further optimised by immobilising the $PSI_{\Delta PsaE}$-MBH_{PsaE} complex in an elegant study where a gold electrode was studded with Ni-NTA, capable of interacting with an affinity tagged version of $PSI_{\Delta PsaE}$ (Figure 5.1). A considerable increase in hydrogen production was measured highlighting the importance of mimicking the *in vivo* (i.e. membrane bound) state (Krassen *et al.*, 2009). If even greater hydrogen production is to be realised using oxygen-tolerant [NiFe]-hydrogenases in systems similar to this, the proton reducing capacity of these enzymes must be optimised. Electrochemical characterisations of oxygen-tolerant hydrogenases from *A. aeolicus* (Pandelia et al., 2010), *E. coli* (Lukey *et al.*, 2010) and *Salmonella* (Parkin *et al.*, 2012) have established that at negative potentials, these enzymes are not capable of proton reduction. A characteristic of this unique subclass of hydrogenase is however the reverse relay of electrons to the active site for oxygen reduction. Therefore it might be considered a possibility that some members of this subclass can also reduce protons. This is supported by the results of a study undertaken by Sawers and Boxer (1986) who demonstrated the ability of *E. coli* Hyd-1 to produce hydrogen using methyl viologen as an artificial electron donor. This requires further investigation but would represent a great leap forward for hydrogen producing technologies.

The other option is to use available hydrogen producing [FeFe]-hydrogenases and couple these to PSI systems. This was attempted *in vitro* by directly connecting the Fe-S cluster containing subunit PsaC of PSI to the distal Fe-S cluster of the [FeFe]-hydrogenase from *Clostridium acetobutylicum*. Upon illumination, low hydrogen producing rates were obtained (Lubner *et al.*, 2010). This was further enhanced

following optimisation, resulting in a 2-fold increase in hydrogen evolving rates when compared to natural photosynthetic oxygen evolving rates (Lubner *et al.*, 2011). The main problem with experiments like these is that they are conducted under completely anoxic conditions due to the extreme oxygen-sensitivity of this class of enzyme. If these hydrogenases are to be used in future technologies, oxygen-tolerance will have to be genetically engineered.

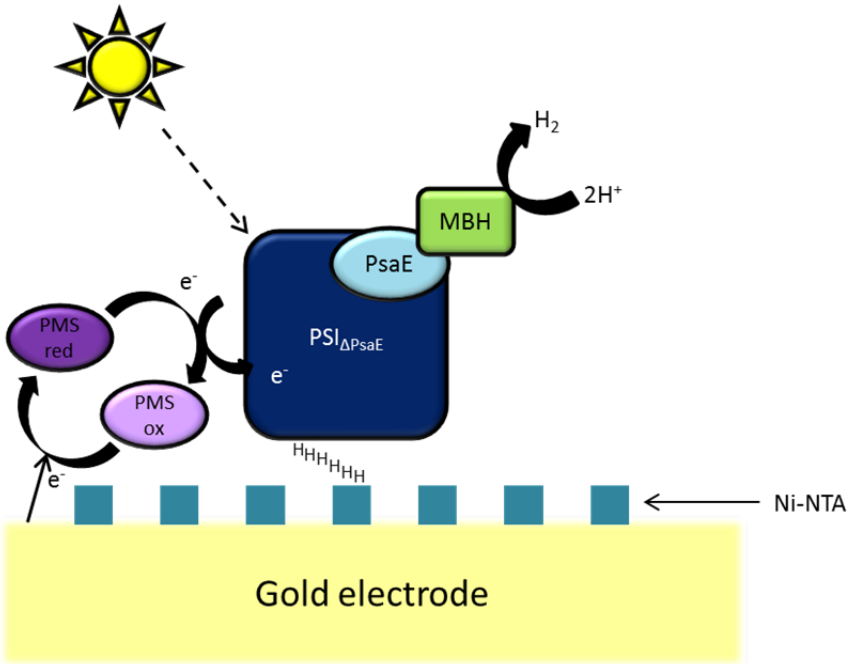

Figure 5.1. Diagrammatic representation of the PSI linked, photobiological hydrogen producing system.
$PSI_{\Delta PsaE}$ is bound to the Ni-NTA studded, gold electrode *via* a hexahistidine affinity tag, which also dictates its orientation. Added MBH_{PsaE} spontaneously attaches to the complex. The soluble electron carrier, *N*-methylphenazonium methyl sulfate (PMS), then mediates the delivery of electrons from the electrode to the PSI complex. Upon illumination, electrons are transferred to the MBH active site, which promotes proton reduction. The diagram is adapted from Krassen *et al*. (2009).

Findings over the last few years have shed much needed light on the molecular basis of oxygen-tolerance. The engineering of robust, bio-inspired catalysts is dependent on the valuable spectroscopic, electrochemical and structural information that has, and is still being gathered. The finding that the proximal Fe-S cluster of oxygen-tolerant hydrogenases could donate two reducing equivalents to the active site was unexpected. The immediate environment surrounding this particular Fe-S cluster, including the presence of two supernumerary cysteines, is obviously crucial in permitting the high potential transition that occurs when this cluster is super oxidised. Engineering cysteine residues into standard oxygen-sensitive hydrogenases,

engineering a catalytic bias towards proton reduction, generating small gas channels and possibly allowing for membrane attachment may result in a hydrogenase with great potential for hydrogen production.

5.1.3 Oxygen-tolerant hydrogenases and their potential

Hydrogenases have a number of attributes that make them excellent electrocatalysts for use in biological fuel cells. Enzyme production is completely renewable; the enzymes have great specificity for hydrogen, high turnover rates and can scavenge fuel under ambient conditions (Cracknell *et al.*, 2008). Fuel cells containing platinum based catalysts on the other hand require a proton exchange membrane due to lack of specificity and are very expensive. It has already been established by Vincent *et al*. (2006) that the oxygen-tolerant hydrogenase from *Ralstonia metallidurans* CH34 is capable of oxidising very low levels (3%) of hydrogen at the anode of a biological fuel cell. With a fungal laccase present at the cathode to reduce oxygen, enough electricity was generated to power a wrist-watch for 24 hours. The design of electrodes is also important and requires attention. The electrode and the enzyme active site must have a good electrical connection, which is mostly achieved through enzyme immobilisation. Unfortunately, this is not possible for some hydrogenase enzymes. A good connection is important and increases the stability of the enzyme. An alternative option is the use of mobile mediators that relay electrons between the electrode and the enzyme, which are currently being researched (Cracknell *et al.*, 2008).

The membrane bound, oxygen-tolerant hydrogenases do represent the subclass of enzyme with the greatest potential to be used in practical applications including fuel cells. These are the best studied of the 'non-standard' [NiFe]-hydrogenases. Although elucidating the conformation of the proximal Fe-S cluster was important, there are other features specific to oxygen-tolerant hydrogenases that remain to be understood. One of these features is the tolerance of this subclass to carbon monoxide, which is not shared by standard hydrogenases. Carbon monoxide and oxygen are similarly sized, hydrophobic gases that are assumed to access the active site in a similar manner. As the oxygen-tolerant enzymes do not appear to be inhibited by carbon monoxide, the suggestion is that the nickel atom does not form a strong enough bond with the carbon monoxide to compete with the binding of

hydrogen (Shafaat *et al.*, 2013). The available structures, however, did not reveal any differences between the electronic structures of the active sites of oxygen-sensitive and oxygen-tolerant hydrogenases (Fritsch *et al.*, 2013). The mechanism behind carbon monoxide tolerance therefore necessitates further probing.

There are however alternative enzymes that have demonstrated a tolerance to oxygen but require further research and better understanding. One of these is the subclass of [NiFe]-hydrogenases known as $NAD(P)^+$ - reducing hydrogenases. These systems are soluble, multimeric enzymes composed of a hydrogenase dimer and a diaphorase module. Although these enzymes predominantly perform hydrogen oxidation, under reducing conditions, the diaphorase module can produce hydrogen. Therefore, these enzymes are known as bidirectional hydrogenases (Vignais and Billoud, 2007). Furthermore, it has been established that the $NAD(P)^+$ - reducing hydrogenase from *R. eutropha* is capable of oxidising hydrogen under oxic conditions (Burgdorf *et al.*, 2005). The mechanism behind oxygen-tolerance is unfortunately unknown at this time. This is due to a lack of spectroscopic and structural information. The NiFeSe [NiFe]-hydrogenases are another fascinating subgroup that have a higher overall enzymatic activity, are biased toward proton reduction and display a decreased sensitivity to oxygen. Although these enzymes have not demonstrated the ability to oxidise hydrogen under oxic conditions, they are capable of aerobic hydrogen production at low potentials (Shafaat *et al.*, 2013). Again the mechanism behind this tolerance is not yet appreciated and requires further research.

The design of bio-inspired synthetic hydrogenase enzymes requires a complete understanding of the mechanisms responsible for desired characteristics such as oxygen-tolerance. It will also be necessary to understand the involvement of specific components (e.g. accessory proteins) in the biosynthesis of these enzymes.

5.2 Hydrogenases in medicine

The development and spread of antibiotic resistance represents a global threat and requires an immediate response. Multi-drug resistant bacteria are thought to have been responsible for an estimated 400 000 infections, 25 000 of which resulted in death, within Europe in 2007. The financial cost associated with this is thought to have exceeded 1.5 billion euros (Bush *et al.*, 2011). It was not long after the discovery of penicillin that Sir Alexander Fleming warned of bacterial antibiotic resistance and urged caution with antibiotic use (Gould and Bal, 2013). Dedicated research into antimicrobials and a continuous stream of new antibiotic classes is required to keep up with the remarkable adaptability of microorganisms. Unfortunately, research is in fact declining and as result the rate of antibiotic resistance infections is rising while the stock of new antibiotics is not. This is mainly due to the lower rate of return that pharmaceutical companies obtain from antibiotics. In contrast to drugs used to treat the symptoms of chronic infections that are taken for life, antibiotics are used for a very small length of time every now and again (Spellberg *et al.*, 2008). The threat of antibiotic resistance has to be taken seriously and deserves financial support that will allow antibiotic research and development against unique drug targets.

Hydrogen is an important energy substrate for a number of pathogenic bacteria including *H. pylori* and *Salmonella* (Maier, 2005). It has been established that removal of the hydrogen uptake [NiFe]-hydrogenase from *H. pylori* results in a strain severely compromised in its colonisation ability (Olson and Maier, 2002). Moreover, deletion of the three hydrogen oxidising [NiFe]-hydrogenases from *Salmonella* results in the acquisition of an avirulent strain unable to cause disease in mice (Maier *et al.*, 2004). Therefore it is clear that as well as being essential for hydrogen respiration, [NiFe]-hydrogenases appear to be essential for infection. Although the removal of these enzymes does not affect bacterial viability, the fact that it impacts bacterial pathogenicity makes hydrogenases attractive drug targets. The presence of a very unique active site containing the metals Ni and Fe and its coordination by the two biologically rare molecules CO and CN, again validate this enzyme as a target for inhibitors.

Due to the availability of hydrogenase crystal structures similar to the one solved in this study, a hit-discovery program could be employed with the intention of eventually, generating a new anti-microbial or anti-infective drug. First of all, a random binding screen using a variety of existing compounds, or fragments of compounds, should be performed using a high-throughput surface plasmon resonance (SPR) system in order to test the binding affinity of these to hydrogenase. If a compound does bind to the enzyme, as the *Salmonella* Hyd-5 enzyme has already been successfully crystallised in-house, it might be possible to assay that enzyme and crystallise the enzyme when bound to the compound. A process of compound optimisation can then be performed in order to obtain a more efficient inhibitor. Phagocyte infection assays and whole animal experiments should also eventually be implemented. Alternatively, rather than starting with a compound binding technique, it may be possible to develop a miniaturised hydrogenase enzyme assay in order to screen for inhibitors directly. Pinske *et al*. (2012) recently showed that oxygen-tolerant [NiFe]-hydrogenases can reduce nitro blue tetrazolium directly *in vitro*, which forms a permanent purple precipitate. Taken together with the high affinity that oxygen-tolerant enzymes appear to have for hydrogen (K_m ~1 μM), it is conceivable that hydrogen-saturated buffers can be safely used in high throughput, automated, inhibitor screens.

Another antimicrobial option may be to prevent the biosynthesis of [NiFe]-hydrogenases. This requires a clear understanding of the assembly and maturation process and the molecular mechanisms involved. The successful incorporation of active site metals and Fe-S clusters is crucial for biosynthesis of active enzyme. Therefore targeting and inhibiting the function of accessory proteins responsible for these insertions would be valuable. Since most of the accessory proteins are water soluble, and their structures are known, setting up a high throughput SPR hit discovery screen would not be impossible. However, as the accessory proteins are cytoplasmic proteins there may be future problems in getting inhibitory compounds inside the cell. Finally, as the Tat system is important for correct localisation of many [NiFe]-hydrogenase enzymes, the design of a drug that would interrupt this transport process, be it through the inhibition of an essential chaperone or the disruption of signal peptide recognition, would also be attractive.

5.3 Concluding remarks

In this work, it was demonstrated that genetic removal of the extended signal peptide n-region results in complete inactivity of *E. coli* [NiFe]-hydrogenase 1. Furthermore, although transcription of the *hya* operon is unaffected, neither the large or small subunit was synthesised in a stable form, indicative of a defective maturation process. The use of reporter protein constructs and pulse-chase labelling experiments have demonstrated that removal of the signal peptide results in a faster rate of protein transport. Therefore, it appears likely that the n-region functions to stall protein export, which may be necessary for successful incorporation of essential cofactors. It is evident that signal peptides of [NiFe]-hydrogenase fulfil a number of different roles, with the proposition here being that the n-region functions in a regulatory capacity.

Salmonella strains have been generated as part of this study, which allow high level expression of hydrogenase enzymes. This method of up-regulated expression will no doubt prove useful in further hydrogenase studies. The findings of this thesis have provided further insight into the mechanism of oxygen tolerance. The acquisition of a Hyd-5 crystal structure revealed the presence of an unusual [4Fe-3S] proximal Fe-S cluster, unique to oxygen-tolerant hydrogenases. Although coordinated by six cysteine residues of the small subunit, this Fe-S cluster was also found to be ligated by a histidine (HisL229) of the large subunit. Here, mutagenesis and electrochemical studies have provided evidence to suggest that residue HisL229 is important for the catalytic activity and oxygen tolerance of Hyd-5.

The involvement of accessory proteins in the biosynthesis of Hyd-5 has also been investigated in this study. It has been demonstrated that proteins HydG and HydH appear to be important for the assembly of an active Hyd-5 enzyme. The deletion of *hydH* in particular appears to have the greatest impact on hydrogen oxidising activity and enzyme processing. This is interesting as homologs of HydH are not encoded by anaerobically expressed operons and are predicted to have a specific role in the assembly of oxygen tolerant hydrogenases.

Hydrogenase enzymes have great potential for use in future biotechnologies including biological fuels cells. In addition, the importance of hydrogen as an energy source for bacterial pathogens such as *Salmonella*, make hydrogenase enzymes

attractive drug targets. Studies into understanding the structure, function and biosynthesis of these enzymes therefore contribute to both fields of biotechnology and biomedicine.

6 Materials and methods

6.1 Bacterial strains

All strains used in this study were derived from either *Escherichia coli* K-12 or *Salmonella enterica* serovar Typhimurium LT2a and are listed in Table 6.1. DH5α was chosen as the *E. coli* strain used for general cloning and transformation of vectors, although M15 [pREP4] was used in some cases. K38 was the host strain used for radiolabelling experiments where the expression of T7 polymerase was encoded on a separate plasmid, pGP1-2.

Name	Description	Antibiotic Resistance	Reference
Escherichia coli K12			
DH5α	F−, *endA1, glnV44, thi-1, recA1, relA1, gyrA96, deoR, nupG, Φ80dlacZΔM15,* Δ(*lacZYA-argF*)*U169, hsdR17*(*rK- mK+*), *λ*−		Grant *et al*. (1990)
M15 [pREP4]	*F-, lac, ara, gal, mtl* [(Kan^R, *lacI*]	Kan (from plasmid)	Villarejo and Zabin (1974)
MG1655	wild-type *E. coli* K12 strain, F$^-$ λ$^-$ ilvG- rfb-50 rph-1		Blattner *et al.* (1997)
MC4100	F- [araD139]B/r Δ(argF-lac)169 λ- e14-flhD5301 Δ(fruK-yeiR)725 (fruA25)‡ relA1 rpsL150(strR) rbsR22 Δ(fimB-fimE)632(::IS1) deoC1		Casadaban and Cohen (1979)
K38[pGP1-2]	*HfrC phoA4 pit-10, tonA22 ompF 627, relA1 spoT1 λ$^+$*, pGP1-2 encodes T7 RNA polymerase	Kan (from plasmid)	Lyons and Zinder (1972) Tabor and Richardson (1985)
FTD67	MC4100, Δ*hybC*		Dubini *et al*. (2002)
FTD147	MC4100, Δ*hyaB*, Δ*hybC*, Δ*hycE*		Deplanche *et al*. (2010)
IC009	FTD67, Δ*hycE*		Deplanche *et al*. (2010)
IC009 E5W	IC009 with a E5W QuikChange substitution introduced by pMAK705		This study
IC009 Y8W	IC009 with a Y8W QuikChange substitution introduced by pMAK705		This study
IC009 ΔNR	IC009 with a n-region deletion introduced by pMAK705		This study
FTH004	MC4100, *hyaA*^{his}		Dubini *et al*. (2002)
Salmonella enterica serovar Typhimurium			
LT2a	Wild type *Salmonella enterica* serovar		McClelland *et al*.

	Typhimurium strain but with a mutation in the *rpoS* gene resulting in avirulence (Swords *et al.*, 1997; Wilmes-Riesenberg *et al.*, 1997)		(2001)
SFTH01	LT2a, *hyd*A^{His}		This study (Parkin *et al.*, 2012)
SFTH05	SFTH01, p_{tat}-*hydA*^{His}		This study (Parkin *et al.*, 2012)
SFTH06a	SFTH01, p_{T5}-*hydA*^{His}		This study (Parkin *et al.*, 2012)
LB03	SFTH06a, ΔTM		This study
LB03 E73A	LB03 carrying a E73A substitution in HydB		This study
LB03 H229A	LB03 carrying a H229A substitution in HydB		This study
LB04	LB03, Δ*hydG* (STM1533)		This study
LB05	LB03, Δ*hydF* (STM1534)		This study
LB06	LB03, Δ*hydH* (STM1532)		This study
LB03T	LB03, Δ*tatABC* (STM3973-3975)	Apra	This study
LB03H1	LB03, Δ*hyaAB* (STM1786/STM 1787)	Apra	This study

Table 6.1. *E. coli* K-12 and *Salmonella* LT2a strains used in this study.

6.2 Materials

6.2.1 Media, supplements and growth conditions

Media used in this study are listed in Table 6.2 and were prepared by the Media Service at the College of Life Science, Dundee. Aerobic growth of *E. coli* strains was achieved by culturing the bacteria in Luria Bertani (LB) medium at 37°C with shaking at 200 rpm. A minimum liquid to air ratio of 1:4 was maintained in each case. Anaerobic growth of *E. coli* was ensured by completely filling the growth vessel with LB medium and incubating, without agitation, at 37°C. For growth on solid media, LB containing 1.5% agar was utilised and incubated at 37°C. These growth conditions were also used to grow *Salmonella* strains, although in this case, low salt LB media was used. Peptone-Iron (PI) agar plates were used as a selective media to detect *Salmonella*. Inoculated PI agar plates were incubated inside a BD BBL GasPak system where an anaerobic atmosphere was generated using an Oxoid Anareogen sachet. Anaerobiosis was confirmed using an Anaerotest (Merck) strip. For radiolabelling experiments, K38 [pGP1-2] was sub-cultured into minimal M9 medium containing the additions detailed in Table 6.2. Supplements and antibiotics were added to the relevant media at the concentrations specified in Table 6.3 and Table 6.4.

Inoculated plates were stored at 4°C for no more than 14 days. In the long term, strain and plasmid stocks (in DH5α) were flash frozen in liquid nitrogen and then stored at -80°C as 25% (v/v) glycerol stock cultures in cryogenic vials.

To test for Tat-compromised strains, agar plates containing 2% SDS, and the appropriate antibiotics, were inoculated and incubated at 37°C overnight (Stanley *et al.*, 2001).

Medium	Components	Quantity (L^{-1})
Luria Bertani (LB) agar (Russell and Sambrook, 2001)	NaCl	10g
	Tryptone	10g
	Yeast extract	5g
	Agar	15g
LB medium	NaCl	10g
	Tryptone	10g
	Yeast extract	5g
Low salt LB agar	NaCl	5g
	Tryptone	10g
	Yeast extract	5g

	Agar	15g
Low salt LB medium	NaCl	5g
	Tryptone	10g
	Yeast extract	5g
M9 medium + amino acids	10 X M9 salts	100 ml
	100 mM $CaCl_2$*	1 ml
	1 M $MgSO_4$*	2 ml
	1% (w/v) Thiamine*	1 ml
	20% (w/v) glucose*	10 ml
	1% (w/v) non-sulphur amino acids*	10 ml x 18
Peptone-Iron (PI) Agar	Agar	16g
	Bacto peptone	15g
	Proteose peptone	5g
	$C_6H_{11}FeNO_7$	0.5g
	$C_3H_7Na_2O_6P$	1g
	$Na_2S_2O_3$	10g

Table 6.2. Growth media used in this study and their components.

Media and components were autoclaved at 121°C for 20 minutes. Components marked with an asterisk, however, were filter sterilised and added to the media prior to use.

Media Supplement	Stock Concentration	Final concentration
Glycerol	50% (v/v)	0.5% (v/v)
Sodium fumarate	16%	0.4% (w/v)
IPTG	1M	2 mM
Sodium Dodecyl Sulphate (SDS)	20% (w/v)	2%
L-arabinose	1 M	10 mM
$NiS0_4$	250 mM	10 µM

Table 6.3. Media supplements and their concentrations.

Each stock solution was prepared in distilled water and filter sterilised prior to use.

Antibiotic	Stock concentration (mg ml^{-1})	Prepared in	Final concentration (µg ml^{-1})
Ampicillin (Amp)	125	Distilled water	50
Apramycin (Apra)	50	Distilled water	50
Chloramphenicol (Cml)	25	80% (v/v) ethanol	25 (*E. coli*) 12.5 (*Salmonella*)
Kanamycin (Kan)	50	Distilled water	50
Rifampicin	20	100% (v/v) methanol	400

Table 6.4. Antibiotics used in this study and their concentrations.

Each stock solution was filter sterilised prior to use.

6.2.2 Buffers and solutions

6.2.2.1 General buffers and solutions

Buffer/Solution	Components	Concentration
Ammonium persulphate (APS)		10% (w/v)
Carbonate transfer buffer	$NaCHO_3$	10 mM
	Na_2CO_3	3 mM
	Methanol	20% (v/v)
Colloidal coomassie stain	Coomassie brilliant blue G-250	0.1% (w/v)
	Methanol	50% (v/v)
Destain	Methanol	50% (v/v)
Dithionite	Dithionite	1% (w/v)
	NaOH	1 mM
DNA loading dye (10x)	Orange G dye	5 mg ml^{-1}
	Glycerol	50% (v/v)
Fixing solution	Methanol	40% (v/v)
	Acetic acid	10% (v/v)
Laemmli sample buffer (2x)	Tris.HCl, pH 6.8	62.5 mM
	SDS	2% (w/v)
	β-mercaptoethanol	5% (v/v)
	Glycerol	25% (v/v)
	Bromophenol blue	0.01% (w/v) bromophenol blue
M9 salts (10x)	NH_4Cl	1% (w/v)
	NaCl	0.5% (w/v)
	KH_2P0_4	3% (w/v)
	Na_2HP0_4	6% (w/v)
Ponceau S solution	Ponceau S	0.1% (w/v)
	Acetic acid	5% (w/v)
Resuspension buffer	Tris.HCl, pH 7.5	50 mM
Rocket immunoelectrophoresis running buffer, pH 8.6	Sodium barbitone.HCl	20 mM
	Triton X-100	0.1% (v/v)
SDS-PAGE running buffer, pH8.3 (10X)	Tris.HCl	250 mM
	Glycine	1.92 M
	SDS	1% (w/v)
TAE buffer	Tris.HCl	40 mM, pH 8.0
	Acetic acid	1.142% (v/v)
	EDTA	1 mM
TBS/Tween	Tris.HCl	20 mM, pH 7.6
	NaCl	137 mM
	Tween®20	0.1 % (v/v)
Transformation buffer (TSB)	1 M $MgS0_4$	5 ml
	DMSO	5ml
	PEG 6000	10g (per 100 ml LB)

Tris buffered saline (TBS)	Tris.HCl	20 mM, pH 7.6
	NaCl	137 mM
Tris-sucrose buffer	Tris.HCl	50 mM, pH 7.5
	Sucrose	40% (w/v)

Table 6.5. General buffers and solutions used in this study.

6.2.2.2 Chromatography buffers

Nickel Affinity Buffers (M)	Components	Concentration
Nickel buffer A (M)	Tris.HCl, pH 7.5	50 mM
	NaCl	150 mM
	Imidazole	50 mM (75 mM for
	Triton X-100	*Salmonella* enzymes)
		0.1% (v/v)
Nickel buffer B (M)	Tris.HCl, pH 7.5	50 mM
	NaCl	500 mM
	Imidazole	1 M (500 mM for
		Salmonella enzymes)
	Triton X-100	0.1% (v/v)

Table 6.6. Nickel affinity chromatography buffers for purification of membrane bound hydrogenases.

M = membrane.

Nickel Affinity Buffers (S)	Components	Concentration
Nickel buffer A (S)	Tris.HCl, pH 7.5	50 mM
	NaCl	150 mM
	Imidazole	75 mM
Nickel buffer B (S)	Tris.HCl, pH 7.5	50 mM
	NaCl	500 mM
	Imidazole	75 mM

Table 6.7. Nickel affinity chromatography buffers for purification of soluble hydrogenases.

S = soluble.

Anion Exchange Buffers	Components	Concentration
Anion exchange buffer A	Tris.HCl, pH 7.5	50 mM
	NaCl	20 mM
Anion exchange buffer B	Tris.HCl, pH 7.5	50 mM
	NaCl	1M

Table 6.8. Anion exchange buffers.

Size Exclusion Buffer	Components	Concentration
SEC buffer	Tris.HCl, pH 7.5	50 mM
	NaCl	150 mM

Table 6.9. Size exclusion buffers.

6.3 Molecular biology techniques

6.3.1 Plasmid DNA preparation

Plasmids were extracted from *E. coli* strains using the QIAprep® Spin Miniprep Kit (Qiagen). The protocol followed is based on the alkaline lysis method of extracting plasmid DNA developed by Bimhoim and Doly (Birnboim and Doly, 1979). Cells were harvested from a 5 ml overnight culture of *E. coli* containing the plasmid of interest, and any required antibiotics, by centrifugation at 2773 x *g* for 10 minutes in an Accuspin™ 1 bench-top centrifuge (Fisher Scientific). The pellet was resuspended and cells lysed in an alkaline solution. Following neutralisation and centrifugation at 16 000 x *g* for 10 minutes in an Eppendorf 5415D centrifuge, lysate was washed over a silica membrane, where plasmid DNA was selectively adsorbed in the presence of a high salt buffer. Plasmid DNA was then eluted in the elution buffer supplied. Plasmids used in this study are listed in Table 6.10.

DNA was quantified spectrophotometrically using a NanoDrop ND-1000 system (Thermo Scientific). A 1.5 µl sample was pipetted on a clean sample pedestal and the absorbance peak of nucleic acid in the sample measured at 260 nm.

6.3.2 Preparation and transformation of competent cells

6.3.2.1 Chemical transformation

5 ml of LB medium, containing the necessary antibiotics, was inoculated with the host strain and grown overnight at 37°C, with shaking. This was subcultured into fresh LB medium, containing the relevant antibiotics, at a dilution of 1:100 and grown aerobically at 37°C, shaking at 200 rpm until an OD_{600} of 0.3-0.4 was reached. Cells were harvested by centrifugation at 2773 x *g* for 10 minutes in an Accuspin™ 1 bench-top centrifuge (Fisher Scientific) and then resuspended in 500 µl of ice cold TSB. Cells were maintained on ice until transformed.

Transformation was performed by incubating 100 µl of competent cells with 1 µl of DNA (0.1-0.6 µg) on ice for 20-30 minutes. Cells were then transferred to 42°C for 90 seconds in a 'heat shock' and chilled on ice for 2 minutes. To the cells, 1 ml of LB medium was added and the culture grown for 1 hour, shaking at 200 rpm at 37°C.

Cells were then harvested by centrifugation at 16 000 x *g* in an Eppendorf 5415D centrifuge for 1 minute, resuspended in 100 µl of LB medium, spread on LB agar plates containing the relevant antibiotics and incubated overnight at 37°C. If transforming the temperature sensitive vector pMAK705, culturing conditions required growth at 30°C.

6.3.2.2 Electroporation

An overnight culture was used to inoculate 25 ml low salt LB medium containing the required antibiotics at a dilution of 1:100, which was then incubated at 37°C, shaking at 200 rpm. Once an OD_{600} of 0.4-0.6 was reached, cultures were incubated on ice for 40 minutes before centrifugation at 2773 x *g* for 10 minutes at 4°C. Cells were resuspended in ice cold 10% glycerol and harvested once more. This was repeated a further two times before a final resuspension in 250 µl of ice cold 10% glycerol. Cells were either used immediately or aliquoted and flash frozen in liquid nitrogen, and then stored at -80°C.

To an aliquot of 50 µl of electrocompetent cells, 1 µl (0.1-0.6 µg) of plasmid DNA was added and incubated on ice for 10 minutes. Cells were then transferred to a chilled 2 mm electroporation cuvette and an electrical pulse applied using the following settings: 2.5 kV, 25 µF capacitance, 200 Ω resistance, 2 mm cuvette length of a Bio-Rad (Hercules, CA) GenePulser Xcell electroporator. Following electroporation, 1 ml of low salt LB medium was added to the cuvette, the cells gently mixed and then transferred to an eppendorf, which was incubated at 37°C for 1 hour with shaking. Cells were then harvested by centrifugation at 16 000 x *g* and resuspended in 100 µl of low salt LB medium before being spread onto low salt agar containing the necessary antibiotics and incubated at 37°C overnight. If transforming pMAK705, culturing conditions required growth at 30°C.

Name	Description	Antibiotic Resistance	Reference
Plasmids used in *Escherichia coli* study			
pUNI-PROM	pT7.5 (Tabor and Richardson, 1985) with the *tatA* promoter cloned *Eco*RI-*Bam*HI	Amp	Jack *et al*. (2004)
pUniREP (pUniCAT)	pUNI-PROM with the *cat* gene cloned in *Xba*I-*Hind*III	Amp	Maillard *et al.* (2007)
pUniCAT-HyaA	pUniCAT with HyaA signal peptide cloned in *Bam*HI-*Xba*I	Amp	T. Palmer (Unpublished)
pUniREP-HyaAlong	pUnirep carrying the HyaA signal peptide and part of the mature sequence cloned *Bam*HI-*Xba*I	Amp	T. Palmer (Unpublished)
pUniCAT-HyaAsstrunc	pUniCAT-HyaA with a truncated HyaA signal peptide (n-region deletion)	Amp	T. Palmer (Unpublished)
pUniCAT-HybO	pUniCAT with HybO signal peptide cloned in *Bam*HI-*Xba*I	Amp	T. Palmer (Unpublished)
pUniCAT-HybOlong	pUnirep carrying the HybO signal peptide and part of the mature sequence cloned *Bam*HI-*Xba*I	Amp	T. Palmer (Unpublished)
pUniCat-HybOsstrunc	pUniCAT-HybO with a truncated HybO signal peptide (n-region deletion)	Amp	T. Palmer (Unpublished)
pUniCAT-HyaA N2W	pUniCAT-HyaA with signal sequence Quikchange substitution N2W	Amp	This work
pUniCAT-HyaA N3W	pUniCAT-HyaA with signal sequence Quikchange substitution N3W	Amp	This work
pUniCAT-HyaA E4W	pUniCAT-HyaA with signal sequence Quikchange substitution E4W	Amp	This work
pUniCAT-HyaA E5W	pUniCAT-HyaA with signal sequence Quikchange substitution E5W	Amp	This work
pUniCAT-HyaA 6TW	pUniCAT-HyaA with signal sequence Quikchange substitution 6TW	Amp	This work
pUniCAT-HyaA F7W	pUniCAT-HyaA with signal sequence Quikchange substitution F7W	Amp	This work
pUniCAT-HyaA Y8W	pUniCAT-HyaA with signal sequence Quikchange substitution Y8W	Amp	This work
pUniCAT-HyaA Q9W	pUniCAT-HyaA with signal sequence Quikchange substitution Q9W	Amp	This work
pUniCAT-HyaA A10W	pUniCAT-HyaA with signal sequence Quikchange substitution A10W	Amp	This work
pUniCAT-HyaA M11W	pUniCAT-HyaA with signal sequence Quikchange substitution M11W	Amp	This work
pUniCAT-HyaA R12W	pUniCAT-HyaA with signal sequence Quikchange substitution R12W	Amp	This work
pUniCAT-HyaA R13W	pUniCAT-HyaA with signal sequence Quikchange substitution R13W	Amp	This work
pUniCAT-HyaA Q14W	pUniCAT-HyaA with signal sequence Quikchange substitution Q14W	Amp	This work
pUniCAT-HyaA G15W	pUniCAT-HyaA with signal sequence Quikchange substitution G15W	Amp	This work
pUniCAT-HyaA V16W	pUniCAT-HyaA with signal sequence Quikchange substitution V16W	Amp	This work
pBluescript II KS^+	pBluescript cloning vector with polylinker oriented in the KS orientation	Amp	Stratagene

pMAK705	Suicide vector for *E. coli* chromosomal mutations	Cml	Hamilton *et al*. (1989)
pKS_E5W	pBluescript II KS$^+$ with 500bp upstream and downstream of HyaA containing the E5W substitution, cloned in *Xba*I-*Kpn*I	Amp	This work
pMAK705_E5W	pMAK705 with 500bp upstream and downstream of HyaA containing the E5W substitution, cloned in *Xba*I-*Kpn*I. Used to generate IC009 E5W	Cml	This work
pKS_Y8W	pBluescript II KS$^+$ with 500bp upstream and downstream of HyaA containing the Y8W substitution, cloned in *Xba*I-*Kpn*I	Amp	This work
pMAK705_Y8W	pMAK705 with 500bp upstream and downstream of HyaA containing the Y8W substitution, cloned in *Xba*I-*Kpn*I. Used to generate IC009 Y8W	Cml	This work
pJET1.2LBsynNdeI	pJET1.2/blunt with 500bp upstream and downstream of HyaA n-region blunt cloned. Insert can be released using *Xba*I-*Kpn*-I. Used to generate IC009 ΔNR	Amp	Biomatik
pUniprom-HyaA	pUniprom with HyaA sequence cloned in *Eco*RI-*Hind*III	Amp	T. Palmer (unpublished)
pQE80-HyaA	pQE80L (Qiagen) with HyaA sequence cloned in *Eco*RI-*Hind*III	Amp	This work

Plasmids used in *Salmonella enterica* serovar Typhimurium study

pFAT210	pBluescript II KS$^+$ with the multicloning site and the C-terminal hexahistidine tag from pQE60 (Qiagen) cloned in *Sal*I-*Cla*I	Amp	Dubini *et al*. (2002)
pFAT210_HydAH1-H2	pFAT210 with DNA covering part of the *hydA* gene up to the final codon cloned in *Kpn*I-*Bgl*II	Amp	This work (Parkin *et al.*, 2012)
pFAT210_HyaAH1-H4	pFAT210_HydAH1-H2 with DNA covering the start codon of *hydB* (including the upstream sequence containing a putative ribosome binding site) cloned in *Hind*III-*Xba*I	Amp	This work (Parkin *et al.*, 2012)
pMAK705 Sal hydAhis	pMAK705 containing *Kpn*I-*Xba*I fragment excised from pFAT210_HyaAH1-H4. Used to generate SFTH01 (*hydA*^{His})	Cml	This work (Parkin *et al.*, 2012)
pKSHydA500up	pBluescript II KS$^+$ with DNA sequence upstream of *hydA* promoter region cloned in HindIII-EcoRI	Amp	This work (Parkin *et al.*, 2012)
pHydApromswap	pKS$^+$ HydA500up with DNA sequence downstream of *hydA* promoter region (including *hydA* start codon) cloned in *Bam*HI-*Xba*I	Amp	This work (Parkin *et al.*, 2012)
pKS Hyd1-6 Ec tat promoter	pHydApromswap with the *tatABCD* operon promoter region (from *E. coli* K-12) excised from pUNIPROM and cloned in *Eco*RI-*Bam*HI	Amp	This work (Parkin *et al.*, 2012)

pKS Hyd1-6 t5 promoter	pHydApromswap with the T5 promoter region (from pQE60) cloned in *Eco*RI-*Bam*HI	Amp	This work (Parkin *et al.*, 2012)
pMAK705 Hyd1-6 Ec tat promoter	pMAK705 with the *tat* promoter region excised from pKS Hyd1-6 Ec tat promoter and cloned in *Xba*I-*Hind*III. Used to generate SFT06 (p_{tat}-*hydA*^{His})	Cml	This work (Parkin *et al.*, 2012)
pMAK705 Hyd1-6 t5 promoter	pMAK705 with the T5 promoter region excised from pKS Hyd1-6 t5 promoter and cloned in *Xba*I-*Hind*III. Used to generate SFT06 (p_{T5}-*hydA*^{His})	Cml	This work (Parkin *et al.*, 2012)
pKS_dhydATMup	pBluescript II KS$^+$ with upstream region of HydA TM domain cloned in *Xba*I-*Bam*HI	Amp	This work
pKS_dhydATMdown	pBluescript II KS$^+$ with downstream region of HydA TM domain cloned in *Bam*HI-*Kpn*I	Amp	This work
pMAK_dhydATM	pMAK705 with regions upstream and downstream of HydA TM domain cloned in *Xba*I-*Kpn*I. Used to generate LB03 (ΔTM)	Cml	This work
pKS_dhydFup	pBluescript II KS$^+$ with upstream region of HydF (STM 1534) cloned in *Xba*I-*Bam*HI	Amp	This work
pKS_dhydFdown	pBluescript II KS$^+$ with downstream region of HydF (STM 1534) cloned in *Bam*HI-*Hind*III	Amp	This work
pMAK_dhydF	pMAK705 with upstream and downstream regions of HydF cloned in *Hind*III-*Xba*I. Used to generate LB05 (Δ*hydF*)	Cml	This work
pKS_dhydGup	pBluescript II KS$^+$ with upstream region of HydG (STM 1533) cloned in *Xba*I-*Bam*HI	Amp	This work
pKS_dhydGup	pBluescript II KS$^+$ with downstream region of HydG (STM 1533) cloned in *Bam*HI-*Hind*III	Amp	This work
pMAK_dhydGup	pMAK705 with upstream and downstream regions of HydG cloned in *Hind*III-*Xba*I. Used to generate LB04 (Δ*hydG*)	Cml	This work
pKS_dhydHup	pBluescript II KS$^+$ with upstream region of HydH (STM 1532) cloned in *Hind*III-*Bam*HI	Amp	This work
pKS_dhydHdown	pBluescript II KS$^+$ with downstream region of HydH (STM 1532) cloned in *Bam*HI-*Xba*I	Amp	This work
pMAK_dhydH	pMAK705 with upstream and downstream regions of HydH cloned in *Hind*III-*Xba*I. Used to generate LB06 (Δ*hydH*)	Cml	This work
pKS_Glu73	pBluescript II KS$^+$ with HydB Glu73 region cloned in *Xba*I-*Kpn*I	Amp	This work
pMAK_E73A	pMAK with region of HydB Glu73 region (carrying E73A substitution) cloned in *Xba*I-*Kpn*I. Used to generate LB03 E73A	Cml	This work

pKS_His229	pBluescript II KS$^+$ with HydB His229region cloned in *Xba*I-*Kpn*I	Amp	This work
pMAK_H229A	pMAK with region of HydB His229 region (carrying H229A substitution) cloned in *Xba*I-*Kpn*I. Used to generate LB03 H229A	Cml	This work
pKSApra	pBluescript II KS$^+$ with apramycin cassette cloned in *Hind*III-*Apa*I	Amp/Apra	T. Palmer (unpublished)
pKSApra_ΔtatLT2	pKS Apra with upstream and downstream regions of the tat operon cloned in *Not*I-*Hind*III, *Apa*I-*Kpn*I	Amp/Apra	T. Palmer (unpublished)
pKSApra_ΔhyaABLT2	pKS Apra with upstream and downstream regions of hyaA and hyaB cloned in *Eco*RI-*Hind*III, *Apa*I-*Kpn*I	Amp/Apra	This work
pIJ790	λ RED recombinase vector; *[oriR101]*, *[repA101*(ts)*]*, *araBp-gam-be-exo*	Cml	Datsenko and Wanner (2000)

Table 6.10. Plasmids used in this study.

6.3.3 Polymerase Chain Reaction (PCR)

DNA fragments were amplified by performing the polymerase chain reaction (PCR). The reaction typically involves the use a pair of specific oligonucleotide primers, four different dNTPs, DMSO, DNA template, DNA polymerase and polymerase specific buffer as shown in Table 6.11. *Taq* DNA polymerase (Roche) was typically used for PCR. On occasion, GoTaq® DNA polymerase was utilised, requiring the addition of $MgCl_2$ at a final concentration of 1.5 mM. These two DNA polymerases were used for general PCR (for e.g. where confirmation of a gene deletion or gene insertion was required). Herculase II (Agilent Technologies) was used for high fidelity PCR and to amplify DNA fragments used for cloning. Around 200 ng of plasmid DNA or purified genomic DNA was used as the DNA template for PCR. Genomic DNA from whole bacterial colonies was also used as template, where a single colony was picked from solid media and resuspended in 50 µl of Milli-Q water. 1 µl of resuspension was then added as template.

Component	Volume
10x Buffer	5 µl
DMSO	2.5 µl
dNTPs (20 mM)	1.0 µl
Forward primer (100 µM)	1.0 µl
Reverse primer (100 µM)	1.0 µl
DNA template	1.0 µl
DNA polymerase	0.5 µl
Water	38 µl
Final volume	**50 µl**

Table 6.11. General PCR mixture used in this study.

General PCR cycling conditions are listed in Table 6.12 and were performed in a Techne TC-3000 PCR Thermal Cycler. An initial step at 94°C was used to denature the DNA and separate the complementary strands of the template. The next three steps were repeated in a series of 30 cycles. First, another denaturation step at 94°C was included, followed by a primer annealing step where specific oligonucleotides bind to single stranded DNA by hybridisation. This was performed at a variable temperature of between 50 and 60°C. An elongation step was then carried out at 72°C; the optimum temperature for most thermostable DNA polymerases. One minute per kilobase of sequence was required for complete extension of the sequence using the

oligonucleotides. The primers used in this study are listed in Table 6.13 and were synthesised by Sigma-Aldrich. The program was concluded by a final elongation step at 72°C.

Step	Temperature (°C)	Time (m:s)	Cycles
Initial denaturation	94	2:00	1
Denaturation	94	0:45	
Annealing	54	0:30	30
Elongation	72	1:00/kb of sequence length	
Final elongation	72	5:00	1

Table 6.12. General PCR cycling conditions used in this study.

Name	Sequence 5’ to 3’	Restriction sites	Details
Escherichia coli primers			
HyaAssN2Wfor	CTACCACAGAGGAGGATCCATG**TGG**AACGAGGAAACATTTTAC		Forward primer for generating Quikchange substitution N2W in pUniCAT-HyaA
HyaAssN2Wrev	GTAAAATGTTTCCTCGTT**CCA**CATGGATCCTCCTCTGTGGTAG		Reverse primer for generating Quikchange substitution N2W in pUniCAT-HyaA
HyaAssN3Wfor	GAGGAGGATCCATGAAT**TGG**GAGGAAACATTTTACCAG		Forward primer for generating Quikchange substitution N3W in pUniCAT-HyaA
HyaAssN3Wrev	CTGGTAAAATGTTTCCTC**CCA**ATTCATGGATCCTCCTC		Reverse primer for generating Quikchange substitution N3W in pUniCAT-HyaA
HyaAssE4Wfor	GGAGGATCCATGAATAAC**TGG**GAAACATTTTACCAGGCC		Forward primer for generating Quikchange substitution E4W in pUniCAT-HyaA
HyaAssE4Wrev	GGCCTGGTAAAATGTTTC**CCA**GTTATTCATGGATCCTCC		Reverse primer for generating Quikchange substitution E4W in pUniCAT-HyaA
HyaAssE5Wfor	GGATCCATGAATAACGAG**TGG**ACATTTTACCAGGCCATG		Forward primer for generating Quikchange substitution E5W in pUniCAT-HyaA
HyaAssE5Wrev	CATGGCCTGGTAAAATGT**CCA**CTCGTTATTCATGGATCC		Reverse primer for generating Quikchange substitution E5W in pUniCAT-HyaA
HyaAssT6Wfor	CCATGAATAACGAGGAA**TGG**TTTTACCAGGCCATGCGG		Forward primer for generating Quikchange substitution T6W in pUniCAT-HyaA
HyaAssT6Wrev	CCGCATGGCCTGGTAAAA**CCA**TTCCTCGTTATTCATGG		Reverses primer for generating Quikchange substitution T6W in pUniCAT-HyaA
HyaAssF7Wfor	GGATCCATGAATAACGAGGAAACA**TGG**TACCAGGCCATGCGGCG		Forward primer for generating Quikchange substitution F7W in pUniCAT-HyaA
HyaAssF7Wrev	CGCCGCATGGCCTGGTA**CCA**TGTTTCCTCGTTATTCATGGATCC		Reverse primer for generating Quikchange substitution F7W in pUniCAT-HyaA
HyaAssY8Wfor	GAATAACGAGGAAACATTT**TGG**CAGGCCATGCGGCGTCAG		Forward primer for generating Quikchange substitution Y8W in pUniCAT-HyaA
HyaAssY8Wrev	CTGACGCCGCATGGCCTG**CCA**AAATGTTTCCTCGTTATTC		Reverse primer for generating Quikchange substitution Y8W in pUniCAT-HyaA
HyaAssQ9Wfor	CGAGGAAACATTTTAC**TGG**GCCATGCGGCGTCAGGGC		Forward primer for generating Quikchange substitution Q9W in pUniCAT-HyaA
HyaAssQ9Wrev	GCCCTGACGCCGCATGGC**CCA**GTAAAATGTTTCCTCG		Reverse primer for generating Quikchange

			substitution Q9W in pUniCAT-HyaA
HyaAssA10Wfor	CGAGGAAACATTTTACCAG**TGG**ATGCGGCGTCAGGGCGTTAC		Forward primer for generating Quikchange substitution A10W in pUniCAT-HyaA
HyaAssA10Wrev	GTAACGCCCTGACGCCGCAT**CCA**CTGGTAAAATGTTTCCTCG		Reverse primer for generating Quikchange substitution A10W in pUniCAT-HyaA
HyaAssM11Wfor	GGAAACATTTTACCAGGCC**TGG**CGGCGTCAGGGCGTTACC		Forward primer for generating Quikchange substitution M11W in pUniCAT-HyaA
HyaAssM11Wrev	GGTAACGCCCTGACGCCG**CCA**GGCCTGGTAAAATGTTTCC		Reverse primer for generating Quikchange substitution M11W in pUniCAT-HyaA
HyaAssR12Wfor	CATTTTACCAGGCCATG**TGG**CGTCAGGGCGTTACCCGG		Forward primer for generating Quikchange substitution R12W in pUniCAT-HyaA
HyaAssR12Wrev	CCGGGTAACGCCCTGACG**CCA**CATGGCCTGGTAAAATG		Reverse primer for generating Quickchange substitution R12W in pUniCAT-HyaA
HyaAssR13Wfor	CATTTTACCAGGCCATGCGG**TGG**CAGGGCGTTACCCGGCGC		Forward primer for generating Quikchange substitution R13W in pUniCAT-HyaA
HyaAssR13Wrev	GCGCCGGGTAACGCCCTG**CCA**CCGCATGGCCTGGTAAAATG		Reverse primer for generating Quikchange substitution R13W in pUniCAT-HyaA
HyaAssQ14Wfor	CCAGGCCATGCGGCGT**TGG**GGCGTTACCCGGCGCAGC		Forward primer for generating Quikchange substitution Q14W in pUniCAT-HyaA
HyaAssQ14Wrev	GCTGCGCCGGGTAACGCC**CCA**ACGCCGCATGGCCTGG		Reverse primer for generating Quikchange substitution Q14W in pUniCAT-HyaA
HyaAssG15Wfor	CCAGGCCATGCGGCGTCAG**TGG**GTTACCCGGCGCAGCTTTC		Forward primer for generating Quikchange substitution G15W in pUniCAT-HyaA
HyaAssG15Wrev	GAAAGCTGCGCCGGGTAAC**CCA**CTGACGCCGCATGGCCTGG		Reverse primer for generating Quikchange substitution G15W in pUniCAT-HyaA
HyaAssV16Wfor	GCCATGCGGCGTCAGGGC**TGG**ACCCGGCGCAGCTTTCTC		Forward primer for generating Quikchange substitution V16W in pUniCAT-HyaA
HyaAssV16Wrev	GAGAAAGCTGCGCCGGGT**CCA**GCCCTGACGCCGCATGGC		Reverse primer for generating Quikchange substitution V16W in pUniCAT-HyaA
HyaAnregfor	GCGCTCTAGAATTCGAACTCTGGAACC	*Xba*I	Forward primer for amplification of *hyaA* fragment required for IC009 *hyaA* substitutions
HyaAnregrev	GCGCGGTACCTGATGACTTTGTCGATAGG	*Kpn*I	Reverse primer for amplification of *hyaA* fragment required for IC009 *hyaA* substitutions

HyaAnregQC_E5 Wfor	GATATGAATAACGAG**TGG**ACATTTTACCAGGC	Forward primer for generating Quikchange substitution E5W in IC009 *hyaA*
HyaAnregQC_E5 Wrev	GCCTGGTAAAATGT**CCA**CTCGTTATTCATATC	Reverse primer for generating Quikchange substitution E5W in IC009 *hyaA*
HyaAnregQC_Y8 Wfor	CGAGGAAACATTT**TGG**CAGGCCATGCGGC	Forward primer for generating Quikchange substitution Y8W in IC009 *hyaA*
HyaAnregQC_Y8 Wrev	GCCGCATGGCCTGC**CAA**AATGTTTCCTCG	Reverse primer for generating Quikchange substitution Y8W in IC009 *hyaA*
HyaAspcheckFOR	GCGCTACTTTCTGGCGACGTGC	Forward sequencing primer for IC009 *hyaA* substitutions and n-region deletion
HyaAspcheckREV	GCGCTAATCGAGGGAAATCAGG	Reverse sequencing primer for IC009 *hyaA* substitutions and n-region deletion
HyaA_RTPCRfor	GCGCATACTTTGATGGCTGCC	Forward primer to amplify *hyaA* fragment for RT-PCR analysis
HyaA_RTPCRrev	GCGCATCATCCCAACTCTGG	Reverse primer to amplify *hyaA* fragment for RT-PCR analysis
HyaB_RTPCRfor	GCGCAATATGGAACGCCTGAACC	Forward primer to amplify *hyaB* fragment for RT-PCR analysis
HyaB_RTPCRrev	GCGCATAAGCGATTAACGTGC	Reverse primer to amplify *hyaB* fragment for RT-PCR analysis
HyaE_RTPCRfor	GCGCACGACACGCCATTTGATGC	Forward primer to amplify *hyaE* fragment for RT-PCR analysis
HyaE_RTPCRrev	GCGCTGAGGCACGCTCCTGCTGC	Reverse primer to amplify *hyaE* fragment for RT-PCR analysis
M13 For	GGAAAACGACGGCCAGT	Forward primer from M13 site
M13 Rev	GGAAACAGCTATGACCATG	Reverse primer from M13 site
pT7.5 For	GGTTTTCACCGTCATCACC	Forward primer to amplify inserts in pT7.5
pT7.5 Rev	CGCTGAGATAGGTGCC	Reverse primer to amplify inserts in pT7.5

Salmonella enterica serovar Typhimurium primers

SalHydA-H1	GCGCGGTACCGCGCATCATGGGGCTGCGTGCAGGC	*Kpn*I	Forward primer to amplify *hydA* DNA fragment for cloning into pFAT210 (incorporation of HydA hexahistidine tag)
SalHydA-H2	GCGCAGATCTTTTTTTCTCTTCCGGAGCGTTTTC	*Bgl*II	Reverse primer to amplify *hydA* DNA

			fragment for cloning into pFAT210 (incorporation of HydA hexahistidine tag)
SalHydA-H3	GCGCAAGCTTGCTCCGGAAGAGAAAAAATAATTAT	*Hind*III	Forward primer to amplify *hydB* DNA fragment for cloning into pFAT210_H1-H2 (incorporation of HydA hexahistidine tag)
SalHydA-H4	GCGCTCTAGAATTCAAGATAGTGGGCGACCGCCAGC	*Xba*I	Forward primer to amplify *hydB* DNA fragment for cloning into pFAT210_H1-H2 (incorporation of HydA hexahistidine tag)
HydX1	GCGCAAGCTTCTTATCCCCTGGCTGCCATCCGGCG	*Hind*III	Forward primer to amplify DNA upstream of the native *hydA* promoter region for cloning into pBluescript II KS^+
HydX2	GCGCGAATTCCCCAAACCACTATAGTTAGTGTGGGG	*Eco*RI	Reverse primer to amplify DNA upstream of the native *hydA* promoter region for cloning into pBluescript II KS^+
HydX5	GCGCGGATCCATGCAAACACAAGATACATTTTATC	*Bam*HI	Forward primer to amplify DNA dowstream of the native *hydA* promoter (including *hydA* start codon) region for cloning into pKS^+ HydA500up
HydX6	GCGCTCTAGAATTCAGGTATAGGCGGGCAGCCTGGC	*Xba*I	Reverse primer to amplify DNA downstream of the native *hydA* promoter region for cloning into pKS^+ HydA500up
T5 forward	GCGCGAATTCAAATCATAAAAAATTTATTTGC	*Eco*RI	Forward primer to amplify the T5 promoter from pQE60 (Qiagen) for cloning into pHydApromswap (to generate SFTH06)
T5 reverse	GGCCGGATCCTTTCTCCTCTTTAATGTATTCTGTGTGAA ATTGTTATCC	*Bam*HI	Reverse primer to amplify the T5 promoter from pQE60 (Qiagen) for cloning into pHydApromswap (to generate SFTH06). A base change has been incorporated to remove the *Eco*RI site from the promoter
HyaATMupfor	CGCGTCTAGAGATGTTTTGCATACTGGCTGG	*Xba*I	Forward primer for amplifying upstream region of *hyaA* to generate LB03 (ΔTM strain)
HyaATMuprev	CGCGGGATCCCGTTGCCCGGCTGTAAAAAG	*Bam*HI	Reverse primer for amplifying upstream of *hydA* TM (ending at Thr313) to generate LB03 (ΔTM strain)

HyaATMdownfor	CGCGGGATCCAGATCTCATCACCATCACCATCAC	*Bam*HI*/Bgl*II	Forward primer for amplifying downstream region of *hydA* to generate LB03 (ΔTM strain)
HyaATMdownrev	GCGCGGTACCATCCCGGCGAGGATAGC	*Kpn*I	Reverse primer for amplifying downstream region of *hydA* to generate LB03 (ΔTM strain)
HydFupXba	GCGCTCTAGAGCAACTGATGCCTGCGGTCTATCTCG	*XbaI*	Forward primer for amplifying upstream region of *hydF* (STM1534) to generate *hydF* deletion strain (LB05)
HydFupBam	GCGCGGATCCGATAGTCATTTTTTTAAATGCTCCGG	*Bam*HI	Reverse primer for amplifying upstream region of *hydF* (STM1534) to generate *hydF* deletion strain (LB05)
HydFdownBam	GCGCGGATCCACGCAATAGAATGAAAGGTAACACACG	*Bam*HI	Forward primer for amplifying downstream region of *hydF* (STM1534) to generate *hydF* deletion strain (LB05)
HydFdownHind	GCGCAAGCTTGCGGCAATTCTGGCGTAATCGGCG	*Hind*III	Reverse primer for amplifying downstream region of *hydF* (STM1534) to generate *hydF* deletion strain (LB05)
HydGupXba	GCGCTCTAGACCTTAGCAGGCGCATGGCTGCTGAC	*Xba*I	Forward primer for amplifying upstream region of *hydG* (STM1533) to generate *hydG* deletion strain (LB04)
HydGupBam	GCGCGGATCCATGATTCACGTGTGTTACCTTTCATTC	*Bam*HI	Reverse primer for amplifying upstream region of *hydG* (STM1533) to generate *hydG* deletion strain (LB04)
HydGdownBam	GCGCGGATCCATCGATGAAGGTAATAGTTCGTGC	*Bam*HI	Forward primer for amplifying downstream region of *hydG* (STM1533) to generate *hydG* deletion strain (LB04)
HydGdown Hind	GCGCAAGCTTCGATAGCCAGAGGCGAGACATCCAGG	*Hind*III	Reverse primer for amplifying downstream region of *hydG* (STM1533) to generate *hydG* deletion strain (LB04)
HydHdelupfor	GCGCAAGCTTCGTAAAACAGCCGG	*Hind*III	Forward primer for amplifying upstream region of *hydH* (STM1532) to generate *hydH* deletion strain (LB06)
HydHdeluprev	GCGCGGATCCCACGAACTATTACC	*Bam*HI	Reverse primer for amplifying upstream region of *hydH* (STM1532) to generate

			hydH deletion strain (LB06)
HydHdeldownfor	GCGCGGATCCTGAAGGAGCTGGCC	*Bam*HI	Forward primer for amplifying downstream region of *hydH* (STM1532) to generate *hydH* deletion strain (LB06)
HydHdeldownrev	GCGCTCTAGACAGTTTAGGGATACC	*Xba*I	Reverse primer for amplifying downstream region of *hydH* (STM1532) to generate *hydH* deletion strain (LB06)
HydHcheckfor	GCGCTATCATTAACTTAACGC		Forward sequencing primer to confirm *hydH* (STM1532) deletion
HydHcheckrev	GCGCAGTTTTGATAAAACTTGC		Reverse sequencing primer to confirm *hydH* (STM1532) deletion
HydBGlufor	GCGCTCTAGACATGACAAATGTTACC	*Xba*I	Forward primer to amplify region around *hydB* (STM1538) Glu73
HydBGlurev	GCGCGGTACCTTCGTCAAGGTTGATGG	*Kpn*I	Reverse primer to amplify region around *hydB* (STM1538) Glu73
HydBHisfor	GCGCTCTAGAAAGGTCGCGATCC	*Xba*I	Forward primer to amplify region around *hydB* (STM1538) His229
HydBHisrev	GCGCGGTACCTAGCGGACTCATCC	*Kpn*I	Forward primer to amplify region around *hydB* (STM1538) His229
QCHydBE73Afor	GGGCATTCGTT**GCG**CGCATTTGCGGC		Forward primer for generating Quikchange substitution E73A in LB03
QCHydBE73Arev	GCCGCAAATGCG**CGC**AACGAATGCCC		Reverse primer for generating Quikchange substitution E73A in LB03
QCHydBH229Afor	GGTAAAAACCCG**GCG**CCTAACTGGCTG		Forward primer for generating Quikchange substitution H229A in LB03
QCHydBH229Arev	CAGCCAGTTAGG**CGC**CGGGTTTTTACC		Reverse primer for generating Quikchange substitution H229A in LB03
QCcheckfor	GCGCTATCCTTATCAGACTCAGG		Forward sequencing primer to confirm *hydB* quick change substitutions
QCcheckrev	GCGCCTGGCAATCAGCAAGACG		Forward sequencing primer to confirm *hydB* quick change substitutions
HyaABdelupfor	GCGCGAATTCACCACAGTGCTCAGGC	*Eco*RI	Forward primer to amplify DNA upstream of *hyaA* (STM1786) for generating LB03 Hyd-1 λRED deletion strain
HyaABdeluprev	GCGCAAGCTTTGCACCACGCTCCGCC	*Hind*III	Reverse primer to amplify DNA upstream

			of *hyaA* (STM1786) for generating LB03 Hyd-1 λRED deletion strain
HyaABdeldownfor	GCGCGGGCCCCGCTAAGCGTTAAGGAAAAGAACG	*Apa*I	Forward primer to amplify DNA downstream of *hyaB* (STM1787) for generating LB03 Hyd-1 λred deletion strain
HyaABdeldownrev	GCGCGGTACCAGATGGCGTACTGGCTATGC	*Kpn*I	Reverse primer to amplify DNA downstream of *hyaB* (STM1787) for generating LB03 Hyd-1 λred deletion strain
Apra to start	GCAGCACACCGCGGG		Reverse primer from apramycin cassette outwards
Apra to end	GCCAGAGGCGGGATGC		Forward primer form apramycin cassette outwards

Table 6.13. Primers used in this study.

Restriction sites are underlined and Quikchange codons highlighted in bold.

6.3.4 Reverse Transcriptase-PCR (RT-PCR)

For RT-PCR analysis, total RNA was extracted from anaerobically cultured strains in the stationary phase of growth using the RNeasy® minikit (Qiagen) following manufacturer's instructions. Two volumes of RNAprotect® Bacteria Reagent were added to 1 ml culture in order to stabilise the RNA. Cells were lysed by adding 100 µl of TE buffer containing 1 mg/ml of lysozyme to the mixture, which was then incubated at room temperature for 5 minutes. After washing, the lysate was transferred to an RNeasy Mini spin column and centrifuged in an Eppendorf 5415D centrifuge at 8000 x *g* for 15 seconds. Any contaminating genomic DNA was digested on-column by the addition of DNase I. Following various washes to rid of salts and non-specifically bound biomolecules, RNA was eluted into 50 µl of RNase-free water.

To synthesise cDNA, the following protocol was followed: 500 ng RNA was mixed with 1 µl of random hexamer primers, 1 µl of dNTPs and 5 µl RNase-free water, which was incubated at 65°C for 5 minutes and then placed on ice for 1 minute. Next, 4 µl of first strand buffer, 1 µl of 0.1 M DTT, 1 µl Superscript III reverse transcriptase (Invitrogen) and 1 µl RNaseOUT™ Recombinant Ribonuclease Inhibitor (Invitrogen) was added to the mixture. This was then incubated at 25°C for 5 minutes, 50°C for 50 minutes and 70 °C for 15 minutes as set on the Techne TC-3000 PCR Thermal Cycler. A negative control reaction was included where the addition of reverse transcriptase was omitted. RNase H (Invitrogen) was added to digest any residual RNA template and the mixture incubated at 37°C for 20 minutes. RNase free water was then added to give a final volume of 100 µl. Oligonucleotides designed to amplify gene regions were used for general PCR analysis of the generated cDNA. Positive control and negative control reactions were performed using genomic DNA and RT minus cDNA templates. PCR products were analysed following agarose gel electrophoresis and GelRed (Biotium) staining.

6.3.5 QuikChange site-directed mutagenesis

QuikChange site-directed mutagenesis was used to introduce amino acid substitutions into plasmid-encoded inserts. This method utilises two synthetic oligonucleotides that contain sequence complementary to opposite strands of the vector, but also have the desired mutation incorporated. Oligonucleotides were designed to be at least 25 bp in length with the desired mutation arranged in the

middle of the sequence. Also of importance, was the presence of one or more G or C nucleotides at both the 3' and 5' ends to ensure strong hybridisation. The oligonucleotide primers used for QuikChange were synthesised by Sigma-Aldrich and can be found in Table 6.13. The complementary oligonucleotides were extended by *PfuTurbo* (Agilent Technologies) DNA polymerase to generate nicked, circular plasmid DNA possessing the incorporated mutation. The reaction mixture and QuikChange cycling conditions are given in Table 6.14 and Table 6.15 respectively. QuikChange PCR was performed in a Techne TC-3000 PCR Thermal Cycler.

Component	Volume
10x buffer	5 µl
DMSO	2.5 µl
dDNTPs (20 mM)	1 µl
Forward primer (100 µM)	1.25 µl
Reverse primer (100 µM)	1.25 µl
DNA template	1 µl
Pfu turbo	1 µl
Water	35
Final volume	50 µl

Table 6.14. Quikchange PCR mixture.

Step	Temperature (°C)	Time (m:s)	Cycles
Initial denaturation	95	0:30	1
Denaturation	95	0:30	
Annealing	50	1:00	18
Elongation	68	12:00	
Final elongation	68	5:00	1

Table 6.15. Quikchange PCR cycling conditions.

Following QuikChange PCR temperature cycling, *dam* methylated parental DNA template was digested for one hour at 37°C with ten units of the restriction endonuclease *Dpn*I. Therefore, mutation-containing synthesised DNA was selected for. Competent *E. coli* DH5α were then transformed with 1 µl of the *DpnI* treated DNA, where the nicked circular DNA was closed to provide plasmids containing the mutated insert. The insert of interest was then sequenced to confirm successful incorporation of the desired mutation.

6.3.6 PCR product purification

To remove impurities (including enzymes, primers and unincorporated nucleotides) from PCR products, PCR purification was performed using the QIAquick® PCR Purification Kit following manufacturer's instructions. A high-salt buffer was added to the reaction mixture, which was then applied to a silica membrane present within a spin column and washed through during centrifugation at 16 000 x *g* for 10 minutes in an Eppendorf 5415D centrifuge. DNA is selectively adsorbed onto the membrane and contaminants pass through. Salts are then washed through using an ethanol containing buffer and the DNA eluted into ultrapure water or into elution buffer as provided.

6.3.7 Agarose gel electrophoresis and extraction

Agarose gel electrophoresis was used for analytical purposes but also to prepare DNA fragments for cloning. DNA fragments were electrophoresed into 1% (w/v) agarose gels prepared in 1 x TAE and containing a 1:10 000 dilution of GelRed (Biotium). DNA samples were mixed with 10 x DNA loading dye and added to the wells of a gel immersed in 1 x TAE buffer. A DNA standard (1 kb ladder, Roche) was loaded adjacent to the DNA samples to allow for estimation of fragment size. Electrophoresis and fragment separation was then performed at 100 V for 20-30 minutes. DNA fragments were visualised by exposure to UV light using a Bio-Rad Gel Doc™ XR+ system.

For use in further applications, DNA was extracted from agarose gels using the QIAquick® Gel Extraction Kit (Qiagen) following manufacturer's instructions. The DNA fragment was excised from the gel following visualisation by UV and the agarose gel slice dissolved in a high salt buffer at 42°C. This was then added to a spin column containing a silica membrane and DNA adsorbed to the membrane. DNA was washed with a high salt buffer containing ethanol and then eluted into 30 µl of EB buffer as supplied.

6.3.8 Digestion of DNA and preparation for cloning

Purified DNA was digested by restriction endonuclease enzymes in the appropriate buffers supplied by the manufacturer. Where two enzymes were used, an

appropriate buffer was chosen that would enable efficient activity of both endonucleases. If no such buffer existed, a reaction containing one of the enzymes was performed first, the DNA purified and then the second reaction performed. Restriction digests were typically performed in a total volume of 50 µl and contained 10 U of each restriction enzyme and about 1500 ng of DNA. Diagnostic digests were performed in a total volume of 20 µl. Reactions were incubated at 37°C (except in the case of *Apa*I, which requires incubation at 30°C) for two hours or overnight.

PCR products digested with restriction enzymes were purified using the QIAquick PCR Purification Kit (Qiagen [6.3.6]). Digested vector DNA was treated with 5 units of rAPid alkaline phosphatase (Roche) at 37°C for 20 minutes to remove 5'-monophosphate groups and prevent vector religation. Vector DNA was then separated by agarose gel electrophoresis and purified using the QIAquick Gel Extraction Kit (Qiagen[6.3.7]), removing the alkaline phosphatase.

6.3.9 DNA ligation

DNA fragments were ligated into linearised vector DNA using T4 DNA Ligase (Roche), which catalyses the formation of phosphodiester bonds between neighbouring 3'-hydroxyl and 5'-phosphate ends in double stranded DNA. Vector and insert were mixed at a ratio of either 1:1, 1:3 or 1:5 and incubated in a 10 µl reaction mixture containing 1 x ligation buffer and 1 unit of T4 DNA Ligase at room temperature overnight. The entire ligation mixture was then used to transform competent DH5α or M15[pREP4] cells.

6.3.10 DNA sequencing

DNA sequencing was essential for confirming the correct sequence of PCR products and vector inserts after cloning, and was performed by the DNA Sequencing and Services at the College of Life Sciences, University of Dundee. For PCR product sequencing, a single 30 µl reaction consisted of 2-80 ng of DNA, depending on the length of product, and a primer at a final concentration of 3.2 picomoles. For plasmid sequencing, a single 30 µl reaction consisted of 600 ng of DNA and 3.2 picomoles of primer.

6.3.11 Chromosomal gene replacements using the λ RED recombinase method

Targeted gene replacements in *Salmonella* were performed by following an adaptation of the REDIRECT protocol for gene disruption by PCR targeting developed for *Streptomyces coelicolor* (Gust *et al.*, 2004) and *E. coli* (Datsenko and Wanner, 2000). This method permits the replacement of a target genetic sequence on the chromosome with an apramycin resistance cassette through a homologous recombination event with a linear PCR product. DNA covering approximately 500 bp upstream of the gene(s) to be deleted, including the start site, and DNA covering approximately 500 bp downstream of the gene(s) to be deleted, including the termination site, were amplified by PCR (Figure 6.1). These DNA fragments were then cloned into pKSApra, flanking the apramycin resistance gene. The apramycin resistance gene is also flanked by FRT (FLP recognition target) sites, which if desired, could be used to eliminate the resistance gene upon expression of FLP recombinase. Primers M13 For and M13 Rev were then used to amplify the entire insert present in pKSApra (Figure 6.1).

The resulting PCR product was incubated with 1 µl (10 U) of *Dpn*I to digest *dam* methylated DNA for 4 hours at 37°C. The PCR product was analysed following agarose gel electrophoresis, excised and extracted from the gel using the QIAquick Gel Extraction Kit (Qiagen[6.3.7]), where DNA was eluted into 50 µl of ultrapure water. *Salmonella* electrocompetent cells harbouring the temperature sensitive pIJ790 were then transformed with 8 µl of PCR product. Electrocompetent cells were prepared as described before (6.3.2) but with a number of modifications. An overnight culture of the strain harbouring pIJ790 was grown in low salt LB medium supplemented with 10 mM arabinose in order to induce expression of the recombinase genes at 30°C, with shaking. This was subcultured into fresh low salt LB medium containing arabinose and electrocompetent cells prepared. Transformed cells were spread onto low salt LB agar containing apramycin and incubated overnight at 30°C. Colonies were then patched onto low salt LB agar containing apramycin and low salt LB agar containing ampicillin. Replacement of the target gene on the chromosome (Figure 6.1) was tested by PCR of apramycin resistant, ampicillin sensitive colonies using primers specific to within the apramycin resistance cassette. A dysfunctional Tat system was tested for by streaking the strain onto LB agar containing 2% SDS.

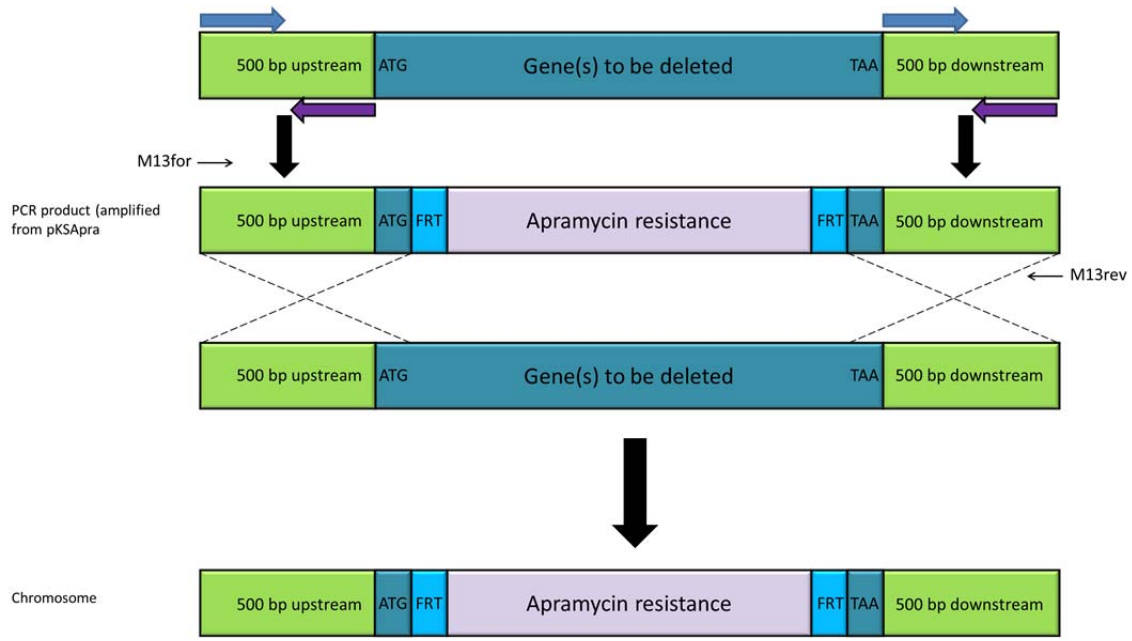

Figure 6.1. λRED protocol for generating targeted gene replacements.

DNA covering 500 bp upstream (including ATG) and 500 bp downstream (including TAA) of the gene(s) to be deleted were amplified using PCR. The two fragments were then cloned separately into pKSApra so as to flank the apramycin resistance gene and FRT sites. The entire pKSApra insert was then amplified using M13 for and M13 rev by PCR and the PCR product used to transform electrocompetent *Salmonella* cells. The gene(s) to be deleted were then replaced with the apramycin resistance gene in a homologous recombination event.

6.3.12 pMAK homologous recombination method for gene deletions and insertions

This method of allelic exchange is used to generate gene and amino acid replacements as well as gene deletions as described by Hamilton *et al*. (1989). The technique involves use of a chloramphenicol resistant, temperature sensitive vector that carries the gene sequence to be recombined onto the chromosome. This integration occurs through homologous recombination.

DNA sequence (500 bp upstream and downstream) surrounding the amino acid to be substituted or the gene to be deleted was amplified and cloned into the suicide vector pMAK705 (Hamilton *et al.*, 1989). The recombinant plasmid was then transformed into the host strain and an overnight culture grown in LB (if *E. coli*) or low salt LB medium (if *Salmonella*) supplemented with chloramphenicol, at 30°C. Serial dilutions (10^{-3}, 10^{-4} and 10^{-5}) were then spread onto the relevant chloramphenicol containing LB agar media and incubated at 44°C overnight. As pMAK705 is temperature sensitive and only replicates at 30°C, any chloramphenicol colonies must be the result of cointegrate formation. A control was also included where cells were diluted at 1 x10^{-7} and incubated at 30°C. Next, five cultures, each containing five

colonies were incubated in the relevant antibiotic containing LB medium at 30°C for 24 hours to allow plasmid regeneration within the cell. Two more cycles of this growth was carried out by transferring a loopful of culture into fresh antibiotic containing medium. A loopful of each culture was then streaked onto the relevant LB media containing chloramphenicol and incubated at 30°C overnight. The final step involved curing plasmid from the strain. Twelve cultures containing single colonies were grown in the relevant LB media, without any added antibiotic at 44°C for at least 16 hours. A loopful from each culture was then streaked onto the relevant LB agar medium (without antibiotic) and incubated at 44°C overnight. Single colonies were then patched onto LB agar and LB agar medium containing chloramphenicol and then incubated at 30°C overnight. Chloramphenicol sensitive colonies were tested for successful integration or deletion by PCR using primers with homology to DNA sequence upstream and downstream of the selected region. PCR products were then analysed following agarose gel electrophoresis and DNA sequencing.

6.4 Protein methods

6.4.1 Purification of affinity-tagged proteins by nickel-affinity chromatography

A 5 ml LB/low salt LB culture, inoculated with the desired strain and containing the relevant antibiotics and supplements was grown overnight at 37°C with shaking at 200rpm. This was used to inoculate fresh medium at a 1:1000 dilution. *Salmonella* strains grown aerobically were cultured in 4 x 2L baffled flasks containing 200 ml low salt LB supplemented with 0.5% glycerol. Flasks were then incubated overnight at 37°C with shaking at 200 rpm. *E. coli* and *Salmonella* strains grown anaerobically were cultured in 5 L Duran bottles, completely filled with LB/low salt LB containing the relevant supplements and antibiotics. The bottles were then incubated at 37°C overnight without agitation.

Cells were harvested by centrifugation at 5009 x *g* for 30-40 minutes, in a Beckman J6-MI centrifuge. For purification of membrane-bound hydrogenases, cell pellets were resuspended in 50 ml of B-PER solution (Thermo Scientific) supplemented with DNase I (Sigma-Aldrich), lysozyme (Sigma-Aldrich), 0.5 ml of protease inhibitor set III (Calbiochem) and 50 mM imidazole to lyse the bacterial cells. This mixture was then incubated at room temperature with agitation for 30 minutes, and centrifuged at 17 387 x *g* for 15 minutes in a Beckman Avanti J-26 XP centrifuge to rid of cell debris. The crude extract was immediately placed on ice. For purification of soluble hydrogenases, a different protocol was followed. Cell pellets were resuspended in Nickel buffer A (S) and lysed under a pressure of 15 000 psi using the EmulsiFlex®-C3 high pressure homogeniser (Avestin). The lysis mixture was then centrifuged at 17 387 x *g* for 15 minutes in a Beckman Avanti J-26 XP centrifuge to rid of cell debris.

Nickel-affinity chromatography was used to isolate C-terminally His-tagged proteins using an ÄKTA FPLC system (Amersham Biosciences). Crude extracts were applied to 5 ml HisTrap HP affinity columns (GE Healthcare) at a flow rate of 1 ml min^{-1}. The column was previously equilibrated with either Nickel buffer A (M) or Nickel buffer A (S) depending on whether a membrane bound (Table 6.6) or soluble hydrogenase (Table 6.7) was being purified respectively. Fifteen column volumes of Nickel buffer A (M/S) were used to wash any unbound protein from the column. A linear gradient of 0-100% Nickel buffer B (M) or Nickel buffer (S) was then applied to the column to elute

bound proteins over a time period of 30 minutes. Eluted protein was collected in 5 ml fraction tubes and samples mixed with Laemmli sample buffer at a ratio of 2:1. Protein samples were then analysed following SDS-PAGE [6.4.8]. Fractions containing the desired protein were concentrated using Vivaspin 20, 50 kDa cut-off spin concentrators (Sartorius Stedim).

6.4.1.1 Antibody Production

Purified *E. coli* Hyd-1^{His} and *Salmonella* Hyd-5^{His} were shipped to Eurogentec (Liege, Belgium) for anti-protein polyclonal antibody production. Approximately 1 mg of each protein was sent to allow for the production of antibodies from two rabbits.

6.4.2 Anion exchange chromatography

Anion exchange chromatography was used to separate proteins according to charge. Concentrated protein was diluted with 50 mM Tris. HCl, pH7.5 to give a final volume of 10 ml. Protein was applied to a HiTrap Q FF (GE Healthcare) Q sepharose column previously equilibrated with anion exchange buffer A (Table 6.8) at a rate of 0.5 ml min^{-1}. Unbound protein was then washed from the column using 10 column volumes of anion exchange buffer A. Bound protein was eluted into 5 ml fraction collection tubes by applying a linear gradient of 0-100% anion exchange buffer B (Table 6.8) over a time period of 30 minutes. Eluted protein samples were mixed with Laemmli sample buffer at a ratio of 1:1. Protein samples were then analysed following SDS-PAGE [6.4.8]. Fractions containing the desired protein were concentrated using Vivaspin 20, 50 kDa cut-off spin concentrators (Sartorius Stedim).

6.4.3 Size Exclusion Chromatography (SEC)

Size exclusion chromatography was performed using a Superdex 200 10/300 GL gel filtration column (GE Healthcare) in order to further purify protein for crystallisation trials. The column was first equilibrated with 1.5 column volumes of SEC buffer (Table 6.9). A small volume of concentrated protein (< 500 µl) was then applied to the column at a flow rate of 0.5 ml min^{-1} and eluted fractions collected in 5 ml fraction collection tubes. Samples were mixed with Laemmli sample buffer at a ratio of 2:1 and then analysed following SDS-PAGE. Fractions containing the desired protein

were concentrated using Vivaspin 20, 50 kDa cut-off spin concentrators (Sartorius Stedim).

6.4.4 Protein crystallisation trials

The hanging drop vapour diffusion method of protein crystallisation was attempted using concentrated protein purified by IMAC and then SEC. A 24 well plate was used to set up various reservoir conditions containing PEG-4000 ranging from a concentration of 16-23% (w/v) and 0.1 M MES ranging from a pH of 5.5 to 6.5. Each reservoir contained 0.24 M lithium sulphate and was made up to a final volume of 1 ml. A small volume (0.5 µl) of protein solution was mixed with 0.5 µl of reservoir, with 1 µl reservoir and with 1 µl of the next reservoir. The three mixtures were dropped onto a coverslip and arranged hanging over the 1 ml reservoir. Crystal trays were maintained at room temperature and checked regularly for crystal formation.

6.4.5 Limited trypsinolysis

To ascertain whether limited trypsinolysis was a viable option to generate stable, soluble enzyme, purified protein was incubated with 0.2% (w/v) Proteomic Grade Trypsin (Sigma-Aldrich) at 37°C for 1 hour. 5 µl samples were removed every 10 minutes and mixed with Laemmli sample buffer at a ratio of 1:1. Samples were boiled for 2 minutes and centrifuged at 16 000 x *g* for 5 minutes in an Eppendorf 5415D centrifuge. Samples were analysed following SDS-PAGE and stained with InstantBlue (Expedion), a Coomassie based staining solution [6.4.8]. A sample untreated with trypsin was also included for molecular weight comparisons. As trypsinolysis was evident within the first 10 minutes, the concentration of trypsin used was lowered to 0.02 % (w/v) and protein incubated with the enzyme for 1 hour at 37°C. To remove trypsin from the concentrated protein, anion exchange chromatography was performed (6.4.2).

6.4.6 Pulse-chase labelling

Pulse-chase experiments were performed to analyse the rate of protein processing. *E. coli* K38[pGP1-2] was used as the host strain where pGP1-2 encodes T7 polymerase and expression is induced by heat shock. K38[pGP1-2] was transformed

with the appropriate pT7 recombinant plasmid where the gene of interest was under control of the T7 promoter. A 5ml culture of transformed K38[pGP1-2] was grown aerobically in LB medium containing ampicillin, overnight at 30°C. The strain was then subcultured at 1:100 into fresh LB medium containing ampicillin and incubated aerobically at 30°C for 3.5 hours. 1 ml of cells were harvested at 16 000 x *g* in an Eppendorf 5415D centrifuge and then resuspended in 5 ml 1 x M9 salts. This was repeated a further two times. Following the final centrifugation, supernatant was removed and the washed cells resupended in 5 ml of a M9 medium + amino acid mixture (lacking cysteine and methionine). This was cultured for one further hour at 30°C in order to deplete the cellular content of cysteine and methionine. The culture was then moved to a temperature of 42°C for 10 minutes to induce synthesis of T7 polymerase from pGP1-2. pGP1-2 not only encodes T7 RNA polymerase, which is under control of the inducible phage λ P_L promoter, but also a constitutively expressed temperature sensitive λ repressor (Tabor and Richardson, 1985). The temperature transition therefore results in induced expression of genes under the control of T7 promoter. Rifampicin was added to a final concentration of 400 µg/ml to inhibit the action of *E. coli* RNA polymerases, and the culture maintained at 42°C for a further 15 minutes before being returned to a temperature of 30°C for 20 minutes. 50 µCi of ^{35}S radiolabelled methionine was then added to the culture to allow specific 'pulse' labelling of the T7 controlled protein. This was then 'chased' with the addition of unlabelled methionine to a final concentration of 0.75 mg/ml two minutes later. 0.5 ml samples were withdrawn at 0, 0.5, 1, 2, 5, 15, 30 and 60 minutes after this addition and added to 1.5 ml screw-cap conical tubes (StarLabs) containing 50 µl of Laemmli sample buffer. Each tube was immediately flash frozen in liquid nitrogen. After gentle thawing, samples were boiled for two minutes and then centrifuged for five minutes at 16 000 x *g* in an Eppendorf 5415D centrifuge. Samples were separated by SDS-PAGE on 12% poly-acrylamide gels. Gels were immersed in fixing solution, vacuum dried on filter paper at 80°C and then exposed to BioMax MR scientific imaging film (Kodak), which was developed in the medical film processor SRX-101A (Konica Minolta). Quantification of protein was undertaken using the Quantity One® Analysis software provided with the Bio-Rad Gel Doc™ XR+ system.

6.4.7 Rocket immunoelectrophoresis

Rocket immunoelectrophoresis is a quick and simple technique that gives an indication of the amount of protein present in a given sample. Periplasm, cytoplasm and membrane samples were used directly for analysis by rocket immunoelectrophoresis. 1% (w/v) agarose gels containing rocket immunoelectrophoresis buffer and antisera specific to the protein being investigated were assembled on small glass plates and small wells introduced. Plates were then placed in an electrophoresis tank containing rocket immunoelectrophoresis buffer and 1-2 µl samples added to the wells. Two Whatman paper electrode wicks were then placed in the buffer, at both the cathode and the anode, and arranged in such a way as to touch the gels. Samples were electrophoresed at 2 mA per plate for 16 hours at 4°C. As the protein migrates through the gel, antibody begins to bind forming a precipitin, which eventually stalls electrophoresis of the complex. Plates were then removed, blotted dry and placed in petri dishes where they were immersed in a 50 mM Tris.HCl pH 7.5 buffer containing a small spatula-full of benzyl viologen (BV) and Tetrazolium Red. BV acts as an artificial electron acceptor while Tetrazolium Red is a redox indicator used to stain active precipitin arcs red. Plates were then enclosed within an Equitron anaerobic jar and incubated under an atmosphere of hydrogen for 16 hours. Hydrogen oxidising activity was detected as intense red precipitin arcs.

6.4.8 SDS-PAGE

SDS polyacrylamide gel electrophoresis (SDS-PAGE) was employed to separate proteins under denaturing conditions according to their molecular weight (Laemmli, 1970) using the Bio-Rad Mini-PROTEAN II System. The resolving gel was prepared as indicated in Table 6.16 and was poured between two glass plates, leaving enough room for comb insertion. Water was then poured on top of the resolving gel, which was left to polymerise. Following polymerisation, the water was removed and the stacking gel added. This was prepared as detailed in Table 6.16. A comb was immediately inserted into the stacking gel to create sample wells.

Resolving Gel constituents	Concentration/ %
Acrylamide/bisacrylamide (37:5:1)	8-16%
Tris.HCl pH 8.8	0.375 M
SDS	0.1% (w/v)
APS	0.1% (w/v)
TEMED	0.1% (v/v)

Stacking Gel constituents	Concentration/ %
Acrylamide/bisacrylamide (37:5:1)	6%
Tris.HCl pH 6.8	0.125 M
SDS	0.1% (w/v)
APS	0.1% (w/v)
TEMED	0.1% (v/v)

Table 6.16. The constituents of the resolving and stacking gels used in SDS-PAGE.

Following polymerisation of the stacking gel, the combs were gently removed and the plates placed into the electrophoresis tank, which was then filled with 1 x SDS running buffer (Table 6.5). Protein samples were mixed in a 1:1 or 2:1 ratio with Laemmli sample buffer prior to loading. Samples were loaded into the wells of each gel along with a pre-stained molecular weight protein standard (Precision Plus, Bio-Rad). Proteins were electrophoresed into the stacking gel at a constant voltage of 100 V. On entry into the resolving gel, the voltage was increased to 200 V and left for the desired length of time. Upon removal of the gels, protein bands were visualised using InstantBlue (Expedion), and left incubating overnight with gentle shaking. Gels were destained in water with gentle shaking, arranged between two pieces of acetate and scanned.

6.4.9 Semi-dry Western immunoblotting

Following SDS-PAGE, the gel was transferred from the electrophoresis tank into carbonate transfer buffer for five minutes (Table 6.5). At the same time, a piece of Amersham™ Hybond™-ECL nitrocellulose membrane (GE Healthcare) and four pieces of Whatman filter paper were also immersed in carbonate transfer buffer. Two pieces of Whatman were placed on the semi-dry transfer apparatus (Bio-Rad) with the nitrocellulose membrane and poly-acrylamide gel placed on top of this. A further two pieces of Whatman were arranged as the final layer. Protein bands were transferred to the nitrocellulose membrane at 175 mA for 45 minutes.

Following protein transfer, the membrane was blocked in 1 x TBS containing 5% milk overnight at 4°C. The membrane was washed in Milli-Q water to remove the milk solution and then incubated with the primary antibody in either 1 x TBS/Tween or in a 1 x TBS solution containing 5% milk and 0.5 % (w/v) BSA, shaking at room temperature.

The monoclonal Penta-His primary antibody (Qiagen) was used at a dilution of 1:4000 whereas use of the polyclonal *E. coli* Hyd-1 and *Salmonella* Hyd-5 antiserum required various methods of 'cleaning up'. The Hyd-5 antiserum was 'purified' by incubating the serum with crude extract of an anaerobically-cultured Hyd-1-deletion strain (LB03H1). LB03H1 was cultured anaerobically in low salt LB overnight at 37°C without shaking. Following centrifugation at 2773 x *g* for 10 minutes, the cell pellet was resuspended in 5 ml 1 x TBS and sonicated to lyse cells. Crude extract was obtained following centrifugation. 5 µl of antiserum was added to 1 ml of crude extract, which was then incubated at 37°C for 30 minutes with shaking. The mixture was then centrifuged at 16 000 x *g* for 10 minutes and antiserum used at a dilution of 1:100.

For detection of the *E. coli* Hyd-1 large subunit, it was sufficient to incubate the polyclonal Hyd-1 antiserum with the crude extract of FTD147, centrifuge to remove precipitates, and then use for immunoblotting at a dilution of 1:100. For detection of the small subunit, purified Hyd-1 was separated by SDS-PAGE, immunoblotted and stained with ponceau solution. The section of nitrocellulose membrane containing the small subunit was blocked in 1 x TBS containing 5% (w/v) milk overnight. Following three washes with 1 x TBS, membranes were incubated with 800 µl of 1 x TBS and 200 µl of antiserum overnight at room temperature with shaking. After washing, 1 ml of 100 mM glycine pH 2.5 was added to strip the antibody from the membrane. The pH was increased by the addition of 100 µl of 1M Tris. HCl to prevent antibody denaturation and then used for immunoblotting at a dilution of 1:500.

Membranes were then washed in approximately 100 ml TBS/Tween for 10 minutes, shaking at room temperature. This was repeated a further two times to rid of excess antibody. Secondary antibody diluted in in either 1 x TBS/Tween or in a 1 x TBS solution containing 5% milk and 0.5% (w/v) BSA was then added to the membrane and incubated at room temperature with shaking. The membrane was washed three times in 1 x TBS/Tween, shaking at room temperature, again to remove unbound antibody. Anti-mouse IgG and anti-rabbit IgG HRP conjugate (Bio-Rad) was used at a dilution of 1:10 000. Immunoreactive protein bands were detected using Immobilon™ Western Chemiluminescent HRP Substrate and exposure to BioMax MR scientific imaging film (Kodak). Films were developed in the medical film processor SRX-101A (Konica Minolta).

6.4.10 Determining protein concentrations

Protein concentrations were determined by following a modified Lowry method (Lowry *et al.*, 1951), using the DC Protein Assay Kit (Bio-Rad). A 2 mg ml^{-1} BSA solution (Sigma-Aldrich) was used to obtain a standard curve ranging between 2-10 µg of protein. This was performed in triplicate in a 96 well plate. Protein samples were diluted 1:2, 1:4 and 1:8 in 50 mM Tris. HCl pH 7.5 and 5 µl samples aliquoted into the same 96 well plate. Reagent A was added to each sample at a volume of 25 µl, followed by the addition of 200 µl of reagent B. This was incubated at room temperature for 15 minutes and the absorbance read at a wavelength of 750 nm in the ELx808™ Absorbance Microplate Reader (BioTek). Protein concentrations were calculated using the measured absorbance and applying it to the standard BSA curve.

6.5 Antibiotic sensitivity assays

MG1655 transformed with the appropriate recombinant plasmid was cultured in LB medium containing ampicillin overnight at 37°C with shaking. Cells were diluted 1:200 into fresh LB medium containing ampicillin and either 100 µg/ml or no added chloramphenicol. 150 µl of the inoculated medium was then added to a 96 well plate and was performed in triplicate. Cell density was measured at 750 nm every 20 minutes at 37°C with shaking on the ELx808™ Absorbance Microplate Reader (BioTek). One of the wells contained LB medium and ampicillin only, and was used as a background reading.

6.6 Cell fractionation

Subcellular fractionation was performed on cells grown either aerobically or anaerobically in LB media containing relevant supplements and antibiotics, at 37°C. Cells were harvested at 2773 x *g*, washed in 50 mM Tris.HCl pH 7.5 and resuspended in Tris-sucrose buffer [6.2.2] at 10 ml g^{-1} wet weight. EDTA and lysozyme were added to a final concentration of 5 mM and 0.6 mg/ml respectively and the suspension incubated, without agitation, at 37°C for 30 minutes. The suspension was centrifuged at 17 387 x *g* for 12 minutes in a Beckman Avanti J-26 XP centrifuge to obtain sphaeroplasts. Sphaeroplasts were resuspended in 50 mM Tris.HCl pH 7.5 at a volume of 10 ml g^{-1} of original wet weight and DNase I added. Cell suspensions were lysed at 8000 psi using a French® Press cell disruptor (Thermo Scientific) and the sample then centrifuged at 27 000 x *g* for 20 minutes to remove cell debris. The supernatant was then centrifuged at 278 000 x *g* for 30 minutes in an Optima™ TLX ultracentrifuge (Beckman) to obtain membranes. The supernatant containing cytoplasm was added to an equal volume of Laemmli sample buffer and flash frozen in liquid nitrogen. The remaining supernatant was removed; membranes resuspended in 50 mM Tris.HCl pH 7.5 and 250 mM NaCl and suspensions centrifuged again at 278 000 x *g* for 30 minutes. For Western immunoblotting, membranes were resuspended in 50 mM Tris.HCl pH 7.5 following removal of the supernatant and then re-centrifuged. For rocket immunoelectrophoresis, membranes were solubilised in 50mM Tris.HCl pH 7.6 containing 0.4% Triton X-100 (v/v), incubated on ice for 20 minutes and then centrifuged at 278 000 x *g* for a further 30 minutes. Supernatants containing membranes were added to an equal volume of Laemmli sample buffer and flash frozen in liquid nitrogen.

6.7 Enzyme assays

6.7.1 Hydrogen-oxidising activity assays

Using hydrogenase activity assays, the oxidation of hydrogen can be coupled *in vitro* to the reduction of an artificial electron donor, which in this case is benzyl viologen (BV). Whereas oxidised BV is colourless, reduced BV is purple. BV reduction can then therefore be detected by measuring the A_{600} in a spectrometer. For whole cell hydrogenase activity assays on anaerobically grown *Salmonella*, Duran bottles containing 500 ml low salt LB were inoculated with 0.5 ml of pre-culture and incubated for 16 hours without agitation, at 37°C. For whole cell hydrogenase activity assays on aerobically grown *Salmonella,* flasks containing 25 ml of low salt LB supplemented with 0.5% glycerol were inoculated and incubated at 37°C overnight with shaking. Cells were harvested at 2773 x *g* for 10 minutes, washed twice in 50 mM Tris.HCl pH 7.5, re-centrifuged and 100 mg of cells resuspended in 200 µl of 50 mM Tris.HCl, pH 7.5. Cuvettes containing benzyl viologen (BV) were completely filled with 50 mM Tris.HCl, pH 7.5 buffer saturated with hydrogen and titrated with a 1% (w/v) sodium dithionite solution until the A_{600} was steady at between 0.3 and 0.7. Between 1 and 2.5 µl of intact cells were added to the cuvette and the reduction of BV measured at A_{600} at room temperature.

Hydrogenase specific activity assays were performed on protein purified by IMAC. Following protein purification, fractions containing the desired protein were pooled and concentrated. The volume of protein added to the cuvette varied upon enzyme but measurements were taken as detailed above. Protein concentrations were determined using the Lowry method (6.4.10). Hydrogenase activity was calculated using Equation 6.1.

$$\frac{\mu M \text{ oxidised BV}}{mg^{-1}\ min^{-1}} = \frac{\Delta A_{600}\ min^{-1} \times \text{cuvette volume (L)} \times 1000}{2 \times \varepsilon_{600}\ (mM^{-1}\ cm^{-1}) \times \text{protein/cells (mg)} \times \text{path length}}$$

Equation 6.1. The equation used for determining hydrogen oxidising activity. ε_{600} BV = 7.4 mM-1 cm-1; cuvette volume = 0.0018 L and the path length = 1cm.

6.8 In-gel digestion of proteins for phospho-peptide analysis

This method of in-gel digestion was used to prepare proteins for a phospho-peptide search that was conducted by Dr David Campbell of the MRC-PPU proteomics facility run by Dr Matthias Trost in the MRC Protein Phosphorylation and Ubiquitylation Unit, Dundee.

Following IMAC, fractions containing the respective protein were pooled. A sample was then removed and mixed with Laemmli sample buffer in a ratio of 1:1 before boiling for 1 minute. Iodoacetamide was added to the sample at a final concentration of 50 mM to alkylate cysteine residues. This was then incubated in the dark, at room temperature for 30 minutes. DTT was added to a final concentration of 50 mM to quench the reaction. Next, samples were loaded into the wells of a pre-cast 4-15% Mini-PROTEAN® TGX gel (BioRad) placed within a SDS-PAGE apparatus containing fresh, filtered 1 x SDS-PAGE running buffer. Following electrophoresis, bands were stained with InstantBlue (Expedion) for two hours and then destained with water while shaking. Every effort was taken to minimise keratin contamination. Therefore, the majority of the subsequent steps were performed within a laminar flow hood and gloves worn at all times.

Gel bands were excised using clean scalpels and cut into 1 mm cubes, before being placed into Eppendorf tubes. Gel pieces were washed in 0.5 ml Milli-Q water, followed by 0.5 ml 50% acetonitrile/50% MilliQ water and lastly 0.5 ml 50% acetonitrile/50 mM NH_4HC0_3. Each wash was performed for 10 minutes with shaking and liquid removed between washes. To obtain colourless gel bands, the 0.5 ml 50% acetonitrile/50 mM NH_4HC0_3 wash was repeated overnight. Once colourless, 0.3 ml acetonitrile was added for 15 minutes to dehydrate the gel pieces. Supernatant was then removed and the tubes placed in a Speed-Vac (Thermo Scientific) to completely dry the gel pieces. Gel pieces were then swollen by the addition of 30 µl of 25 mM Triethylammonium bicarbonate containing 5 µl/ml of protease and were incubated at 30°C for 30 minutes with shaking. Gel bands were checked to ensure they were still immersed in the digest solution and were then returned to 30°C overnight. The equivalent volume of acetonitrile was added to the digest, which was shaken for a further 15 minutes. The supernatant was removed to a clean tube, flash frozen at -

80°C in liquid nitrogen and then dried using the SpeedVac. Meanwhile, 100 µl of 50% acetonitrile/2.5% formic acid was added to the gel pieces, which were shaken for another 10 minutes. The supernatant from this step was then combined with the dried first extract, flash frozen in liquid nitrogen and then completely dried in the SpeedVac. Samples were now transferred to the MRC-PPU proteomics facility for phospho-peptide screening.

7 Bibliography

Abou Hamdan, A., Burlat, B., Gutierrez-Sanz, O., Liebgott, P. P., Baffert, C., De Lacey, A. L., Rousset, M., Guigliarelli, B., Leger, C. and Dementin, S. (2013) O2-independent formation of the inactive states of NiFe hydrogenase. Nature chemical biology **9**: 15-17

Akhtar, M. K. and Jones, P. R. (2008) Deletion of iscR stimulates recombinant clostridial Fe-Fe hydrogenase activity and H2-accumulation in *Escherichia coli* BL21(DE3). Applied microbiology and biotechnology **78**: 853-862

Alami, M., Luke, I., Deitermann, S., Eisner, G., Koch, H. G., Brunner, J. and Muller, M. (2003) Differential interactions between a twin-arginine signal peptide and its translocase in *Escherichia coli*. Molecular cell **12**: 937-946

Albareda, M., Manyani, H., Imperial, J., Brito, B., Ruiz-Argueso, T., Bock, A. and Palacios, J. M. (2012) Dual role of HupF in the biosynthesis of [NiFe] hydrogenase in *Rhizobium leguminosarum*. BMC microbiology **12**: 256

Andrews, S. C., Berks, B. C., McClay, J., Ambler, A., Quail, M. A., Golby, P. and Guest, J. R. (1997) A 12-cistron *Escherichia coli* operon (hyf) encoding a putative proton-translocating formate hydrogenlyase system. Microbiology **143 (Pt 11)**: 3633-3647

Ballantine, S. P. and Boxer, D. H. (1985) Nickel-containing hydrogenase isoenzymes from anaerobically grown *Escherichia coli* K-12. Journal of bacteriology **163**: 454-459

Ballantine, S. P. and Boxer, D. H. (1986) Isolation and characterisation of a soluble active fragment of hydrogenase isoenzyme 2 from the membranes of anaerobically grown *Escherichia coli*. European journal of biochemistry / FEBS **156**: 277-284

Baradaran, R., Berrisford, J. M., Minhas, G. S. and Sazanov, L. A. (2013) Crystal structure of the entire respiratory complex I. Nature **494**: 443-448

Barreto, L., Makihiro, A. a. and Riahi, K. (2003) The hydrogen economy in the 21st century: a sustainable development scenario. International journal of Hydrogen Energy **28**: 267-284

Bayer, T. S., Booth, L. N., Knudsen, S. M. and Ellington, A. D. (2005) Arginine-rich motifs present multiple interfaces for specific binding by RNA. RNA **11**: 1848-1857

Bechet, E., Guiral, S., Torres, S., Mijakovic, I., Cozzone, A. J. and Grangeasse, C. (2009) Tyrosine-kinases in bacteria: from a matter of controversy to the status of key regulatory enzymes. Amino acids **37**: 499-507

Berggren, G., Adamska, A., Lambertz, C., Simmons, T. R., Esselborn, J., Atta, M., Gambarelli, S., Mouesca, J. M., Reijerse, E., Lubitz, W., Happe, T., Artero, V. and Fontecave, M. (2013) Biomimetic assembly and activation of [FeFe]-hydrogenases. Nature **499**: 66-69

Berks, B. C., Palmer, T. and Sargent, F. (2005) Protein targeting by the bacterial twin-arginine translocation (Tat) pathway. Current opinion in microbiology **8**: 174-181

Berks, B. C., Sargent, F. and Palmer, T. (2000) The Tat protein export pathway. Molecular microbiology **35**: 260-274

Berney, M. and Cook, G. M. (2010) Unique flexibility in energy metabolism allows mycobacteria to combat starvation and hypoxia. PloS one **5**: e8614

Bernhard, M., Schwartz, E., Rietdorf, J. and Friedrich, B. (1996) The *Alcaligenes eutrophus* membrane-bound hydrogenase gene locus encodes functions involved in maturation and electron transport coupling. Journal of bacteriology **178**: 4522-4529

Berrisford, J. M. and Sazanov, L. A. (2009) Structural basis for the mechanism of respiratory complex I. The Journal of biological chemistry **284**: 29773-29783

Birnboim, H. C. and Doly, J. (1979) A rapid alkaline extraction procedure for screening recombinant plasmid DNA. Nucleic acids research **7**: 1513-1523

Blattner, F. R., Plunkett, G., 3rd, Bloch, C. A., Perna, N. T., Burland, V., Riley, M., Collado-Vides, J., Glasner, J. D., Rode, C. K., Mayhew, G. F., Gregor, J., Davis, N. W., Kirkpatrick, H. A., Goeden, M. A., Rose, D. J., Mau, B. and Shao, Y. (1997) The complete genome sequence of *Escherichia coli* K-12. Science **277**: 1453-1462

Blokesch, M., Albracht, S. P., Matzanke, B. F., Drapal, N. M., Jacobi, A. and Bock, A. (2004a) The complex between hydrogenase-maturation proteins HypC and HypD is an intermediate in the supply of cyanide to the active site iron of [NiFe]-hydrogenases. Journal of molecular biology **344**: 155-167

Blokesch, M., Paschos, A., Bauer, A., Reissmann, S., Drapal, N. and Bock, A. (2004b) Analysis of the transcarbamoylation-dehydration reaction catalyzed by the hydrogenase maturation proteins HypF and HypE. European journal of biochemistry / FEBS **271**: 3428-3436

Blokesch, M., Paschos, A., Theodoratou, E., Bauer, A., Hube, M., Huth, S. and Bock, A. (2002) Metal insertion into NiFe-hydrogenases. Biochemical Society transactions **30**: 674-680

Bogsch, E. G., Sargent, F., Stanley, N. R., Berks, B. C., Robinson, C. and Palmer, T. (1998) An essential component of a novel bacterial protein export system with homologues in plastids and mitochondria. The Journal of biological chemistry **273**: 18003-18006

Bohm, R., Sauter, M. and Bock, A. (1990) Nucleotide sequence and expression of an operon in *Escherichia coli* coding for formate hydrogenlyase components. Molecular microbiology **4**: 231-243

Bothe, H., Schmitz, O., Yates, M. G. and Newton, W. E. (2010) Nitrogen fixation and hydrogen metabolism in cyanobacteria. Microbiology and molecular biology reviews : MMBR **74**: 529-551

Boyington, J. C., Gladyshev, V. N., Khangulov, S. V., Stadtman, T. C. and Sun, P. D. (1997) Crystal structure of formate dehydrogenase H: catalysis involving Mo, molybdopterin, selenocysteine, and an Fe4S4 cluster. Science **275**: 1305-1308

Brito, B., Prieto, R. I., Cabrera, E., Mandrand-Berthelot, M. A., Imperial, J., Ruiz-Argueso, T. and Palacios, J. M. (2010) *Rhizobium leguminosarum* hupE encodes a nickel transporter required for hydrogenase activity. Journal of bacteriology **192**: 925-935

Brock, I. W., Mills, J. D., Robinson, D. and Robinson, C. (1995) The delta pH-driven, ATP-independent protein translocation mechanism in the chloroplast thylakoid membrane. Kinetics and energetics. The Journal of biological chemistry **270**: 1657-1662

Brondsted, L. and Atlung, T. (1994) Anaerobic regulation of the hydrogenase 1 (hya) operon of *Escherichia coli*. Journal of bacteriology **176**: 5423-5428

Bruser, T. and Sanders, C. (2003) An alternative model of the twin arginine translocation system. Microbiological research **158**: 7-17

Buchanan, G., Maillard, J., Nabuurs, S. B., Richardson, D. J., Palmer, T. and Sargent, F. (2008) Features of a twin-arginine signal peptide required for recognition by a Tat proofreading chaperone. FEBS letters **582**: 3979-3984

Buhrke, T., Lenz, O., Krauss, N. and Friedrich, B. (2005) Oxygen tolerance of the H2-sensing [NiFe] hydrogenase from *Ralstonia eutropha* H16 is based on limited access of oxygen to the active site. The Journal of biological chemistry **280**: 23791-23796

Burgdorf, T., Lenz, O., Buhrke, T., van der Linden, E., Jones, A. K., Albracht, S. P. and Friedrich, B. (2005) [NiFe]-hydrogenases of *Ralstonia eutropha* H16: modular enzymes for oxygen-tolerant biological hydrogen oxidation. Journal of molecular microbiology and biotechnology **10**: 181-196

Burstel, I., Hummel, P., Siebert, E., Wisitruangsakul, N., Zebger, I., Friedrich, B. and Lenz, O. (2011) Probing the origin of the metabolic precursor of the CO ligand in the catalytic center of [NiFe] hydrogenase. The Journal of biological chemistry **286**: 44937-44944

Burstel, I., Siebert, E., Winter, G., Hummel, P., Zebger, I., Friedrich, B. and Lenz, O. (2012) A universal scaffold for synthesis of the Fe(CN)2(CO) moiety of [NiFe] hydrogenase. The Journal of biological chemistry **287**: 38845-38853

Bush, K., Courvalin, P., Dantas, G., Davies, J., Eisenstein, B., Huovinen, P., Jacoby, G. A., Kishony, R., Kreiswirth, B. N., Kutter, E., Lerner, S. A., Levy, S., Lewis, K., Lomovskaya, O., Miller, J. H., Mobashery, S., Piddock, L. J., Projan, S., Thomas, C. M., Tomasz, A., Tulkens, P.

M., Walsh, T. R., Watson, J. D., Witkowski, J., Witte, W., Wright, G., Yeh, P. and Zgurskaya, H. I. (2011) Tackling antibiotic resistance. Nature reviews. Microbiology **9**: 894-896

Cardarelli, F., Serresi, M., Bizzarri, R. and Beltram, F. (2008) Tuning the transport properties of HIV-1 Tat arginine-rich motif in living cells. Traffic **9**: 528-539

Cardarelli, F., Serresi, M., Bizzarri, R., Giacca, M. and Beltram, F. (2007) *In vivo* study of HIV-1 Tat arginine-rich motif unveils its transport properties. Molecular therapy : the journal of the American Society of Gene Therapy **15**: 1313-1322

Casadaban, M. J. and Cohen, S. N. (1979) Lactose genes fused to exogenous promoters in one step using a Mu-lac bacteriophage: *in vivo* probe for transcriptional control sequences. Proceedings of the National Academy of Sciences of the United States of America **76**: 4530-4533

Chan Chung, K. C. and Zamble, D. B. (2011) Protein interactions and localization of the Escherichia coli accessory protein HypA during nickel insertion to [NiFe] hydrogenase. The Journal of biological chemistry **286**: 43081-43090

Chatzi, K. E., Sardis, M. F., Karamanou, S. and Economou, A. (2013) Breaking on through to the other side: protein export through the bacterial Sec system. The Biochemical journal **449**: 25-37

Cheng, T., Li, H., Xia, W. and Sun, H. (2012) Multifaceted SlyD from *Helicobacter pylori*: implication in [NiFe] hydrogenase maturation. Journal of biological inorganic chemistry : JBIC : a publication of the Society of Biological Inorganic Chemistry **17**: 331-343

Cheng, T., Li, H., Yang, X., Xia, W. and Sun, H. (2013) Interaction of SlyD with HypB of *Helicobacter pylori* facilitates nickel trafficking. Metallomics : integrated biometal science

Cline, K., Ettinger, W. F. and Theg, S. M. (1992) Protein-specific energy requirements for protein transport across or into thylakoid membranes. Two lumenal proteins are transported in the absence of ATP. The Journal of biological chemistry **267**: 2688-2696

Cline, K. and McCaffery, M. (2007) Evidence for a dynamic and transient pathway through the TAT protein transport machinery. The EMBO journal **26**: 3039-3049

Constant, P., Chowdhury, S. P., Pratscher, J. and Conrad, R. (2010) Streptomycetes contributing to atmospheric molecular hydrogen soil uptake are widespread and encode a putative high-affinity [NiFe]-hydrogenase. Environmental microbiology **12**: 821-829

Cracknell, J. A., Vincent, K. A. and Armstrong, F. A. (2008) Enzymes as working or inspirational electrocatalysts for fuel cells and electrolysis. Chemical reviews **108**: 2439-2461

Cristóbal, S., de Gier, J. W., Nielsen, H. and von Heijne, G. (1999) Competition between Sec- and TAT-dependent protein translocation in *Escherichia coli*. The EMBO journal **18**: 2982-2990

Dabney-Smith, C., Mori, H. and Cline, K. (2006) Oligomers of Tha4 organize at the thylakoid Tat translocase during protein transport. The Journal of biological chemistry **281**: 5476-5483

Datsenko, K. A. and Wanner, B. L. (2000) One-step inactivation of chromosomal genes in *Escherichia coli* K-12 using PCR products. Proceedings of the National Academy of Sciences of the United States of America **97**: 6640-6645

Dawson, C. C., Intapa, C. and Jabra-Rizk, M. A. (2011) "Persisters": survival at the cellular level. PLoS pathogens **7**: e1002121

De Lacey, A. L., Fernandez, V. M., Rousset, M. and Cammack, R. (2007) Activation and inactivation of hydrogenase function and the catalytic cycle: spectroelectrochemical studies. Chemical reviews **107**: 4304-4330

de Pina, K., Navarro, C., McWalter, L., Boxer, D. H., Price, N. C., Kelly, S. M., Mandrand-Berthelot, M. A. and Wu, L. F. (1995) Purification and characterization of the periplasmic nickel-binding protein NikA of *Escherichia coli* K12. European journal of biochemistry / FEBS **227**: 857-865

DeLisa, M. P., Samuelson, P., Palmer, T. and Georgiou, G. (2002) Genetic analysis of the twin arginine translocator secretion pathway in bacteria. The Journal of biological chemistry **277**: 29825-29831

DeLisa, M. P., Tullman, D. and Georgiou, G. (2003) Folding quality control in the export of proteins by the bacterial twin-arginine translocation pathway. Proceedings of the National Academy of Sciences of the United States of America **100**: 6115-6120

Deplanche, K., Caldelari, I., Mikheenko, I. P., Sargent, F. and Macaskie, L. E. (2010) Involvement of hydrogenases in the formation of highly catalytic Pd(0) nanoparticles by bioreduction of Pd(II) using *Escherichia coli* mutant strains. Microbiology **156**: 2630-2640

Dow, J. M., Gabel, F., Sargent, F. and Palmer, T. (2013) Characterisation of a pre-export enzyme-chaperone complex on the twin-arginine transport pathway. The Biochemical journal

Dubini, A., Pye, R. L., Jack, R. L., Palmer, T. and F., S. (2002) How bacteria get energy from hydrogen: a genetic analysis of periplasmic hydrogen oxidation in *Escherichia coli*. International journal of Hydrogen Energy **27**: 1413-1420

Dubini, A. and Sargent, F. (2003) Assembly of Tat-dependent [NiFe] hydrogenases: identification of precursor-binding accessory proteins. FEBS letters **549**: 141-146

Duche, O., Elsen, S., Cournac, L. and Colbeau, A. (2005) Enlarging the gas access channel to the active site renders the regulatory hydrogenase HupUV of *Rhodobacter capsulatus* O2 sensitive without affecting its transductory activity. The FEBS journal **272**: 3899-3908

Dukes, J. S. (2003) Burning buried sunshine: human consumption of ancient solar energy. Climatic Change **61**: 31-44

Efremov, R. G., Baradaran, R. and Sazanov, L. A. (2010) The architecture of respiratory complex I. Nature **465**: 441-445

Efremov, R. G. and Sazanov, L. A. (2012) The coupling mechanism of respiratory complex I - a structural and evolutionary perspective. Biochimica et biophysica acta **1817**: 1785-1795

Elsholz, A. K., Turgay, K., Michalik, S., Hessling, B., Gronau, K., Oertel, D., Mader, U., Bernhardt, J., Becher, D., Hecker, M. and Gerth, U. (2012) Global impact of protein arginine phosphorylation on the physiology of *Bacillus subtilis*. Proceedings of the National Academy of Sciences of the United States of America **109**: 7451-7456

Fincher, V., McCaffery, M. and Cline, K. (1998) Evidence for a loop mechanism of protein transport by the thylakoid Delta pH pathway. FEBS letters **423**: 66-70

Forzi, L., Hellwig, P., Thauer, R. K. and Sawers, R. G. (2007) The CO and CN(-) ligands to the active site Fe in [NiFe]-hydrogenase of *Escherichia coli* have different metabolic origins. FEBS letters **581**: 3317-3321

Forzi, L. and Sawers, R. G. (2007) Maturation of [NiFe]-hydrogenases in *Escherichia coli*. Biometals : an international journal on the role of metal ions in biology, biochemistry, and medicine **20**: 565-578

Friedrich, B., Fritsch, J. and Lenz, O. (2011) Oxygen-tolerant hydrogenases in hydrogen-based technologies. Current opinion in biotechnology **22**: 358-364

Fritsch, J., Lenz, O. and Friedrich, B. (2011a) The maturation factors HoxR and HoxT contribute to oxygen tolerance of membrane-bound [NiFe] hydrogenase in *Ralstonia eutropha* H16. Journal of bacteriology **193**: 2487-2497

Fritsch, J., Lenz, O. and Friedrich, B. (2013) Structure, function and biosynthesis of O(2)-tolerant hydrogenases. Nature reviews. Microbiology **11**: 106-114

Fritsch, J., Loscher, S., Sanganas, O., Siebert, E., Zebger, I., Stein, M., Ludwig, M., De Lacey, A. L., Dau, H., Friedrich, B., Lenz, O. and Haumann, M. (2011b) [NiFe] and [FeS] cofactors in the membrane-bound hydrogenase of *Ralstonia eutropha* investigated by X-ray absorption spectroscopy: insights into O(2)-tolerant H(2) cleavage. Biochemistry **50**: 5858-5869

Fritsch, J., Scheerer, P., Frielingsdorf, S., Kroschinsky, S., Friedrich, B., Lenz, O. and Spahn, C. M. (2011c) The crystal structure of an oxygen-tolerant hydrogenase uncovers a novel iron-sulphur centre. Nature **479**: 249-252

Frobel, J., Rose, P., Lausberg, F., Blummel, A. S., Freudl, R. and Muller, M. (2012a) Transmembrane insertion of twin-arginine signal peptides is driven by TatC and regulated by TatB. Nature communications **3**: 1311

Frobel, J., Rose, P. and Muller, M. (2012b) Twin-arginine-dependent translocation of folded proteins. Philosophical transactions of the Royal Society of London. Series B, Biological sciences **367**: 1029-1046

Fu, C. and Maier, R. J. (1994) Organization of the hydrogenase gene cluster from *Bradyrhizobium japonicum*: sequences and analysis of five more hydrogenase-related genes. Gene **145**: 91-96

Giel, J. L., Rodionov, D., Liu, M., Blattner, F. R. and Kiley, P. J. (2006) IscR-dependent gene expression links iron-sulphur cluster assembly to the control of O2-regulated genes in *Escherichia coli*. Molecular microbiology **60**: 1058-1075

Gohlke, U., Pullan, L., McDevitt, C. A., Porcelli, I., de Leeuw, E., Palmer, T., Saibil, H. R. and Berks, B. C. (2005) The TatA component of the twin-arginine protein transport system forms channel complexes of variable diameter. Proceedings of the National Academy of Sciences of the United States of America **102**: 10482-10486

Goris, T., Wait, A. F., Saggu, M., Fritsch, J., Heidary, N., Stein, M., Zebger, I., Lendzian, F., Armstrong, F. A., Friedrich, B. and Lenz, O. (2011) A unique iron-sulfur cluster is crucial for oxygen tolerance of a [NiFe]-hydrogenase. Nature chemical biology **7**: 310-318

Gould, I. M. and Bal, A. M. (2013) New antibiotic agents in the pipeline and how they can help overcome microbial resistance. Virulence **4**: 185-191

Grahl, S., Maillard, J., Spronk, C. A., Vuister, G. W. and Sargent, F. (2012) Overlapping transport and chaperone-binding functions within a bacterial twin-arginine signal peptide. Molecular microbiology **83**: 1254-1267

Grant, S. G., Jessee, J., Bloom, F. R. and Hanahan, D. (1990) Differential plasmid rescue from transgenic mouse DNAs into *Escherichia coli* methylation-restriction mutants. Proceedings of the National Academy of Sciences of the United States of America **87**: 4645-4649

Greene, N. P., Porcelli, I., Buchanan, G., Hicks, M. G., Schermann, S. M., Palmer, T. and Berks, B. C. (2007) Cysteine scanning mutagenesis and disulfide mapping studies of the TatA component of the bacterial twin arginine translocase. The Journal of biological chemistry **282**: 23937-23945

Grgic, L., Zwicker, K., Kashani-Poor, N., Kerscher, S. and Brandt, U. (2004) Functional significance of conserved histidines and arginines in the 49-kDa subunit of mitochondrial complex I. The Journal of biological chemistry **279**: 21193-21199

Gross, R., Simon, J. and Kroger, A. (1999) The role of the twin-arginine motif in the signal peptide encoded by the hydA gene of the hydrogenase from *wolinella succinogenes*. Archives of microbiology **172**: 227-232

Gust, B., Chandra, G., Jakimowicz, D., Yuqing, T., Bruton, C. J. and Chater, K. F. (2004) Lambda red-mediated genetic manipulation of antibiotic-producing Streptomyces. Advances in applied microbiology **54**: 107-128

Hagelueken, G., Wiehlmann, L., Adams, T. M., Kolmar, H., Heinz, D. W., Tummler, B. and Schubert, W. D. (2007) Crystal structure of the electron transfer complex rubredoxin rubredoxin reductase of *Pseudomonas aeruginosa*. Proceedings of the National Academy of Sciences of the United States of America **104**: 12276-12281

Hakobyan, M., Sargsyan, H. and Bagramyan, K. (2005) Proton translocation coupled to formate oxidation in anaerobically grown fermenting *Escherichia coli*. Biophysical chemistry **115**: 55-61

Hallenbeck, P. C. and Ghosh, D. (2009) Advances in fermentative biohydrogen production: the way forward? Trends in biotechnology **27**: 287-297

Hamilton, C. M., Aldea, M., Washburn, B. K., Babitzke, P. and Kushner, S. R. (1989) New method for generating deletions and gene replacements in *Escherichia coli*. Journal of bacteriology **171**: 4617-4622

Hatzixanthis, K., Clarke, T. A., Oubrie, A., Richardson, D. J., Turner, R. J. and Sargent, F. (2005) Signal peptide-chaperone interactions on the twin-arginine protein transport pathway. Proceedings of the National Academy of Sciences of the United States of America **102**: 8460-8465

Hatzixanthis, K., Palmer, T. and Sargent, F. (2003) A subset of bacterial inner membrane proteins integrated by the twin-arginine translocase. Molecular microbiology **49**: 1377-1390

Hicks, M. G., Lee, P. A., Georgiou, G., Berks, B. C. and Palmer, T. (2005) Positive selection for loss-of-function tat mutations identifies critical residues required for TatA activity. Journal of bacteriology **187**: 2920-2925

Higuchi, Y., Yagi, T. and Yasuoka, N. (1997) Unusual ligand structure in Ni-Fe active center and an additional Mg site in hydrogenase revealed by high resolution X-ray structure analysis. Structure **5**: 1671-1680

Hinsley, A. P., Stanley, N. R., Palmer, T. and Berks, B. C. (2001) A naturally occurring bacterial Tat signal peptide lacking one of the 'invariant' arginine residues of the consensus targeting motif. FEBS letters **497**: 45-49

Holzapfel, E., Eisner, G., Alami, M., Barrett, C. M., Buchanan, G., Luke, I., Betton, J. M., Robinson, C., Palmer, T., Moser, M. and Muller, M. (2007) The entire N-terminal half of TatC is involved in twin-arginine precursor binding. Biochemistry **46**: 2892-2898

Hopper, S. and Bock, A. (1995) Effector-mediated stimulation of ATPase activity by the sigma 54-dependent transcriptional activator FHLA from *Escherichia coli*. Journal of bacteriology **177**: 2798-2803

Horch, M., Lauterbach, L., Lenz, O., Hildebrandt, P. and Zebger, I. (2012) NAD(H)-coupled hydrogen cycling - structure-function relationships of bidirectional [NiFe] hydrogenases. FEBS letters **586**: 545-556

Howlett, R. M., Hughes, B. M., Hitchcock, A. and Kelly, D. J. (2012) Hydrogenase activity in the foodborne pathogen *Campylobacter jejuni* depends upon a novel ABC-type nickel transporter (NikZYXWV) and is SlyD-independent. Microbiology **158**: 1645-1655

Hynds, P. J., Robinson, D. and Robinson, C. (1998) The sec-independent twin-arginine translocation system can transport both tightly folded and malfolded proteins across the thylakoid membrane. The Journal of biological chemistry **273**: 34868-34874

Ihara, M., Nishihara, H., Yoon, K. S., Lenz, O., Friedrich, B., Nakamoto, H., Kojima, K., Honma, D., Kamachi, T. and Okura, I. (2006) Light-driven hydrogen production by a hybrid complex of a [NiFe]-hydrogenase and the cyanobacterial photosystem I. Photochemistry and photobiology **82**: 676-682

Imperial, J., Rey, L., Palacios, J. M. and Ruiz-Argueso, T. (1993) HupK, a hydrogenase-ancillary protein from *Rhizobium leguminosarum*, shares structural motifs with the large subunit of NiFe hydrogenases and could be a scaffolding protein for hydrogenase metal cofactor assembly. Molecular microbiology **9**: 1305-1306

Ize, B., Stanley, N. R., Buchanan, G. and Palmer, T. (2003) Role of the *Escherichia coli* Tat pathway in outer membrane integrity. Molecular microbiology **48**: 1183-1193

Jack, R. L., Buchanan, G., Dubini, A., Hatzixanthis, K., Palmer, T. and Sargent, F. (2004) Coordinating assembly and export of complex bacterial proteins. The EMBO journal **23**: 3962-3972

Jack, R. L., Sargent, F., Berks, B. C., Sawers, G. and Palmer, T. (2001) Constitutive expression of *Escherichia coli* tat genes indicates an important role for the twin-arginine translocase during aerobic and anaerobic growth. Journal of bacteriology **183**: 1801-1804

Jacobi, A., Rossmann, R. and Bock, A. (1992) The hyp operon gene products are required for the maturation of catalytically active hydrogenase isoenzymes in *Escherichia coli*. Archives of microbiology **158**: 444-451

Jordan, D. B., Bowman, M. J., Braker, J. D., Dien, B. S., Hector, R. E., Lee, C. C., Mertens, J. A. and Wagschal, K. (2012) Plant cell walls to ethanol. The Biochemical journal **442**: 241-252

Karp, A. and Richter, G. M. (2011) Meeting the challenge of food and energy security. Journal of experimental botany **62**: 3263-3271

Kashani-Poor, N., Zwicker, K., Kerscher, S. and Brandt, U. (2001) A central functional role for the 49-kDa subunit within the catalytic core of mitochondrial complex I. The Journal of biological chemistry **276**: 24082-24087

Kelley, L. A. and Sternberg, M. J. (2009) Protein structure prediction on the Web: a case study using the Phyre server. Nature protocols **4**: 363-371

Kim, Y. J., Lee, H. S., Kim, E. S., Bae, S. S., Lim, J. K., Matsumi, R., Lebedinsky, A. V., Sokolova, T. G., Kozhevnikova, D. A., Cha, S. S., Kim, S. J., Kwon, K. K., Imanaka, T., Atomi, H., Bonch-Osmolovskaya, E. A., Lee, J. H. and Kang, S. G. (2010) Formate-driven growth coupled with H(2) production. Nature **467**: 352-355

Kipping, M., Lilie, H., Lindenstrauss, U., Andreesen, J. R., Griesinger, C., Carlomagno, T. and Bruser, T. (2003) Structural studies on a twin-arginine signal sequence. FEBS letters **550**: 18-22

Klein, M. J., Grage, S. L., Muhle-Goll, C., Burck, J., Afonin, S. and Ulrich, A. S. (2012) Structure analysis of the membrane-bound PhoD signal peptide of the Tat translocase shows an N-terminal amphiphilic helix. Biochimica et biophysica acta **1818**: 3025-3031

Koch, S., Fritsch, M. J., Buchanan, G. and Palmer, T. (2012) *Escherichia coli* TatA and TatB Proteins Have N-out, C-in Topology in Intact Cells. The Journal of biological chemistry **287**: 14420-14431

Krassen, H., Schwarze, A., Friedrich, B., Ataka, K., Lenz, O. and Heberle, J. (2009) Photosynthetic hydrogen production by a hybrid complex of photosystem I and [NiFe]-hydrogenase. ACS nano **3**: 4055-4061

Kuchenreuther, J. M., Grady-Smith, C. S., Bingham, A. S., George, S. J., Cramer, S. P. and Swartz, J. R. (2010) High-yield expression of heterologous [FeFe] hydrogenases in *Escherichia coli*. PloS one **5**: e15491

Kumar, R., Singh, S. and Singh, O. V. (2008) Bioconversion of lignocellulosic biomass: biochemical and molecular perspectives. Journal of industrial microbiology & biotechnology **35**: 377-391

Kurisu, G., Zhang, H., Smith, J. L. and Cramer, W. A. (2003) Structure of the cytochrome b6f complex of oxygenic photosynthesis: tuning the cavity. Science **302**: 1009-1014

Laemmli, U. K. (1970) Cleavage of structural proteins during the assembly of the head of bacteriophage T4. Nature **227**: 680-685

Laffly, E., Garzoni, F. and Fontecilla-Camps, J. C. (2010) Maturation and processing of the recombinant [FeFe] hydrogenase from *Desulfovibrio vulgaris* Hildenborough (DvH) in *Escherichia coli*. . International Journal of Hydrogen Energy **35**: 10761-10769

Lal, R. (2010) Managing soils for a warming earth in a food-insecure and energy-starved world. Journal of Plant Nutrition and Soil Science **173**: 4-15

Lamichhane-Khadka, R., Kwiatkowski, A. and Maier, R. J. (2010) The Hyb hydrogenase permits hydrogen-dependent respiratory growth of *Salmonella enterica* serovar Typhimurium. mBio **1**:

Lee, J. H., Yeo, W. S. and Roe, J. H. (2004) Induction of the sufA operon encoding Fe-S assembly proteins by superoxide generators and hydrogen peroxide: involvement of OxyR, IHF and an unidentified oxidant-responsive factor. Molecular microbiology **51**: 1745-1755

Lennen, R. M. and Pfleger, B. F. (2013) Microbial production of fatty acid-derived fuels and chemicals. Current opinion in biotechnology

Lenz, O., Zebger, I., Hamann, J., Hildebrandt, P. and Friedrich, B. (2007) Carbamoylphosphate serves as the source of CN(-), but not of the intrinsic CO in the active site of the regulatory [NiFe]-hydrogenase from Ralstonia eutropha. FEBS letters **581**: 3322-3326

Lewis, K. (2007) Persister cells, dormancy and infectious disease. Nature reviews. Microbiology **5**: 48-56

Li, H., Chang, L., Howell, J. M. and Turner, R. J. (2010) DmsD, a Tat system specific chaperone, interacts with other general chaperones and proteins involved in the molybdenum cofactor biosynthesis. Biochimica et biophysica acta **1804**: 1301-1309

Liebgott, P. P., Leroux, F., Burlat, B., Dementin, S., Baffert, C., Lautier, T., Fourmond, V., Ceccaldi, P., Cavazza, C., Meynial-Salles, I., Soucaille, P., Fontecilla-Camps, J. C., Guigliarelli, B., Bertrand, P., Rousset, M. and Leger, C. (2010) Relating diffusion along the substrate tunnel and oxygen sensitivity in hydrogenase. Nature chemical biology **6**: 63-70

Lowry, O. H., Rosebrough, N. J., Farr, A. L. and Randall, R. J. (1951) Protein measurement with the Folin phenol reagent. The Journal of biological chemistry **193**: 265-275

Lubner, C. E., Applegate, A. M., Knorzer, P., Ganago, A., Bryant, D. A., Happe, T. and Golbeck, J. H. (2011) Solar hydrogen-producing bionanodevice outperforms natural photosynthesis.

Proceedings of the National Academy of Sciences of the United States of America **108**: 20988-20991

Lubner, C. E., Knorzer, P., Silva, P. J., Vincent, K. A., Happe, T., Bryant, D. A. and Golbeck, J. H. (2010) Wiring an [FeFe]-hydrogenase with photosystem I for light-induced hydrogen production. Biochemistry **49**: 10264-10266

Ludwig, M., Cracknell, J. A., Vincent, K. A., Armstrong, F. A. and Lenz, O. (2009a) Oxygen-tolerant H2 oxidation by membrane-bound [NiFe] hydrogenases of ralstonia species. Coping with low level H2 in air. The Journal of biological chemistry **284**: 465-477

Ludwig, M., Schubert, T., Zebger, I., Wisitruangsakul, N., Saggu, M., Strack, A., Lenz, O., Hildebrandt, P. and Friedrich, B. (2009b) Concerted action of two novel auxiliary proteins in assembly of the active site in a membrane-bound [NiFe] hydrogenase. The Journal of biological chemistry **284**: 2159-2168

Lukey, M. J., Parkin, A., Roessler, M. M., Murphy, B. J., Harmer, J., Palmer, T., Sargent, F. and Armstrong, F. A. (2010) How *Escherichia coli* is equipped to oxidize hydrogen under different redox conditions. The Journal of biological chemistry **285**: 3928-3938

Lukey, M. J., Roessler, M. M., Parkin, A., Evans, R. M., Davies, R. A., Lenz, O., Friedrich, B., Sargent, F. and Armstrong, F. A. (2011) Oxygen-tolerant [NiFe]-hydrogenases: the individual and collective importance of supernumerary cysteines at the proximal Fe-S cluster. Journal of the American Chemical Society **133**: 16881-16892

Lutz, S., Jacobi, A., Schlensog, V., Bohm, R., Sawers, G. and Bock, A. (1991) Molecular characterization of an operon (hyp) necessary for the activity of the three hydrogenase isoenzymes in *Escherichia coli*. Molecular microbiology **5**: 123-135

Lyons, L. B. and Zinder, N. D. (1972) The genetic map of the filamentous bacteriophage f1. Virology **49**: 45-60

Maeda, T., Sanchez-Torres, V. and Wood, T. K. (2007) Enhanced hydrogen production from glucose by metabolically engineered *Escherichia coli*. Applied microbiology and biotechnology **77**: 879-890

Magalon, A. and Bock, A. (2000) Dissection of the maturation reactions of the [NiFe] hydrogenase 3 from *Escherichia coli* taking place after nickel incorporation. FEBS letters **473**: 254-258

Maier, R. J. (2005) Use of molecular hydrogen as an energy substrate by human pathogenic bacteria. Biochemical Society transactions **33**: 83-85

Maier, R. J., Olczak, A., Maier, S., Soni, S. and Gunn, J. (2004) Respiratory hydrogen use by *Salmonella enterica* serovar Typhimurium is essential for virulence. Infection and immunity **72**: 6294-6299

Maillard, J., Spronk, C. A., Buchanan, G., Lyall, V., Richardson, D. J., Palmer, T., Vuister, G. W. and Sargent, F. (2007) Structural diversity in twin-arginine signal peptide-binding proteins. Proceedings of the National Academy of Sciences of the United States of America **104**: 15641-15646

Manyani, H., Rey, L., Palacios, J. M., Imperial, J. and Ruiz-Argueso, T. (2005) Gene products of the hupGHIJ operon are involved in maturation of the iron-sulfur subunit of the [NiFe] hydrogenase from *Rhizobium leguminosarum* bv. viciae. Journal of bacteriology **187**: 7018-7026

Matias, P. M., Soares, C. M., Saraiva, L. M., Coelho, R., Morais, J., Le Gall, J. and Carrondo, M. A. (2001) [NiFe] hydrogenase from *Desulfovibrio desulfuricans* ATCC 27774: gene sequencing, three-dimensional structure determination and refinement at 1.8 A and modelling studies of its interaction with the tetrahaem cytochrome c3. Journal of biological inorganic chemistry : JBIC : a publication of the Society of Biological Inorganic Chemistry **6**: 63-81

Maurer, C., Panahandeh, S., Jungkamp, A. C., Moser, M. and Muller, M. (2010) TatB functions as an oligomeric binding site for folded Tat precursor proteins. Molecular biology of the cell **21**: 4151-4161

McClelland, M., Sanderson, K. E., Spieth, J., Clifton, S. W., Latreille, P., Courtney, L., Porwollik, S., Ali, J., Dante, M., Du, F., Hou, S., Layman, D., Leonard, S., Nguyen, C., Scott, K., Holmes, A., Grewal, N., Mulvaney, E., Ryan, E., Sun, H., Florea, L., Miller, W., Stoneking, T., Nhan, M., Waterston, R. and Wilson, R. K. (2001) Complete genome sequence of *Salmonella enterica* serovar Typhimurium LT2. Nature **413**: 852-856

McKinlay, J. B. and Harwood, C. S. (2010) Photobiological production of hydrogen gas as a biofuel. Current opinion in biotechnology **21**: 244-251

Menon, N. K., Chatelus, C. Y., Dervartanian, M., Wendt, J. C., Shanmugam, K. T., Peck, H. D., Jr. and Przybyla, A. E. (1994) Cloning, sequencing, and mutational analysis of the hyb operon encoding *Escherichia coli* hydrogenase 2. Journal of bacteriology **176**: 4416-4423

Menon, N. K., Robbins, J., Wendt, J. C., Shanmugam, K. T. and Przybyla, A. E. (1991) Mutational analysis and characterization of the *Escherichia coli* hya operon, which encodes [NiFe] hydrogenase 1. Journal of bacteriology **173**: 4851-4861

Meyer, J. (2007) [FeFe] hydrogenases and their evolution: a genomic perspective. Cellular and molecular life sciences : CMLS **64**: 1063-1084

Montet, Y., Amara, P., Volbeda, A., Vernede, X., Hatchikian, E. C., Field, M. J., Frey, M. and Fontecilla-Camps, J. C. (1997) Gas access to the active site of Ni-Fe hydrogenases probed by X-ray crystallography and molecular dynamics. Nature structural biology **4**: 523-526

Mouesca, J. M., Fontecilla-Camps, J. C. and Amara, P. (2013) The structural plasticity of the proximal [4Fe3S] cluster is responsible for the O2 tolerance of membrane-bound [NiFe] hydrogenases. Angewandte Chemie **52**: 2002-2006

Mould, R. M. and Robinson, C. (1991) A proton gradient is required for the transport of two lumenal oxygen-evolving proteins across the thylakoid membrane. The Journal of biological chemistry **266**: 12189-12193

Mulder, D. W., Shepard, E. M., Meuser, J. E., Joshi, N., King, P. W., Posewitz, M. C., Broderick, J. B. and Peters, J. W. (2011) Insights into [FeFe]-hydrogenase structure, mechanism, and maturation. Structure **19**: 1038-1052

Naik, S. N., Goud, V. V., Rout, P. K. a. and Dalai, A. K. (2010) Production of first and second generation biofuels: A comprehensive review. Renewable and Sustainable Energy Reviews **14**: 578-597

Navarro, C., Wu, L. F. and Mandrand-Berthelot, M. A. (1993) The nik operon of *Escherichia coli* encodes a periplasmic binding-protein-dependent transport system for nickel. Molecular microbiology **9**: 1181-1191

Nawabi, P., Bauer, S., Kyrpides, N. and Lykidis, A. (2011) Engineering *Escherichia coli* for biodiesel production utilizing a bacterial fatty acid methyltransferase. Applied and environmental microbiology **77**: 8052-8061

Nesbit, A. D., Fleischhacker, A. S., Teter, S. J. and Kiley, P. J. (2012) ArcA and AppY antagonize IscR repression of hydrogenase-1 expression under anaerobic conditions, revealing a novel mode of O2 regulation of gene expression in *Escherichia coli*. Journal of bacteriology **194**: 6892-6899

Nicolet, Y., Piras, C., Legrand, P., Hatchikian, E. C. and Fontecilla-Camps, J. C. (1999) *Desulfovibrio desulfuricans* iron hydrogenase: the structure shows unusual coordination to an active site Fe binuclear centre. Structure **7**: 13-23

Niviere, V., Wong, S. L. and Voordouw, G. (1992) Site-directed mutagenesis of the hydrogenase signal peptide consensus box prevents export of a beta-lactamase fusion protein. Journal of general microbiology **138**: 2173-2183

Ochsner, U. A., Snyder, A., Vasil, A. I. and Vasil, M. L. (2002) Effects of the twin-arginine translocase on secretion of virulence factors, stress response, and pathogenesis. Proceedings of the National Academy of Sciences of the United States of America **99**: 8312-8317

Ogata, H., Kellers, P. and Lubitz, W. (2010) The crystal structure of the [NiFe] hydrogenase from the photosynthetic bacterium *Allochromatium vinosum*: characterization of the oxidized enzyme (Ni-A state). Journal of molecular biology **402**: 428-444

Okoro, C. K., Kingsley, R. A., Connor, T. R., Harris, S. R., Parry, C. M., Al-Mashhadani, M. N., Kariuki, S., Msefula, C. L., Gordon, M. A., de Pinna, E., Wain, J., Heyderman, R. S., Obaro, S., Alonso, P. L., Mandomando, I., MacLennan, C. A., Tapia, M. D., Levine, M. M., Tennant, S. M., Parkhill, J. and Dougan, G. (2012) Intracontinental spread of human invasive *Salmonella Typhimurium* pathovariants in sub-Saharan Africa. Nature genetics **44**: 1215-1221

Olson, J. W. and Maier, R. J. (2002) Molecular hydrogen as an energy source for *Helicobacter* pyilori. Science **298**: 1788-1790

Oresnik, I. J., Ladner, C. L. and Turner, R. J. (2001) Identification of a twin-arginine leader-binding protein. Molecular microbiology **40**: 323-331

Palmer, T. and Berks, B. C. (2012) The twin-arginine translocation (Tat) protein export pathway. Nature reviews. Microbiology **10**: 483-496

Palmer, T., Sargent, F. and Berks, B. C. (2005) Export of complex cofactor-containing proteins by the bacterial Tat pathway. Trends in microbiology **13**: 175-180

Palmer, T., Sargent, F. and Berks, B. C. (2011). The Tat protein export pathway, D. ASM Press.

Pandelia, M. E., Fourmond, V., Tron-Infossi, P., Lojou, E., Bertrand, P., Leger, C., Giudici-Orticoni, M. T. and Lubitz, W. (2010) Membrane-bound hydrogenase I from the hyperthermophilic bacterium *Aquifex aeolicus*: enzyme activation, redox intermediates and oxygen tolerance. Journal of the American Chemical Society **132**: 6991-7004

Pandelia, M. E., Lubitz, W. and Nitschke, W. (2012) Evolution and diversification of Group 1 [NiFe] hydrogenases. Is there a phylogenetic marker for O(2)-tolerance? Biochimica et biophysica acta **1817**: 1565-1575

Pandelia, M. E., Nitschke, W., Infossi, P., Giudici-Orticoni, M. T., Bill, E. and Lubitz, W. (2011) Characterization of a unique [FeS] cluster in the electron transfer chain of the oxygen tolerant [NiFe] hydrogenase from *Aquifex aeolicus*. Proceedings of the National Academy of Sciences of the United States of America **108**: 6097-6102

Papish, A. L., Ladner, C. L. and Turner, R. J. (2003) The twin-arginine leader-binding protein, DmsD, interacts with the TatB and TatC subunits of the *Escherichia coli* twin-arginine translocase. The Journal of biological chemistry **278**: 32501-32506

Parish, D., Benach, J., Liu, G., Singarapu, K. K., Xiao, R., Acton, T., Su, M., Bansal, S., Prestegard, J. H., Hunt, J., Montelione, G. T. and Szyperski, T. (2008) Protein chaperones Q8ZP25_SALTY from *Salmonella typhimurium* and HYAE_ECOLI from *Escherichia coli* exhibit thioredoxin-like structures despite lack of canonical thioredoxin active site sequence motif. Journal of structural and functional genomics **9**: 41-49

Parkin, A., Bowman, L., Roessler, M. M., Davies, R. A., Palmer, T., Armstrong, F. A. and Sargent, F. (2012) How *Salmonella* oxidises H(2) under aerobic conditions. FEBS letters **586**: 536-544

Parkin, A., Goldet, G., Cavazza, C., Fontecilla-Camps, J. C. and Armstrong, F. A. (2008) The difference a Se makes? Oxygen-tolerant hydrogen production by the [NiFeSe]-hydrogenase from *Desulfomicrobium baculatum*. Journal of the American Chemical Society **130**: 13410-13416

Parkin, A. and Sargent, F. (2012) The hows and whys of aerobic H2 metabolism. Current opinion in chemical biology **16**: 26-34

Paschos, A., Glass, R. S. and Bock, A. (2001) Carbamoylphosphate requirement for synthesis of the active center of [NiFe]-hydrogenases. FEBS letters **488**: 9-12

Penfold, D. W., Sargent, F. and Macaskie, L. E. (2006) Inactivation of the *Escherichia coli* K-12 twin-arginine translocation system promotes increased hydrogen production. FEMS microbiology letters **262**: 135-137

Peralta-Yahya, P. P., Zhang, F., del Cardayre, S. B. and Keasling, J. D. (2012) Microbial engineering for the production of advanced biofuels. Nature **488**: 320-328

Pereira, S. F., Goss, L. and Dworkin, J. (2011) Eukaryote-like serine/threonine kinases and phosphatases in bacteria. Microbiology and molecular biology reviews : MMBR **75**: 192-212

Peters, J. W., Lanzilotta, W. N., Lemon, B. J. and Seefeldt, L. C. (1998) X-ray crystal structure of the Fe-only hydrogenase (CpI) from *Clostridium pasteurianum* to 1.8 angstrom resolution. Science **282**: 1853-1858

Peters, J. W., Stowell, M. H., Soltis, S. M., Finnegan, M. G., Johnson, M. K. and Rees, D. C. (1997) Redox-dependent structural changes in the nitrogenase P-cluster. Biochemistry **36**: 1181-1187

Pichon, C. and Felden, B. (2007) Proteins that interact with bacterial small RNA regulators. FEMS microbiology reviews **31**: 614-625

Pilak, O., Mamat, B., Vogt, S., Hagemeier, C. H., Thauer, R. K., Shima, S., Vonrhein, C., Warkentin, E. and Ermler, U. (2006) The crystal structure of the apoenzyme of the iron-sulphur cluster-free hydrogenase. Journal of molecular biology **358**: 798-809

Pinske, C., Kruger, S., Soboh, B., Ihling, C., Kuhns, M., Braussemann, M., Jaroschinsky, M., Sauer, C., Sargent, F., Sinz, A. and Sawers, R. G. (2011) Efficient electron transfer from hydrogen to benzyl viologen by the [NiFe]-hydrogenases of *Escherichia coli* is dependent on the coexpression of the iron-sulfur cluster-containing small subunit. Archives of microbiology **193**: 893-903

Pinske, C. and Sawers, R. G. (2012) Delivery of iron-sulfur clusters to the hydrogen-oxidizing [NiFe]-hydrogenases in *Escherichia coli* requires the A-type carrier proteins ErpA and IscA. PloS one **7**: e31755

Punginelli, C., Ize, B., Stanley, N. R., Stewart, V., Sawers, G., Berks, B. C. and Palmer, T. (2004) mRNA secondary structure modulates translation of Tat-dependent formate dehydrogenase N. Journal of bacteriology **186**: 6311-6315

Redwood, M. D., Mikheenko, I. P., Sargent, F. and Macaskie, L. E. (2008) Dissecting the roles of *Escherichia coli* hydrogenases in biohydrogen production. FEMS microbiology letters **278**: 48-55

Reissmann, S., Hochleitner, E., Wang, H., Paschos, A., Lottspeich, F., Glass, R. S. and Bock, A. (2003) Taming of a poison: biosynthesis of the NiFe-hydrogenase cyanide ligands. Science **299**: 1067-1070

Rey, L., Murillo, J., Hernando, Y., Hidalgo, E., Cabrera, E., Imperial, J. and Ruiz-Argueso, T. (1993) Molecular analysis of a microaerobically induced operon required for hydrogenase synthesis in *Rhizobium leguminosarum* biovar viciae. Molecular microbiology **8**: 471-481

Richard, D. J., Sawers, G., Sargent, F., McWalter, L. and Boxer, D. H. (1999) Transcriptional regulation in response to oxygen and nitrate of the operons encoding the [NiFe] hydrogenases 1 and 2 of *Escherichia coli*. Microbiology **145 (Pt 10)**: 2903-2912

Rittmann, S. and Herwig, C. (2012) A comprehensive and quantitative review of dark fermentative biohydrogen production. Microbial cell factories **11**: 115

Rodrigue, A., Boxer, D. H., Mandrand-Berthelot, M. A. and Wu, L. F. (1996) Requirement for nickel of the transmembrane translocation of NiFe-hydrogenase 2 in *Escherichia coli*. FEBS letters **392**: 81-86

Rodrigue, A., Chanal, A., Beck, K., Muller, M. and Wu, L. F. (1999) Co-translocation of a periplasmic enzyme complex by a hitchhiker mechanism through the bacterial tat pathway. The Journal of biological chemistry **274**: 13223-13228

Rodriguez, F., Rouse, S. L., Tait, C. E., Harmer, J., De Riso, A., Timmel, C. R., Sansom, M. S., Berks, B. C. and Schnell, J. R. (2013) Structural model for the protein-translocating element of the twin-arginine transport system. Proceedings of the National Academy of Sciences of the United States of America **110**: E1092-1101

Rollauer, S. E., Tarry, M. J., Graham, J. E., Jaaskelainen, M., Jager, F., Johnson, S., Krehenbrink, M., Liu, S. M., Lukey, M. J., Marcoux, J., McDowell, M. A., Rodriguez, F., Roversi, P., Stansfeld, P. J., Robinson, C. V., Sansom, M. S., Palmer, T., Hogbom, M., Berks, B. C. and Lea, S. M. (2012) Structure of the TatC core of the twin-arginine protein transport system. Nature **492**: 210-214

Roseboom, W., Blokesch, M., Bock, A. and Albracht, S. P. (2005) The biosynthetic routes for carbon monoxide and cyanide in the Ni-Fe active site of hydrogenases are different. FEBS letters **579**: 469-472

Rossmann, R., Maier, T., Lottspeich, F. and Bock, A. (1995) Characterisation of a protease from *Escherichia* cioli involved in hydrogenase maturation. European journal of biochemistry / FEBS **227**: 545-550

Rossmann, R., Sauter, M., Lottspeich, F. and Bock, A. (1994) Maturation of the large subunit (HYCE) of *Escherichia coli* hydrogenase 3 requires nickel incorporation followed by C-terminal processing at Arg537. European journal of biochemistry / FEBS **220**: 377-384

Rude, M. A. and Schirmer, A. (2009) New microbial fuels: a biotech perspective. Current opinion in microbiology **12**: 274-281

Russell, D. W. and Sambrook, J. (2001). *Molecular Cloning: A Laboratory Manual*, Cold Spring Harbor, NY: Cold Spring Harbor Laboratory Press.

San Miguel, M., Marrington, R., Rodger, P. M., Rodger, A. and Robinson, C. (2003) An EscherichiIa cIoli twin-arginine signal peptide switches between helical and unstructured conformations depending on the hydrophobicity of the environment. European journal of biochemistry / FEBS **270**: 3345-3352

Sanchez-Torres, V., Maeda, T. and Wood, T. K. (2009) Protein engineering of the transcriptional activator FhlA To enhance hydrogen production in *Escherichia coli*. Applied and environmental microbiology **75**: 5639-5646

Sargent, F. (2007) The twin-arginine transport system: moving folded proteins across membranes. Biochemical Society transactions **35**: 835-847

Sargent, F., Ballantine, S. P., Rugman, P. A., Palmer, T. and Boxer, D. H. (1998a) Reassignment of the gene encoding the *Escherichia coli* hydrogenase 2 small subunit--identification of a soluble precursor of the small subunit in a hypB mutant. European journal of biochemistry / FEBS **255**: 746-754

Sargent, F., Berks, B. C. and Palmer, T. (2006) Pathfinders and trailblazers: a prokaryotic targeting system for transport of folded proteins. FEMS microbiology letters **254**: 198-207

Sargent, F., Bogsch, E. G., Stanley, N. R., Wexler, M., Robinson, C., Berks, B. C. and Palmer, T. (1998b) Overlapping functions of components of a bacterial Sec-independent protein export pathway. The EMBO journal **17**: 3640-3650

Sasahara, K. C., Heinzinger, N. K. and Barrett, E. L. (1997) Hydrogen sulfide production and fermentative gas production by *Salmonella typhimurium* require F0F1 ATP synthase activity. Journal of bacteriology **179**: 6736-6740

Sauter, M., Bohm, R. and Bock, A. (1992) Mutational analysis of the operon (hyc) determining hydrogenase 3 formation in *Escherichia coli*. Molecular microbiology **6**: 1523-1532

Savage, N. (2011) Fuel options: The ideal biofuel. Nature **474**: S9-11

Sawers, G., Blockesch, M. and Bock, A. (2004). Anaerobic Formate and Hydrogen Metabolism, ASM Press.

Sawers, R. G. (2005) Formate and its role in hydrogen production in *Escherichia coli*. Biochemical Society transactions **33**: 42-46

Sawers, R. G., Ballantine, S. P. and Boxer, D. H. (1985) Differential expression of hydrogenase isoenzymes in *Escherichia coli* K-12: evidence for a third isoenzyme. Journal of bacteriology **164**: 1324-1331

Sawers, R. G. and Boxer, D. H. (1986) Purification and properties of membrane-bound hydrogenase isoenzyme 1 from anaerobically grown *Escherichia coli* K12. European journal of biochemistry / FEBS **156**: 265-275

Sawers, R. G., Jamieson, D. J., Higgins, C. F. and Boxer, D. H. (1986) Characterization and physiological roles of membrane-bound hydrogenase isoenzymes from *Salmonella typhimurium*. Journal of bacteriology **168**: 398-404

Sawers, R. G., Zehelein, E. and Bock, A. (1988) Two-dimensional gel electrophoretic analysis of *Escherichia coli* proteins: influence of various anaerobic growth conditions and the fnr gene product on cellular protein composition. Archives of microbiology **149**: 240-244

Schafer, C., Friedrich, B. and Lenz, O. (2013) Characteristics of a novel, oxygen-insensitive group 5 [NiFe]-hydrogenase in *Ralstonia eutropha*. Applied and environmental microbiology

Schlensog, V., Lutz, S. and Bock, A. (1994) Purification and DNA-binding properties of FHLA, the transcriptional activator of the formate hydrogenlyase system from *Escherichia coli*. The Journal of biological chemistry **269**: 19590-19596

Schmitz, O., Boison, G., Salzmann, H., Bothe, H., Schutz, K., Wang, S. H. and Happe, T. (2002) HoxE--a subunit specific for the pentameric bidirectional hydrogenase complex (HoxEFUYH) of cyanobacteria. Biochimica et biophysica acta **1554**: 66-74

Schubert, T., Lenz, O., Krause, E., Volkmer, R. and Friedrich, B. (2007) Chaperones specific for the membrane-bound [NiFe]-hydrogenase interact with the Tat signal peptide of the small subunit precursor in *Ralstonia eutropha* H16. Molecular microbiology **66**: 453-467

Sehested, J., Gelten, J. A. P., Remediakis, I. N., Bengaard, H. and Norskov, J. K. (2004) Sintering of nickel steam-reforming catalysts: effects of temperature and steam and hydrogen pressures. Journal of catalysis **223**: 432-443

Self, W. T., Hasona, A. and Shanmugam, K. T. (2004) Expression and regulation of a silent operon, hyf, coding for hydrogenase 4 isoenzyme in *Escherichia coli*. Journal of bacteriology **186**: 580-587

Shafaat, H. S., Rudiger, O., Ogata, H. and Lubitz, W. (2013) [NiFe] hydrogenases: A common active site for hydrogen metabolism under diverse conditions. Biochimica et biophysica acta **1827**: 986-1002

Shanmugham, A., Bakayan, A., Voller, P., Grosveld, J., Lill, H. and Bollen, Y. J. (2012) The hydrophobic core of twin-arginine signal sequences orchestrates specific binding to Tat-pathway related chaperones. PloS one **7**: e34159

Shepard, E. M., Boyd, E. S., Broderick, J. B. and Peters, J. W. (2011) Biosynthesis of complex iron-sulfur enzymes. Current opinion in chemical biology **15**: 319-327

Shepard, E. M., Duffus, B. R., George, S. J., McGlynn, S. E., Challand, M. R., Swanson, K. D., Roach, P. L., Cramer, S. P., Peters, J. W. and Broderick, J. B. (2010) [FeFe]-hydrogenase maturation: HydG-catalyzed synthesis of carbon monoxide. Journal of the American Chemical Society **132**: 9247-9249

Shima, S., Pilak, O., Vogt, S., Schick, M., Stagni, M. S., Meyer-Klaucke, W., Warkentin, E., Thauer, R. K. and Ermler, U. (2008) The crystal structure of [Fe]-hydrogenase reveals the geometry of the active site. Science **321**: 572-575

Shomura, Y., Yoon, K. S., Nishihara, H. and Higuchi, Y. (2011) Structural basis for a [4Fe-3S] cluster in the oxygen-tolerant membrane-bound [NiFe]-hydrogenase. Nature **479**: 253-256

Skibinski, D. A., Golby, P., Chang, Y. S., Sargent, F., Hoffman, R., Harper, R., Guest, J. R., Attwood, M. M., Berks, B. C. and Andrews, S. C. (2002) Regulation of the hydrogenase-4 operon of *Escherichia coli* by the sigma(54)-dependent transcriptional activators FhlA and HyfR. Journal of bacteriology **184**: 6642-6653

Slauch, J. M. (2011) How does the oxidative burst of macrophages kill bacteria? Still an open question. Molecular microbiology **80**: 580-583

Spear, J. R., Walker, J. J., McCollom, T. M. and Pace, N. R. (2005) Hydrogen and bioenergetics in the Yellowstone geothermal ecosystem. Proceedings of the National Academy of Sciences of the United States of America **102**: 2555-2560

Spellberg, B., Guidos, R., Gilbert, D., Bradley, J., Boucher, H. W., Scheld, W. M., Bartlett, J. G. and Edwards, J., Jr. (2008) The epidemic of antibiotic-resistant infections: a call to action for

the medical community from the Infectious Diseases Society of America. Clinical infectious diseases : an official publication of the Infectious Diseases Society of America **46**: 155-164

Stanley, N. R., Findlay, K., Berks, B. C. and Palmer, T. (2001) *Escherichia coli* strains blocked in Tat-dependent protein export exhibit pleiotropic defects in the cell envelope. Journal of bacteriology **183**: 139-144

Stanley, N. R., Palmer, T. and Berks, B. C. (2000) The twin arginine consensus motif of Tat signal peptides is involved in Sec-independent protein targeting in *Escherichia coli*. The Journal of biological chemistry **275**: 11591-11596

Stanley, N. R., Sargent, F., Buchanan, G., Shi, J., Stewart, V., Palmer, T. and Berks, B. C. (2002) Behaviour of topological marker proteins targeted to the Tat protein transport pathway. Molecular microbiology **43**: 1005-1021

Steen, E. J., Kang, Y., Bokinsky, G., Hu, Z., Schirmer, A., McClure, A., Del Cardayre, S. B. and Keasling, J. D. (2010) Microbial production of fatty-acid-derived fuels and chemicals from plant biomass. Nature **463**: 559-562

Stephenson, M. and Stickland, L. H. (1931) Hydrogenase: a bacterial enzyme activating molecular hydrogen: The properties of the enzyme. The Biochemical journal **25**: 205-214

Stephenson, M. and Stickland, L. H. (1933) Hydrogenase: The bacterial formation of methane by the reduction of one-carbon compounds by molecular hydrogen. The Biochemical journal **27**: 1517-1527

Swords, W. E., Cannon, B. M. and Benjamin, W. H., Jr. (1997) Avirulence of LT2 strains of *Salmonella typhimurium* results from a defective rpoS gene. Infection and immunity **65**: 2451-2453

Tabor, S. and Richardson, C. C. (1985) A bacteriophage T7 RNA polymerase/promoter system for controlled exclusive expression of specific genes. Proceedings of the National Academy of Sciences of the United States of America **82**: 1074-1078

Tarry, M. J., Schafer, E., Chen, S., Buchanan, G., Greene, N. P., Lea, S. M., Palmer, T., Saibil, H. R. and Berks, B. C. (2009) Structural analysis of substrate binding by the TatBC component of the twin-arginine protein transport system. Proceedings of the National Academy of Sciences of the United States of America **106**: 13284-13289

Thauer, R. K., Kaster, A. K., Goenrich, M., Schick, M., Hiromoto, T. and Shima, S. (2010) Hydrogenases from methanogenic archaea, nickel, a novel cofactor, and H2 storage. Annual review of biochemistry **79**: 507-536

Tian, F., Toon, O. B., Pavlov, A. A. and De Sterck, H. (2005) A hydrogen-rich early Earth atmosphere. Science **308**: 1014-1017

Trchounian, K., Pinske, C., Sawers, R. G. and Trchounian, A. (2012) Characterization of *Escherichia coli* [NiFe]-hydrogenase distribution during fermentative growth at different pHs. Cell biochemistry and biophysics **62**: 433-440

Truant, R. and Cullen, B. R. (1999) The arginine-rich domains present in human immunodeficiency virus type 1 Tat and Rev function as direct importin beta-dependent nuclear localization signals. Molecular and cellular biology **19**: 1210-1217

van Dongen, W., Hagen, W., van den Berg, W. a. and Veeger, C. (1988) Evidence for an unusual mechanism of membrane translocation of the periplasmic hydrogenase of *Desulfovibrio vulgaris* (Hildenborough), as derived from expression in *Escherichia coli*. FEMS microbiology letters **50**: 5-9

Vignais, P. M. (2008) Hydrogenases and H(+)-reduction in primary energy conservation. Results and problems in cell differentiation **45**: 223-252

Vignais, P. M. and Billoud, B. (2007) Occurrence, classification, and biological function of hydrogenases: an overview. Chemical reviews **107**: 4206-4272

Vignais, P. M. and Colbeau, A. (2004) Molecular biology of microbial hydrogenases. Current issues in molecular biology **6**: 159-188

Villarejo, M. R. and Zabin, I. (1974) Beta-galactosidase from termination and deletion mutant strains. Journal of bacteriology **120**: 466-474

Vincent, K. A., Cracknell, J. A., Clark, J. R., Ludwig, M., Lenz, O., Friedrich, B. and Armstrong, F. A. (2006) Electricity from low-level H2 in still air--an ultimate test for an oxygen tolerant hydrogenase. Chemical communications 5033-5035

Vincent, K. A., Parkin, A. and Armstrong, F. A. (2007) Investigating and exploiting the electrocatalytic properties of hydrogenases. Chemical reviews **107**: 4366-4413

Volbeda, A., Amara, P., Darnault, C., Mouesca, J. M., Parkin, A., Roessler, M. M., Armstrong, F. A. and Fontecilla-Camps, J. C. (2012) X-ray crystallographic and computational studies of the O2-tolerant [NiFe]-hydrogenase 1 from *Escherichia coli*. Proceedings of the National Academy of Sciences of the United States of America **109**: 5305-5310

Volbeda, A., Charon, M. H., Piras, C., Hatchikian, E. C., Frey, M. and Fontecilla-Camps, J. C. (1995) Crystal structure of the nickel-iron hydrogenase from *Desulfovibrio gigas*. Nature **373**: 580-587

Volbeda, A., Darnault, C., Parkin, A., Sargent, F., Armstrong, F. A. and Fontecilla-Camps, J. C. (2013) Crystal structure of the O(2)-tolerant membrane-bound hydrogenase 1 from *Escherichia coli* in complex with its cognate cytochrome b. Structure **21**: 184-190

Volbeda, A., Martin, L., Cavazza, C., Matho, M., Faber, B. W., Roseboom, W., Albracht, S. P., Garcin, E., Rousset, M. and Fontecilla-Camps, J. C. (2005) Structural differences between the ready and unready oxidized states of [NiFe] hydrogenases. Journal of biological inorganic chemistry : JBIC : a publication of the Society of Biological Inorganic Chemistry **10**: 239-249

Voordouw, G., Hagen, W. R., Kruse-Wolters, K. M., van Berkel-Arts, A. and Veeger, C. (1987) Purification and characterization of *Desulfovibrio vulgaris* (Hildenborough) hydrogenase expressed in *Escherichia coli*. European journal of biochemistry / FEBS **162**: 31-36

Wait, A. F., Parkin, A., Morley, G. M., dos Santos, L. a. and Armstrong, F. A. (2010) Characteristics of enzyme-based hydrogen fuel cells using an oxygen-tolerant hydrogenase as the anodic catalyst. Journal of physical chemistry c **114**: 12003-12009

Weerakoon, D. R., Borden, N. J., Goodson, C. M., Grimes, J. and Olson, J. W. (2009) The role of respiratory donor enzymes in *Campylobacter jejuni* host colonization and physiology. Microbial pathogenesis **47**: 8-15

Weiner, J. H., Bilous, P. T., Shaw, G. M., Lubitz, S. P., Frost, L., Thomas, G. H., Cole, J. A. and Turner, R. J. (1998) A novel and ubiquitous system for membrane targeting and secretion of cofactor-containing proteins. Cell **93**: 93-101

Wexler, M., Sargent, F., Jack, R. L., Stanley, N. R., Bogsch, E. G., Robinson, C., Berks, B. C. and Palmer, T. (2000) TatD is a cytoplasmic protein with DNase activity. No requirement for TatD family proteins in sec-independent protein export. The Journal of biological chemistry **275**: 16717-16722

Wildschut, J. D., Lang, R. M., Voordouw, J. K. and Voordouw, G. (2006) Rubredoxin:oxygen oxidoreductase enhances survival of *Desulfovibrio vulgaris* hildenborough under microaerophilic conditions. Journal of bacteriology **188**: 6253-6260

Wilmes-Riesenberg, M. R., Foster, J. W. and Curtiss, R., 3rd (1997) An altered rpoS allele contributes to the avirulence of Salmonella typhimurium LT2. Infection and immunity **65**: 203-210

Winstone, T. L., Workentine, M. L., Sarfo, K. J., Binding, A. J., Haslam, B. D. and Turner, R. J. (2006) Physical nature of signal peptide binding to DmsD. Archives of biochemistry and biophysics **455**: 89-97

Witze, A. (2007) Energy: that's oil, folks. Nature **445**: 14-17

Wu, L. F. and Mandrand-Berthelot, M. A. (1986) Genetic and physiological characterization of new *Escherichia coli* mutants impaired in hydrogenase activity. Biochimie **68**: 167-179

Wu, L. F., Mandrand-Berthelot, M. A., Waugh, R., Edmonds, C. J., Holt, S. E. and Boxer, D. H. (1989) Nickel deficiency gives rise to the defective hydrogenase phenotype of hydC and fnr mutants in *Escherichia coli*. Molecular microbiology **3**: 1709-1718

Yahr, T. L. and Wickner, W. T. (2001) Functional reconstitution of bacterial Tat translocation *in vitro*. The EMBO journal **20**: 2472-2479

Zbell, A. L., Benoit, S. L. and Maier, R. J. (2007) Differential expression of NiFe uptake-type hydrogenase genes in *Salmonella enterica* serovar Typhimurium. Microbiology **153**: 3508-3516

Zbell, A. L. and Maier, R. J. (2009) Role of the Hya hydrogenase in recycling of anaerobically produced H2 in *Salmonella enterica* serovar Typhimurium. Applied and environmental microbiology **75**: 1456-1459

Zbell, A. L., Maier, S. E. and Maier, R. J. (2008) *Salmonella enterica* serovar Typhimurium NiFe uptake-type hydrogenases are differentially expressed *in vivo*. Infection and immunity **76**: 4445-4454

Zheng, M., Wang, X., Templeton, L. J., Smulski, D. R., LaRossa, R. A. and Storz, G. (2001) DNA microarray-mediated transcriptional profiling of the *Escherichia coli* response to hydrogen peroxide. Journal of bacteriology **183**: 4562-4570

Zirngibl, C., Hedderich, R. and Thauer, R. K. (1990) N^5, N^{10}-Methylenetetrahydromethanopterin dehydrogenase from *Methanobacterium thermoautotrophicum* has hydrogenase activity. FEBS letters **261**: 112-116

Zirngibl, C., Van Dongen, W., Schworer, B., Von Bunau, R., Richter, M., Klein, A. and Thauer, R. K. (1992) H2-forming methylenetetrahydromethanopterin dehydrogenase, a novel type of hydrogenase without iron-sulfur clusters in methanogenic archaea. European journal of biochemistry / FEBS **208**: 511-520